รายงานวิจัยฉบับสมบูรณ์

โครงการการหาขอบเขตของตัวประกอบวัตถุเทาสำหรับหลุมดำ แบบ Reissner - Nordström และ Schwarzschild - Tangherlini

โดย ผศ.ดร. เพชรอาภา บุญเสริม

2 มิถุนายน 2558

สัญญาเลขที่ MRG5680171

รายงานวิจัยฉบับสมบูรณ์

โครงการการหาขอบเขตของตัวประกอบวัตถุเทาสำหรับหลุมดำ แบบ Reissner - Nordström และ Schwarzschild - Tangherlini

ผู้วิจัย ผศ.ดร. เพชรอาภา บุญเสริม
สังกัดภาควิชาคณิตศาสตร์และวิทยาการคอมพิวเตอร์
คณะวิทยาศาสตร์ จุฬาลงกรณ์มหาวิทยาลัย

สนับสนุนโดยสำนักงานกองทุนสนับสนุนการวิจัย

(ความเห็นในรายงานนี้เป็นของผู้วิจัย
สกว.ไม่จำเป็นต้องเห็นด้วยเสมอไป)

รูปแบบ Abstract (บทคัดย่อ)

Project Code : MRG5680171
(รหัสโครงการ)

Project Title : การหาขอบเขตของตัวประกอบวัตถุเทาสำหรับหลุมดำแบบ Reissner – Nordström และ Schwarzschild - Tangherlini
(ชื่อโครงการ)

Investigator : ผศ.ดร. เพชรอาภา บุญเสริม จุฬาลงกรณ์มหาวิทยาลัย
(ชื่อนักวิจัย)

E-mail Address : Petarpa.Boonserm@gmail.com

Project Period : 2 ปี
(ระยะเวลาโครงการ)

บทคัดย่อ

Semiclassical black holes emit radiation called the Hawking radiation. Such radiation, as seen by an asymptotic observer far outside the black hole, differs from the original radiation near the horizon of the black hole by a redshift factor and the so-called 'greybody factor'. In this project, we concentrate on the greybody factor. Various bounds for the greybody factors of non-rotating black holes are obtained, with major focus on the charged Reissner - Nordström and the Schwarzschild - Tangherlini black holes. These bounds can be derived using a 2×2 transfer matrix formalism. It has been found that the charges of black holes act as efficient barriers. Furthermore, adding extra dimensions to spacetime can shield the Hawking radiation. Finally, the cosmological constant has also been found to increase the emission rate of the Hawking radiation.

Keywords : greybody factors, Hawking radiation, rigorous bound, Reissner – Nordström black hole, Schwarzschild – Tangherlini black hole
(คำหลัก)

วัตถุประสงค์

1) To calculate the greybody factors for the four-dimensional Reissner-Nordström black holes, the Schwarzschild - Tangherlini black holes, the charged dilatonic black holes in (2 + 1) dimensions, and the charged dilatonic black holes in (3 + 1) dimensions.

2) To investigate what factors have an effect on the greybody factors.

3) To compare the 2×2 transfer matrix method with the WKB approximation and the matching techniques.

4) To apply the approach to other black holes.

วิธีดำเนินงานวิจัย

1) Derivation of the Schrödinger -like equation and the extraction of potential from the equation, for each type of black hole.

A static and spherically symmetric black hole in d dimensions can be described by

$$ds^2 = -A(r)dt^2 + \frac{1}{B(r)}dr^2 + r^2 d\Omega^2_{d-2}, \tag{1}$$

where $d\Omega^2_{d-2}$ is the metric on $(d-2)$-sphere and is given by

$$d\Omega^2_{d-2} = d\theta_1^2 + \sin^2\theta_1 d\theta_2^2 + \sin^2\theta_1 \sin^2\theta_2 d\theta_3^2 + \ldots + \sin^2\theta_1 \cdots \sin^2\theta_{d-3} d\theta^2_{d-2}. \tag{2}$$

We are interested in a massless uncharged scalar field emitted from this black hole. The equation of motion of this scalar field on the black hole background is

$$\frac{1}{\sqrt{-g}}\partial_\mu\left(\sqrt{-g}g^{\mu\nu}\partial_\nu\Phi\right) = 0. \tag{3}$$

By separating variables

$$\Phi(t,r,\Omega) = e^{i\omega t} r^{(2-d)/2}\psi_\ell(r)Y_{\ell m}(\Omega), \tag{4}$$

we obtain the Schrödinger -like equation governing the modes, which is given by

$$\frac{d^2\psi_\ell(r)}{dr_*^2} + \left[\omega^2 - V_\ell(r)\right]\psi_\ell(r) = 0, \tag{5}$$

where r_* is the standard "tortoise coordinate" given by

$$\frac{dr_*}{dr} = \frac{1}{\sqrt{A(r)B(r)}} \tag{6}$$

and $V(r)$ is the potential produced by the black hole

$$V_\ell(r) = \frac{\ell(\ell+d-3)A(r)}{r^2} + \frac{(d-2)\sqrt{A(r)B(r)}}{2r^{(d-2)/2}}\frac{d}{dr}\left[r^{(d-4)/2}\sqrt{A(r)B(r)}\right]. \tag{7}$$

Its shape depends on the type of black hole. Black holes can be classified into four different types. The first is the uncharged, non-rotating black hole called the Schwarzschild black hole, which is the simplest type of black hole. The second is the Reissner-Nordström black hole, which is a charged, non-rotating black hole. The third is the Kerr black hole, which is an uncharged, rotating black hole. The last type of black hole is the Kerr-Newman black hole, which is a charged, rotating black hole. Here is a summary of the different types of black holes [15].

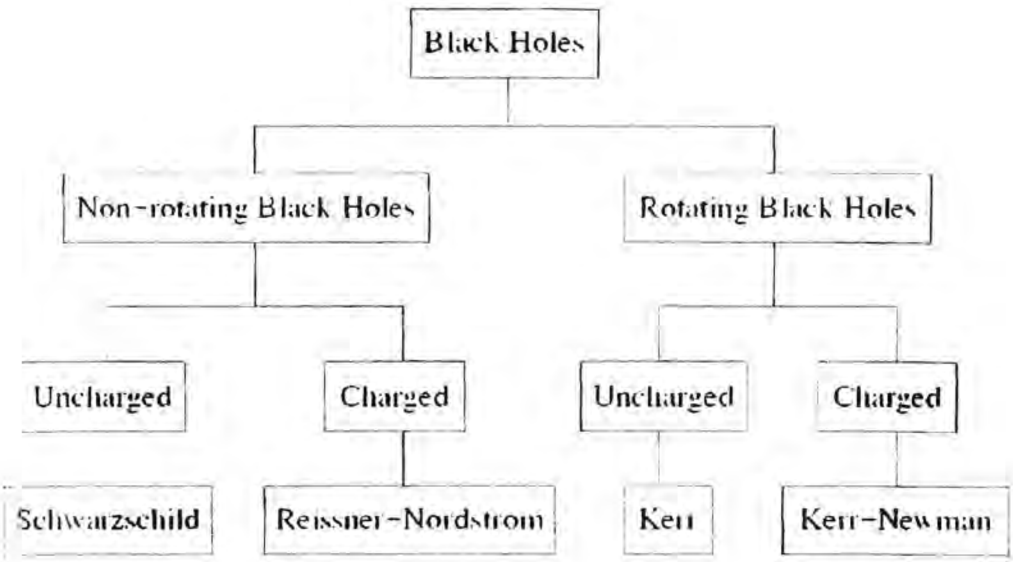

If a Schwarzschild black hole is surrounded by matter, it becomes a dirty black hole. In higher dimensions, the generalization of the Schwarzschild black holes to d dimensions is referred to as Schwarzschild-Tangherlini black holes. Similarly, the generalization of the Kerr-Newman black holes to $(4 + n)$ dimensions is called as the Myers-Perry black holes. Moreover, there are black holes which are considered as the solutions to the low-energy string theory. Each of these black holes is associated with a dilaton field called the charged dilatonic black hole. In this project, we will study them in both (2 + 1) and (3 + 1) dimensions.

2) Calculation of the bounds on the greybody factors of the black holes using the 2×2 transfer matrix techniques.

A greybody factor is a transmission probability of Hawking radiation to penetrate a potential barrier produced by a black hole. It is an important quantity which helps us understand the quantum nature of a black hole. Properties of greybody factors depend on the type of black hole. In this project, greybody factors are calculated using rigorous bounds developed by the 2×2 transfer matrices. We start by rewriting the second order differential equation

$$\frac{d^2\psi(r)}{dr_*^2} + \left[\omega^2 - V(r)\right]\psi(r) = 0$$

as two first order differential equations in the 2×2 transfer matrix form

$$\frac{d}{dr_*}\begin{bmatrix} \psi \\ \pi / k_0 \end{bmatrix} = \begin{bmatrix} 0 & k_0 \\ -k^2(r_*)/k_0 & 0 \end{bmatrix}\begin{bmatrix} \psi \\ \pi / k_0 \end{bmatrix},$$

where

$$k^2(r_*) = \omega^2 - V(r) \text{ and } \pi = \frac{dk(r_*)}{dr_*}.$$

Using the inequality for real numbers

$$x^2 + y^2 \geq 2|xy|,$$

we can obtain the rigorous bounds on the greybody factors [16]

$$T \geq \operatorname{sech}^2\left(\int_{-\infty}^{\infty} \frac{\sqrt{(h')^2 + \left(\omega^2 - V - h^2\right)^2}}{2h} dr_*\right), \tag{8}$$

where V is a potential barrier produced by a black hole, ω is a frequency of Hawking radiation, and h is any positive function which will be chosen to optimize the bounds. Calculating the greybody factor using this technique is relatively more precise than other methods such as the matching techniques. Moreover, the rigorous bounds are powerful in providing the qualitative understanding of black holes.

3) Analytical determination of what variables the results depend on.

From the above formula, we can see that the rigorous bounds on the greybody factors mainly depend on V, a potential barrier produced by a black hole. To analyze the results, we will set the values of some parameters such as GM and ω so that the bounds are functions of just one variable. They can, therefore, be plotted using a program such as MAPLE for the analytical computation of the results. In general, the rigorous bounds on the greybody factors depend on the black hole mass, the black hole charge, and the black hole angular momentum as well as the wave frequency and the spacetime dimension. This means that black hole characteristics themselves determine what values of the rigorous bounds on the greybody factors should be.

4) Comparison of results from the 2×2 transfer matrices with results obtained from the WKB approximation and the matching techniques.

Using the WKB approximation, the approximate greybody factor is given by [1]

$$T \approx \exp\left[-\frac{2}{\hbar}\operatorname{Im}\int_a^b p(x)dx\right],$$

where

$$p(x) = \sqrt{2m[E - V(x)]}\,.$$

The matching techniques are a composition of the approximation methods for finding the solutions to the Schrödinger-like equation. First, we find the solutions near the black hole, which are called near solutions, by approximating the relevant parameters in order to make the Schrödinger-like equation simple enough for us to solve it. Second, we find the solutions at the point of infinity by approximating the relevant parameters to obtain the far solutions. Last, we relate the near solutions to the far solutions using the appropriate boundary conditions. Consequently, the approximate greybody factors can be obtained. We will compare the results of the greybody factors acquired using the 2×2 transfer matrices with results from the WKB approximation and the matching techniques.

5) The application of the 2×2 transfer matrix techniques with other black holes.

We will apply the bounds on the greybody factors from the 2×2 transfer matrix to various types of black holes such as the four-dimensional Reissner-Nordström black holes (the charged, non-rotating black holes), the Schwarzschild - Tangherlini black holes (the non-rotating black holes in d dimensions), the charged dilatonic black holes (the black holes associated with the dilaton fields) in (2 + 1) and (3 + 1) dimensions, the dirty black holes, and the Myers-Perry black holes (the charged rotating black holes in (4 + n) dimensions). The Myers-Perry black holes are important in that they are the simplest of the higher-dimensional rotating black holes. In addition, there is a new phenomenon, called superradiance, occurring in the Myers-Perry black holes, which can never arise in non-rotating black holes. Superradiance is a phenomenon by which the reflected wave is larger in its amplitude than the incident wave [14].

ผลการทดลอง

In this section, we will show you how we can obtain the bounds on the greybody factors for various types of black holes by the methodology mentioned above. We will analyze the factors which affect the bounds on the greybody factors and compare those bounds with the approximate greybody factors obtained from the WKB approximation and the matching techniques. Application with various types of black holes are as follows;

1. Reissner-Nordström black holes

The Reissner-Nordström metric is given by [1]

$$ds^2 = -\Delta dt^2 + \Delta^{-1} dr^2 + r^2 d\Omega^2,$$

where $d\Omega^2 = d\theta^2 + \sin^2\theta d\phi^2$ and

$$\Delta = 1 - \frac{2GM}{r} + \frac{G\left(Q^2 + P^2\right)}{r^2}.$$

Here M is the black hole mass, Q is the total electric charge, and P is the total magnetic charge. In this case, from equation (1) we find that

$$A(r) = B(r) = \Delta(r) \text{ and } d = 4.$$

From equation (5), the Schrödinger-like equation is given by

$$\frac{d^2\psi}{dr_*^2} + \left[\omega^2 - V(r)\right]\psi = 0.$$

From equation (6), the tortoise coordinate is given by

$$dr_* = \frac{1}{\Delta} dr.$$

From equation (7), the potential produced by the Reissner-Nordström black hole is given by

$$V(r) = \frac{\ell(\ell+1)\Delta}{r^2} + \frac{\Delta\partial_r\Delta}{r}.$$

where ℓ is the angular momentum.

From equation (8), the bounds on the greybody factors are given by

$$T \geq \text{sech}^2\left[\frac{1}{2\omega}\left\{\frac{\ell(\ell+1)}{GM+A} + \frac{GM+2A}{3(GM+A)^2}\right\}\right],$$

where

$$A^2 \equiv G^2M^2 - G\left(Q^2 + P^2\right).$$

The bounds on the greybody factors versus A are plotted for different angular momenta as shown in Figure 1.

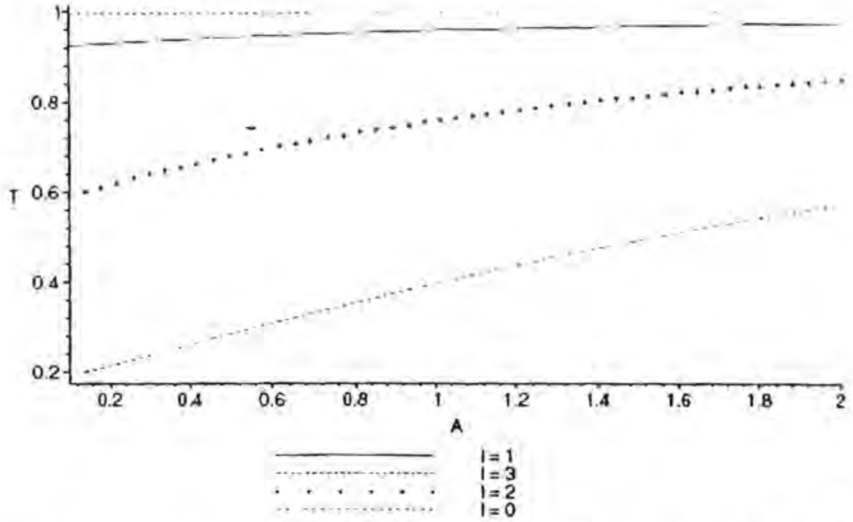

Figure 1. Dependence of the bounds on the greybody factors on A.

Based on the value of A, a decrease in A corresponds to an increase in the magnitude of the charge. The graph shows that when the magnitude of the charge increases, the bounds on the greybody factors decrease. That is, the charge is an effective barrier in resisting the tunneling of uncharged scalar particles [2-7]. Moreover, the bound is smaller in higher angular momenta.

If the energy from the potential barrier is higher than the particle's energy, we can use the WKB approximation to calculate the greybody factor

$$T_{\text{WKB}} = \exp\left[-\frac{2\pi}{\hbar}\left\{2G\omega\left(M-\frac{\omega}{2}\right)-(M-\omega)\sqrt{G^2(M-\omega)^2-G\left(Q^2+P^2\right)}\right.\right.$$
$$\left.\left.+M\sqrt{G^2M^2-G\left(Q^2+P^2\right)}\right\}\right].$$

The asymptotic greybody factor for large ω, obtained from the matching techniques, is given by [8-10]

$$T \approx \frac{e^{\beta\omega}-1}{e^{\beta\omega}+2+3e^{-\beta_i\omega}},$$

where

$$\beta = \frac{8\pi M}{1+Q^2/2GM^2+5Q^4/16G^2M^4} \text{ and } \beta_i = -\frac{2\pi\left[GM-\sqrt{G^2M^2-GQ^2}\right]^2}{\sqrt{G^2M^2-GQ^2}}.$$

The bound on the greybody factor compared with the asymptotic greybody factor for large ω is shown on the graph in Figure 2.

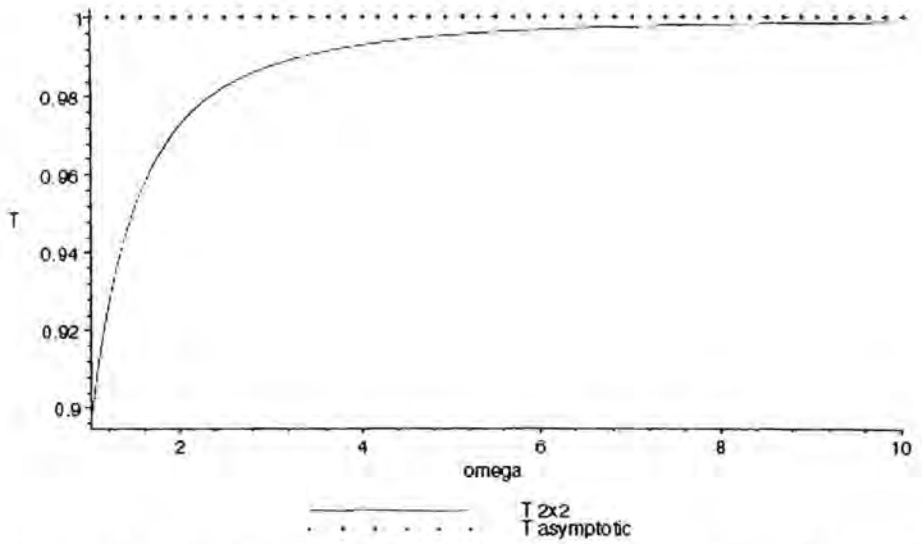

Figure 2. Comparison of the bound on the greybody factor and the asymptotic greybody factor.

The graph shows that the result from the 2×2 transfer matrix is close to the asymptotic result for large ωs. Moreover, the bound on the greybody factor provides a true lower bound.

2. Schwarzschild - Tangherlini black holes in *d* dimensions

The Schwarzschild-Tangherlini metric in *d* dimensions is given by [1]

$$ds^2 = -f(r)dt^2 + \frac{dr^2}{f(r)} + r^2 d\Omega^2_{d-2},$$

where

$$f(r) = 1 - \left(\frac{r_0}{r}\right)^{d-3}.$$

Here, the Schwarzschild radius r_0 in *d* dimensions is given by

$$r_0 = \frac{16\pi GM}{(d-2)\Omega_{d-2}} \text{ and } \Omega_{d-2} = \frac{2\pi^{(d-1)/2}}{\Gamma((d-1)/2)},$$

where *M* is the black hole mass. In this case, from equation (1) we find that

$$A(r) = B(r) = f(r).$$

From equation (5), the Schrödinger -like equation is given by

$$\frac{d^2\psi}{dr_*^2} + \left[\omega^2 - V(r)\right]\psi = 0.$$

From equation (6), the tortoise coordinate is given by

$$dr_* = \frac{1}{f(r)}dr.$$

From equation (7), the potential produced by the Schwarzschild-Tangherlini metric in d dimensions is given by

$$V(r)=\frac{(d-2)(d-4)}{4}\frac{f^2(r)}{r^2}+\frac{(d-2)}{2}\frac{f(r)\partial_r f(r)}{r}+\ell\left(\ell+d-3\right)\frac{f(r)}{r^2}.$$

From equation (8), the bounds on the greybody factors are given by

$$T\geq \operatorname{sech}^2\left[\frac{(d-2)(d-3)+4\ell\left(\ell+d-3\right)}{8\omega r_0}\right].$$

The bounds on the greybody factors versus M are plotted for different spacetime dimensions as shown in Figure 3.

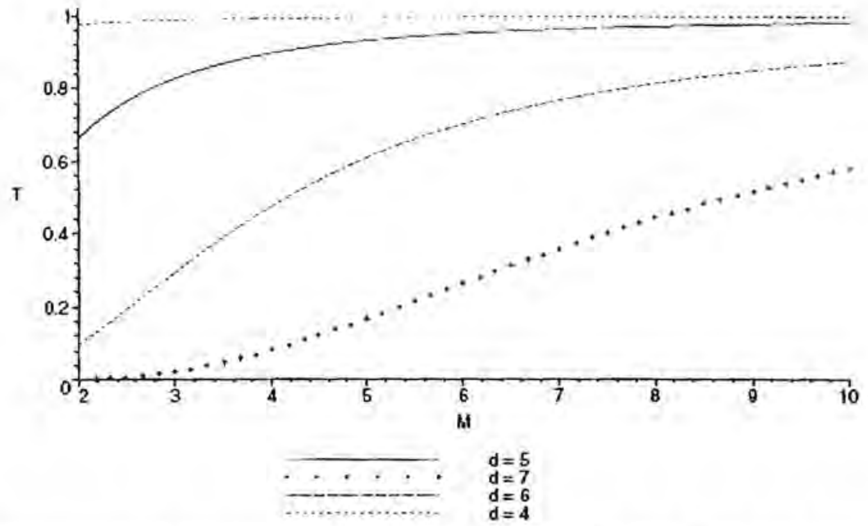

Figure 3. Dependence of the bound on the greybody factor on the black hole mass in various spacetime dimensions.

The graph shows that when the black hole mass increases, the bounds on the greybody factors also increase. However, for the same mass, the bound on the greybody factor is less in higher dimensions [11].

3. Charged dilatonic black holes in (2 + 1) dimensions

The charged dilatonic black holes in (2 + 1) dimensions is given by [1]

$$ds^2=-f(r)dt^2+\frac{4r^2}{f(r)}dr^2+r^2d\theta^2,$$

where

$$f(r)=-2Mr+8\Lambda r^2+8Q^2.$$

Here, M is the black hole mass, Q is the total electric charge, and Λ is the cosmological constant. In this case, from equation (1) we find that

$$A(r) = f(r), B(r) = \frac{f(r)}{4r^2}, \text{ and } d = 3.$$

From equation (5), the Schrödinger-like equation is given by

$$\frac{d^2\psi}{dr_*^2} + \left[\omega^2 - V(r)\right]\psi = 0.$$

From equation (6), the tortoise coordinate is given by

$$dr_* = \frac{2r}{f(r)} dr.$$

From equation (7), the potential produced by the charged dilatonic black holes in (2 + 1) dimensions is given by

$$V(r) = -(8m^2\Lambda + 6m\Lambda) + 14\Lambda^2 r + \left(\frac{5M^2}{8} + 2m^2 M\right)\frac{1}{r} - (4MQ^2 + 8m^2Q^2)\frac{1}{r^2} + \frac{6Q^4}{r^3}.$$

From equation (8), the bounds on the greybody factors are given by

$$T \geq \operatorname{sech}^2\left[\frac{-368\Lambda m(4m+3) + 644M\Lambda - 2576Q^2\Lambda + 115M^2 + 368m^2M}{60\omega\sqrt{M^2 - 64Q^2\Lambda}} - \frac{5\sqrt{M^2 - 64Q^2\Lambda}}{8\omega} + \frac{5M + 16m^2}{16\omega}\ln\left(\frac{M + \sqrt{M^2 - 64Q^2\Lambda}}{M - \sqrt{M^2 - 64Q^2\Lambda}}\right) - \frac{23Q^2(3Q^2 - 2M - 4m^2)}{15\omega\Lambda}\right].$$

The bound on the greybody factor versus Q is plotted as shown in Figure 4.

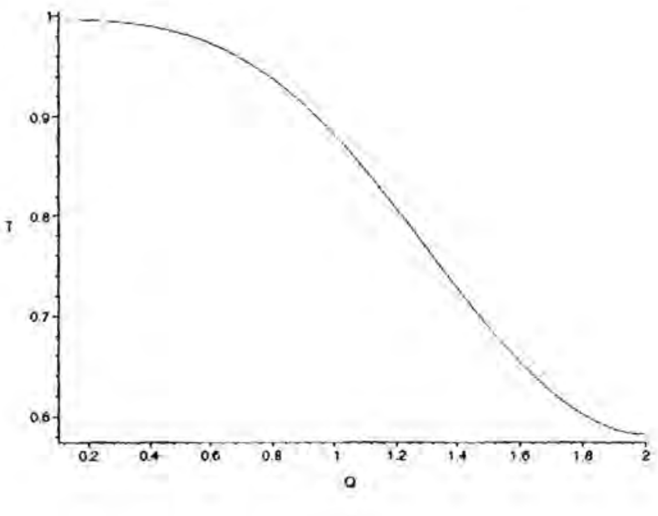

Figure 4. Dependence of the bound on the greybody factor on the charge of the dilatonic black holes in (2 + 1) dimensions.

The graph shows that when the charge increases, the bound on the greybody factor decreases. This result is similar to the Reissner-Nordström black hole's result; that is, the charge behaves as an effective barrier in resisting the tunneling of uncharged scalar particles.

The bound on the greybody factor versus the cosmological constant is plotted as shown in Figure 5.

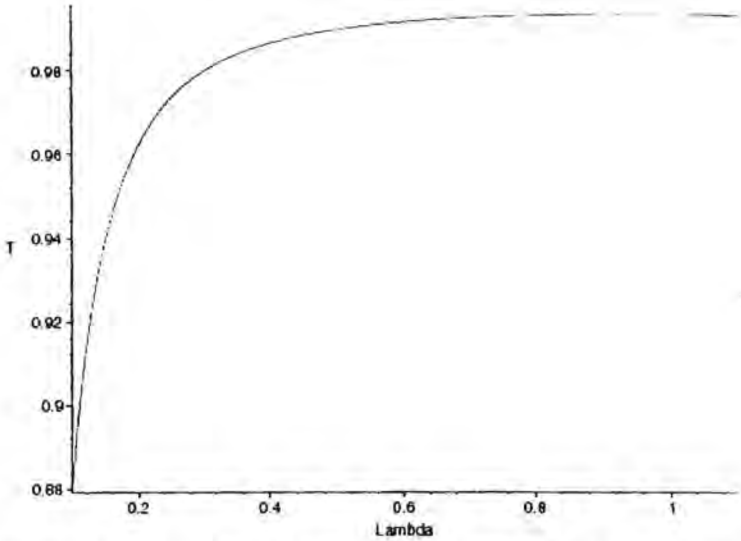

Figure 5. Dependence of the bound on the greybody factor on the cosmological constant for the charged dilatonic black holes in (2 + 1) dimensions.

The graph shows that when the value of the cosmological constant increases, the bound on the greybody factor also increases. That is, the cosmological constant renders the gravitational potential produced by the black hole transparent.

The approximate greybody factor obtained from the matching techniques is given by [12]

$$T \approx 1 - \frac{\cosh\left[\frac{\pi\omega}{4\Lambda} - \frac{\pi}{2}\sqrt{\frac{\omega^2 - 8m^2\Lambda}{4\Lambda^2} - 1}\right]\cosh\left[\frac{\pi\omega(r_+ + r_-)}{4\Lambda(r_+ - r_-)} - \frac{\pi}{2}\sqrt{\frac{\omega^2 - 8m^2\Lambda}{4\Lambda^2} - 1}\right]}{\cosh\left[\frac{\pi\omega}{4\Lambda} + \frac{\pi}{2}\sqrt{\frac{\omega^2 - 8m^2\Lambda}{4\Lambda^2} - 1}\right]\cosh\left[\frac{\pi\omega(r_+ + r_-)}{4\Lambda(r_+ - r_-)} + \frac{\pi}{2}\sqrt{\frac{\omega^2 - 8m^2\Lambda}{4\Lambda^2} - 1}\right]},$$

where

$$r_{\pm} = \frac{M \pm \sqrt{M^2 - 64Q^2\Lambda}}{8\Lambda}.$$

The bound on the greybody factor compared with the approximate greybody factor is shown on the graph in Figure 6.

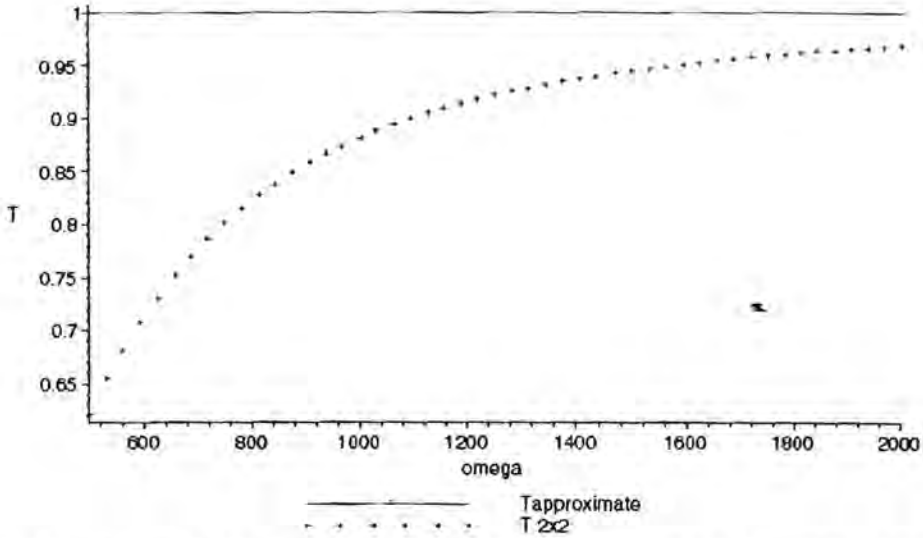

Figure 6. Comparison of the bound on the greybody factor and the approximate greybody factor.

The graph shows that when the energy of an emitted particle increases, the greybody factor also increases. It can be seen that the result derived from the 2×2 transfer matrices is relatively more accurate when compared with the approximate result. Note that the methods of 2×2 transfer matrices used to obtain the lower bound are comparatively less complex than the methods used to obtain the approximate result.

4. Charged dilatonic black holes in (3 + 1) dimensions

The charged dilatonic black holes in (3 + 1) dimensions is given by [1]

$$ds^2 = -f(r)dt^2 + \frac{1}{f(r)}dr^2 + R^2(r)d\Omega^2,$$

where

$$f(r) = 1 - \frac{r_+}{r} \text{ and } R^2(r) = r^2\left(1 - \frac{r_-}{r}\right).$$

For the black hole mass M and the total electric charge Q, r_+ and r_- are given by

$$r_+ = 2M \text{ and } r_- = \frac{Q^2}{M}.$$

In this case, from equation (1) we find that

$$A(r) = B(r) = f(r) \text{ and } d = 4.$$

The equation of motion for the radial part is given by

$$\frac{1}{R^2(r)}\frac{d}{dr}\left[R^2(r)f(r)\frac{du(r)}{dr}\right]+\left[\frac{\omega^2}{f(r)}-\frac{\ell(\ell+1)}{R^2(r)}\right]u(r)=0.$$

From equation (6), the tortoise coordinate is given by

$$dr_* = \frac{1}{f(r)}dr.$$

From equation (7), the potential produced by the charged dilatonic black holes in (3 + 1) dimensions is given by

$$V(r)=\frac{\ell(\ell+1)f(r)}{R^2(r)}.$$

From equation (8), the bounds on the greybody factors are given by

$$T \geq \frac{4\left(2M^2\right)^{\ell(\ell+1)M/\omega Q^2}\left(2M^2-Q^2\right)^{\ell(\ell+1)M/\omega Q^2}}{\left[\left(2M^2\right)^{\ell(\ell+1)M/\omega Q^2}+\left(2M^2-Q^2\right)^{\ell(\ell+1)M/\omega Q^2}\right]^2}.$$

The bound on the greybody factor versus Q is plotted as shown in Figure 7.

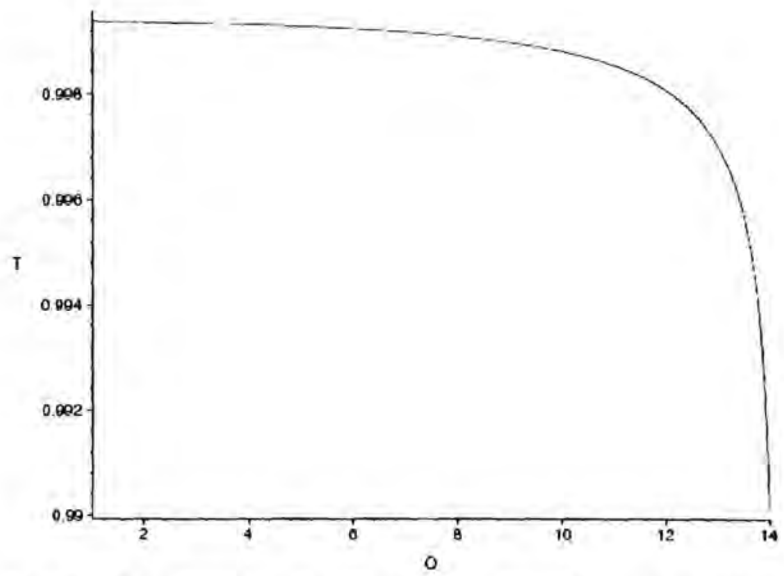

Figure 7. Dependence of the bound on the greybody factor on the charge of the dilatonic black holes in (3 + 1) dimensions.

The graph shows that when the charge increases, the bound on the greybody factor decreases. This result is similar to the Reissner-Nordström and the (2 + 1) dimensional charged dilatonic black holes' results; that is, the charge behaves as an effective barrier in resisting the tunneling of uncharged scalar particles. The rigorous bounds presented here only work for certain potentials. Such potentials have to satisfy $V(\pm\infty) \rightarrow V_{\pm\infty}$.

5. Dirty black holes

A general static spherically symmetric spacetime for a dirty black hole is given by [13]

$$ds^2 = -e^{-2\phi(r)}\left(1-\frac{2m(r)}{r}\right)dt^2 + \frac{dr^2}{1-2m(r)/r} + r^2 d\Omega^2,$$

where $\phi(r)$ is related to the distribution of matter and $m(r)$ is the total mass within the radius r from center of a black hole. In this case, from equation (1) we find that

$$A(r) = e^{-2\phi(r)}\left[1-\frac{2m(r)}{r}\right],\ B(r) = 1-\frac{2m(r)}{r} \text{ and } d = 4.$$

From equation (5), the Schrödinger-like equation is given by

$$\frac{d^2\psi}{dr_*^2} + \left[\omega^2 - V(r)\right]\psi = 0.$$

From equation (6), the tortoise coordinate is given by

$$\frac{dr_*}{dr} = e^{\phi(r)}\left[1-\frac{2m(r)}{r}\right]^{-1}.$$

From equation (7), the potential produced by the Reissner-Nordström black hole is given by

$$V(r) = e^{-2\phi(r)}\left[1-\frac{2m(r)}{r}\right]\left[\frac{\ell(\ell+1)}{r^2} + \frac{2(1-S^2)m(r)}{r^3} - 4(1-S)\pi(\rho - p_r)\right],$$

where ρ is the matter density, p_r is the radial pressure, and S is the spin of a particle which runs from integers 0 to 2.

From equation (8), the bounds on the greybody factors are given by

$$T \geq \operatorname{sech}^2\left[\frac{1}{2\omega r_H}\left\{\ell(\ell+1) + \frac{1-S^2}{2}\right\}\right],$$

where $r_H = 2m(r_H)$. The bound on the greybody factor depends on the frequency wave ω, the angular momentum ℓ, the spin S, and the horizon radius r_H which is related to the contribution of matter.

6. Myers-Perry black holes in (4 + *n*) dimensions

A Myers-Perry black hole in (4 + *n*) dimensions is given by [14]

$$ds^2 = -dt^2 + \frac{\Sigma}{\Delta} dr^2 + \Sigma d\theta^2 + (r^2 + a^2)\sin^2\theta d\varphi^2 + \frac{\mu}{r^{n-1}\Sigma}(dt - a\sin^2\theta d\varphi)^2$$
$$+ r^2\cos^2\theta d\Omega_n^2,$$

where

$$\Delta = r^2 + a^2 - \frac{\mu}{r^{n-1}}, \Sigma = r^2 + a^2\cos^2\theta,$$

and $d\Omega_n^2$ is the line-element on the unit n-sphere S^n. We choose coordinates so that

$$d\Omega_n^2 = d\theta_1^2 + \sin^2\theta_1 d\theta_2^2 + \sin^2\theta_1 \sin^2\theta_2 d\theta_3^2 + \ldots + \left(\prod_{i=1}^{n-1} \sin^2\theta_i\right) d\theta_n^2.$$

The black hole mass M_{BH} and the angular momentum J are defined as follows

$$M_{BH} = \frac{(n+2)2\pi^{(n+3)/2}}{16\pi G\Gamma[(n+3)/2]}\mu \text{ and } J = \frac{2a}{n+2} M_{BH}.$$

In this case, the Schrödinger -like equation is given by

$$\frac{d^2 R_{j\ell m}}{dr_*^2} + \left[(\omega - m\varpi)^2 - V_{j\ell m}(r)\right] R_{j\ell m} = 0,$$

where

$$\varpi(r) = \frac{a}{a^2 + r^2}.$$

The tortoise coordinate is given by

$$dr_* = \frac{r^2 + a^2}{\Delta(r)} dr.$$

The potential produced by the Myers-Perry black holes in (4 + n) dimensions is given by

$$V(r) = \frac{\Delta(r)}{\left(r^2 + a^2\right)^2}\left[\lambda_{j\ell m} + \frac{j(j+n-1)a^2}{r^2} + \frac{n(n-2)\Delta(r)}{4r^2} + \frac{n\Delta'(r)}{2r}\right.$$
$$\left. - \frac{3r^2\Delta(r)}{(r^2 + a^2)^2} + \frac{[r\Delta(r)]'}{r^2 + a^2}\right].$$

From equation (8), the bounds on the greybody factors are given by

$$T \geq \begin{cases} \operatorname{sech}^2\left\{\frac{1}{2}\ln(1-m/m_*)+\frac{1}{2r_H\omega}I_{j\ell m}\right\} & \text{for} \quad m \leq 0 \\ \operatorname{sech}^2\left\{-\frac{1}{2}\ln(1-m/m_*)+\frac{1}{2r_H\omega(1-m/m_*)}I_{j\ell m}\right\} & \text{for} \quad 0 \leq m < m_* \\ \operatorname{sech}^2\left\{-\frac{1}{2}\ln(m/m_*-1)+\frac{1}{2r_H\omega(m/m_*-1)}I_{j\ell m}+J_m^{\text{low}}\right\} & \text{for} \quad m_* \leq m < 2m_* \\ \operatorname{sech}^2\left\{\frac{1}{2}\ln(m/m_*-1)+\frac{1}{2r_H\omega}I_{j\ell m}+J_m^{\text{high}}\right\} & \text{for} \quad m \geq 2m_* \end{cases},$$

where r_H is the horizon radius, $m_* = \omega\left(a^2+r_H^2\right)/a$, and

$$\begin{aligned} I_{j\ell m} = {} & \frac{n(2n-3)}{8}+j(j+n-1)+\frac{a^2}{4(r_H^2+a^2)} \\ & +\left[\frac{2n+1}{2}-j(j+n-1)+\lambda_{j\ell m}(a\omega)\right]\frac{r_H}{a}\arctan\frac{a}{r_H} \\ & +\frac{n(r_H^2+a^2)}{8r_H^2}\,{}_2F_1\left(1,\frac{n+2}{2},\frac{n+4}{2},-\frac{a^2}{r_H^2}\right). \end{aligned}$$

The case where $m < m_*$ is called the non-superradiance mode and the case where $m \geq m_*$ is called the superradiance mode. Superradiance is a phenomenon by which the reflected wave is larger in its amplitude than the incident wave. This phenomenon can arise for rotating black holes only, such as the Myers-Perry black hole.

The bound on the greybody factor versus the wave frequency for a spin zero angular momentum mode is plotted for five (n = 1) and six (n = 2) dimensions as shown in Figure 8.

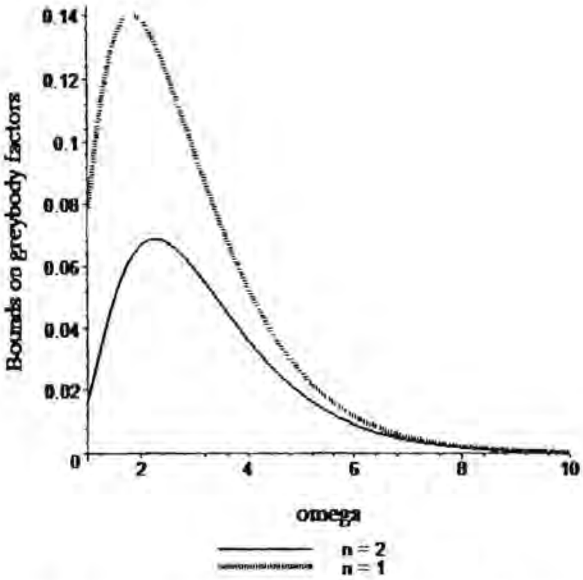

Figure 8. Dependence of the bound on the greybody factor on the wave frequency in five (n = 1) and six (n = 2) dimensions

The graph shows that when the wave frequency increases, the bounds on the greybody factors increase to their maximum and then decrease. Moreover, the bound on the greybody factor is lower in higher dimensions.

The bound on the greybody factor versus the angular momentum of the Myers-Perry black hole is plotted as shown in Figure 9.

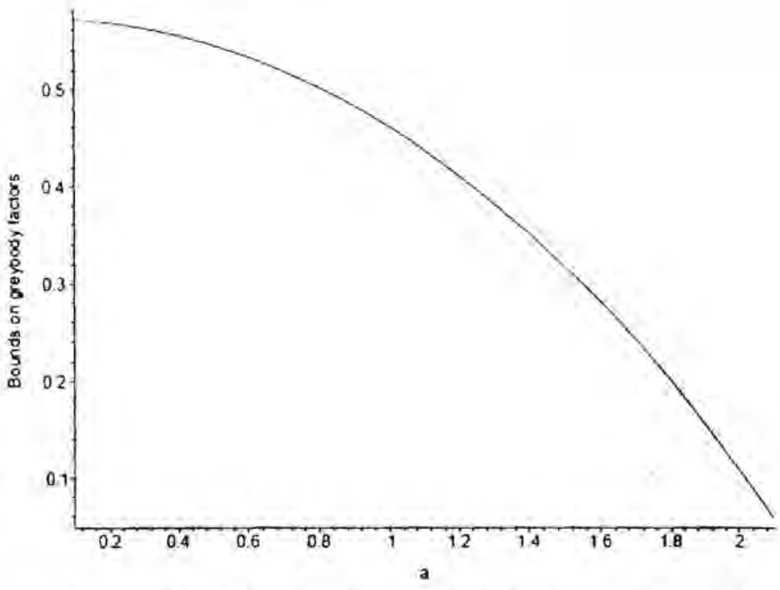

Figure 9. Dependence of the bound on the greybody factor on the angular momentum.

The graph shows that the bound on the greybody factor decreases as the angular momentum of the black hole increases.

References

[1] T. Ngampitipan and P. Boonserm, Int. J. Mod. Phys. D 22 (2013) 9, arXiv:1211.4070 [math-ph].

[2] R. Sini and V. C. Kuriakose, Int. J. Mod. Phys. D 18 (2009) 1, arXiv:0708.3146 [gr-qc].

[3] S. Chen and J. Jing, Phys. Lett. B 691 (2010) 254, arXiv:1005.5601 [gr-qc].

[4] C. Ding, C. Liu, J. Jing and S. Chen, J. High Energy Phys. 11 (2010) 146, arXiv:1007.4240 [gr-qc].

[5] K. Lin and S. Z. Yang, Astrophys. Space Sci. 333 (2011) 369.

[6] K. D. Kokkotas and R. A. Konoplya, Phys. Rev. D 83 (2011) 024031, arXiv:1011.1843 [gr-qc].

[7] L. Yan and J. J. Liang, Chin. Phys. Lett. 29 (2012) 010402.

[8] A. Neitzke, Greybody factors at large imaginary frequencies, arXiv:hep-th/0304080.

[9] K. Nozari and B. Fazlpour, Acta Phys. Pol. B 39 (2008) 1363.

[10] Z. Zhai and W. Liu, Astrophys. Space Sci. 325 (2010) 63.

[11] P. Nicolini and E. Winstanley, J. High Energy Phys. 11 (2011) 75, arXiv:1108.4419 [hep-ph].

[12] S. Fernando, Gen. Relativ. Gravit. 37 (2005) 461.

[13] P. Boonserm, T. Ngampitipan, and M. Visser, Phys. Rev. D 88 (2013) 041502(R) arXiv:1305.1416 [gr-qc].

[14] P. Boonserm, A. Chatrabhuti, T. Ngampitipan, and M. Visser, J. Math. Phys. 55 (2014) 112502 arXiv:1405.5678 [gr-qc].

[15] S. Caroll, Spacetime and geometry: An introduction to general relativity, Addison-Wesley 2004.

[16] P. Boonserm and M. Visser, Ann. Phys. 323 (2008) 2779-2798 arXiv:0801.0610 [quant-ph].

สรุปและวิจารณ์ผลการทดลอง

In this project, we obtain valuable knowledge from developing mathematical techniques to calculate the rigorous bounds on the greybody factors. These bounds are derived for the four-dimensional Reissner - Nordström black holes, the higher dimensional Schwarzschild - Tangherlini black holes, the charged dilatonic black holes in (2 + 1) dimensions, the charged dilatonic black holes in (3 + 1) dimensions, the dirty black holes, and the Myers-Perry black holes. We gain understanding of the key factors that affect the greybody factors. These key factors are summarized as follows;

For the Reissner-Nordström black holes, when the magnitude of the charges increases, the bound on the greybody factor decreases. That is, the charges are an effective barrier in resisting the tunneling of uncharged scalar particles.

For the *d*-dimensional Schwarzschild - Tangherlini black holes, the bound on the greybody factor is lesser in higher dimensions.

For the charged dilatonic black holes in (2 + 1) dimensions, when the charges increase, the bound on the greybody factor decreases. This result is similar to the Reissner-Nordström black hole's result; that is, the charges behave as an effective barrier in resisting the tunneling of uncharged scalar particles. Moreover, when the value of the cosmological constant increases, the bound on the greybody factor increases as well. That is, the cosmological constant renders the gravitational potential produced by the black hole transparent.

For charged dilatonic black holes in (3 + 1) dimensions, when the charges increase, the bound on the greybody factor decreases. This result is also similar to the Reissner-Nordström black hole's and the (2 + 1) dimensional charged dilatonic black hole's result. That is, the charges behave as an effective barrier in resisting the tunneling of the uncharged scalar particles.

For dirty black holes, the bound on the greybody factor depends on the frequency wave, the angular momentum, the spin, and the horizon radius which is related to the contribution of matter. Choosing the appropriate functions $\phi(r)$ and $m(r)$ can generate considerably more specific results.

For the Myers-Perry black holes in (4 + *n*) dimensions, we have established certain rigorous bounds on the greybody factors (mode dependent transmission probabilities). There are possibilities for the emergence of superradiance. Superradiance is a phenomenon by which the reflected wave is larger in its amplitude than the incident wave. The condition under which superradiance occurs entails the wave frequency being lesser than the rotation rate of a given black hole. We have also obtained (mutatis mutandis) certain rigorous bounds on the emission rates for the superradiant modes. In the absence of exact results, (the relevant differential equations seem highly resistant to explicit analytic solution), quantitative bounds along these lines seem to be the best attainable solutions.

Output จากโครงการวิจัยที่ได้รับทุนจาก สกว.

1. ผลงานตีพิมพ์ในวารสารวิชาการนานาชาติ (ระบุชื่อผู้แต่ง ชื่อเรื่อง ชื่อวารสาร ปี เล่มที่ เลขที่ และหน้า) หรือผลงานตามที่คาดไว้ในสัญญาโครงการ

   ผลงานตีพิมพ์ในวารสารวิชาการนานาชาติจำนวน 6 ฉบับ

   1) Petarpa Boonserm, Auttakit Chatrabhuti, Tritos Ngampitipan, and Matt Visser, "Greybody factors for Myers-Perry black holes" Journal of Mathematical Physics 2014 (55) 112502

   Impact factor: 1.296

   2) Petarpa Boonserm, Tritos Ngampitipan, and Matt Visser, "Superradiance and flux conservation" Physical Review D 2014 (90) 064013

   Impact factor: 4.864

   3) Petarpa Boonserm, Tritos Ngampitipan, and Matt Visser, "Bounding the greybody factors for scalar field excitations on the Kerr-Newman spacetime" Journal of High Energy Physics 2014 (03) 113

   Impact factor: 5.618

   4) Petarpa Boonserm and Matt Visser, "Bounds on variable-length compound jumps" Journal of Mathematical Physics 2013 (54) 092105

   Impact factor: 1.296

   5) Petarpa Boonserm, Tritos Ngampitipan, and Matt Visser, "Regge-Wheeler equation, linear stability, and greybody factors for dirty black holes" Physical Review D 2013 (88) 041502(R)

   Impact factor: 4.558

   6) Tritos Ngampitipan and Petarpa Boonserm, "Bounding the greybody factors for non-rotating black holes" International Journal of Modern Physics D 2013 (22) 1350058

   Impact factor: 1.046

2. การนำผลงานวิจัยไปใช้ประโยชน์
   - เชิงวิชาการ (มีการพัฒนาการเรียนการสอน/สร้างนักวิจัยใหม่)

     - จัดตั้งกลุ่มวิจัย Gravity group ซึ่งทำการวิจัยหัวข้อต่าง ๆ ทางด้านทฤษฎีสัมพัทธภาพทั่วไป หลุมดำ กลศาสตร์ควอนตัม สมการเชิงอนุพันธ์

5) Tritos Ngampitipan and Petarpa Boonserm, "Transmission probability for charged dilatonic black holes in various dimensions" JPS Conference Proceedings 2014 (1) 013100

Publications

AIP Journal of Mathematical Physics

Bounds on variable-length compound jumps

Petarpa Boonserm and Matt Visser

Citation: J. Math. Phys. **54**, 092105 (2013); doi: 10.1063/1.4820146
View online: http://dx.doi.org/10.1063/1.4820146
View Table of Contents: http://jmp.aip.org/resource/1/JMAPAQ/v54/i9
Published by the AIP Publishing LLC.

JOURNAL OF MATHEMATICAL PHYSICS 54, 092105 (2013)

Bounds on variable-length compound jumps

Petarpa Boonserm[1,a] and Matt Visser[2,b]
[1]*Department of Mathematics and Computer Science, Faculty of Science, Chulalongkorn University, Phayathai Road, Pathumwan, Bangkok 10330, Thailand*
[2]*School of Mathematics, Statistics, and Operations Research, Victoria University of Wellington, PO Box 600, Wellington 6140, New Zealand*

(Received 7 February 2013; accepted 20 August 2013; published online 9 September 2013)

In Euclidean space there is a trivial upper bound on the maximum length of a compound "walk" built up of variable-length jumps, and a considerably less trivial lower bound on its *minimum* length. The existence of this non-trivial lower bound is intimately connected to the triangle inequalities, and the more general "polygon inequalities." Moving beyond Euclidean space, when a modified version of these bounds is applied in "rapidity space" they provide upper and lower bounds on the relativistic composition of velocities. Similarly, when applied to "transfer matrices" these bounds place constraints either (in a scattering context) on transmission and reflection coefficients or (in a parametric excitation context) on particle production. Physically these are very different contexts, but mathematically there are intimate relations between these superficially very distinct systems. © *2013 AIP Publishing LLC*. [http://dx.doi.org/10.1063/1.4820146]

I. BACKGROUND

One is often confronted with physical or mathematical situations where some complicated process can be built up by compounding (that is, chaining together) a number of simpler but not necessarily equal individual steps. Examples (by no means an exhaustive list) include compounding a series of variable-length jumps in physical space, the relativistic composition of multiple velocities, and the composition of transfer matrices for scattering from multiple distinct (non-overlapping) barriers.

An interesting and pragmatically useful question is whether information concerning the individual steps can be used to place useful bounds on the overall compound process. Herein, we present examples of several such phenomena. From a purely technical perspective, this discussion is largely based on the analysis of compound scattering processes presented in Ref. 1, but the applications will be completely different:

1. There is a simplification of the upper and lower bounds of that article to variable-length compound jumps in ordinary Euclidean physical space.
2. There is a modification of the upper and lower bounds of that article to the special relativistic composition of velocities.

Mathematically, the intimate relationship between the Euclidean translations, special relativistic boosts, and quantum scattering is due to the fact that both the Lorentz group and group of transfer matrices are Lie groups, with closely related though not identical Lie algebras. Specifically, the Lorentz group can be represented by $SO(3, 1)$, which is locally isomorphic to $SL(2, \mathbb{C})$, whereas the set of transfer matrices form a representation of $SU(1, 1)$, which is locally isomorphic to $SL(2, \mathbb{R})$. See, for example, the recent review article[2] and references therein. (For other relevant background

[a]petarpa.boonserm@gmail.com
[b]matt.visser@msor.vuw.ac.nz

material see, for instance, Refs. 3–8 on composition of velocities in special relativity and Refs. 9–18 on quantum scattering.)

It is the structural similarity between the Lie algebras of $SL(2, \mathbb{C})$ and $SL(2, \mathbb{R})$, and the relation between velocities and rapidities, versus the relation between transmission probabilities and Bogoliubov coefficients, that underlies the close mathematical similarities between Euclidean translations, relativistic composition of velocities, and the compounding of transfer matrices. For instance, an arbitrary boost can always, up to a three-dimensional rotation R, be written as

$$\mathcal{B} = R \exp\left(\xi \begin{bmatrix} 0 & 1 & 0 & 0 \\ 1 & 0 & 0 & 0 \\ 0 & 0 & 0 & 0 \\ 0 & 0 & 0 & 0 \end{bmatrix}\right) R^{-1}, \tag{1}$$

with the speed being related to the rapidity by $v = \tanh \xi$. In counterpoint, an arbitrary transfer matrix can always be written in the form[1]

$$\mathcal{T} = \begin{bmatrix} \alpha & \beta^* \\ \beta & \alpha^* \end{bmatrix} = \begin{bmatrix} \cosh\Theta\, e^{i\phi} & \sinh\Theta\, e^{-i\psi} \\ \sinh\Theta\, e^{i\psi} & \cosh\Theta\, e^{-i\phi} \end{bmatrix}. \tag{2}$$

It is then easy to see that

$$\mathcal{T} = \begin{bmatrix} e^{i(\phi-\psi)/2} & 0 \\ 0 & e^{-i(\phi-\psi)/2} \end{bmatrix} \exp\left(\Theta \begin{bmatrix} 0 & 1 \\ 1 & 0 \end{bmatrix}\right) \begin{bmatrix} e^{i(\phi+\psi)/2} & 0 \\ 0 & e^{-i(\phi+\psi)/2} \end{bmatrix}, \tag{3}$$

with the reflection probability being given by $\sqrt{R} = |r| = \tanh\Theta$. (See, for instance, Ref. 1) Furthermore, the appropriate subspaces of the Lie algebras of both of these Lie groups can be mapped homeomorphically (and even monotonically) to the Euclidean translations, which ultimately underlies the close connection to compound jumps in ordinary Euclidean space. Indeed, working with the Euclidean space formulation in some sense "trivializes" the bounds and makes clear the close connection between the lower bound and the triangle inequalities (or more generally the polygon inequalities).

II. VARIABLE LENGTH RANDOM WALKS IN PHYSICAL SPACE

Suppose we have a compound "walk" in physical where the individual step sizes ("jumps") are fixed but variable, $\ell_1, \ell_2, \ell_3, \ldots, \ell_n$, but the directions $\mathbf{n}_i$ are arbitrary. What if anything can we say about upper and lower bounds on the net displacement

$$\mathbf{x}_{12\cdots n} = \sum_{i=i}^{n} \mathbf{n}_i\, \ell_i ?. \tag{4}$$

Consider the two step case

$$\mathbf{x}_{12} = \mathbf{n}_1\, \ell_1 + \mathbf{n}_2\, \ell_2, \tag{5}$$

then it is elementary that

$$|\ell_1 - \ell_2| \leq |\mathbf{x}_{12}| \leq \ell_1 + \ell_2. \tag{6}$$

Furthermore, it is also clear that for n steps

$$|\mathbf{x}_{12\cdots n}| \leq M_{12\cdots n} \equiv \sum_{i=1}^{n} \ell_i. \tag{7}$$

But can one place a *lower bound* on $|\mathbf{x}_{12\cdots n}|$? Yes, by a straightforward modification (and simplification) of the analysis of Ref. 1, for a three-step walk we assert (and shall soon prove)

$$|\mathbf{x}_{123}| \geq \max\{\ell_1 - \ell_2 - \ell_3,\ \ \ell_2 - \ell_3 - \ell_1,\ \ \ell_3 - \ell_1 - \ell_2,\ \ 0\}. \tag{8}$$

More generally, for an n-step walk we assert (and shall soon prove)

$$|\mathbf{x}_{12\cdots n}| \geq \max\left\{\ell_i - \sum_{j\neq i}\ell_j,\ \ 0\right\}, \tag{9}$$

or equivalently

$$|\mathbf{x}_{12\cdots n}| \geq \max\left\{2\ell_i - \sum_{j=1}^{n}\ell_j,\ \ 0\right\}. \tag{10}$$

We can also write this as

$$|\mathbf{x}_{12\cdots n}| \geq m_{12\cdots n} \equiv \max\{2\ell_i - M_{12\cdots n},\ \ 0\}. \tag{11}$$

(So, as is reasonably common notation, we use M to denote the maximum, and m to denote the minimum.)

III. TRIANGLE AND POLYGON INEQUALITIES

To first see *why* these lower bounds have any hope of working, it is useful to consider the triangle inequalities.

A. 3 steps

A key observation is this: *The 3-step lower bound is non-trivial if and only if the three step-lengths, ℓ_1, ℓ_2, and ℓ_3, violate the triangle inequalities.* To see this, recall that for a three-step compound walk in physical space we asserted

$$|\mathbf{x}_{123}| \geq \max\{\ell_1 - \ell_2 - \ell_3, \ell_2 - \ell_3 - \ell_1, \ell_3 - \ell_1 - \ell_2, 0\}. \tag{12}$$

Why this odd combination? This is related to the triangle inequalities in a quite elementary manner. If ℓ_1, ℓ_2, and ℓ_3 are the lengths of the sides of a physical triangle in Euclidean space, then they must satisfy the triangle inequalities: The length of any one side of the triangle must be less than or equal to the sum of the lengths of the other two sides. That is,

$$\ell_1 \leq \ell_2 + \ell_3; \qquad \ell_2 \leq \ell_3 + \ell_1; \qquad \ell_3 \leq \ell_1 + \ell_2. \tag{13}$$

This implies

$$\ell_1 - \ell_2 - \ell_3 \leq 0; \qquad \ell_2 - \ell_3 - \ell_1 \leq 0; \qquad \ell_3 - \ell_1 - \ell_2 \leq 0. \tag{14}$$

Therefore, in this situation

$$\max\{\ell_1 - \ell_2 - \ell_3, \ell_2 - \ell_3 - \ell_1, \ell_3 - \ell_1 - \ell_2, 0\} = 0. \tag{15}$$

That is, *if* the quantities ℓ_1, ℓ_2, and ℓ_3 are the lengths of the sides of a physical triangle in Euclidean space, *then* there is no constraint on $|\mathbf{x}_{123}|$ apart from the trivial one: $|\mathbf{x}_{123}| \geq 0$. Therefore, the lower bound on $|\mathbf{x}_{123}|$ is *non-trivial* if and only if ℓ_1, ℓ_2, and ℓ_3 *cannot* be interpreted as the lengths of the sides of a physical triangle in Euclidean space. Furthermore, if the triangle inequalities are violated, then the non-trivial lower bound specifies the extent to which the 3 edges of the "would-be triangle" *fail to close*.

B. n steps

Generalizing the above observation: *For n steps the lower bound is non-trivial if and only if the polygon inequalities are violated.* To see this, observe that for an n-step random walk the lengths ℓ_i can be interpreted as the physical lengths of an n-sided polygon if and only if all n polygon inequalities are satisfied

$$\forall i \qquad \ell_i \leq \sum_{j\neq i} \ell_j. \tag{16}$$

These polygon inequalities are the natural generalization of the triangle inequalities. They can be built up iteratively by subdividing any polygon into triangles, and then applying the triangle inequalities step-by-step. That is,

$$\forall i \qquad \ell_i - \sum_{j\neq i} \ell_j \leq 0. \tag{17}$$

But then

$$\max\left\{\ell_i - \sum_{j\neq i} \ell_j, 0\right\} = 0. \tag{18}$$

So if the lengths ℓ_i can be interpreted as the physical lengths of an n-sided polygon, then there is no constraint on $|\mathbf{x}_{12\cdots n}|$ apart from the trivial one: $|\mathbf{x}_{12\cdots n}| \geq 0$. Therefore, the lower bound on $|\mathbf{x}_{12\cdots n}|$ is *non-trivial* if and only if the ℓ_i *cannot* be interpreted as the lengths of the sides of a physical n-sided polygon in Euclidean space. Furthermore, if the polygon inequalities are violated, then the non-trivial lower bound specifies the extent to which the n edges of the "would-be polygon" *fail to close*.

These observations, though mathematically rather straightforward, and possibly even trivial, make it much clearer *why* the lower bounds take the form they do, why there is any realistic hope of obtaining any non-trivial lower bound, and also why there is no realistic hope of a lower bound more stringent than the one we have enunciated.

IV. PROOF OF THE LOWER BOUND

Start by defining the sums ($j \in \{1, 2, 3, \ldots, n\}$),

$$M_{123\cdots j} = \sum_{i=1}^{j} \ell_i. \tag{19}$$

Then it is elementary that

$$|\mathbf{x}_{123\cdots j}| \leq M_{123\cdots j} \tag{20}$$

for all $j \in \{1, 2, 3, \ldots, n\}$.

A. Iterative version of the lower bound

Now take

$$m_1 = \ell_1, \tag{21}$$

and, for $j \in \{1, 2, 3, \ldots, n-1\}$, iteratively define the quantities $m_{123\cdots(j+1)}$ by

$$m_{123\cdots(j+1)} = (\ell_{j+1} - M_{123\cdots j})\, H(\ell_{j+1} - M_{123\cdots j}) + (m_{123\cdots j} - \ell_{j+1})\, H(m_{123\cdots j} - \ell_{j+1}), \tag{22}$$

where $H(\cdot)$ is the Heaviside step function. We can equivalently re-write this iterative definition as

$$m_{123\cdots(j+1)} = \max\left\{\ell_{j+1} - M_{123\cdots j}, m_{123\cdots j} - \ell_{j+1}, 0\right\}. \tag{23}$$

Theorem: By iterating the 2-step bounds, one has

$$\forall n: \qquad m_{123\cdots n} \leq |\mathbf{x}_{12\cdots n}| \leq M_{123\cdots n}. \tag{24}$$

Proof by Induction: When we iterate the definitions for $M_{123\cdots j}$ and $m_{123\cdots j}$, then the first two times we obtain

$$M_1 = \ell_1; \qquad m_1 = \ell_1; \tag{25}$$

$$M_{12} = \ell_1 + \ell_2; \qquad m_{12} = |\ell_1 - \ell_2|. \tag{26}$$

Thus the claimed theorem is certainly true for $n = 2$. Now apply mathematical induction: Assume that at each stage the interval $[m_{123\cdots j}, M_{123\cdots j}]$ characterizes the highest possible and lowest possible values of $|\mathbf{x}_{12\cdots j}|$. Applying the 2-step bound to the pair $|\mathbf{x}_{12\cdots j}|$ and ℓ_{j+1} leads trivially to $|\mathbf{x}_{12\cdots(j+1)}|$ being bounded from above by

$$M_{123\cdots(j+1)} = M_{123\cdots j} + \ell_{j+1}, \tag{27}$$

and less trivially to being bounded from below by

$$m_{123\cdots(j+1)} = \max\left\{\ell_{j+1} - M_{123\ldots j}, m_{123\cdots j} - \ell_{j+1}, 0\right\}. \tag{28}$$

This completes the inductive step. That is,

$$|\mathbf{x}_{12\ldots(j+1)}| \in [m_{123\cdots(j+1)}, M_{123\cdots(j+1)}], \tag{29}$$

as claimed.

However, these bounds are currently defined in a relatively messy iterative manner. Can this be usefully simplified? Can we make the bounds explicit?

B. Symmetry properties for the lower bound

When we iterate the definitions of $M_{123\cdots j}$ and $m_{123\cdots j}$, a third time we see

$$M_{123} = \ell_1 + \ell_2 + \ell_3; \qquad m_{123} = \max\{\ell_3 - (\ell_1 + \ell_2), |\ell_1 - \ell_2| - \ell_3, 0\}. \tag{30}$$

We can further simplify this by rewriting m_{123} as

$$m_{123} = \max\{\ell_1 - \ell_2 - \ell_3,\ \ell_2 - \ell_3 - \ell_1,\ \ell_3 - \ell_1 - \ell_2,\ 0\}. \tag{31}$$

Note that this form of m_{123} is manifestly symmetric under arbitrary permutations of the labels 123. One suspects that there is a good reason for this. In fact there is.

Theorem: The quantity $m_{123\cdots j}(\ell_i)$ is a totally symmetric function of the j parameters ℓ_i, where $i \in \{1, 2, 3, \cdots, j\}$.

Proof: By inspection the result is true for m_1, m_{12}, and m_{123}. But this argument now generalizes. In fact, the easiest way of completing the argument is to provide an explicit formula, which we shall do in Sec. IV C.

C. Non-iterative formula for the lower bound

Theorem:

$$\forall n : m_{123\cdots n} = \max_{i\in\{1,2,\ldots n\}} \{2\ell_i - M_{123\cdots n}, 0\} = \max_{i\in\{1,2,\ldots n\}} \left\{\ell_i - \sum_{k=1,k\neq i}^{n} \ell_k, 0\right\}. \tag{32}$$

Proof by Induction: We have already seen that the iterative definition of $m_{123\cdots j}$ can be written as

$$m_{123\cdots(j+1)} = \max\{\ell_{j+1} - M_{123\cdots j}, m_{123\cdots j} - \ell_{j+1}, 0\}, \tag{33}$$

which we can also rewrite as

$$m_{123\cdots(j+1)} = \max\{2\ell_{j+1} - M_{123\cdots(j+1)}, m_{123\cdots j} - \ell_{j+1}, 0\}. \tag{34}$$

Now apply induction. The assertion of the theorem is certainly true for $n = 1$ and $n = 2$, and has even been explicitly verified for $n = 3$. Now assume it holds up to some j, then

$$\begin{aligned} m_{123\cdots(j+1)} &= \max\{2\ell_{j+1} - M_{123\cdots(j+1)}, m_{123\cdots j} - \ell_{j+1}, 0\} \\ &= \max\left\{2\ell_{j+1} - M_{123\cdots(j+1)}, \max_{i\in\{1,2,\ldots j\}}\{2\ell_i - M_{123\cdots j}, 0\} - \ell_{j+1}, 0\right\} \\ &= \max\left\{2\ell_{j+1} - M_{123\cdots(j+1)}, \max_{i\in\{1,2,\ldots j\}}\{2\ell_i - M_{123\cdots(j+1)}, 0\}, 0\right\} \\ &= \max_{i\in\{1,2,\ldots,j,(j+1)\}}\{2\ell_i - M_{123\cdots(j+1)}, 0\}. \end{aligned} \tag{35}$$

This proves the inductive step. Consequently,

$$\forall n: \quad m_{123\cdots n} = \max_{i\in\{1,2,\ldots n\}}\{2\ell_i - M_{123\cdots n}, 0\}, \tag{36}$$

as claimed.

To simplify the formalism even further, let us now define

$$\ell_{\text{peak}} = \max_{i\in\{1,2,\ldots n\}} \ell_i. \tag{37}$$

(We shall use the subscript "peak" for the maximum of the individual ℓ_i's; the words "max" and "min" will be reserved for bounds on the n-fold composition of the ℓ_i.) Then we can simply write

$$\forall n: \quad m_{123\cdots n} = \max\{2\ell_{\text{peak}} - M_{123\cdots n}, 0\}. \tag{38}$$

This is perhaps the simplest way of presenting the lower bound.

V. RELATIVISTIC COMPOSITION OF VELOCITIES

Let us now apply the Euclidean space result derived above to a more subtle situation; the relativistic composition of velocities. (For general background see Refs. 3–8.)

A. Collinear velocities

When it comes to the relativistic composition of velocities the key thing is to note that for a pair of collinear (parallel or anti-parallel) velocities we have

$$v_{12} = \frac{v_1 + v_2}{1 + v_1 v_2}, \tag{39}$$

which implies

$$\frac{|\,|v_1| - |v_2|\,|}{1 - |v_1||v_2|} \leq |v_{12}| \leq \frac{|v_1| + |v_2|}{1 + |v_1||v_2|}. \tag{40}$$

If we work with the (non-negative) rapidities ζ_i defined by

$$|v_i| = \tanh \zeta_i, \tag{41}$$

then

$$\tanh|\zeta_1 - \zeta_2| \leq |v_{12}| \leq \tanh(\zeta_1 + \zeta_2). \tag{42}$$

That is

$$\tanh|\zeta_1 - \zeta_2| \leq \tanh(\zeta_{12}) \leq \tanh(\zeta_1 + \zeta_2), \tag{43}$$

which implies

$$|\zeta_1 - \zeta_2| \leq \zeta_{12} \leq \zeta_1 + \zeta_2. \tag{44}$$

It is this version that is closest in spirit to the Euclidean result, and this version that is more likely to lead to a suitable constraint on the composition of n relative velocities. We could also write the 2-velocity constraint as

$$\tanh\left|\tanh^{-1}|v_1| - \tanh^{-1}|v_2|\right| \leq |v_{12}| \leq \tanh\left(\tanh^{-1}|v_1| + \tanh^{-1}|v_2|\right). \tag{45}$$

B. Non-collinear velocities

If the velocities are *not collinear*, there is a more complicated rule for combining velocities

$$\vec{v}_{12} = \vec{v}_1 \oplus \vec{v}_2. \tag{46}$$

Fortunately, we will not need to be explicit about the details. (For more details see, for instance, almost any medium-level technical book on special relativity,[3,4] or for example, Refs. 5–8.) If we further define a rapidity *vector*

$$\vec{\zeta} = \left\{\tanh^{-1}|v|\right\}\ \hat{v}, \tag{47}$$

there will be an analogous vectorial composition rule in rapidity space

$$\vec{\zeta}_{12} = \vec{\zeta}_1 \boxplus \vec{\zeta}_2. \tag{48}$$

Fortunately, we do not need the full power of the non-collinear composition rule, we only need to know the simple result obtained by looking at the extreme case of collinear (parallel/anti-parallel) motion

$$\left| |\vec{\zeta}_1| - |\vec{\zeta}_2| \right| \leq |\vec{\zeta}_1 \boxplus \vec{\zeta}_2| \leq |\vec{\zeta}_1| + |\vec{\zeta}_2|. \tag{49}$$

That is,

$$\left| |\vec{\zeta}_1| - |\vec{\zeta}_2| \right| \leq |\vec{\zeta}_{12}| \leq |\vec{\zeta}_1| + |\vec{\zeta}_2|. \tag{50}$$

So even for non-collinear motion, we still have

$$|\zeta_1 - \zeta_2| \leq \zeta_{12} \leq \zeta_1 + \zeta_2. \tag{51}$$

We can now immediately apply the bound we have already derived for compound walks in physical Euclidean space.

C. Bounds on the composition of velocities

1. Upper bounds

For n velocities the upper bound is straightforward, we just iterate the two-step result to obtain

$$\zeta_{12\cdots n} \leq \sum_{i=1}^{n} \zeta_i, \tag{52}$$

whence

$$|v_{12\cdots n}| \leq \tanh\left[\sum_{i=1}^{n} \zeta_i\right]. \tag{53}$$

We can also write this as

$$|v_{12\cdots n}| \leq \tanh\left[\sum_{i=1}^{n} \tanh^{-1}|v_i|\right]. \tag{54}$$

Here are some explicit special cases obtained by straightforward manipulation of hyperbolic trig identities. Relativistically combining three velocities, one has

$$|v_{123}| \leq \frac{|v_1| + |v_2| + |v_3| + |v_1||v_2||v_3|}{1 + |v_1||v_2| + |v_2||v_3| + |v_3||v_1|}. \tag{55}$$

Similarly, relativistically combining four velocities, one has

$$|v_{1234}| \leq \frac{|v_1| + |v_2| + |v_3| + |v_4| + |v_1||v_2||v_3| + |v_2||v_3||v_4| + |v_3||v_4||v_1| + |v_4||v_1||v_2|}{1 + |v_1||v_2| + |v_2||v_3| + |v_3||v_4| + |v_4||v_1| + |v_1||v_3| + |v_2||v_4| + |v_1||v_2||v_3||v_4|}. \tag{56}$$

If one additionally knows that all velocities are collinear, then instead of bounds one has the related *equalities*

$$v_{123} = \frac{v_1 + v_2 + v_3 + v_1 v_2 v_3}{1 + v_1 v_2 + v_2 v_3 + v_3 v_1} \tag{57}$$

and

$$v_{1234} = \frac{v_1 + v_2 + v_3 + v_4 + v_1 v_2 v_3 + v_2 v_3 v_4 + v_3 v_4 v_1 + v_4 v_1 v_2}{1 + v_1 v_2 + v_2 v_3 + v_3 v_4 + v_4 v_1 + v_1 v_3 + v_2 v_4 + v_1 v_2 v_3 v_4}. \tag{58}$$

(There does not seem to be any more pleasant reformulation of these results, and in the completely general n-velocity case the general the "tanh" formula above seems to be the best one can do.)

2. Lower bounds

Obtaining an explicit lower bound is again a lot trickier than the upper bound. When relativistically combining three velocities then, (because of the monotonicity of the tanh function), one has

$$|v_{123}| \geq \tanh\left[\max\{\zeta_1 - \zeta_2 - \zeta_3,\ \zeta_2 - \zeta_3 - \zeta_1,\ \zeta_3 - \zeta_1 - \zeta_2,\ 0\}\right]. \tag{59}$$

When relativistically combining n velocities the best one can do is this

$$|v_{12\cdots n}| \geq \tanh\left[\max\left\{\zeta_i - \sum_{j\neq i}\zeta_j,\ 0\right\}\right]. \tag{60}$$

We can also write this as

$$|v_{12\cdots n}| \geq \tanh\left[\max\left\{2\zeta_i - \sum_{j=1}^{n}\zeta_j,\ 0\right\}\right]. \tag{61}$$

Now defining

$$M_{12\cdots n} \equiv \tanh\left[\sum_{j=1}^{n}\zeta_j\right], \tag{62}$$

and

$$v_{\text{peak}} = \max_i\{|v_i|\}, \tag{63}$$

and setting

$$m_{12\cdots n} \equiv \tanh\left[\max\left\{2\tanh^{-1} v_{\text{peak}} - \tanh^{-1} M_{12\cdots n},\ 0\right\}\right], \tag{64}$$

we can also write this as

$$m_{12\cdots n} \leq |v_{12\cdots n}| \leq M_{12\cdots n}. \tag{65}$$

So there certainly are quite non-trivial constraints, one can place on the relativistic combination of velocities, but they are a little less obvious than one might at first suspect.

VI. SCATTERING

Compound scattering processes were extensively discussed in Ref. 1. (For additional background see Refs. 2, 12–18; for various explicit bounds on transmission and reflection probabilities for scattering processes see Refs. 19–27; for a survey of exact results see Ref. 28.) Rather than unnecessarily repeating the results of Ref. 1, we shall herein content ourselves with a few explicit comments regarding 2-barrier, 3-barrier, and 4-barrier systems. The key point is that for the transfer matrix as represented in Eqs. (2) and (3) the reflection probability is $\sqrt{R} = \tanh(\Theta)$, and that composing transfer matrices corresponds to composing Euclidean jumps of length $|\Theta|$, see Ref. 1.

Specifically, for two non-overlapping barriers the transmission and reflection probabilities are bounded by

$$\frac{T_1 T_2}{\left\{1+\sqrt{1-T_1}\sqrt{1-T_2}\right\}^2} \leq T_{12} \leq \frac{T_1 T_2}{\left\{1-\sqrt{1-T_1}\sqrt{1-T_2}\right\}^2} \tag{66}$$

and

$$\left\{\frac{\sqrt{R_1}-\sqrt{R_2}}{1-\sqrt{R_1}\sqrt{R_2}}\right\}^2 \leq R_{12} \leq \left\{\frac{\sqrt{R_1}+\sqrt{R_2}}{1+\sqrt{R_1}\sqrt{R_2}}\right\}^2. \tag{67}$$

For three non-overlapping barriers, the results of Ref. 1, combined with a little work using hyperbolic trigonometric identities, lead to

$$T_{123} \geq \frac{T_1 T_2 T_3}{\left\{1+\sqrt{(1-T_2)(1-T_3)}+\sqrt{(1-T_3)(1-T_1)}+\sqrt{(1-T_1)(1-T_2)}\right\}^2} \tag{68}$$

and

$$R_{123} \leq \left\{\frac{\sqrt{R_1R_2R_3}+\sqrt{R_1}+\sqrt{R_2}+\sqrt{R_3}}{1+\sqrt{R_2R_3}+\sqrt{R_3R_1}+\sqrt{R_1R_2}}\right\}^2. \tag{69}$$

For four non-overlapping barriers, a completely analogous calculation straightforwardly yields

$$T_{1234} \geq \frac{T_1T_2T_3T_4}{\left\{1+\sum_{i<j}\sqrt{(1-T_i)(1-T_j)}+\sqrt{(1-T_1)(1-T_2)(1-T_3)(1-T_4)}\right\}^2} \tag{70}$$

and

$$R_{1234} \leq \left\{\frac{\sqrt{R_1}+\sqrt{R_2R_3R_4}+\text{(cyclic permutations)}}{1+\sum_{i<j}\sqrt{R_iR_j}+\sqrt{R_1R_2R_3R_4}}\right\}^2. \tag{71}$$

That is, explicitly,

$$R_{1234} \leq \tag{72}$$
$$\left\{\frac{\sqrt{R_1}+\sqrt{R_2}+\sqrt{R_3}+\sqrt{R_4}+\sqrt{R_2R_3R_4}+\sqrt{R_3R_4R_1}+\sqrt{R_4R_1R_2}+\sqrt{R_1R_2R_3}}{1+\sum_{i<j}\sqrt{R_iR_j}+\sqrt{R_1R_2R_3R_4}}\right\}^2.$$

Upper bounds on T, and lower bounds on R, are less algebraically tractable, (at least in explicit closed form), and we refer the reader to Ref. 1 for more details.

VII. PARAMETRIC EXCITATIONS

By working in the temporal rather than spatial domain, particle scattering processes can be re-phrased in terms of particle production via parametric excitation. (See Ref. 1 for details). In this context, the net particle production due to two non-overlapping excitation events is bounded by

$$\left\{\sqrt{N_1(N_2+1)}-\sqrt{N_2(N_1+1)}\right\}^2 \leq N_{12} \leq \left\{\sqrt{N_1(N_2+1)}+\sqrt{N_2(N_1+1)}\right\}^2. \tag{73}$$

For three non-overlapping excitation events, one obtains

$$N_{123} \leq \left\{\sqrt{N_1(1+N_2)(1+N_3)} + \sqrt{N_2(1+N_3)(1+N_1)} + \sqrt{N_3(1+N_1)(1+N_2)} + \sqrt{N_1 N_2 N_3}\right\}^2. \tag{74}$$

For four non-overlapping excitation events a straightforward (but rather tedious) calculation yields

$$N_{1234} \leq \left\{\sqrt{N_1(1+N_2)(1+N_3)(1+N_4)} + \sqrt{N_1 N_2 N_3(1+N_4)} + \text{(cyclic permutations)}\right\}^2. \tag{75}$$

Further "explicit" algebraic formulae would be rather unwieldy, and for all practical purposes one is better off using the somewhat less "explicit" formulae in presented terms of hyperbolic functions in Ref. 1. Similarly lower bounds on N are less algebraically tractable, (at least in explicit closed form), and we again refer the reader to Ref. 1 for more details.

VIII. DISCUSSION

That particle scattering in the spatial domain is mathematically intimately related to particle production in the temporal domain is a very standard result, ultimately going back to the relationship between scattering and transmission amplitudes and the Bogoliubov coefficients. (See, for instance, Refs. 1, 2, 13, and 28 for more details on this specific point.) The intimate mathematical relationship between particle scattering and relativistic composition of velocities is less well-known, but is quite standard. The $SO(3, 1)$ Lorentz group is locally isomorphic to $SL(2, \mathbb{C})$, while the group of transfer matrices $SU(1, 1)$ is locally isomorphic to $SL(2, \mathbb{R})$. Ultimately, it is the fact that their Lie algebras are both isomorphic to Euclidean space that ties the three problems (physical Euclidean space, relativistic composition of velocities, and composition of scattering processes) together. The overall result of the current article is to rigorously establish several clearly motivated and robust mathematical bounds on these three closely inter-related physical problems.

ACKNOWLEDGMENTS

M.V. was supported by the Marsden Fund, and by a James Cook fellowship, both administered by the Royal Society of New Zealand. P.B. was supported by a scholarship from the Royal Government of Thailand, and partially supported by a travel grant from FQXi, and by a grant for the professional development of new academic staff from the Ratchadapisek Somphot Fund at Chulalongkorn University, by the Thailand Toray Science Foundation (TTSF), by the Thailand Research Fund (TRF), the Office of the Higher Education Commission (OHEC), Chulalongkorn University (MRG5680171), and by the Research Strategic plan program (A1B1), Faculty of Science, Chulalongkorn University.

[1] P. Boonserm and M. Visser, "Compound transfer matrices: Constructive and destructive interference," J. Math. Phys. 53, 012104 (2012); e-print arXiv:1101.4014 [math-ph].
[2] L. L. Sanchez-Soto, J. J. Monzon, A. G. Barriuso, and J. F. Cariñena, "The transfer matrix: A geometrical perspective," Phys. Rep. 513, 191–227 (2012).
[3] C. Møller, *The Theory of Relativity* (Oxford University Press, London, 1952).
[4] J. D. Jackson, *Classical Electrodynamics*, 3rd ed. (Wiley, New York, 1998).
[5] K. O'Donnell and M. Visser, "Elementary analysis of the special relativistic combination of velocities, Wigner rotation, and Thomas precession," Eur. J. Phys. 32, 1033 (2011); e-print arXiv:1102.2001 [gr-qc].
[6] H. P. Stapp, "Relativistic theory of polarization phenomena," Phys. Rev. 103, 425–434 (1956).
[7] G. P. Fisher, "Thomas precession," Am. J. Phys. 40, 1772 (1972).
[8] M. Ferraro and R. Thibeault, "Generic composition of boosts: An elementary derivation of the Wigner rotation," Eur. J. Phys. 20, 143 (1999).
[9] E. Merzbacher, *Quantum Mechanics* (Wiley, New York, 1965).
[10] P. M. Mathews and K. Venkatesan, *A Textbook of Quantum Mechanics* (McGraw-Hill, New York, 1978).
[11] J. Singh, *Quantum Mechanics: Fundamentals and Applications to Technology* (Wiley, New York, 1997).
[12] L. L. Sanchez-Soto, J. F. Cariñena, A. G. Barriuso, and J. J. Monzon, "Vectorlike representation of one-dimensional scattering," Eur. J. Phys. 26, 469 (2005); e-print arXiv:quant-ph/0411081.

[13] P. Boonserm and M. Visser, "One dimensional scattering problems: A pedagogical presentation of the relationship between reflection and transmission amplitudes," Thai J. Math. **8** (Special Issue), 83–97 (2010).
[14] A. Peres, "Transfer matrices for one-dimensional potentials," J. Math. Phys. **24**, 1110–1119 (1983).
[15] J. M. Kowalski and J. L. Fry, "Tunneling in one-dimensional ideal barriers," J. Math. Phys. **28**, 2407–2415 (1987).
[16] S. Khorasani and A. Adibi, "Analytical solution of linear ordinary differential equations by a differential transfer matrix method," Electron. J. Differ. Equations **2003**, No. 79, 1–18 (2003); http://ejde.math.txstate.edu/Volumes/2003/79/adibi.pdf.
[17] A. G. Barriuso, J. J. Monzon, L. L. Sanchez-Soto, and J. F. Cariñena, "A vectorlike representation of multilayers," J. Opt. Soc. Am. A **21**, 2386–2391 (2004); e-print arXiv:physics/0403140.
[18] A. G. Barriuso, J. J. Monzon, L. L. Sanchez-Soto, and J. F. Cariñena, "Geometrical aspects of first-order optical systems," J. Opt. A, Pure Appl. Opt. **7**, 451–456 (2005); e-print arXiv:physics/0506112 [physics.optics].
[19] M. Visser, "Some general bounds for 1-D scattering," Phys. Rev. A **59**, 427–438 (1999); e-print arXiv:quant-ph/9901030.
[20] P. Boonserm and M. Visser, "Bounding the Bogoliubov coefficients," Ann. Phys. **323**, 2779–2798 (2008); e-print arXiv:quant-ph/0801.0610.
[21] P. Boonserm and M. Visser, "Bounding the greybody factors for Schwarzschild black holes," Phys. Rev. D **78**, 101502 (2008); e-print arXiv:0806.2209 [gr-qc].
[22] P. Boonserm and M. Visser, "Transmission probabilities and the Miller-Good transformation," J. Phys. A **42**, 045301 (2009); e-print arXiv:0808.2516 [math-ph].
[23] P. Boonserm and M. Visser, "Analytic bounds on transmission probabilities," Ann. Phys. **325**, 1328–1339 (2010); e-print arXiv:0901.0944 [gr-qc].
[24] P. Boonserm and M. Visser, "Reformulating the Schrödinger equation as a Shabat–Zakharov system," J. Math. Phys. **51**, 022105 (2010); e-print arXiv:0910.2600 [math-ph].
[25] P. Boonserm, "Rigorous bounds on transmission, reflection, and Bogoliubov coefficients," Ph.D. thesis (Victoria University of Wellington, 2009); e-print arXiv:0907.0045 [math-ph].
[26] T. Ngampitipan and P. Boonserm, "Bounding the greybody factors for non-rotating black holes," Int. J. Mod. Phys. D **22**, 1350058 (2013); e-print arXiv:1211.4070 [math-ph].
[27] T. Ngampitipan and P. Boonserm, "Bounding the greybody factors for the Reissner–Nordström black holes," in *Proceedings of the International Conference on Advancement in Science and Technology, ICAST, Kuantan, Malaysia, 2012*; [J. Phys.: Conf. Ser. **435**, 012027 (2013)].
[28] P. Boonserm and M. Visser, "Quasi-normal frequencies: Key analytic results," J. High Energy Phys. 1103 (**2011**) 073; e-print arXiv:1005.4483v2 [math-ph].

1 28202338

PUBLISHED FOR SISSA BY SPRINGER

RECEIVED: *January 13, 2014*
ACCEPTED: *March 2, 2014*
PUBLISHED: *March 25, 2014*

Bounding the greybody factors for scalar field excitations on the Kerr-Newman spacetime

Petarpa Boonserm,[a] Tritos Ngampitipan[b] and Matt Visser[c]

[a] *Department of Mathematics and Computer Science, Chulalongkorn University, Phayathai Road, Pathumwan, Bangkok 10330, Thailand*
[b] *Department of Physics, Chulalongkorn University, Phayathai Road, Pathumwan, Bangkok 10330, Thailand*
[c] *School of Mathematics, Statistics, and Operations Research, Victoria University of Wellington, PO Box 600, Wellington 6140, New Zealand*

E-mail: petarpa.boonserm@gmail.com, tritos.ngampitipan@gmail.com, matt.visser@msor.vuw.ac.nz

ABSTRACT: Finding exact solutions for black-hole greybody factors is generically impractical; typically one resorts either to making semi-analytic or numerical estimates, or alternatively to deriving rigorous analytic bounds. Indeed, rigorous bounds have already been established for the greybody factors of Schwarzschild and Riessner-Nordström black holes, and more generally for those of arbitrary static spherically symmetric asymptotically flat black holes. Adding rotation to the problem greatly increases the level of difficulty, both for purely technical reasons (the Kerr or Kerr-Newman black holes are generally much more difficult to work with than the Schwarzschild or Reissner-Nordström black holes), but also at a *conceptual* level (due to the generic presence of super-radiant modes). In the current article we analyze bounds on the greybody factors for scalar field excitations on the Kerr-Newman geometry in some detail, first for zero-angular-momentum modes, then for the non-super-radiant modes, and finally for the super-radiant modes.

KEYWORDS: Classical Theories of Gravity, Black Holes

ARXIV EPRINT: 1401.0568

doi:10.1007/JHEP03(2014)113

JHEP03(2014)113

Contents

1 Introduction

The spacetime geometry of a black hole, in the region that interpolates between the horizon and spatial infinity, (the domain of outer communication), generically acts as a potential barrier that partially reflects both ingoing and outgoing excitations. (See for instance [1–4].) In the case of outgoing excitations (Hawking quanta) the resulting transmission probabilities are called "greybody factors". Calculation of these greybody factors, when practical, is based on analyzing the excitations in terms of a Regge-Wheeler equation, (or closely related variant thereof, such as the Zerilli or Teukolsky equations), which in the non-super-radiant case reduces the problem to a one-dimensional barrier-penetration problem.

Even then, finding exact solutions is mostly impractical, and one typically resorts either to making semi-analytic or numerical estimates, or to deriving rigorous analytic bounds. Indeed, rigorous bounds have already been established for the greybody factors of the Schwarzschild [5] and Riessner-Nordström [6, 7] black holes, and more generally for arbitrary static spherically symmetric asymptotically flat black holes [8]. Some preliminary work on the Kerr-Newman spacetime is presented in reference [9]. Some of the new issues

JHEP03(2014)113

raised in dealing with rotating black holes are purely technical — the specific form of the metric is much more complicated. But there are new conceptual issues to deal with as well — the presence of super-radiant modes now adding extra conceptual overhead.

The technique we are using to derive rigorous bounds on the greybody factors is a technique of general applicability to bounding transmission probabilities for one-dimensional barrier penetration problems. First developed in reference [10], this quite general technique has subsequently been extended in several different ways [11–14], before then being specifically applied to the analysis of black-hole greybody factors in references [5–9]. In the current article we shall analyze bounds on the greybody factors for scalar field excitations on the Kerr-Newman geometry in some detail, first for the zero-angular-momentum $m = 0$ mode, secondly for generic non-super-radiant modes, and finally for the super-radiant modes.

2 Radial Teukolsky equation for scalar fields

The radial Teukolsky equation for scalar field excitations on the Kerr-Newman spacetime is discussed in references [15],[1] [16],[2] and [17]. The radial Teukolsky equation is considerably more complicated than the Regge-Wheeler equation for scalar field excitations on non-rotating spacetimes [15].[3] Particularly useful recent references are [18–20], though a wealth of other relevant material is also available [21–24]. The scalar field excitations are described by the curved-spacetime Klein-Gordon equation, which is in this context the spin-zero case of the Teukolsky master equation; the radial Teukolsky equation for scalar fields then corresponds to the radial part of this Klein-Gordon equation. (Nomenclature is not entirely consistent in this field, but this seems to be the consensus.)

Begin by writing the Kerr-Newman geometry in the form [25, 26]

$$\mathrm{d}s^2 = -\frac{\Delta}{\Sigma}\left(\mathrm{d}t - a\sin^2\theta\,\mathrm{d}\phi\right)^2 + \frac{\sin^2\theta}{\Sigma}\left[a\,\mathrm{d}t - (r^2+a^2)\,\mathrm{d}\phi\right]^2 + \frac{\Sigma}{\Delta}\,\mathrm{d}r^2 + \Sigma\,\mathrm{d}\theta^2, \tag{2.1}$$

where

$$\Delta = r^2 - 2Mr + a^2 + Q^2 = (r-r_+)(r-r_-); \qquad \Sigma = r^2 + a^2\cos^2\theta. \tag{2.2}$$

Here M is the mass of the black hole, $J = Ma$ is its angular momentum, and Q is its charge. The quantities $r_\pm$ denote the locations of the inner and outer horizons. Setting $Q \to 0$ gives the Kerr spacetime [27–29].[4] Now consider a massless electrically neutral minimally coupled scalar field. (Adding mass and electric charge to the scalar field is not intrinsically difficult [18], but is somewhat tedious, so we shall not do so for now.)

---

[1] See especially page 128.

[2] See especially pages 114–115.

[3] See especially pages 89–90. There they make it clear, just after (4.2.7), that while the phrase "Regge-Wheeler equation" originally applied only to (axial) gravitational perturbations of the Schwarzschild geometry, it is now customary to apply that phrase also to the perturbations of a scalar field. More generally this terminology is now commonly applied to all manner of perturbations on generic spherically symmetric spacetimes where separation of variables leads to similar-looking equations.

[4] Reference [29] is published as a chapter in reference [28].

JHEP03(2014)113

2.1 Spheroidal harmonics

It is a standard result, see Carter [30], that one can then use separation of variables to consider field modes of the form

$$\Psi(r,\theta,\phi,t) = \frac{R_{\ell m}(r)\, S_{\ell m}(\theta)\, \exp(-i\omega t + im\phi)}{\sqrt{r^2+a^2}}. \tag{2.3}$$

It is now a standard but quite tedious computation to verify that the "spheroidal harmonics" $S_{\ell m}(\theta)\, e^{im\phi}$ generalize the usual "spherical harmonics" $Y_{\ell m}(\theta,\phi)$, and satisfy the differential equation:

$$\left\{ \frac{1}{\sin\theta}\frac{\mathrm{d}}{\mathrm{d}\theta}\left[\sin\theta\frac{\mathrm{d}}{\mathrm{d}\theta}\right] - a^2\omega^2\sin^2\theta - \frac{m^2}{\sin^2\theta} + 2ma\omega + \lambda_{\ell m}(a\omega) \right\} S_{\ell m}(\theta) = 0. \tag{2.4}$$

(See for instance [31] pp 26–27.) Note this differential equation is independent of M and Q, though it does indirectly depend on the angular momentum via the dimensionless combination $a\omega = (J/M)\omega$. Here the separation constant $\lambda_{\ell m}(a\omega)$ generalizes the usual quantity $\ell(\ell+1)$ occurring for spherical harmonics, and in fact in the slow-rotation limit we have

$$\lambda_{\ell m}(a\omega) = \ell(\ell+1) - 2m\, a\omega + \{H_{\ell+1,m} - H_{\ell m}\}\, (a\omega)^2 + \mathcal{O}[(a\omega)^3], \tag{2.5}$$

with

$$H_{\ell m} = \frac{2\ell(\ell^2-m^2)}{4\ell^2-1}. \tag{2.6}$$

Some useful background references are [32–35]. Note that since the differential operator is negative definite we automatically have the constraint that $\lambda_{\ell m}(a\omega) + 2ma\omega \geq 0$. (To establish this, simply multiply the differential equation by $\sin^2\theta\, S_{\ell m}(\theta)$, and integrate by parts.) In fact, re-writing the differential equation as

$$\left\{ \frac{1}{\sin\theta}\frac{\mathrm{d}}{\mathrm{d}\theta}\left[\sin\theta\frac{\mathrm{d}}{\mathrm{d}\theta}\right] - \left(a\omega\sin\theta - \frac{m}{\sin\theta}\right)^2 + \lambda_{\ell m}(a\omega) \right\} S_{\ell m}(\theta) = 0, \tag{2.7}$$

we can also see that $\lambda_{\ell m}(a\omega) \geq 0$, an observation that will prove to be useful in the calculation below. Furthermore, the differential equation for the $S_{\ell m}(\theta)$ can be *explicitly solved* in terms of the confluent Heun functions. Unfortunately, this observation is less useful than one might hope, simply because despite valiant efforts not enough is yet known about the mathematical properties of Heun functions [36–39].

2.2 Effective potential

With these preliminaries out of the way, it is now straightforward to write down the Teukolsky equation for the radial modes [18]

$$\left\{ \frac{\mathrm{d}^2}{\mathrm{d}r_*^2} - U_{\ell m}(r) \right\} R_{\ell m}(r) = 0. \tag{2.8}$$

Here we use the "tortoise coordinate" defined by

$$\mathrm{d}r_* = \frac{r^2+a^2}{\Delta}\,\mathrm{d}r = \frac{r^2+a^2}{(r-r_+)(r-r_-)}\,\mathrm{d}r. \tag{2.9}$$

JHEP03(2014)113

Explicitly

$$r_* = r + \frac{a^2 + r_+^2}{r_+ - r} \ln(r - r_+) - \frac{a^2 + r_-^2}{r_+ - r_-} \ln(r - r_-). \tag{2.10}$$

Thus r_* runs from $+\infty$ at spatial infinity to $-\infty$ at the outer horizon, located at $r = r_+$. This region, the "domain of outer communication", is the only part of the spacetime geometry relevant for current purposes. The "effective potential" $U_{\ell m}(r)$ is:

$$U_{\ell m}(r) = \frac{\Delta}{(r^2 + a^2)^2} \left(\lambda_{\ell m}(a\omega) + \frac{(r\Delta)'}{r^2 + a^2} - \frac{3r^2\Delta}{(r^2 + a^2)^2} \right) - \left(\omega - \frac{ma}{r^2 + a^2} \right)^2. \tag{2.11}$$

For calculational purpose it is now useful to define quantities

$$\varpi = \frac{a}{a^2 + r^2}, \qquad \text{and more specifically,} \qquad \Omega_+ = \frac{a}{a^2 + r_+^2}. \tag{2.12}$$

Here $\varpi(r)$ is (perhaps somewhat vaguely) related to frame dragging, while Ω_+ is the angular velocity of the event horizon. We can now write

$$U_{\ell m}(r) = V_{\ell m}(r) - (\omega - m\varpi)^2, \tag{2.13}$$

with

$$V_{\ell m}(r) = \frac{\Delta}{(r^2 + a^2)^2} \left\{ \lambda_{\ell m}(a\omega) + W_{MQJ}(r) \right\}. \tag{2.14}$$

Here we have separated out the quantity

$$W_{MQJ}(r) = \frac{(r\Delta)'}{r^2 + a^2} - \frac{3r^2\Delta}{(r^2 + a^2)^2}, \tag{2.15}$$

which depends only on the spacetime geometry, not on the multipole (ℓm) under consideration. This definition of $V_{\ell m}(r)$ is now as close as possible to our earlier usage in references [5–8], and to the general (non-relativistic quantum mechanical) analyses of references [10–14]. If one switches off rotation, $a \to 0$, then this radial Teukolsky equation reduces to the Regge-Wheeler equation [15? –17].

2.3 Positivity properties

We have already seen that the separation constant $\lambda_{\ell m}(a\omega)$ is positive. More subtly the quantity $W_{MQJ}(r)$ is also positive. (This result depends implicitly on the Einstein equations and the resulting special properties of the Kerr-Newman spacetime.)

To check the positivity of $W_{MQJ}(r)$, we write

$$\Delta = (r - r_+)(r - r_-); \qquad r_+ + r_- = 2M; \qquad r_+ r_- = a^2 + Q^2. \tag{2.16}$$

In particular note that

$$0 \le \frac{a^2}{r_+} \le r_- \le r_+, \qquad \text{and} \qquad 0 \le \frac{Q^2}{r_+} \le r_- \le r_+. \tag{2.17}$$

Furthermore

$$a \le M; \qquad |Q| \le M. \tag{2.18}$$

Now consider

$$
\begin{aligned}
(r\Delta)' &= [r(r-r_+)(r-r_-)]' \\
&= (r-r_+)(r-r_-) + r(r-r_+) + r(r-r_-) \\
&= 3r^2 - 2r(r_+ + r_-) + r_+ r_- .
\end{aligned}
\tag{2.19}
$$

Then

$$
\begin{aligned}
W_{MQJ}(r) &\propto (r\Delta)'(r^2+a^2) - 3r^2\Delta \\
&= (3r^2 - 2r(r_+ + r_-) + r_+r_-)(r^2+a^2) - 3r^2(r-r_+)(r-r_-) \\
&= [0]r^4 + [-2(r_+ + r_-) + 3(r_+ + r_-)]r^3 + [3a^2 + r_+r_- - 3r_+r_-]r^2 \\
&\qquad + [-2a^2(r_+ + r_-)]r + [a^2 r_+ r_-]r^0 \\
&= (r_+ + r_-)r^3 + [3a^2 - 2r_+r_-]r^2 - 2a^2(r_+ + r_-)r + a^2 r_+ r_- \\
&= r^2(rr_+ + rr_- - 2r_+r_-) + a^2 r(2r - r_+ - r_-) + a^2\Delta \\
&\geq 0.
\end{aligned}
\tag{2.20}
$$

Here in the penultimate line all three terms are manifestly positive outside the outer horizon (for $r \geq r_+$).

Furthermore $\lim_{r\to\infty} W_{MQJ} = 0$ and $W_{MQJ}(r_+) = r_+(r_+ - r_-)/(r_+^2 + a^2)$. Thence we see that $V_{\ell m} \to 0$ both at the outer horizon r_+ and at spatial infinity.

2.4 Super-radiance

It is the trailing term in the effective potential, the $(\omega - m\varpi)^2$ term, that is responsible for the qualitatively new phenomenon of super-radiance, which never occurs in ordinary non-relativistic quantum mechanics. The reason for this is that the Schrödinger equation is first-order in time derivatives, so the effective potential for Schrödinger-like barrier-penetration problems is generically of the form

$$
U(r) = V(r) - \omega. \tag{2.21}
$$

In contrast, for problems based on the Klein-Gordon equation (second-order in time derivatives) the qualitative structure of the effective potential is

$$
U(r) = V(r) - (\omega - m\varpi)^2. \tag{2.22}
$$

We shall soon see that it is when the quantity $\omega - m\varpi$ changes sign that the possibility of super-radiance arises. (See for instance the general discussion by Richartz *et al* [40].) In the current set-up super-radiance is related to the rotation of the black hole, but if the scalar field additionally carries electric charge there is another contribution to ϖ coming from the electrostatic potential, and so a separate route to super-radiance [18, 40].

While the Dirac equation, being first-order in both space and time, might seem to side-step this phenomenon, it is a standard result that iterating the Dirac differential operator twice produces a Klein-Gordon-like differential equation. In terms of the Dirac matrices we have:

$$
\not{D}^2 = 2(\nabla - iqA)^2 + qF_{ab}\,[\gamma^a, \gamma^b]. \tag{2.23}
$$

JHEP03(2014)113

So, once one factors out the spinorial components, and concentrates attention on the second-order differential equation for the amplitude of the Dirac field, even the Klein paradox for charged relativistic fermions can be put into this framework. It is the trailing $(\omega - m\varpi)^2$ term, and more specifically the change in sign of $\omega - m\varpi$, that is the harbinger of super-radiance. Indeed, assuming ϖ is monotonic (which it certainly is in the situations we shall be interested in) let us define the quantity $m_* = \omega/\Omega_+$. Then:

- the modes $m < m_*$ are not super-radiant;
- the modes $m \geq m_*$ are super-radiant.

We shall soon see much more detail regarding the super-radiance phenomenon in the subsequent discussion.

3 Non-super-radiant modes ($m < m_*$)

It is convenient to split the discussion of the non-super-radiant modes into three sub-cases:

- $m = 0$, zero-angular-momentum modes;
- $m < 0$, negative-angular-momentum modes;
- $m \in (0, m_*)$, low-lying positive-angular-momentum modes.

3.1 Zero-angular-momentum modes ($m = 0$)

This sub-case is both particularly simple, and is in many ways a guiding template for all the other cases. Some preliminary work on these zero-angular-momentum modes in the Kerr-Newman spacetime is presented in reference [9]. We note that from reference [10] pp. 427–428 we have the very generic bound:

$$T_{\ell m} \geq \operatorname{sech}^2 \left\{ \int_{-\infty}^{+\infty} \frac{\sqrt{[h'(r)]^2 + [U_{\ell m}(r) + h(r)^2]^2}}{2h(r)} \, \mathrm{d}r_* \right\}; \qquad \forall h(r) > 0. \tag{3.1}$$

Note that we need $h(r) > 0$ everywhere in order for this bound to hold. Suppose we set $m = 0$, then

$$U_{\ell,m=0}(r) = -\omega^2 + \frac{\Delta}{(r^2+a^2)^2} \left[\lambda_{\ell,m=0} + W_{MQJ}(r)\right]. \tag{3.2}$$

Now choose $h(r) = \omega > 0$, and change the integration variable from $\mathrm{d}r_*$ to $\mathrm{d}r$, so that

$$T_{\ell,m=0} \geq \operatorname{sech}^2 \left\{ \frac{1}{2\omega} \int_{r_+}^{+\infty} \left| \frac{1}{(r^2+a^2)} \left[\lambda_{\ell,m=0} + W_{MQJ}(r)\right] \right| \mathrm{d}r \right\}. \tag{3.3}$$

(This corresponds to the Case I bound of reference [10].) As long as $\lambda_{\ell m}$ and $W_{MQJ}(r)$ are always positive (and we have already checked that above) we can dispense with the absolute value symbols and write

$$T_{\ell,m=0} \geq \operatorname{sech}^2 \left\{ \frac{1}{2\omega} \int_{r_+}^{+\infty} \frac{1}{(r^2+a^2)} \left[\lambda_{\ell,m=0} + W_{MQJ}(r)\right] \, \mathrm{d}r \right\}. \tag{3.4}$$

This now decouples the problem to considering two integrals, each of which can be explicitly evaluated in closed form.

JHEP03(2014)113

First integral: we note that

$$\int_{r_+}^{+\infty} \frac{\lambda_{\ell,m=0}}{(r^2+a^2)} \mathrm{d}r = \lambda_{\ell,m=0}(a\omega)\ \frac{\arctan(a/r_+)}{a}. \tag{3.5}$$

This quantity is independent of M and Q.

Second integral: when it comes to evaluating the integral involving W_{MQJ} it is best to define the dimensionless quantity

$$K_{MQJ} = r_+ \int_{r_+}^{+\infty} \frac{W_{MQJ}}{(r^2+a^2)} \mathrm{d}r = r_+ \int_{r_+}^{+\infty} \frac{1}{(r^2+a^2)} \left(\frac{(r\Delta)'}{r^2+a^2} - \frac{3r^2\Delta}{(r^2+a^2)^2} \right) \mathrm{d}r. \tag{3.6}$$

To evaluate this the best trick is to integrate by parts:

$$K_{MQJ} = r_+ \int_{r_+}^{+\infty} \left(-(r\Delta)[(r^2+a^2)^{-2}]' - \frac{3r^2\Delta}{(r^2+a^2)^3} \right) \mathrm{d}r. \tag{3.7}$$

(Note that the boundary terms vanish.) This then equals:

$$K_{MQJ} = r_+ \int_{r_+}^{+\infty} \left(\frac{(4-3)r^2\Delta}{(r^2+a^2)^3} \right) \mathrm{d}r = r_+ \int_{r_+}^{+\infty} \left(\frac{r^2\Delta}{(r^2+a^2)^3} \right) \mathrm{d}r. \tag{3.8}$$

So finally

$$K_{MQJ} = \frac{r_+}{8} \frac{(r_+^2+a^2)(3a^2+r_+r_-)\arctan(a/r_+) + a(a^2[r_+ - 2r_-] - r_+^2 r_-)}{a^3(r_+^2+a^2)}. \tag{3.9}$$

This dimensionless quantity is independent of the parameters characterizing the scalar mode (ℓ, m, ω), and depends only on the parameters characterizing the spacetime geometry (a, r_+, r_-), which in turn implicitly depend only on (M, Q, J).

Consistency check: if you look carefully this quantity K_{MQJ} does have a finite limit as $a \to 0$, as it should do to be consistent with the physics of the Reissner-Nordström spacetime. (The limit is a little tricky.) We can recast K_{MQJ} as

$$K_{MQJ} = \frac{3}{8} \frac{\arctan(a/r_+)}{a/r_+} + \frac{r_+^2 r_-}{8} \frac{([r_+^2+a^2]\arctan(a/r_+) - ar_+)}{a^3(r_+^2+a^2)} + \frac{1}{8} \frac{r_+(3a+r_+-2r_-)}{r_+^2+a^2}, \tag{3.10}$$

with limit

$$\to \frac{3}{8} + \frac{1}{12}\frac{r_-}{r_+} + \frac{1}{8}\frac{r_+ - 2r_-}{r_+} = \frac{1}{24} \frac{9r_+ + 2r_- + 3r_+ - 6r_-}{r_+} = \frac{3r_+ - r_-}{6r_+}. \tag{3.11}$$

Final result: collecting terms, we can write the bound on the transmission probability as

$$T_{\ell,m=0} \geq \operatorname{sech}^2 \left[\frac{I_{\ell,m=0}}{2r_+\omega} \right], \tag{3.12}$$

with

$$I_{\ell,m=0} = \lambda_{\ell,m=0}(a\omega)\ \frac{\arctan(a/r_+)}{a/r_+} + K_{MQJ}. \tag{3.13}$$

This cleanly separates out the mode dependence (ℓm) from the purely geometrical piece K_{MQJ}. Note $I_{\ell,m=0}$ is now a dimensionless number that depends only dimensionless ratios such as a/r_+ and r_-/r_+, and implicitly (via $\lambda_{\ell,m=0}$) on ℓ and $a\omega$. In view of the known slow rotation expansion for $\lambda_{\ell,m=0}(a\omega)$ we know that

$$I_{\ell,m=0}(\omega \to 0) = \ell(\ell+1)\,\frac{\arctan(a/r_+)}{a/r_+} + K_{MQJ}. \tag{3.14}$$

So at low frequencies the transmission bound is dominated by the $1/\omega$ pole in the argument of the hyperbolic secant function. If we wish to be very explicit we can write

$$\begin{aligned} I_{\ell,m=0} = {} & \left(\lambda_{\ell,m=0}(a\omega) + \frac{3}{8}\right)\frac{\arctan(a/r_+)}{a/r_+} \\ & + \frac{r_+ r_-}{8}\,\frac{r_+([r_+^2 + a^2]\arctan(a/r_+) - a r_+)}{a^3(r_+^2 + a^2)} + \frac{1}{8}\frac{r_+(3a + r_+ - 2r_-)}{r_+^2 + a^2}. \end{aligned} \tag{3.15}$$

There are certainly other ways of re-writing this quantity, but this version is sufficient for exhibiting key aspects of the physics.

3.2 Non-zero-angular-momentum modes ($m \neq 0$)

What if anything can we do once $m \neq 0$? Recall the basic result

$$T_{\ell m} \geq \operatorname{sech}^2\left\{\int_{-\infty}^{+\infty} \frac{\sqrt{[h'(r)]^2 + [U_{\ell m}(r) + h(r)^2]^2}}{2h(r)}\,\mathrm{d}r_*\right\}; \qquad \forall h(r) > 0. \tag{3.16}$$

Now by the triangle inequality we certainly have

$$T_{\ell m} \geq \operatorname{sech}^2\left\{\frac{1}{2}\int_{-\infty}^{+\infty}\left|\frac{h'}{h}\right|\mathrm{d}r_* + \frac{1}{2}\int_{-\infty}^{+\infty}\frac{|U_{\ell m}(r) + h(r)^2|}{2h(r)}\,\mathrm{d}r_*\right\}; \qquad \forall h(r) > 0. \tag{3.17}$$

We are now free to pick $h(r)$ so that it is monotone, $h'(r) > 0$ or $h'(r) < 0$. Then subject to this condition

$$T_{\ell m} \geq \operatorname{sech}^2\left\{\frac{1}{2}\left|\ln\left[\frac{h(\infty)}{h(-\infty)}\right]\right| + \frac{1}{2}\int_{-\infty}^{+\infty}\frac{|U_{\ell m}(r) + h(r)^2|}{2h(r)}\,\mathrm{d}r_*\right\}; \qquad \forall h(r) > 0. \tag{3.18}$$

Apply this general result to our specific situation

$$U_{\ell m}(r) = V_{\ell m} - (\omega - m\varpi)^2, \tag{3.19}$$

by choosing

$$h(r) = \omega - m\varpi. \tag{3.20}$$

(This construction is now as close as one can get to the Case I bound of reference [10].) Note this choice for $h(r)$ is, since $\varpi = a/(a^2 + r^2)$, always monotonic as a function of r. In contrast, (remember that $\omega > 0$ and $a > 0$), we see that this $h(r)$ is positive throughout the domain of outer communication *if and only if* $\omega > m\Omega_+$, which is completely equivalent to $m < \omega/\Omega_+$, or $m < m_*$. This is easily recognized as the quite standard condition that the mode does *not* suffer from super-radiant instability. Let us now see where we can go with this.

3.2.1 Negative-angular-momentum modes ($m < 0$)

First note that in this situation, for the specific function $h(r)$ chosen above, we have

$$\frac{h(\infty)}{h(-\infty)} = \frac{\omega}{\omega - m\Omega_+} = \frac{1}{1 - m\Omega_+/\omega} < 1. \tag{3.21}$$

Then

$$\frac{1}{2}\left|\ln\left[\frac{h(\infty)}{h(-\infty)}\right]\right| = \frac{1}{2}\ln(1 - m\Omega_+/\omega). \tag{3.22}$$

Also in this case we have $\omega - m\Omega_+ > h(r) > \omega$, so

$$\int_{-\infty}^{+\infty} \frac{|U_{\ell m}(r) + h(r)^2|}{2h(r)}\, \mathrm{d}r_* = \int_{-\infty}^{+\infty} \frac{|V_{\ell m}|}{2h(r)}\, \mathrm{d}r_* < \int_{-\infty}^{+\infty} \frac{V_{\ell m}}{2\omega}\, \mathrm{d}r_*. \tag{3.23}$$

Then

$$T_{\ell,m<0} \geq \operatorname{sech}^2\left\{\frac{1}{2}\ln(1 - m\Omega_+/\omega) + \int_{-\infty}^{+\infty} \frac{V_{\ell,m<0}}{2\omega}\, \mathrm{d}r_*\right\}. \tag{3.24}$$

But that last integral is almost identical to that we performed for $m = 0$, the only change being the replacement $\lambda_{\ell,m=0} \to \lambda_{\ell,m<0}$. Therefore

$$T_{\ell,m<0} \geq \operatorname{sech}^2\left\{\frac{1}{2}\ln(1 - m\Omega_+/\omega) + \frac{I_{\ell,m<0}}{2r_+\,\omega}\right\}, \tag{3.25}$$

where in comparison we previously had

$$T_{\ell,m=0} \geq \operatorname{sech}^2\left\{\frac{I_{\ell,m=0}}{2r_+\omega}\right\}. \tag{3.26}$$

Explicitly

$$I_{\ell m} = \lambda_{\ell m}(a\omega)\,\frac{\arctan(a/r_+)}{a/r_+} + K_{MQJ}, \tag{3.27}$$

and

$$T_{\ell,m<0} \geq \operatorname{sech}^2\left\{\frac{1}{2}\ln(1 - m\Omega_+/\omega) + \frac{\lambda_{\ell m}(a\omega)\,\dfrac{\arctan(a/r_+)}{a/r_+} + K_{MQJ}}{2r_+\,\omega}\right\}. \tag{3.28}$$

Note that for $m < 0$ we have $-m \leq \ell$, so we could also write the weaker (but perhaps slightly simpler) bound

$$T_{\ell,m<0} \geq \operatorname{sech}^2\left\{\frac{1}{2}\ln(1 + \ell\Omega_+/\omega) + \frac{I_{\ell,m<0}}{2r_+\,\omega}\right\}. \tag{3.29}$$

3.2.2 Low-lying positive-angular-momentum modes ($m \in (0, m_*)$)

For this situation we first note that

$$\frac{h(\infty)}{h(-\infty)} = \frac{\omega}{\omega - m\Omega_+} = \frac{1}{1 - m\Omega_+/\omega} > 1. \tag{3.30}$$

Then we see

$$\frac{1}{2}\left|\ln\left[\frac{h(\infty)}{h(-\infty)}\right]\right| = -\frac{1}{2}\ln(1-m\Omega_+/\omega). \tag{3.31}$$

Also, in this case $\omega - m\Omega_+ < h(r) < \omega$, so

$$\int_{-\infty}^{+\infty}\frac{|U_{\ell m}(r)+h(r)^2|}{2h(r)}\,\mathrm{d}r_* = \int_{-\infty}^{+\infty}\frac{|V_{\ell,m>0}|}{2h(r)}\,\mathrm{d}r_* < \int_{-\infty}^{+\infty}\frac{V_{\ell,m>0}}{2(\omega-m\Omega_+)}\,\mathrm{d}r_*. \tag{3.32}$$

Then

$$T_{\ell,m>0} \geq \operatorname{sech}^2\left\{-\frac{1}{2}\ln(1-m\Omega_+/\omega)+\frac{1}{2}\int_{-\infty}^{+\infty}\frac{|V_{\ell,m>0}|}{(\omega-\Omega_+)}\,\mathrm{d}r_*\right\}. \tag{3.33}$$

But that remaining integral is qualitatively the same as that which we performed for the $m=0$ and $m<0$ cases, therefore

$$T_{\ell,m>0} \geq \operatorname{sech}^2\left\{-\frac{1}{2}\ln(1-m\Omega_+/\omega)+\frac{I_{\ell,m>0}}{2r_+(\omega-m\Omega_+)}\right\}, \tag{3.34}$$

where in comparison

$$T_{\ell,m=0} \geq \operatorname{sech}^2\left\{\frac{I_{\ell,m=0}}{2r_+\,\omega}\right\}. \tag{3.35}$$

Explicitly

$$I_{\ell m} = \lambda_{\ell m}(a\omega)\,\frac{\arctan(a/r_+)}{a/r_+} + K_{MQJ}, \tag{3.36}$$

and

$$T_{\ell,m>0} \geq \operatorname{sech}^2\left\{-\frac{1}{2}\ln(1-m\Omega_+/\omega)+\frac{\lambda_{\ell m}(a\omega)\,\dfrac{\arctan(a/r_+)}{a/r_+}+K_{MQJ}}{2r_+(\omega-m\Omega_+)}\right\}. \tag{3.37}$$

Note that for $m>0$ we have $m\leq\ell$, so we could also write the weaker (but perhaps slightly simpler) bound

$$T_{\ell,m>0} \geq \operatorname{sech}^2\left\{-\frac{1}{2}\ln(1-\ell\Omega_+/\omega)+\frac{I_{\ell m}}{2r_+(\omega-\ell\Omega_+)}\right\}. \tag{3.38}$$

3.3 Summary (non-super-radiant modes)

Define

$$I_{\ell m} = \lambda_{\ell m}(a\omega)\,\frac{\arctan(a/r_+)}{a/r_+} + K_{MQJ}, \tag{3.39}$$

where

$$K_{MQJ} = \frac{r_+}{8}\,\frac{(r_+^2+a^2)(3a^2+r_+r_-)\arctan(a/r_+)+a(a^2[r_+-2r_-]-r_+^2r_-)}{a^3(r_+^2+a^2)}. \tag{3.40}$$

Then for the non-super-radiant modes

$$T_{\ell,m\leq 0} \geq \operatorname{sech}^2\left\{\frac{1}{2}\ln(1-m\Omega_+/\omega)+\frac{I_{\ell,m\leq 0}}{2r_+\,\omega}\right\}, \tag{3.41}$$

JHEP03(2014)113

and

$$T_{\ell,m\in(0,m_*)} \geq \operatorname{sech}^2\left\{-\frac{1}{2}\ln(1-m\Omega_+/\omega)+\frac{I_{\ell,m>0}}{2r_+(\omega-m\Omega_+)}\right\}. \tag{3.42}$$

These bounds can also be written as

$$T_{\ell,m\leq 0} \geq \operatorname{sech}^2\left\{\frac{1}{2}\ln(1-m/m_*)+\frac{I_{\ell,m\leq 0}}{2r_+\,\omega}\right\}, \tag{3.43}$$

and

$$T_{\ell,m\in(0,m_*)} \geq \operatorname{sech}^2\left\{-\frac{1}{2}\ln(1-m/m_*)+\frac{I_{\ell,m>0}}{2r_+\,\omega\,(1-m/m_*)}\right\}. \tag{3.44}$$

These are the best general bounds we have been able to establish for the non-super-radiant modes.

4 Super-radiant modes ($m \geq m_*$)

For the super-radiant modes we must be more careful. Inspection of the original derivation in reference [10] shows that fundamentally the analysis works by placing bounds on the Bogoliubov coefficients:

$$|\alpha| \leq \cosh \oint \vartheta \, \mathrm{d}r; \qquad |\beta| \leq \sinh \oint \vartheta \, \mathrm{d}r, \tag{4.1}$$

where

$$\Theta = \oint \vartheta \, \mathrm{d}r = \int_{-\infty}^{+\infty} \frac{\sqrt{[h'(r)]^2+[U_{\ell m}(r)+h(r)^2]^2}}{2h(r)}\,\mathrm{d}r_*; \qquad \forall h(r)>0. \tag{4.2}$$

In the non-super-radiant case these constraints on the Bogoliubov coefficients quickly and directly lead to a bound on the transmission coefficient $T=|\alpha|^{-2}$. In counterpoint, in the super-radiant case the Bogoliubov coefficients also have an additional physical interpretation: the near-horizon quantum vacuum state now contains a nontrivial density of quanta when viewed from the region near spatial infinity [40]. The number of quanta per unit length in each mode is $n = k\,|\beta|^2$, corresponding to an emission rate

$$\Gamma = \omega\,|\beta|^2. \tag{4.3}$$

Explicitly, the emission rate in each specific mode is bounded by

$$\Gamma_{\ell m}(\omega) \leq \omega \sinh^2\Theta, \tag{4.4}$$

where

$$\Theta = \int_{-\infty}^{+\infty} \frac{\sqrt{[h'(r)]^2+[U_{\ell m}(r)+h(r)^2]^2}}{2h(r)}\,\mathrm{d}r_*; \qquad \forall h(r)>0. \tag{4.5}$$

The net result is that one is still interested in the same integral, but now under different conditions, and with an additional physical interpretation. To be more explicit about this, note that

$$\Theta = \int_{-\infty}^{+\infty} \frac{\sqrt{[h'(r)]^2+[V_{\ell m}(r)-(\omega-m\varpi(r))^2+h(r)^2]^2}}{2h(r)}\,\mathrm{d}r_*; \quad \forall h(r)>0. \tag{4.6}$$

The art comes now in *choosing* a specific $h(r)$ to in some sense optimize the bound, (either by making it a particularly tight bound, or by making it a particularly simple bound), subject now to the condition that $\omega - m\varpi(r)$ is assumed to change sign at some finite value of r, and subject to the condition that one wants the integral to be finite, (implying in particular that the integrand should vanish both on the outer horizon and at spatial infinity).
Now the triangle inequality implies ($\forall h(r) > 0$) that

$$\Theta \leq \frac{1}{2}\int_{-\infty}^{+\infty} \frac{|h'(r)|}{h(r)}\,\mathrm{d}r_* + \int_{-\infty}^{+\infty} \frac{|V_{\ell m}(r) - (\omega - m\varpi(r))^2 + h(r)^2|}{2h(r)}\,\mathrm{d}r_*. \tag{4.7}$$

Additionally we know that $V_{\ell m} \to 0$ at both the outer horizon and spatial infinity, so to keep the integral finite we need both $h(\infty)^2 = \omega^2$ and $h(r_+)^2 = (\omega - m\Omega_+)^2$. Based on this observation, it is now a good strategy to again use the triangle inequality to split the integral as follows

$$\Theta \leq \frac{1}{2}\int_{-\infty}^{+\infty} \frac{|h'(r)|}{h(r)}\,\mathrm{d}r_* + \int_{-\infty}^{+\infty} \frac{V_{\ell m}(r)}{2h(r)}\,\mathrm{d}r_* + \int_{-\infty}^{+\infty} \frac{|h(r)^2 - (\omega - m\varpi(r))^2|}{2h(r)}\,\mathrm{d}r_*. \tag{4.8}$$

Now split the super-radiant modes into two sub-cases depending on the relative sizes of ω^2 and $(\omega - m\Omega_+)^2$. But note that in the super-radiant regime $\omega^2 = (\omega - m\Omega_+)^2$ when $m = 2\omega/\Omega_+ = 2m_*$. This suggests splitting the super-radiant regime into two distinct sub-cases:

- $m \in [m_*, 2m_*)$.
- $m \in [2m_*, \infty)$.

4.1 Low-lying super-radiant modes ($m \in [m_*, 2m_*)$)

In this region we have $\omega^2 > (\omega - m\Omega_+)^2$ and so we could take:

$$h(r) = \max\left\{\omega - \frac{ma}{(a^2 + r^2)}, m\Omega_+ - \omega\right\}. \tag{4.9}$$

This quantity is positive and monotone decreasing as we move from spatial infinity to the horizon, and becomes a flat horizontal line near the horizon. Note that by construction $h(r) \geq m\Omega_+ - \omega$ everywhere. First, from the definition of $h(r)$, in this situation we have

$$\int_{-\infty}^{+\infty} \frac{|h'(r)|}{h(r)}\,\mathrm{d}r_* = |\ln h(r)|_{r_+}^{\infty} = \ln\left(\frac{\omega}{m\Omega_+ - \omega}\right) = -\ln(m/m_* - 1). \tag{4.10}$$

Second

$$\int_{-\infty}^{+\infty} \frac{V_{\ell m}(r)}{2h(r)}\,\mathrm{d}r_* \leq \int_{-\infty}^{+\infty} \frac{V_{\ell m}(r)}{2(m\Omega_+ - \omega)} = \frac{I_{\ell m}}{2(m\Omega_+ - \omega)} = \frac{I_{\ell m}}{2\omega(m/m_* - 1)}, \tag{4.11}$$

where the $I_{\ell m}$ integral is the same quantity we have considered several times before. Finally, the remaining integral to be performed is

$$J_m^{\mathrm{low}} = \int_{-\infty}^{+\infty} \frac{h(r)^2 - (\omega - m\varpi(r))^2}{2h(r)}\,\mathrm{d}r_*, \tag{4.12}$$

with the integrand being both independent of ℓ, and carefully chosen to be zero over much of the relevant range. Indeed, unwrapping all of the definitions, we are interested in

$$J_m^{\text{low}} = \int_{r_+}^{r_0} \frac{(\omega - m\Omega_+)^2 - (\omega - m\varpi(r))^2}{2(m\Omega_+ - \omega)} \; \frac{r^2 + a^2}{\Delta} \, \mathrm{d}r. \tag{4.13}$$

The upper limit of integration r_0 is defined by

$$m[\Omega_+ + a/(a^2 + r_0^2)] = 2\omega, \tag{4.14}$$

that is, by

$$r_0^2 - r_+^2 = \frac{2(m - m_*)}{2m_* - m} \, (r_+^2 + a^2). \tag{4.15}$$

Explicitly

$$r_0 = \sqrt{r_+^2 + \frac{2(m - m_*)}{2m_* - m} \, (r_+^2 + a^2)}. \tag{4.16}$$

Note $r_0 > r_+$ for $m \in [m_*, 2m_*)$. Then

$$J_m^{\text{low}} = \frac{m}{2(\omega - \Omega_+)} \int_{r_+}^{r_0} (\Omega_+ - \varpi)(2\omega - m\varpi(r) - m\Omega_+) \; \frac{r^2 + a^2}{\Delta} \, \mathrm{d}r. \tag{4.17}$$

But over the relevant domain $0 \leq (2\omega - m\varpi(r) - m\Omega_+ \leq 2(\omega - m\Omega_+)$, therefore

$$J_m^{\text{low}} \leq m \int_{r_+}^{r_0} (\Omega_+ - \varpi) \; \frac{r^2 + a^2}{\Delta} \, \mathrm{d}r. \tag{4.18}$$

The remaining integral is now simple and manifestly finite.

$$J_m^{\text{low}} \leq m \int_{r_+}^{r_0} (\Omega_+ - \varpi) \; \frac{r^2 + a^2}{\Delta} \, \mathrm{d}r = \frac{ma}{r_+^2 + a^2} \int_{r_+}^{r_0} \frac{r - r_+}{r - r_-} \, \mathrm{d}r. \tag{4.19}$$

(In fact we could have evaluated J_m^{low} exactly, but given the other approximations being made in deriving the bounds, there is no real point in doing so.) Assembling the pieces we have:

$$T_{\ell, m \in [m_*, 2m_*)} \geq \operatorname{sech}^2 \left\{ -\frac{1}{2} \ln(m/m_* - 1) + \frac{I_{\ell, m \in [m_*, 2m_*)}}{2r_+\omega\,(m/m_* - 1)} + J_m^{\text{low}} \right\}. \tag{4.20}$$

Furthermore:

$$\Gamma_{\ell, m \in [m_*, 2m_*)} \leq \omega \; \sinh^2 \left\{ -\frac{1}{2} \ln(m/m_* - 1) + \frac{I_{\ell, m \in [m_*, 2m_*)}}{2r_+\omega\,(m/m_* - 1)} + J_m^{\text{low}} \right\}. \tag{4.21}$$

4.2 Highly super-radiant modes ($m \geq 2m_*$)

In this region we have $(\omega - m\Omega_+)^2 > \omega^2$ and so we could take:

$$h(r) = \max \left\{ \frac{ma}{(a^2 + r^2)} - \omega, \omega \right\}. \tag{4.22}$$

This is now both positive and monotone decreasing as we move from the horizon to spatial infinity, and becomes a flat horizontal line near spatial infinity. Note $h(r) \geq \omega$ everywhere. First, from the definition of $h(r)$, in this situation we have

$$\int_{-\infty}^{+\infty} \frac{|h'(r)|}{h(r)} \, \mathrm{d}r_* = |\ln h(r)|_{r_+}^{\infty} = \ln\left(\frac{m\Omega_+ - \omega}{\omega}\right) = \ln(m/m_* - 1). \tag{4.23}$$

Second

$$\int_{-\infty}^{+\infty} \frac{V_{\ell m}(r)}{2h(r)} \, \mathrm{d}r_* \leq \int_{-\infty}^{+\infty} \frac{V_{\ell m}(r)}{2\omega} = \frac{I_{\ell m}}{2\omega}, \tag{4.24}$$

where the $I_{\ell m}$ integral is the same quantity we have considered before. Finally, the remaining integral is

$$J_m^{\mathrm{high}} = \int_{-\infty}^{+\infty} \frac{h(r)^2 - (\omega - m\varpi(r))^2}{2h(r)} \, \mathrm{d}r_*, \tag{4.25}$$

with the integrand being zero over much of the relevant range. Indeed we are now interested in

$$J_m^{\mathrm{high}} = \int_{r_0}^{\infty} \frac{\omega^2 - (\omega - m\varpi(r))^2}{2\omega} \, \frac{r^2 + a^2}{\Delta} \, \mathrm{d}r\,. \tag{4.26}$$

The lower limit of integration r_0 is now defined by $ma/(a^2 + r_0^2) = 2\omega$, that is, by

$$r_0 = a\sqrt{\frac{m}{2\omega a} - 1}. \tag{4.27}$$

Note that since $m \geq 2m_*$ we have

$$r_0 \geq a\sqrt{\frac{m_*}{\omega a} - 1} = a\sqrt{\frac{a^2 + r_+^2}{a^2} - 1} = r_+, \tag{4.28}$$

so we are safely outside (or possibly just on) the outer horizon. If $m > 2m_*$ then $r_0 > r_+$ and the integrand is manifestly finite over the entire range of interest, while falling of asymptotically as $1/r^2$, so the integral J_m^{high} is finite. If $m = 2m_*$ so $r_0 = r_+$, then both the numerator and denominator of the integrand to zero at the outer horizon, though the ratio is finite. So the integrand again remains finite over the entire range of interest, while falling of asymptotically as $1/r^2$, so the integral J_m^{high} is again finite. (In fact we can evaluate J_m^{low} exactly, but the result is algebraically messy, and given the other approximations being made in deriving the bounds, there is no real point in doing so.) Assembling the pieces we have:

$$T_{\ell, m\geq 2m_*} \geq \mathrm{sech}^2\left\{\frac{1}{2}\ln(m/m_* - 1) + \frac{I_{\ell, m\geq 2m_*}}{2r_+\omega} + J_m^{\mathrm{high}}\right\}. \tag{4.29}$$

Furthermore:

$$\Gamma_{\ell, m\geq 2m_*} \leq \omega\, \sinh^2\left\{\frac{1}{2}\ln(m/m_* - 1) + \frac{I_{\ell, m\geq 2m_*}}{2r_+\omega} + J_m^{\mathrm{high}}\right\}. \tag{4.30}$$

JHEP03(2014)113

4.3 Summary (super-radiant modes)

Pulling the results for the low-lying and highly super-radiant modes together we see that for the transmission probabilities we have:

$$T_{\ell,m\in[m_*,2m_*)} \geq \operatorname{sech}^2\left\{-\frac{1}{2}\ln(m/m_*-1)+\frac{I_{\ell,m\in[m_*,2m_*)}}{2r_+\omega\,(m/m_*-1)}+J_m^{\text{low}}\right\}. \tag{4.31}$$

$$T_{\ell,m\geq 2m_*} \geq \operatorname{sech}^2\left\{\frac{1}{2}\ln(m/m_*-1)+\frac{I_{\ell,m\geq 2m_*}}{2r_+\omega}+J_m^{\text{high}}\right\}. \tag{4.32}$$

Furthermore for the super-radiant emission rates we have:

$$\Gamma_{\ell,m\in[m_*,2m_*)} \leq \omega\,\sinh^2\left\{-\frac{1}{2}\ln(m/m_*-1)+\frac{I_{\ell,m\in[m_*,2m_*)}}{2r_+\omega\,(m/m_*-1)}+J_m^{\text{low}}\right\}. \tag{4.33}$$

$$\Gamma_{\ell,m\geq 2m_*} \leq \omega\,\sinh^2\left\{\frac{1}{2}\ln(m/m_*-1)+\frac{I_{\ell,m\geq 2m_*}}{2r_+\omega}+J_m^{\text{high}}\right\}. \tag{4.34}$$

5 Discussion

The net result of this article is to establish certain rigorous bounds on the greybody factors (mode dependent transmission probabilities) for scalar fields on Kerr-Newman black holes. As a side effect, we have also obtained certain rigorous bounds on the emission rates for the super-radiant modes. An interesting feature of these bounds is the ubiquity of the basic quantity $I_{\ell,m}$ which itself is simply linear in the spheroidal harmonic eigenvalue $\lambda_{\ell m}(a\omega)$. (Recall that $\lambda_{\ell m}(a\omega) \to \ell(\ell+1)$ as rotation is switched off, $a \to 0$.) This seems to indicate that it is the use of separable spheroidal coordinates that is in many ways more crucial than the specific form of the metric components.

We do not claim that these bounds are in any sense optimal. (Except, perhaps, in the restricted sense that these seem to be the easiest bounds to establish.) It is quite possible that making different choices at various stages of the analysis could lead to tighter bounds, but there are no really obvious routes to guaranteeing tighter bounds. Possible routes to explore might include the "Case II" bounds of reference [10], the Miller-Good version of the bounds presented in reference [11], or the general considerations of [12–14]. In a rather different direction, since transmission probabilities are intimately related to quasi-normal modes, it may prove useful to adapt the formalism and techniques of [41–44].

More prosaically, there would be in principle no obstruction to adding mass and charge to the scalar field, (see for instance the Teukolsky/Regge-Wheeler analysis in reference [18]), but the results are likely to be algebraically messy. Other possibilities to explore might include the behaviour of spin-1/2, spin-1, and spin-2 fields, or the consideration of other interesting spacetime geometries.

Acknowledgments

PB was supported by a grant for the professional development of new academic staff from the Ratchadapisek Somphot Fund at Chulalongkorn University, by the Thailand Toray Science Foundation (TTSF), by the Thailand Research Fund (TRF), the Office of the

JHEP03(2014)113

Higher Education Commission (OHEC), Chulalongkorn University (MRG5680171), and by the Research Strategic plan program (A1B1), Faculty of Science, Chulalongkorn University.

TN was supported by a scholarship from the Development and Promotion of Science and Technology talent project (DPST).

MV was supported by the Marsden Fund, and by a James Cook fellowship, both administered by the Royal Society of New Zealand.

References

[1] D.N. Page, *Particle emission rates from a black hole: massless particles from an uncharged, nonrotating hole*, *Phys. Rev.* **D 13** (1976) 198 [INSPIRE].

[2] D.N. Page, *Particle emission rates from a black hole. 2. Massless particles from a rotating hole*, *Phys. Rev.* **D 14** (1976) 3260 [INSPIRE].

[3] J.D. Bekenstein and A. Meisels, *Einstein A and B coefficients for a black hole*, *Phys. Rev.* **D 15** (1977) 2775 [INSPIRE].

[4] J. Escobedo, *Greybody factors: Hawking radiation in disguise*, M.Sc. thesis, U. Amsterdam, Amsterdam The Netherlands (2008).

[5] P. Boonserm and M. Visser, *Bounding the greybody factors for Schwarzschild black holes*, *Phys. Rev.* **D 78** (2008) 101502 [arXiv:0806.2209] [INSPIRE].

[6] T. Ngampitipan and P. Boonserm, *Bounding the greybody factors for non-rotating black holes*, *Int. J. Mod. Phys.* **D 22** (2013) 1350058 [arXiv:1211.4070] [INSPIRE].

[7] T. Ngampitipan and P. Boonserm, *Bounding the greybody factors for the Reissner-Nordström black holes*, *J. Phys. Conf. Ser.* **435** (2013) 012027 [arXiv:1301.7527] [INSPIRE].

[8] P. Boonserm, T. Ngampitipan and M. Visser, *Regge-Wheeler equation, linear stability and greybody factors for dirty black holes*, *Phys. Rev.* **D 88** (2013) 041502 [arXiv:1305.1416] [INSPIRE].

[9] T. Ngampitipan, P. Boonserm and M. Visser, *Rigorous bound on transmission probability for $m = 0$ scalar excitations of Kerr-Newman black holes*, in *SPC2014 (Siam Physics Congress)*, Thailand (2014).

[10] M. Visser, *Some general bounds for 1D scattering*, *Phys. Rev.* **A 59** (1999) 427 [quant-ph/9901030] [INSPIRE].

[11] P. Boonserm and M. Visser, *Transmission probabilities and the Miller-Good transformation*, *J. Phys.* **A 42** (2009) 045301 [arXiv:0808.2516] [INSPIRE].

[12] P. Boonserm and M. Visser, *Bounding the Bogoliubov coefficients*, *Annals Phys.* **323** (2008) 2779 [arXiv:0801.0610] [INSPIRE].

[13] P. Boonserm and M. Visser, *Analytic bounds on transmission probabilities*, *Annals Phys.* **325** (2010) 1328 [arXiv:0901.0944] [INSPIRE].

[14] P. Boonserm and M. Visser, *Reformulating the Schrödinger equation as a Shabat-Zakharov system*, *J. Math. Phys.* **51** (2010) 022105 [arXiv:0910.2600] [INSPIRE].

[15] V. Frolov and I.D. Novikov, *Black hole physics: basic concepts and new developments*, Kluwer, Dordrecht The Netherlands (1998) [ISBN-10:0792351452] [ISBN-13:978-0792351450].

[16] D.J. Raine and E.G. Thomas, *Black holes: an introduction*, Imperial College, London U.K. (2005) [ISBN-10:1860945880] [ISBN-13:978-1860945885].

[17] V.D. Kazazakis, *Quasi-normal modes of scalar fields in Kerr background*, M.Sc. thesis, U. Amsterdam, Amsterdam The Netherlands (2012).

[18] K.D. Kokkotas, R.A. Konoplya and A. Zhidenko, *Quasinormal modes, scattering and Hawking radiation of Kerr-Newman black holes in a magnetic field*, *Phys. Rev.* **D 83** (2011) 024031 [arXiv:1011.1843] [INSPIRE].

[19] R.A. Konoplya and A. Zhidenko, *Quasinormal modes of black holes: from astrophysics to string theory*, *Rev. Mod. Phys.* **83** (2011) 793 [arXiv:1102.4014] [INSPIRE].

[20] R.A. Konoplya and A. Zhidenko, *Massive charged scalar field in the Kerr-Newman background I: quasinormal modes, late-time tails and stability*, *Phys. Rev.* **D 88** (2013) 024054 [arXiv:1307.1812] [INSPIRE].

[21] K.D. Kokkotas and B.G. Schmidt, *Quasinormal modes of stars and black holes*, *Living Rev. Rel.* **2** (1999) 2 [gr-qc/9909058] [INSPIRE].

[22] V. Ferrari, *Stellar perturbations*, *Lect. Notes Phys.* **617** (2003) 89.

[23] L. Samuelsson and N. Andersson, *Neutron star asteroseismology. Axial crust oscillations in the Cowling approximation*, *Mon. Not. Roy. Astron. Soc.* **374** (2007) 256 [astro-ph/0609265] [INSPIRE].

[24] V. Ferrari, *Gravitational waves from perturbed stars*, *Bull. Astron. Soc. India* **39** (2011) 203 [arXiv:1105.1678] [INSPIRE].

[25] E.T. Newman and A.I. Janis, *Note on the Kerr spinning particle metric*, *J. Math. Phys.* **6** (1965) 915 [INSPIRE].

[26] E.T. Newman et al., *Metric of a rotating, charged mass*, *J. Math. Phys.* **6** (1965) 918 [INSPIRE].

[27] R.P. Kerr, *Gravitational field of a spinning mass as an example of algebraically special metrics*, *Phys. Rev. Lett.* **11** (1963) 237 [INSPIRE].

[28] D.L. Wiltshire, M. Visser and S.M. Scott eds., *The Kerr spacetime: rotating black holes in general relativity*, Cambridge University Press, Cambridge U.K. (2009).

[29] M. Visser, *The Kerr spacetime: a brief introduction*, arXiv:0706.0622 [INSPIRE].

[30] B. Carter, *Hamilton-Jacobi and Schrödinger separable solutions of Einstein's equations*, *Commun. Math. Phys.* **10** (1968) 280 [INSPIRE].

[31] M. Sasaki and H. Tagoshi, *Analytic black hole perturbation approach to gravitational radiation*, *Living Rev. Rel.* **6** (2003) 6 [gr-qc/0306120] [INSPIRE].

[32] W.H. Press and S.A. Teukolsky, *Perturbations of a rotating black hole. II. Dynamical stability of the Kerr metric*, *Astrophys. J.* **185** (1973) 649 [INSPIRE].

[33] E.D. Fackerell and R.G. Crossman, *Spin-weighted angular spheroidal functions*, *J. Math. Phys.* **18** (1997) 1849.

JHEP03(2014)113

[34] M. Shibata, M. Sasaki, H. Tagoshi and T. Tanaka, *Gravitational waves from a particle orbiting around a rotating black hole: postNewtonian expansion*, *Phys. Rev.* **D 51** (1995) 1646 [gr-qc/9409054] [INSPIRE].

[35] H. Tagoshi, M. Shibata, T. Tanaka and M. Sasaki, *PostNewtonian expansion of gravitational waves from a particle in circular orbits around a rotating black hole: up to $O(v^8)$ beyond the quadrupole formula*, *Phys. Rev.* **D 54** (1996) 1439 [gr-qc/9603028] [INSPIRE].

[36] R.S. Maier, *The* 192 *solutions of the Heun equation*, *Math. Comput.* **76** (2007) 811 [math.CA/0408317].

[37] A. Ronveaux ed., *Heun's differential equations*, Clarendon Press, Oxford University Press, Oxford U.K. (1995) [ISBN:978-0-19-859695-0].

[38] B.D. Sleeman and V.B. Kuznetzov, *Heun functions*, in *NIST handbook of mathematical functions*, F.W.J. Olver, D.M. Lozier, R.F. Boisvert and C.W. Clark eds., Cambridge University Press, Cambridge U.K. (2010) [ISBN:978-0521192255].

[39] G. Valent, *Heun functions versus elliptic functions*, in *Difference equations, special functions and orthogonal polynomials*, World Scientific, Singapore (2007), pg. 664 [math-ph/0512006].

[40] M. Richartz, S. Weinfurtner, A.J. Penner and W.G. Unruh, *General universal superradiant scattering*, *Phys. Rev.* **D 80** (2009) 124016 [arXiv:0909.2317] [INSPIRE].

[41] P. Boonserm and M. Visser, *Quasi-normal frequencies: key analytic results*, *JHEP* **03** (2011) 073 [arXiv:1005.4483] [INSPIRE].

[42] P. Boonserm and M. Visser, *One dimensional scattering problems: a pedagogical presentation of the relationship between reflection and transmission amplitudes*, *Thai J. Math.* **8** (2010) 83.

[43] P. Boonserm and M. Visser, *Compound transfer matrices: constructive and destructive interference*, *J. Math. Phys.* **53** (2012) 012104 [arXiv:1101.4014] [INSPIRE].

[44] P. Boonserm and M. Visser, *Bounds on variable-length compound jumps*, *J. Math. Phys.* **54** (2013) 092105 [arXiv:1301.7524].

JHEP03(2014)113

International Journal of Modern Physics D
Vol. 22, No. 9 (2013) 1350058 (16 pages)

DOI: 10.1142/S0218271813500582

BOUNDING THE GREYBODY FACTORS FOR NON-ROTATING BLACK HOLES

TRITOS NGAMPITIPAN
Department of Physics, Faculty of Science, Chulalongkorn University, Bangkok 10330, Thailand
tritos.ngampitipan@gmail.com

PETARPA BOONSERM*
Department of Mathematics and Computer Science, Faculty of Science, Chulalongkorn University, Bangkok 10330, Thailand
petarpa.boonserm@gmail.com

Received 16 January 2013
Revised 8 May 2013
Accepted 8 May 2013
Published 12 June 2013

Semiclassical black holes emit radiation called Hawking radiation. Such radiation, as seen by an asymptotic observer far outside the black hole, differs from the original radiation near the horizon of the black hole by a redshift factor and the so-called "greybody factor." In this paper, we concentrate on the greybody factor; various bounds for the greybody factors of non-rotaging black holes are obtained, concentrating primarily on charged Reissner–Nordström (RN) and RN de Sitter black holes. These bounds can be derived using a 2×2 transfer matrix formalism. It is found that the charges of black holes act as efficient barriers. Furthermore, adding extra dimensions to spacetime can shield Hawking radiation. Finally, it is also found that the cosmological constant can increase the emission rate of Hawking radiation.

Keywords: Hawking radiation; greybody factor; bounding; Reissner–Nordström black holes; charged dilatonic black holes.

PACS Number(s): 04.50.Gh, 04.60.−m, 04.70.Dy, 04.20−q, 02.40.−k

1. Introduction

Classically, a black hole is associated with the concept that anything which enters the gravitational field of a black hole cannot escape. In 1974, Stephen Hawking,

*Corresponding author.

however, showed that semi-classically a black hole could indeed emit quantum radiation, an effect which became known as Hawking radiation.[1] This effect was derived by studying quantum field theory in a black hole background. In the context of quantum field theory, creation and annihilation of particles are possible. If pair production occurs near a black hole horizon, one can picture Hawking radiation as one of the particles from pair production falling in, with the other moving away from the black hole. An observer outside the black hole would see this particle as Hawking radiation. But according to general relativity, a black hole curves spacetime around it. This nontrivial spacetime behaves as gravitational potential under which particles move. Some of them are reflected back into the black hole and others are transmitted out of the black hole. Therefore, Hawking radiation seen by an observer far outside the black hole differs from radiation which has not yet been scattered by the gravitational potential. This difference can be measured by the so-called "greybody factor."

There has been a number of studies devoted to calculating these greybody factors. Some used the WKB approximation to calculate the greybody factors of the four-dimensional Schwarzschild and Reissner–Nordström (RN) black holes.[2–4] Some solved the wave equation in a black hole background by various approximations.[5–7] However, there is a rather different analytic technique to derive rigorous bounds on the greybody factors.[8–10] By using this method, bounds on the greybody factors of the four-dimensional Schwarzschild black holes was obtained in Ref. 11. In this paper, we extend the analysis and derive rigorous bounds for the greybody factors of the four-dimensional RN black holes, the higher-dimensional Schwarzschild–Tangherlini black holes, the charged dilatonic black holes in $(2+1)$ dimensions, and the charged dilatonic black holes in $(3+1)$ dimensions.

2. The RN Black Holes

The RN metric is given by

$$ds^2 = -\Delta dt^2 + \Delta^{-1} dr^2 + r^2 d\Omega^2, \tag{1}$$

where $d\Omega^2 = d\theta^2 + \sin^2\theta d\phi^2$ and

$$\Delta = 1 - \frac{2GM}{r} + \frac{G(Q^2 + P^2)}{r^2}. \tag{2}$$

The Schrödinger-like equation governing the modes is given by

$$\frac{d^2\psi}{dr_*^2} + [\omega^2 - V(r)]\psi = 0, \tag{3}$$

where r_* is the standard "tortoise coordinate"

$$dr_* = \frac{1}{\Delta} dr \tag{4}$$

and

$$V(r) = \frac{l(l+1)\Delta}{r^2} + \frac{\Delta \partial_r \Delta}{r}. \tag{5}$$

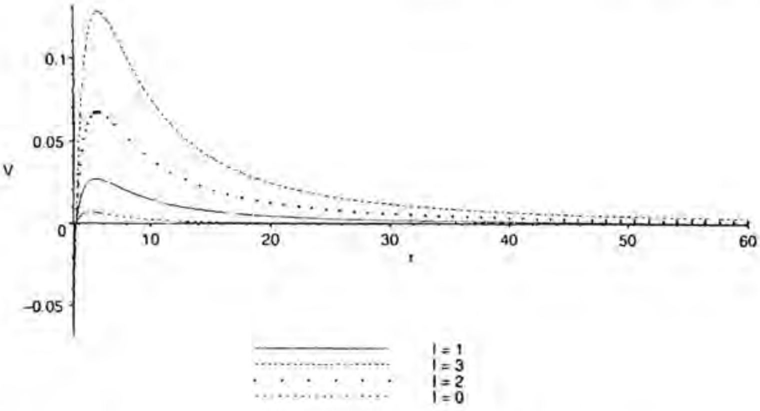

Fig. 1. The RN potential with $Q = 1$ and $M = 2$ in different angular momenta.

We can see the structure of the RN potential with $Q = 1$ and $M = 2$ from Fig. 1.

Using the analysis of Refs. 8–10, lower bounds on the transmission probabilities are given by

$$T \geq \operatorname{sech}^2\left(\int_{-\infty}^{\infty} \vartheta dr_*\right), \tag{6}$$

where

$$\vartheta = \frac{\sqrt{(h')^2 + (\omega^2 - V - h^2)^2}}{2h}, \tag{7}$$

for some positive function h. We set $h = \omega$, then

$$\begin{aligned} T &\geq \operatorname{sech}^2\left(\frac{1}{2\omega}\int_{-\infty}^{\infty} V dr_*\right) \\ &= \operatorname{sech}^2\left[\frac{1}{2\omega}\left\{\frac{l(l+1)}{GM+A} + \frac{GM+2A}{3(GM+A)^2}\right\}\right], \end{aligned} \tag{8}$$

where

$$A^2 \equiv G^2M^2 - G(Q^2 + P^2). \tag{9}$$

If the black holes have no electric charges or magnetic charges, it is found that $A = GM$ and the above bound is reduced to

$$T \geq \operatorname{sech}^2\left[\frac{2l(l+1)+1}{8GM\omega}\right], \tag{10}$$

which is exactly the bound for the Schwarzschild black holes emitting spinless particles.[11] From Fig. 2, the graph is plotted by setting $GM = 2$ and $\omega = 2$. The point $A = 2$ corresponds to the uncharged RN black hole (which is the Schwarzschild black hole). The point $A < 2$ describes the effects of charges on the bound of the greybody factor. Based on the value of A, the decrease in A corresponds to the

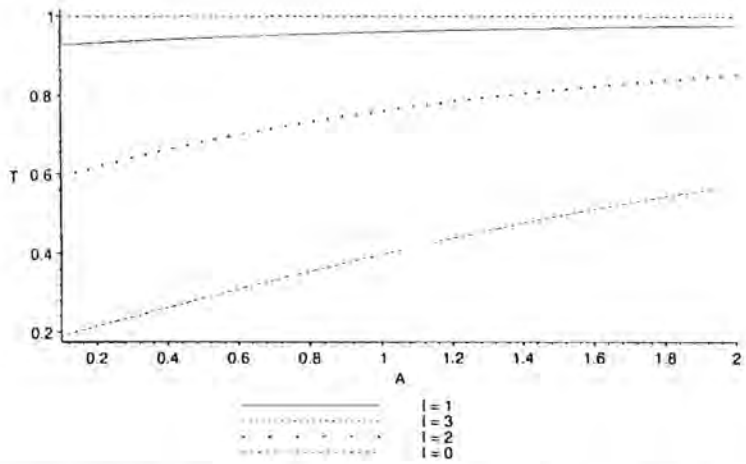

Fig. 2. Dependence of the bound of the greybody factor on the RN black hole charges in different angular momenta.

increase in the magnitude of the charges. The graph shows that when the magnitude of the charges increase, the bound of the greybody factor decreases. That is, the charges are good barriers to resist tunneling of uncharged scalar particles.[12–17] Moreover, the transmission coefficients is smaller in higher angular momenta.

By using the WKB approximation, the approximate transmission coefficient is given by[4]

$$T \approx T_{\mathrm{WKB}} = \exp\left[-\frac{2}{\hbar}\mathrm{Im}\int_a^b p(x)dx\right], \tag{11}$$

where

$$p(x) = \sqrt{2m[E - V(x)]}. \tag{12}$$

We find that

$$T_{\mathrm{WKB}} = \exp\left[-\frac{2\pi}{\hbar}\left\{2G\omega\left(M - \frac{\omega}{2}\right) - (M-\omega)\sqrt{G^2(M-\omega)^2 - G(Q^2+P^2)} + M\sqrt{G^2M^2 - G(Q^2+P^2)}\right\}\right]. \tag{13}$$

Derivation of this equation is given in Appendix A. Another WKB formula developed by Konoplya and Zhidenko can be found in Ref. 18. The bound of the greybody factor of the RN black hole from the 2×2 transfer matrix compared with one obtained from the WKB approximation is shown in Fig. 3. Now turning to an asymptotic analysis inspired by studies of quasi-normal modes, the approximate transmission coefficient for large ω is given by[19–21]

$$T \approx T_{\mathrm{asymptotic}} = \frac{e^{\beta\omega} - 1}{e^{\beta\omega} + 2 + 3e^{-\beta_I\omega}}, \tag{14}$$

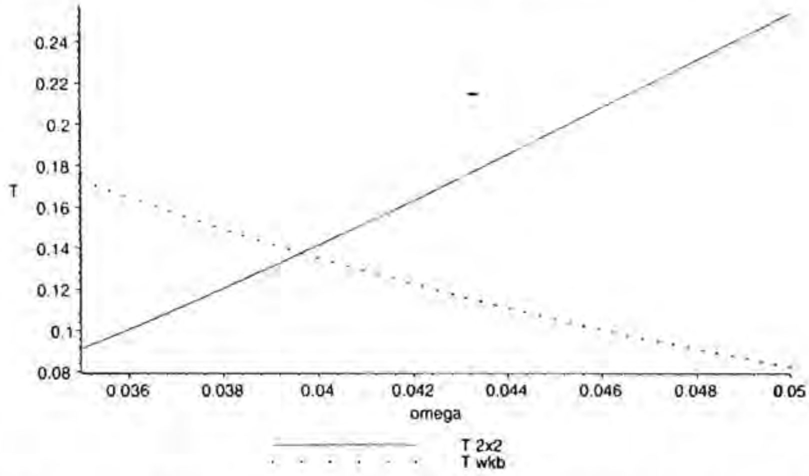

Fig. 3. Comparison of the greybody factor bound of the RN black hole from the 2×2 transfer matrix and the WKB approximation.

where

$$\begin{aligned} \beta &= \frac{8\pi M}{1 + \dfrac{Q^2}{2GM^2} + \dfrac{5Q^4}{16G^2M^4}}, \\ \beta_I &= -\frac{2\pi[GM - \sqrt{G^2M^2 - GQ^2}]^2}{\sqrt{G^2M^2 - GQ^2}}. \end{aligned} \tag{15}$$

The greybody factors obtained from the 2×2 transfer matrix formalism (Eq. (8)) are compared with the asymptotic result (Eq. (14)) on the graph shown in Fig. 4.

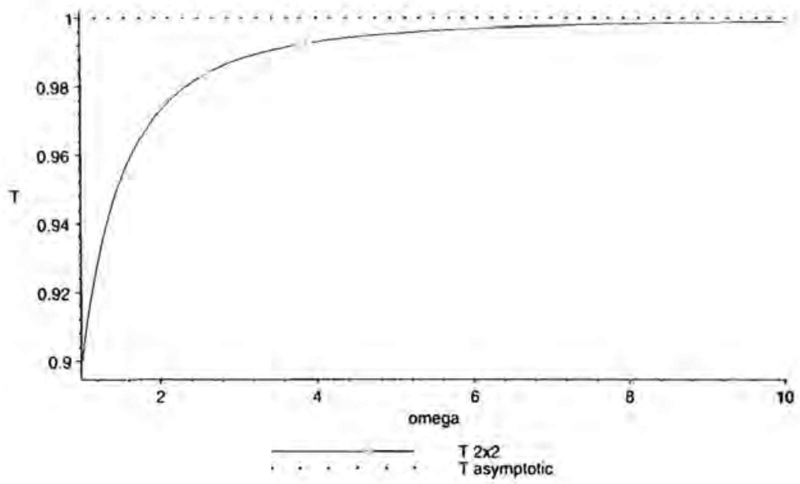

Fig. 4. Comparison of the greybody factor bound of the RN black hole from the 2×2 transfer matrix and the asymptotic result.

The graph shows that the result from the 2×2 transfer matrix is close to the asymptotic result at large ω. Moreover, the 2×2 transfer matrix gives a true lower bound.

3. The Schwarzschild–Tangherlini Black Holes

The Schwarzschild–Tangherlini metric in d dimensions is given by[7]

$$ds^2 = -\left[1 - \left(\frac{r_0}{r}\right)^{d-3}\right] dt^2 + \left[1 - \left(\frac{r_0}{r}\right)^{d-3}\right]^{-1} dr^2 + r^2 d\Omega_{d-2}^2, \tag{16}$$

where the Schwarzschild radius r_0 in d dimensions is given by

$$r_0 = \frac{16\pi GM}{(d-2)\Omega_{d-2}}, \tag{17}$$

with

$$\Omega_{d-2} = \frac{2\pi^{(d-1)/2}}{\Gamma\left(\dfrac{d-1}{2}\right)}. \tag{18}$$

The black holes in $d > 4$ dimensions with Gauss–Bonnet (GB) correction term can be found in Ref. 22. The Schrödinger-like equation is given by

$$\left[\frac{d^2}{dr_*^2} + \omega^2 - V(r)\right] r^{(d-2)/2}\varphi = 0, \tag{19}$$

where

$$dr_* = \frac{1}{f(r)} dr \tag{20}$$

and

$$V(r) = \frac{(d-2)(d-4)}{4}\frac{f^2(r)}{r^2} + \frac{(d-2)}{2}\frac{f(r)\partial_r f(r)}{r} + l(l+d-3)\frac{f(r)}{r^2}, \tag{21}$$

with

$$f(r) = 1 - \left(\frac{r_0}{r}\right)^{d-3}. \tag{22}$$

From Fig. 5, the Schwarzschild–Tangherlini potential is plotted with $l = 1$ and $GM = 1$ in various dimensions.

The lower bound on the transmission probability for $h = \omega$ is

$$\begin{aligned} T &\geq \operatorname{sech}^2\left(\frac{1}{2\omega}\int_{-\infty}^{\infty} V dr_*\right) \\ &= \operatorname{sech}^2\left[\frac{1}{2\omega}\int_{r_0}^{\infty}\left\{\frac{(d-2)(d-4)}{4}\frac{f(r)}{r^2} + \frac{(d-2)}{2}\frac{\partial_r f(r)}{r} + \frac{l(l+d-3)}{r^2}\right\} dr\right] \\ &= \operatorname{sech}^2\left[\frac{(d-2)(d-3) + 4l(l+d-3)}{8\omega r_0}\right]. \end{aligned} \tag{23}$$

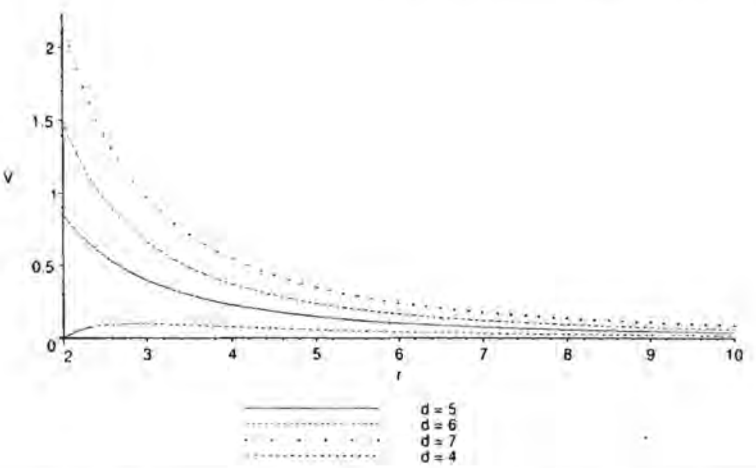

Fig. 5. The higher-dimensional potential with $l = 1$ and $GM = 1$ in various dimensions.

If $d = 4$, this bound is reduced to

$$T \geq \operatorname{sech}^2 \left[\frac{2l(l+1)+1}{8GM\omega} \right], \tag{24}$$

which is, again, exactly the bound for the four-dimensional Schwarzschild black holes emitting spinless particles. Figure 6 shows the plot between the transmission coefficients and the black hole mass in various dimensions. The graph is plotted by setting $l = 1$ and $\omega = 2$. The line $d = 4$ corresponds to the four-dimensional Schwarzschild black hole. The graph shows that when the black hole mass increases, the bound of the greybody factor also increases. However, for the same mass, the bound of the greybody factor is less in higher dimensions.[23]

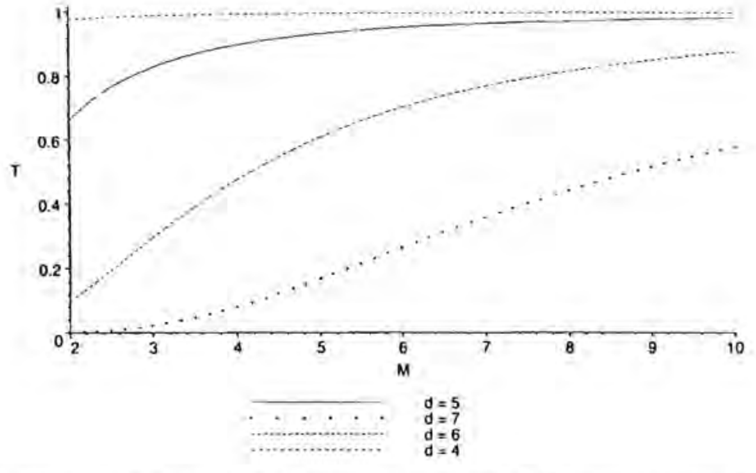

Fig. 6. Dependence of the greybody factor bound on the black hole mass in various dimensions.

4. The Charged Dilatonic Black Holes in (2 + 1) Dimensions

The charged dilatonic metric in $(2+1)$ dimensions is given by[5]

$$ds^2 = -f(r)dt^2 + \frac{4r^2}{f(r)}dr^2 + r^2 d\theta^2, \tag{25}$$

where

$$f(r) = -2Mr + 8\Lambda r^2 + 8Q^2. \tag{26}$$

For $M > 8Q\sqrt{\Lambda}$, this spacetime describes a black hole with two event horizons

$$r_\pm = \frac{M \pm \sqrt{M^2 - 64Q^2\Lambda}}{8\Lambda}. \tag{27}$$

The Schrödinger-like equation is given by

$$\left[\frac{d^2}{dr_*^2} + \omega^2 - V(r)\right] u(r) = 0, \tag{28}$$

where

$$dr_* = \frac{2r}{f(r)}dr \tag{29}$$

and

$$V(r) = -(8m^2\Lambda + 6m\Lambda) + 14\Lambda^2 r + \left(\frac{5M^2}{8} + 2m^2 M\right)\frac{1}{r} - (4MQ^2 + 8m^2Q^2)\frac{1}{r^2} + \frac{6Q^4}{r^3}. \tag{30}$$

We are only interested in r between r_- and r_+. The $(2+1)$ charged dilatonic potential is plotted with $m = 1$, $\Lambda = 0.1$, $Q = 1$ and $M = 10$ as shown in Fig. 7. The coordinate r_* can explicitly be written as

$$r_* = \frac{1}{4\Lambda(r_+ - r_-)}[r_+ \ln|r - r_+| - r_- \ln|r - r_-|], \tag{31}$$

when $r \to r_+$, $r_* \to -\infty$ and when $r \to r_-$, $r_* \to \infty$. The lower bound on the transmission probability for $h = \omega$ is

$$\begin{aligned} T &\geq \operatorname{sech}^2\left[\frac{1}{2\omega}\int_{-\infty}^{\infty} V dr_*\right] \\ &= \operatorname{sech}^2\left[\frac{1}{2\omega}\int_{r_+}^{r_-}\left\{-(8m^2\Lambda + 6m\Lambda) + 14\Lambda^2 r + \left(\frac{5M^2}{8} + 2m^2M\right)\frac{1}{r}\right.\right. \\ &\left.\left. - (4MQ^2 + 8m^2Q^2)\frac{1}{r^2} + \frac{6Q^4}{r^3}\right\}\frac{2r}{f(r)}dr\right] \end{aligned}$$

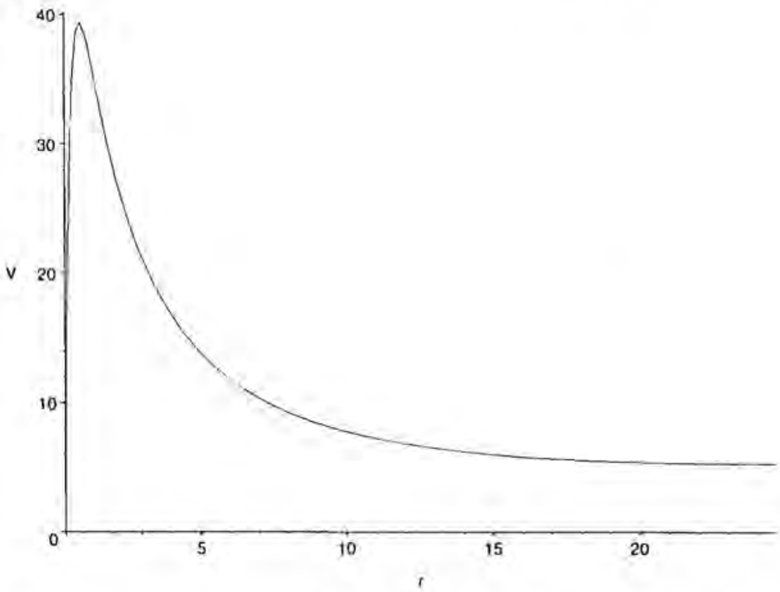

Fig. 7. The $(2+1)$ charged dilatonic potential with $m=1$, $\Lambda=0.1$, $Q=1$ and $M=10$.

$$= \operatorname{sech}^2\left[\frac{-368\Lambda m(4m+3)+644M\Lambda-2576Q^2\Lambda+115M^2+368m^2M}{60\omega\sqrt{M^2-64Q^2\Lambda}}\right.$$
$$-\frac{5\sqrt{M^2-64Q^2\Lambda}}{8\omega}+\frac{5M+16m^2}{16\omega}\ln\left(\frac{M+\sqrt{M^2-64Q^2\Lambda}}{M-\sqrt{M^2-64Q^2\Lambda}}\right)$$
$$\left.-\frac{23Q^2(3Q^2-2M-4m^2)}{15\omega\Lambda}\right]. \tag{32}$$

The approximate transmission coefficient is given by[5]

$$T \approx 1-\frac{\cosh\left[\frac{\pi\omega}{4\Lambda}-\frac{\pi}{2}\sqrt{\frac{\omega^2-8m^2\Lambda}{4\Lambda^2}-1}\right]\cosh\left[\frac{\pi\omega(r_++r_-)}{4\Lambda(r_+-r_-)}-\frac{\pi}{2}\sqrt{\frac{\omega^2-8m^2\Lambda}{4\Lambda^2}-1}\right]}{\cosh\left[\frac{\pi\omega}{4\Lambda}+\frac{\pi}{2}\sqrt{\frac{\omega^2-8m^2\Lambda}{4\Lambda^2}-1}\right]\cosh\left[\frac{\pi\omega(r_++r_-)}{4\Lambda(r_+-r_-)}+\frac{\pi}{2}\sqrt{\frac{\omega^2-8m^2\Lambda}{4\Lambda^2}-1}\right]}. \tag{33}$$

Figure 8 shows the greybody factors of the charged dilatonic black holes in $(2+1)$ dimensions obtained from the 2×2 transfer matrices (Eq. (32)) and from[5] (Eq. (33)). The graph is plotted by setting $m=1$, $M=10$, $Q=1$ and $\Lambda=0.1$. The graph shows that when the energies of the emitted particles increase, the greybody factors also increase. It can be seen that the result derived from the 2×2 transfer matrices is quite accurate when compared with the approximate result. Note that the 2×2

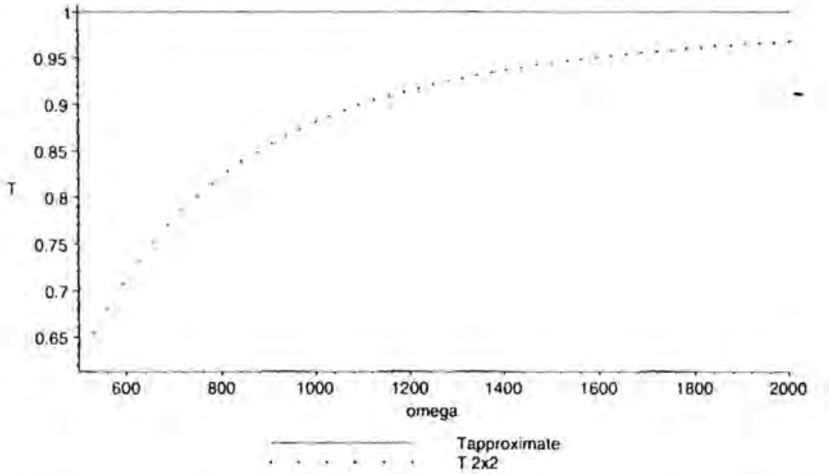

Fig. 8. Dependence of the greybody factor bound on the energies of the particles emitted from the uncharged dilatonic black holes in $(2 + 1)$ dimensions.

transfer matrices used to obtain the lower bound (32) are relatively less complex than the methods used to obtain the approximate result in Eq. (33).

Figure 9 shows the effect of the charges on the bound of the greybody factor. The graph is plotted by setting $m = 1$, $M = 10$, $\omega = 1000$ and $\Lambda = 0.1$. The graph shows that when the charges increase, the bound of the greybody factor decreases.

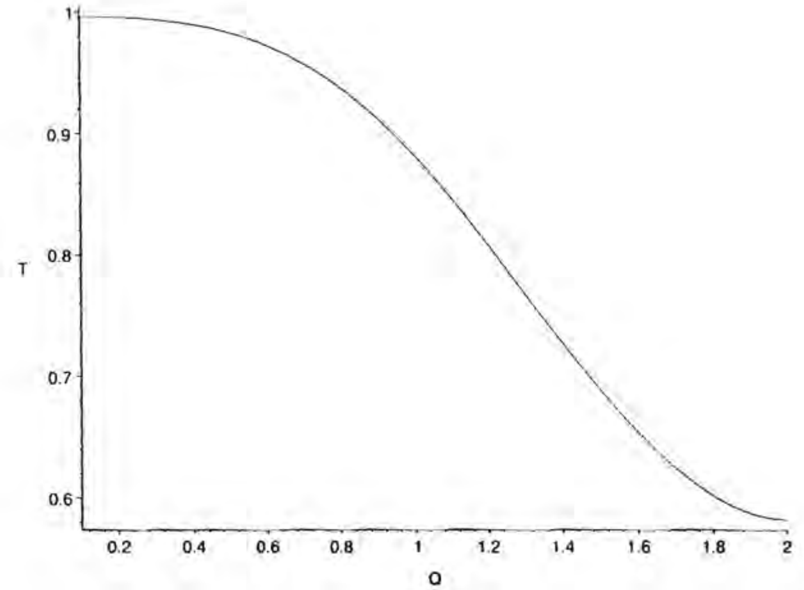

Fig. 9. Dependence of the greybody factor bound on the charges for the charged dilatonic black holes in $(2 + 1)$ dimensions.

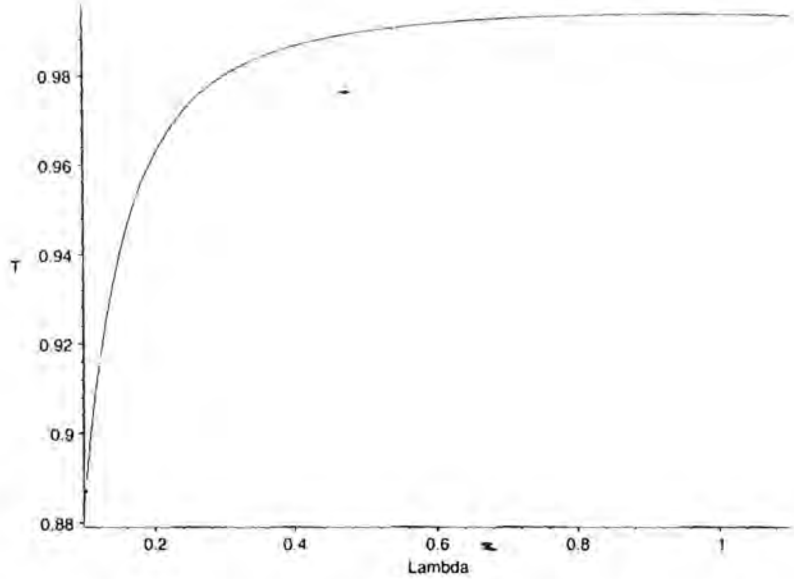

Fig. 10. Dependence of the greybody factor bound on the cosmological constant for the charged dilatonic black holes in (2 + 1) dimensions.

This result is similar to the RN black hole's result; that is, the charges behave as good barriers to resist tunneling of uncharged scalar particles.

Figure 10 shows the effect of the cosmological constant on the bound of the greybody factor. The graph is plotted by setting $m = 1$, $M = 10$, $\omega = 1000$ and $Q = 1$. The graph shows that when the value of the cosmological constant increases, the transmission coefficient also increases. That is, the cosmological constant makes the gravitational potential produced by the black hole transparent.

5. The Charged Dilatonic Black Holes in (3 + 1) Dimensions

The charged dilatonic metric in (3 + 1) dimensions is given by[6]

$$ds^2 = -f(r)dt^2 + \frac{1}{f(r)}dr^2 + R^2(r)d\Omega^2, \tag{34}$$

where

$$f(r) = 1 - \frac{r_+}{r} \quad \text{and} \quad R^2(r) = r^2\left(1 - \frac{r_-}{r}\right), \tag{35}$$

with

$$r_+ = 2M \quad \text{and} \quad r_- = \frac{Q^2}{M}. \tag{36}$$

The equation of motion for the radial part is given by

$$\frac{1}{R^2(r)}\frac{d}{dr}\left[R^2(r)f(r)\frac{du(r)}{dr}\right] + \left[\frac{\omega^2}{f(r)} - \frac{l(l+1)}{R^2(r)}\right]u(r) = 0. \tag{37}$$

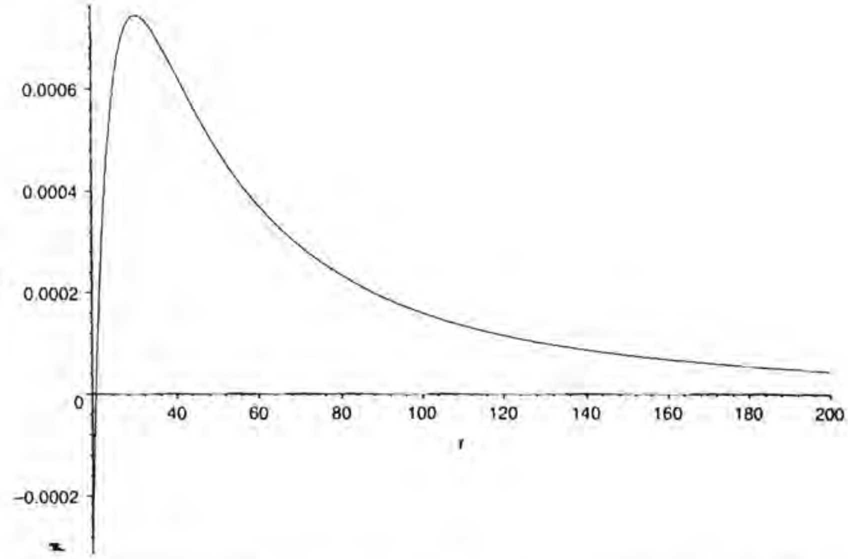

Fig. 11. The (3 + 1) charged dilatonic potential with $l = 1$, $Q = 1$ and $M = 10$.

Let

$$dr_* = \frac{1}{f(r)}dr, \tag{38}$$

then

$$\frac{d^2u(r)}{dr_*^2} + \frac{(r-r_+)(2r-r_-)}{r^2(r-r_-)}\frac{du(r)}{dr_*} + \left[\omega^2 - \frac{l(l+1)f(r)}{R^2(r)}\right]u(r) = 0. \tag{39}$$

The potential is given by

$$V(r) = \frac{l(l+1)f(r)}{R^2(r)}. \tag{40}$$

The (3 + 1) charged dilatonic potential is plotted with $l = 1$, $Q = 1$ and $M = 10$ as shown in Fig. 11. The lower bound on the transmission probability for $h = \omega$ is

$$T \geq \operatorname{sech}^2\left[\frac{1}{2\omega}\int_{-\infty}^{\infty}\frac{l(l+1)f(r)}{R^2(r)}dr_*\right] = \operatorname{sech}^2\left[\frac{1}{2\omega}\int_{r_+}^{\infty}\frac{l(l+1)}{R^2(r)}dr\right]$$
$$= \frac{4(2M^2)^{l(l+1)M/\omega Q^2}(2M^2-Q^2)^{l(l+1)M/\omega Q^2}}{[(2M^2)^{l(l+1)M/\omega Q^2} + (2M^2-Q^2)^{l(l+1)M/\omega Q^2}]^2}.$$

Figure 12 shows the effect of the charges on the bound of the greybody factor. The graph is plotted by setting $M = 10$, $\omega = 2$ and $l = 1$. The graph shows that when the charges increase, the bound of the greybody factor decreases. This result is also similar to the RN black hole's and the (2 + 1) dimensional charged dilatonic black hole's result. That is, the charges behave as good barriers to resist the tunneling of the uncharged scalar particles.

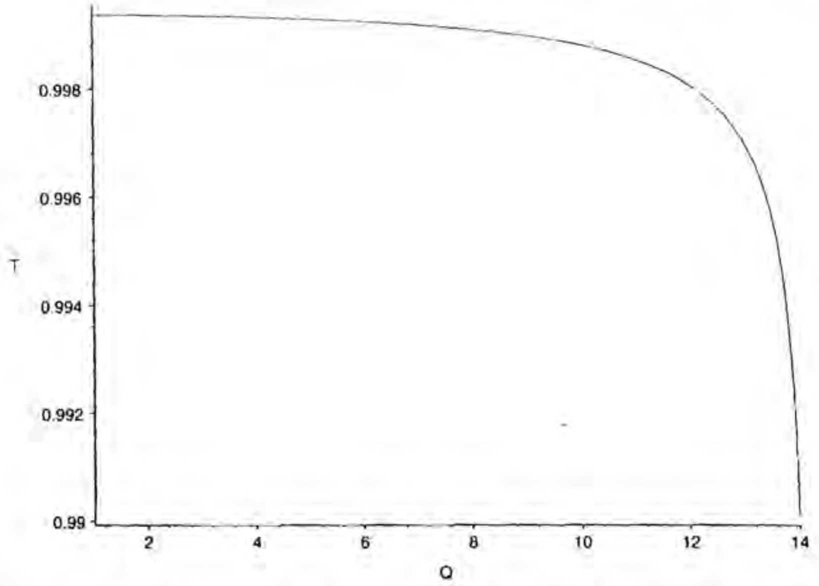

Fig. 12. Dependence of the greybody factor bound on the charges for the charged dilatonic black holes in $(3 + 1)$ dimensions.

6. Conclusion

The rigorous bounds presented in this paper only work for some potentials. Such potentials have to satisfy $V(\pm\infty) \to V_{\pm\infty}$. In this paper, the bounds have been applied to various types of black holes.

For the four-dimensional RN black holes, the charges act as a good barrier. This can also occur for the charged dilatonic black holes, both in $(2 + 1)$ and $(3 + 1)$ dimensions. For the Schwarzschild–Tangherlini black holes, a number of dimensions can shield Hawking radiation.

Acknowledgments

This research has been supported by a grant for the professional development of new academic staff from the Ratchadapisek Somphot Fund at Chulalongkorn University, by Thailand Toray Science Foundation (TTSF), by the Thailand Research Fund (TRF), the Office of the Higher Education Commission (OHEC), Chulalongkorn University and by the Research Strategic plan program (A1B1), Faculty of Science, Chulalongkorn University. P.B. was additionally supported by a scholarship from the Royal Government of Thailand. T.N. was also additionally supported by a scholarship from the Development and Promotion of Science and Technology talent project (DPST). T.N. gives special thanks to Dr. Auttakit Chatrabuti for his invaluable advice. We also thank Prof. Matt Visser for extremely useful suggestions and comments.

Appendix A. Greybody Factor from the WKB Approximation; Derivation of Eq. (13)

By using the WKB method, the approximate transmission coefficient is given by[4]

$$T \approx T_{\rm WKB} = \exp\left[-\frac{2}{\hbar}\mathrm{Im}\int_a^b p(x)dx\right], \tag{A.1}$$

where

$$p(x) = \sqrt{2m[E - V(x)]}. \tag{A.2}$$

In particular, we want to compute

$$\int_{r_{\rm in}}^{r_{\rm out}} p_r dr.$$

The radial momentum can be written as an integral

$$\int_{r_{\rm in}}^{r_{\rm out}} p_r dr = \int_{r_{\rm in}}^{r_{\rm out}} \int_0^{p_r} dp_r' dr. \tag{A.3}$$

From the Hamilton equation

$$\frac{dH}{dp_r} = \dot{r}, \tag{A.4}$$

the above integral becomes

$$\int_{r_{\rm in}}^{r_{\rm out}} p_r dr = \int_{r_{\rm in}}^{r_{\rm out}} \int_M^{M-\omega} \frac{dH}{\dot{r}} dr. \tag{A.5}$$

We change the variable H to ω'

$$\int_{r_{\rm in}}^{r_{\rm out}} p_r dr = -\int_{r_{\rm in}}^{r_{\rm out}} \int_0^{\omega} \frac{d\omega'}{\dot{r}} dr. \tag{A.6}$$

We have to know $\dot{r}$. Starting from the RN metric in Eq. (1)

$$ds^2 = -\Delta dt_{\rm RN}^2 + \Delta^{-1}dr^2 + r^2 d\Omega^2, \tag{A.7}$$

we shift the RN time $t_{\rm RN}$ by a function of r to avoid the singularities

$$\begin{aligned} t_{\rm RN} &= t + f(r), \\ dt_{\rm RN} &= dt + f'(r)dr, \\ dt_{\rm RN}^2 &= dt^2 + 2f'(r)dtdr + [f'(r)]^2 dr^2. \end{aligned}$$

Therefore,

$$ds^2 = -\Delta dt^2 - 2\Delta f'(r)dtdr - \Delta[f'(r)]^2 dr^2 + \Delta^{-1}dr^2 + r^2 d\Omega^2. \tag{A.8}$$

We choose $f(r)$ such that the coefficient of dr^2 is equal to one

$$\begin{aligned} \Delta f'(r) &= \pm\sqrt{\frac{2GM}{r} - \frac{G(Q^2+P^2)}{r^2}} \\ &= \pm\sqrt{1-\Delta}. \end{aligned} \tag{A.9}$$

Putting it in Eq. (A.8), the new metric can be written as

$$ds^2 = -\Delta dt^2 + 2\sqrt{1-\Delta}\,dt\,dr + dr^2 + r^2 d\Omega^2. \tag{A.10}$$

The radial null geodesics can be found by

$$0 = ds^2 = -\Delta dt^2 + 2\sqrt{1-\Delta}\,dt\,dr + dr^2, \tag{A.11}$$

leading to

$$\dot{r} = \begin{cases} 1-\sqrt{1-\Delta}, \\ -1-\sqrt{1-\Delta}. \end{cases} \tag{A.12}$$

Therefore, integral (A.6) becomes

$$\int_{r_{\rm in}}^{r_{\rm out}} p_r dr = -\int_{r_{\rm in}}^{r_{\rm out}} \int_0^{\omega} \frac{r}{r-x} d\omega' dr, \tag{A.13}$$

where

$$x = \sqrt{2G(M-\omega')r - G(Q^2+P^2)}. \tag{A.14}$$

Thus, $dx = -(Gr/x)d\omega'$ and we obtain

$$\begin{aligned}\int_{r_{\rm in}}^{r_{\rm out}} p_r dr &= \int_{r_{\rm in}}^{r_{\rm out}} \int_{\sqrt{2GMr-G(Q^2+P^2)}}^{\sqrt{2G(M-\omega)r-G(Q^2+P^2)}} \frac{r}{r-x}\frac{x}{Gr} dx dr \\ &= \pi i \left[2G\omega\left(M-\frac{\omega}{2}\right) - (M-\omega)\sqrt{G^2(M-\omega)^2 - G(Q^2+P^2)}\right. \\ &\quad \left. + M\sqrt{G^2M^2 - G(Q^2+P^2)}\right]. \end{aligned} \tag{A.15}$$

Therefore, from Eq. (A.1)

$$\begin{aligned} T &\approx T_{\rm WKB} \\ &= \exp\left[-\frac{2\pi}{\hbar}\left\{2G\omega\left(M-\frac{\omega}{2}\right) - (M-\omega)\sqrt{G^2(M-\omega)^2 - G(Q^2+P^2)}\right.\right. \\ &\quad \left.\left. + M\sqrt{G^2M^2 - G(Q^2+P^2)}\right\}\right]. \end{aligned} \tag{A.16}$$

References

1. S. W. Hawking, *Commun. Math. Phys.* **43** (1975) 199.
2. M. K. Parikh and F. Wilczek, *Phys. Rev. Lett.* **85** (2000) 5042, arXiv:hep-th/9907001.
3. C. H. Fleming, Hawking Radiation as Tunneling, http://www.physics.umd.edu/grt/taj/776b/fleming.pdf (2005).
4. P. Lange, Calculation of Hawking Radiation as Quantum Mechanical Tunneling, thesis, Uppsala Universitet (2007).
5. S. Fernando, *Gen. Relativ. Gravit.* **37** (2005) 461.
6. W. Kim and J. J. Oh, *J. Korean Phys. Soc.* **52** (2008) 986.
7. J. Escobedo, Greybody factors: Hawking Radiation in Disguise, M.S. thesis, University of Amsterdam (2008).

8. M. Visser, *Phys. Rev. A* **59** (1999) 427, arXiv:quant-ph/9901030.
9. P. Boonserm and M. Visser, *Ann. Phys. (NY)* **323** (2008) 2779, arXiv:0801.0610 [quant-ph].
10. P. Boonserm, Rigorous bounds on transmission, reflection, and bogoliubov coefficients, Ph.D. thesis, Victoria University of Wellington (2009), arXiv:0907.0045 [math-ph].
11. P. Boonserm and M. Visser, *Phys. Rev. D* **78** (2008) 101502, arXiv:0806.2209 [gr-qc].
12. R. Sini and V. C. Kuriakose, *Int. J. Mod. Phys. D* **18** (2009) 1, arXiv:0708.3146 [gr-qc].
13. S. Chen and J. Jing, *Phys. Lett. B* **691** (2010) 254, arXiv:1005.5601 [gr-qc].
14. C. Ding, C. Liu, J. Jing and S. Chen, *J. High Energy Phys.* **11** (2010) 146, arXiv:1007.4240 [gr-qc].
15. K. Lin and S. Z. Yang, *Astrophys. Space Sci.* **333** (2011) 369.
16. K. D. Kokkotas and R. A. Konoplya, *Phys. Rev. D* **83** (2011) 024031, arXiv:1011.1843 [gr-qc].
17. L. Yan and J. J. Liang, *Chin. Phys. Lett.* **29** (2012) 010402.
18. R. A. Konoplya and A. Zhidenko, *Phys. Rev. D* **81** (2010) 124036, arXiv:1004.1284 [hep-th].
19. A. Neitzke, Greybody factors at large imaginary frequencies, arXiv:hep-th/0304080.
20. K. Nozari and B. Fazlpour, *Acta Phys. Pol. B* **39** (2008) 1363.
21. Z. Zhai and W. Liu, *Astrophys. Space Sci.* **325** (2010) 63.
22. R. A. Konoplya and A. Zhidenko, *Phys. Rev. D* **82** (2010) 084003, arXiv:1004.3772 [hep-th].
23. P. Nicolini and E. Winstanley, *J. High Energy Phys.* 11 (2011) 75, arXiv:1108.4419 [hep-ph].

PHYSICAL REVIEW D 90, 064013 (2014)

Superradiance and flux conservation

Petarpa Boonserm*
Department of Mathematics and Computer Science, Faculty of Science, Chulalongkorn University, Bangkok 10330, Thailand

Tritos Ngampitipan†
Department of Physics, Faculty of Science, Chulalongkorn University, Bangkok 10330, Thailand

Matt Visser‡
School of Mathematics, Statistics, and Operations Research, Victoria University of Wellington, PO Box 600, Wellington 6140, New Zealand
(Received 30 July 2014; published 9 September 2014)

The theoretical foundations of the phenomenon known as superradiance still continue to attract considerable attention. Despite many valiant attempts at pedagogically clear presentations, the effect nevertheless still continues to generate some significant confusion. Part of the confusion arises from the fact that superradiance in a quantum field theory context is not the same as superradiance (superfluorescence) in some condensed matter contexts; part of the confusion arises from traditional but sometimes awkward normalization conventions, and part is due to sometimes unnecessary confusion between fluxes and probabilities. We shall argue that the key point underlying the effect is flux conservation (and, in the presence of dissipation, a controlled amount of flux nonconservation), and that attempting to phrase things in terms of reflection and transmission *probabilities* only works in the *absence* of superradiance. To help clarify the situation we present a simple exactly solvable toy model exhibiting both superradiance and damping.

DOI: 10.1103/PhysRevD.90.064013 PACS numbers: 04.70.Dy, 04.40.-b, 47.35.Rs, 98.80.Qc

I. INTRODUCTION

The phenomenon of quantum field theory (QFT)-induced superradiance has a long and quite tortuous history. Key high points are the articles by Zeldovich [1] and Manogue [2], and the more recent work by Richartz *et al.* [3,4]. There are close connections with the so-called "Klein paradox" for relativistic fermions [2,5–7], and also some significant differences. Specific applications to black hole physics include the issues explored in Refs. [3,4,8–17]. In our own research, when dealing with black hole greybody factors, we have had to deal with superradiance for Kerr, Kerr-Newman, and Myers-Perry black holes, see [18,19] and a related conference article [20].

Despite all efforts, the superradiance effect nevertheless still continues to generate significant confusion. Part of the confusion is purely linguistic—arising from the fact that superradiance in a traditional QFT context is not the same as superradiance (superfluorescence; Dicke superradiance) in traditional condensed matter contexts [21]. Part of the confusion arises from the use of utterly traditional and standard but sometimes awkward normalization conventions [2,22]. Part of the confusion is due to sometimes neglecting the necessary distinction between fluxes and probabilities.

Extending and modifying the analysis of Richartz *et al.* [3], we shall argue that the key point underlying the effect is flux conservation (and, in the presence of dissipation, a controlled amount of flux nonconservation). We shall see that attempting to phrase things in terms of reflection and transmission *probabilities* only works in the *absence* of superradiance.

To illustrate and clarify the situation we shall present a particularly simple and exactly solvable toy model, one which explicitly exhibits both superradiance and damping. While our own interest in these issues was strongly influenced by research into black hole physics, it should be emphasized that the underlying issues and related phenomena are much more general.

II. SUPERRADIANCE: BACKGROUND

One key observation is to note that superradiance never occurs when one is dealing with the Schrödinger equation, and at a minimum requires something like the Klein-Gordon equation [18,19]. For instance, in any axially symmetric stationary background, once one applies separation of variables $\psi(x,t) = \psi(r,\theta)e^{-i\omega t}e^{-im\varphi}$ to a neutral scalar field [23,24], the Klein-Gordon equation becomes

*petarpa.boonserm@gmail.com
†tritos.ngampitipan@gmail.com
‡matt.visser@msor.vuw.ac.nz

$$\Delta_2\psi(r,\theta) = [V(r,\theta) - (\omega - m\varpi(r,\theta))^2]\psi(r,\theta). \quad (1)$$

It is the trailing term in the effective potential, the $(\omega - m\varpi)^2$ term, that is responsible for the qualitatively new phenomenon of superradiance, which never occurs in ordinary nonrelativistic quantum mechanics.

The reason for this is that the Schrödinger equation is first order in time derivatives, so the effective potential for Schrödinger-like barrier-penetration problems is generically of the simple form

$$U(r) = V(r) - \omega. \quad (2)$$

In contrast, for problems based on the Klein-Gordon equation (second order in time derivatives) the qualitative structure of the effective potential is

$$U(r) = V(r) - (\omega - m\varpi)^2. \quad (3)$$

Similar phenomena occur for charged particles where one has a $(\omega - q\Phi)^2$ contribution to the effective potential. We shall soon see that it is when the quantity $\omega - m\varpi$ (or more generally, the quantity $\omega - m\varpi - q\Phi$) changes sign that the possibility of superradiance arises. (See for instance the general discussion by Richartz *et al.* [3,4].) For our purposes in Refs. [18,19] superradiance is related to the rotation of the black hole [25,26], but if the scalar field additionally carries electric charge there is a separate route to superradiance [2,27–29].

While the Dirac equation, being first order in both space and time, might seem to completely sidestep this phenomenon, it is a standard result that iterating the Dirac differential operator twice produces a Klein-Gordon-like differential equation. In terms of the Dirac matrices we have

$$\not{D}^2 = 2(\nabla - iqA)^2 + qF_{ab}[\gamma^a, \gamma^b]. \quad (4)$$

So, once one factors out the spinorial components, and concentrates attention on the second-order differential equation for the amplitude of the Dirac field, even the Klein paradox for charged relativistic fermions can be put into a closely related (though distinct) framework [2]. It is the trailing $(\omega - m\varpi - q\Phi)^2$ term in the effective potential, and more specifically the change in sign of $\omega - m\varpi - q\Phi$, that is now the harbinger of the so-called "Klein paradox." (Which, of course, is not really a paradox [2,5–7].)

III. SUPERRADIANCE: FLUXES

We shall argue that in the long run it is best to phrase things in terms of relative *fluxes* rather than *probabilities*. For a unit incoming flux, consider the equation

$$F_{\text{reflected}} + F_{\text{transmitted}} = 1 - F_{\text{dissipated}}. \quad (5)$$

As long as there is some flux conservation law, as for the Klein-Gordon equation, we can *always* say this, with these signs. [Dissipation can be dealt with by giving the potential $V(r,\theta)$ an imaginary contribution, see the discussion below.] In *some* cases this general result simplifies, and we can reduce this statement about *fluxes* to a statement about *probabilities*.

For example:

(1) If there is no dissipation ($F_{\text{dissipated}} = 0$), and if the transmitted flux is non-negative ($F_{\text{transmitted}} \geq 0$), then we can simply set $R \leftarrow F_{\text{reflected}}$ and $T \leftarrow F_{\text{transmitted}}$, and reinterpret these (relative) *fluxes* as *probabilities* with

$$R + T = 1. \quad (6)$$

(2) If there is some dissipation ($F_{\text{dissipated}} > 0$), and if the transmitted flux is non-negative ($F_{\text{transmitted}} \geq 0$), then we can set $R \leftarrow F_{\text{reflected}}$ and $T \leftarrow F_{\text{transmitted}}$ and $P_D \leftarrow F_{\text{dissipated}}$, and then reinterpret these (relative) *fluxes* as *probabilities* with P_D now being the probability of decay:

$$R + T + P_D = 1. \quad (7)$$

(3) In contrast, if $F_{\text{transmitted}} < 0$, then we *cannot* phrase things in terms of probabilities that add up to 1. We have to work in terms of fluxes. In particular in this superradiant regime we have

$$F_{\text{transmitted}} = -|t|^2 \leq 0. \quad (8)$$

Note the *sign*. It is the possibility of *negative transmitted flux* that lies at the heart of superradiance; in this situation:

$$\begin{aligned} F_{\text{reflected}} &= 1 - F_{\text{transmitted}} - F_{\text{dissipated}} \\ &= 1 + |F_{\text{transmitted}}| - F_{\text{dissipated}}. \end{aligned} \quad (9)$$

The reflected flux can then easily become over unity.

IV. SUPERRADIANCE: TOY MODEL

To see how this all works in detail, it is best to choose a highly idealized but exactly solvable model. Working in $1+1$ dimensions, consider the partial differential equation

$$[-(\partial_t - i\varpi(x))^2 + c^2\partial_x^2 - V(x)]\psi(t,x) = 0. \quad (10)$$

For simplicity we are working with a massless particle (e.g. photon), as this cuts to the heart of the matter. Adding particle rest masses is not particularly difficult (see e.g. Manogue [21]), but adds technical complications that are not central to the issues we wish to discuss.

Taking $\psi(t,x) = e^{-i\omega t}\psi(x)$ this is now equivalent to considering the ordinary differential equation (ODE)

$$c^2\partial_x^2\psi(x) = [V(x) - (\omega - \varpi(x))^2]\psi(x). \tag{11}$$

Setting $\varpi(x) \to 0$ then yields a "Schrödinger-like" equation, with no possibility of superradiance, whereas $\varpi(x) \neq 0$ is essential for superradiance.

Let us now brutally simplify the problem (in the interests of making it *analytically solvable*), by setting $V(x) \to 0$ and taking

$$\varpi(x) = \Omega\text{sign}(x). \tag{12}$$

This toy model is a tractable stand-in for generic situations where $\varpi(x)$ satisfies boundary conditions $\varpi(\pm\infty) = \pm\Omega$. We also take units where $c \to 1$. Then we are interested in

$$\partial_x^2\psi(x) = -(\omega - \Omega\text{sign}(x))^2\psi(x). \tag{13}$$

We shall soon see that for $|\omega| > |\Omega|$ we obtain ordinary scattering, with no superradiance; whereas for $|\omega| < |\Omega|$ we obtain superradiance, plus spontaneous emission.

Now for $x \neq 0$ this ODE has solutions of the form

$$\psi(t,x) = e^{-i(\omega t - k_\pm x)}; \qquad k_\pm^2 = (\omega \mp \Omega)^2. \tag{14}$$

But which root should we take? As is standard, let us consider the *group velocity*

$$v_g = \frac{\partial\omega}{\partial k_\pm} = \frac{1}{\partial k_\pm/\partial\omega} = \frac{1}{(\omega \mp \Omega)/k_\pm} = \frac{k_\pm}{\omega \mp \Omega}. \tag{15}$$

So for the mode with positive group velocity we must have $\text{sign}(k_\pm) = \text{sign}(\omega \mp \Omega)$, whence

$$k_\pm = \text{sign}(\omega \mp \Omega)|\omega \mp \Omega| = \omega \mp \Omega; \qquad v_g = +1. \tag{16}$$

This is valid for *all* ω, positive or negative. Furthermore

$$k_+k_- = \omega^2 - \Omega^2; \qquad \text{sign}(k_+k_-) = \text{sign}(\omega^2 - \Omega^2). \tag{17}$$

Note in contrast that for the phase velocity

$$v_p^\pm = \frac{\omega}{\omega \mp \Omega}. \tag{18}$$

This easily flips sign in some regions, in fact:

$$\text{sign}(v_p^\pm) = \text{sign}(\omega)\text{sign}(\omega \mp \Omega). \tag{19}$$

Now consider something incoming from the left, *and for the time being don't worry about the normalization.* Matching across the origin we have

$$e^{ik_-x} + re^{-ik_-x} \leftrightarrow te^{ik_+x}. \tag{20}$$

From continuity of the wave function and its derivative we have

$$1 + r = t; \qquad k_-(1 - r) = k_+t. \tag{21}$$

Therefore

$$k_-(1 - r) = k_-(1 + r), \tag{22}$$

implying

$$r = -\frac{k_+ - k_-}{k_+ + k_-} = -\frac{(\omega - \Omega) - (\omega + \Omega)}{(\omega - \Omega) + (\omega + \Omega)} = +\frac{\Omega}{\omega}. \tag{23}$$

This is valid for all ω, and normalization independent (*since the reflected mode automatically has the same normalization as the incoming mode*). The reflected flux (more precisely, the ratio of reflected to incident flux) is thus

$$F_{\text{reflected}} = |r|^2 = \frac{\Omega^2}{\omega^2}. \tag{24}$$

However, *if we want to fully understand transmitted flux, we need to normalize properly.*

Now consider something incoming from the left, and normalize relativistically:

$$\frac{e^{ik_-x}}{\sqrt{2|k_-|}}. \tag{25}$$

The $\sqrt{2}$ is standard for the relativistic Klein-Gordon equation, to make the flux simple. One must remember to include both $\psi^*(-i\partial_x)\psi$ *and its hermitian conjugate* when calculating the flux. (For odd historical reasons, for the nonrelativistic Schrödinger equation people do not put the $\sqrt{2}$ in the normalization of the modes, they instead put an explicit $\frac{1}{2}$ in the definition of the current.) With this normalization we now have (*note that this new amplitude "t" will be different from the previous one*)

$$\frac{e^{ik_-x}}{\sqrt{2|k_-|}} + r\frac{e^{-ik_-x}}{\sqrt{2|k_-|}} \leftrightarrow t\frac{e^{ik_+x}}{\sqrt{2|k_+|}}. \tag{26}$$

From continuity of wave function and derivative we have

$$\frac{1+r}{\sqrt{2|k_-|}} = \frac{t}{\sqrt{2|k_+|}}; \quad \frac{k_-}{\sqrt{2|k_-|}}(1-r) = \frac{k_+}{\sqrt{2|k_+|}}t. \tag{27}$$

So *we still have*

$$k_-(1 - r) = k_+(1 + r), \tag{28}$$

implying

$$r = -\frac{k_+ - k_-}{k_+ + k_-} = -\frac{(\omega - \Omega) - (\omega + \Omega)}{(\omega - \Omega) + (\omega + \Omega)} = +\frac{\Omega}{\omega}. \tag{29}$$

Consequently, as before,

$$F_{\text{reflected}} = |r|^2 = \frac{\Omega^2}{\omega^2}. \tag{30}$$

But now, for the transmission amplitude we have

$$t = \sqrt{\frac{|k_-|}{|k_-|}}\left(1+\frac{\Omega}{\omega}\right) = \sqrt{\frac{|\omega-\Omega|}{|\omega+\Omega|}}\left(\frac{\omega+\Omega}{\omega}\right). \tag{31}$$

— If $|\omega| > |\Omega|$ (the usual situation), then we see

$$t = \sqrt{\frac{\omega-\Omega}{\omega+\Omega}}\left[\frac{\omega+\Omega}{\omega}\right] = \frac{\sqrt{\omega^2-\Omega^2}}{\omega} = \text{sign}(\omega)\sqrt{1-\frac{\Omega^2}{\omega^2}}, \tag{32}$$

and so

$$|t|^2 = 1-\frac{\Omega^2}{\omega^2} \geq 0; \qquad F_{\text{reflected}} + |t|^2 = 1. \tag{33}$$

So in the usual situation we can meaningfully write

$$F_{\text{transmitted}} = |t|^2 \geq 0. \tag{34}$$

— However, if $|\omega| < |\Omega|$ (the superradiant case), then

$$\begin{aligned} t &= \sqrt{-\frac{(\omega-\Omega)}{(\omega+\Omega)}}\left(\frac{\omega+\Omega}{\omega}\right) \\ &= \frac{\sqrt{\Omega^2-\omega^2}}{\omega} \\ &= \text{sign}(\omega)\sqrt{\frac{\Omega^2}{\omega^2}-1}, \end{aligned} \tag{35}$$

and so in this situation

$$|t|^2 = \frac{\Omega^2}{\omega^2} - 1; \qquad F_{\text{reflected}} - |t|^2 = 1. \tag{36}$$

Note the sign flip in the flux conservation law. In the superradiant situation we *must* write

$$F_{\text{transmitted}} = -|t|^2 \leq 0. \tag{37}$$

To get a deeper understanding of where the minus sign came from, note that the flux for a "properly normalized" state is

$$(\text{flux}) = \left(\frac{e^{ik_\pm x}}{\sqrt{2|k_\pm|}}\right)^* \left[-i\partial_x\left(\frac{e^{ik_\pm x}}{\sqrt{2|k_\pm|}}\right)\right] + (\text{conjugate}). \tag{38}$$

But then

$$(\text{flux}) = \frac{k_\pm}{|k_\pm|} = \text{sign}(k_\pm) = \text{sign}(\omega \mp \Omega). \tag{39}$$

So the flux may not be in the direction one naively expects. We can summarize the situation by saying that in *both* cases

$$F_{\text{transmitted}} = \text{sign}(k_+k_-)|t|^2 = 1 - \frac{\Omega^2}{\omega^2}. \tag{40}$$

This formula is now equally valid for both normal and superradiant regimes, and for particles incoming from either the left or the right, and easily leads one to verify that in this situation (that is, with no dissipation)

$$F_{\text{reflected}} + F_{\text{transmitted}} = 1. \tag{41}$$

We could also write this more explicitly as

$$|r|^2 + \text{sign}(k_+k_-)|t|^2 = 1. \tag{42}$$

This is manifestly *not* conservation of *probability*; but is the perhaps more interesting statement that we have conservation of *flux*. In particular, we see that superradiance can be adequately understood using first quantization.

Warning: Because of the way some authors (specifically Manogue [2], and Richartz *et al.* [3,4], and even textbook presentations such as Messiah [22]) choose to normalize the transmission amplitude, their key result is instead

$$|r|^2 + \frac{k_-}{k_+}|t|^2 = 1. \tag{43}$$

This is not physically different, but is perhaps a little less transparent.

V. SPONTANEOUS EMISSION

To understand spontaneous emission we need to bring in some foundational ideas from second quantization. The key point in second quantization is to understand the vacuum state; choosing a vacuum state amounts to (what is called) choosing the division between "positive and negative frequencies," an issue which is now just a little more subtle than one might at first expect. Recall that $k_\pm = \omega \mp \Omega$, and that the unit flux modes are singular at $k_\pm = 0$ (that is at $\omega = \Omega$ in the right-hand half line, and at $\omega = -\Omega$ in the left-hand half line).

This observation now leads us, on the two half lines, to identify "particle modes" as

$$\frac{\exp(-i[\omega t - [\omega \mp \Omega]x)}{\sqrt{2|\omega \mp \Omega|}}; \quad \omega > \pm\Omega; \quad (\text{flux}) = +1. \tag{44}$$

$$\frac{\exp(-i[\omega t + [\omega \mp \Omega]x)}{\sqrt{2|\omega \mp \Omega|}}; \quad \omega > \pm\Omega; \quad (\text{flux}) = -1. \tag{45}$$

and to identify "vacuum modes" as

$$\frac{\exp(-i[\omega t-|\omega\mp\Omega|x)}{\sqrt{2|\omega\mp\Omega|}};\quad \omega<\pm\Omega;\quad (\text{flux})=-1. \tag{46}$$

$$\frac{\exp(-i[\omega t+|\omega\mp\Omega|x)}{\sqrt{2|\omega\mp\Omega|}};\quad \omega<\pm\Omega;\quad (\text{flux})=+1. \tag{47}$$

Once these modes have been identified, the rest of the analysis is relatively prosaic.

— For $\omega>|\Omega|$ we are dealing with particle modes on both sides of the barrier; the usual scattering rules apply, regardless of the direction the particle is initially moving in.

— For $\omega<-|\Omega|$ we are dealing with vacuum modes on both sides of the barrier; this situation is not physically relevant for our current purposes, regardless of which direction the particle is initially moving in.

— For $\omega\in(-|\Omega|,+|\Omega|)$, then on one side of the barrier you are dealing with particle modes and on the other side with vacuum modes, this is the tricky situation. Suppose for definiteness $\Omega>0$ is positive, and $\omega\in(-\Omega,+\Omega)$, then in the left-hand half-space we are dealing with particle modes, and in the right-hand half-space we are dealing with vacuum modes.

For particles incident from the left we have already done the calculation and found superradiance. In the right-hand half space we have a right-moving vacuum mode carrying a leftward flux. But what happens if a left-moving vacuum mode comes from the right and hits the barrier? It may partially reflect to a right-moving vacuum mode, but partially transmit to form a left-moving particle mode in the left-hand half-space. This is spontaneous emission. Let us do the relevant calculation. We now have

$$t\frac{\exp(-i[\omega t+k_-x])}{\sqrt{2|k_-|}}\leftrightarrow\frac{\exp(-i[\omega t+k_+x])}{\sqrt{2|k_+|}}+r\frac{\exp(-i[\omega t-k_+x])}{\sqrt{2|k_+|}}. \tag{48}$$

Continuity of wave function and derivatives now implies

$$\frac{t}{\sqrt{2|k_-|}}=\frac{1+r}{\sqrt{2|k_+|}};\qquad \frac{tk_-}{\sqrt{2|k_-|}}=\frac{(1-r)k_+}{\sqrt{2|k_+|}}. \tag{49}$$

Note several strategic sign flips compared to the previous calculation. We now have

$$(1+r)k_-=(1-r)k_+, \tag{50}$$

so that

$$r=\frac{k_+-k_-}{k_++k_-}=\frac{(\omega-\Omega)-(\omega+\Omega)}{(\omega-\Omega)+(\omega+\Omega)}=-\frac{\Omega}{\omega}. \tag{51}$$

Similarly

$$t=\sqrt{\frac{|k_-|}{|k_+|}}\left(1-\frac{\Omega}{\omega}\right)=\sqrt{\frac{\Omega+\omega}{\Omega-\omega}}\left(\frac{\omega-\Omega}{\omega}\right) \tag{52}$$

$$=\frac{\sqrt{\Omega^2-\omega^2}}{\omega}=\text{sign}(\omega)\sqrt{\frac{\Omega^2}{\omega^2}-1}. \tag{53}$$

Since the amplitude t is associated with a left-moving particle in the left half line, the flux in the left-hand half line is

$$(\text{flux})=-|t|^2=-\left(\frac{\Omega^2}{\omega^2}-1\right)<0. \tag{54}$$

The flux is leftward. Particles are being emitted by the barrier and escaping to the left. (Vacuum modes from the right are escaping from the barrier and moving to the left, the region in which they become particle modes.) Unfortunately this flux is dimensionless, it is a relative flux—the ratio of the flux of left-moving particle modes on the left half line to the flux of left-moving vacuum modes on the right half line.

To convert this to an absolute flux we note that the "unit flux" condition corresponds to

$$\frac{d^2N}{dtd\omega}=1. \tag{55}$$

That is, one particle *per unit time per unit frequency*. Then the absolute spontaneous emission rate of left-moving particles is

$$\frac{d^2N}{dtd\omega}=\left(\frac{\Omega^2}{\omega^2}-1\right);\quad \omega^2\le\Omega^2. \tag{56}$$

Note spontaneous emission occurs only within the superradiant regime.

VI. CONSISTENCY CHECK

Note that for the specific toy model we have considered, the amplitudes t and r are infinite at $\omega=0$. An observation along these lines is hidden in Manogue's article [2], buried in appendix 1, near the top of page 278.

Ultimately this infinity is a kinematic singularity due to the fact that $k_+(\omega=0)=-k_-(\omega=0)$. More generally we could consider a "shifted" effective potential by taking

$$\varpi(x)=\bar\Omega+\Delta\text{sign}(x). \tag{57}$$

Then whenever one encounters $\pm\Omega$ it would be replaced by $\Omega_\pm=\bar\Omega\pm\Delta$. It is easy to see that one now has

$$k_\pm=\omega\mp\Omega_\pm=(\omega-\bar\Omega)\pm\Delta. \tag{58}$$

and that now $k_+k_- = (\omega - \bar{\Omega})^2 - \Delta^2$. Redoing the remainder of the relevant calculations one now finds

$$|r|^2 = \frac{\Delta^2}{(\omega - \bar{\Omega})^2}; \qquad |t|^2 = \left|1 - \frac{\Delta^2}{(\omega - \bar{\Omega})^2}\right|. \tag{59}$$

Note one still has

$$|r|^2 + \mathrm{sign}(k_+k_-)|t|^2 = 1. \tag{60}$$

The kinematic infinity has now moved, from $\omega = 0$ to $\omega = \bar{\Omega}$, but the basic form of the flux conservation law is unaltered. The stability of the flux conservation law under the introduction of and shifts in $\bar{\Omega}$ is encouraging.

Indeed, the basic form of the flux conservation law cannot depend on the particular toy model, which was adopted only for simplicity of presentation. As long as well-defined asymptotic states exist in the infinite left and infinite right (so $\varpi(\pm\infty)$ must be well defined and finite), then the form of the relevant second-order ODE guarantees the existence of a transfer matrix [30,31], and also permits (with a suitable change in normalization) a Wronskian analysis along the lines of Richartz *et al.* [3].

VII. ADDING DISSIPATION

We had earlier alluded to the fact that dissipation can be modeled by adding an imaginary contribution to the potential. Let us now see how this works in practice. Set $V(x) \to i\Gamma\delta(x)$ so that we are now interested in the ODE

$$\partial_x^2\psi(x) = [i\Gamma\delta(x) - (\omega - \Omega\mathrm{sign}(x))^2]\psi(x). \tag{61}$$

For an imaginary delta-function potential the scattering calculation is an easy modification of the quite standard calculation for a real delta-function potential. The key point is that while the wave function is still continuous at the origin, there will now be a discontinuity in the derivative at the origin:

$$\partial_x\psi(0^+) - \partial_x\psi(0^-) = i\Gamma\psi(0). \tag{62}$$

A. Dissipation in Schrödinger-like situations

If we (temporarily) set $\Omega \to 0$, thereby (temporarily) banishing even the possibility of superradiance, we will be in a Schrödinger-like situation with damping. Then matching wave functions at the origin

$$\exp(+ikx) + r\exp(-ikx) \leftrightarrow t\exp(+ikx), \tag{63}$$

leads to

$$1 + r = t; \qquad [k(1 - r) - kt] = \Gamma t, \tag{64}$$

or equivalently (since now $k_\pm = k = \omega$ under the current hypotheses),

$$1 + r = t; \qquad [\omega(1 - r) - \omega t] = \Gamma t. \tag{65}$$

Thence $2\omega(1 - t) = \Gamma t$ and we have

$$t = \frac{\omega}{\omega + \frac{1}{2}\Gamma}. \tag{66}$$

Note that ω is intrinsically positive, and under normal conditions $\Gamma \geq 0$. The transmission probability is

$$T = |t|^2 = \frac{\omega^2}{(\omega + \frac{1}{2}\Gamma)^2} \in [0, 1]. \tag{67}$$

For the reflection amplitude we now obtain

$$r = t - 1 = -\frac{\frac{1}{2}\Gamma}{\omega + \frac{1}{2}\Gamma}. \tag{68}$$

Then for the reflection probability we have

$$R = |r|^2 = \frac{\frac{1}{4}\Gamma^2}{(\omega + \frac{1}{2}\Gamma)^2} \in [0, 1]. \tag{69}$$

But now $T + R \neq 1$ and in fact

$$T + R = 1 - \frac{\omega\Gamma}{(\omega + \frac{1}{2}\Gamma)^2}. \tag{70}$$

So the decay probability is identified as

$$P_D = \frac{\omega\Gamma}{(\omega + \frac{1}{2}\Gamma)^2} \in [0, 1]. \tag{71}$$

This can be viewed as the probability of absorption by the barrier. Note that

$$P_D = \frac{\Gamma T}{\omega}. \tag{72}$$

Dissipation can actually be negative (antidissipation) whenever $\Gamma < 0$ (this occurs in nonstandard situations where the imaginary part of the potential is negative). This observation is compatible with the results of the Wronskian-based analysis of Richartz *et al.* [3].

B. Dissipation and superradiance

Now let us turn Ω back on, taking $\Omega \neq 0$, and see how dissipation interacts with superradiance, and the mere possibility of having superradiance. From what we have previously seen, it is now important to focus on *fluxes*, not *probabilities*. In first-quantized formalism with the unit flux normalization we wish to match the wave functions

$$\frac{e^{ik_- x}}{\sqrt{2|k_-|}} + r\frac{e^{-ik_- x}}{\sqrt{2|k_-|}} \leftrightarrow t\frac{e^{ik_+ x}}{\sqrt{2|k_+|}}. \tag{73}$$

From continuity of the wave function, and discontinuity of the derivative, we have

$$\frac{1+r}{\sqrt{2|k_-|}} = \frac{t}{\sqrt{2|k_+|}}; \tag{74}$$

and

$$\frac{k_-}{\sqrt{2|k_-|}}(1-r) - \frac{k_+}{\sqrt{2|k_+|}}t = \frac{\Gamma}{\sqrt{2|k_+|}}t. \tag{75}$$

So *we now have*

$$k_-(1-r) - k_+(1+r) = \Gamma(1+r). \tag{76}$$

implying

$$r = -\frac{k_+ - k_- + \Gamma}{k_+ + k_- + \Gamma} = -\frac{(\omega-\Omega)-(\omega+\Omega)+\Gamma}{(\omega-\Omega)+(\omega+\Omega)+\Gamma}. \tag{77}$$

Consequently,

$$r = \frac{\Omega - \frac{1}{2}\Gamma}{\omega + \frac{1}{2}\Gamma}; \qquad F_{\text{reflected}} = |r|^2 = \frac{(\Omega-\frac{1}{2}\Gamma)^2}{(\omega+\frac{1}{2}\Gamma)^2}. \tag{78}$$

But now for the transmission amplitude we have

$$t = \sqrt{\frac{|k_+|}{|k_-|}}\left(1 + \frac{\Omega-\frac{1}{2}\Gamma}{\omega+\frac{1}{2}\Gamma}\right) = \sqrt{\frac{|\omega-\Omega|}{|\omega+\Omega|}}\left(\frac{\omega+\Omega}{\omega+\frac{1}{2}\Gamma}\right). \tag{79}$$

— If $|\omega| > |\Omega|$ (the nonsuperradiant situation), then

$$t = \sqrt{\frac{\omega-\Omega}{\omega+\Omega}}\left[\frac{\omega+\Omega}{\omega+\frac{1}{2}\Gamma}\right] = \frac{\sqrt{\omega^2-\Omega^2}}{\omega+\frac{1}{2}\Gamma}, \tag{80}$$

and so

$$|t|^2 = \frac{\omega^2-\Omega^2}{(\omega+\frac{1}{2}\Gamma)^2} \geq 0. \tag{81}$$

In this nonsuperradiant case we can meaningfully write

$$F_{\text{transmitted}} = |t|^2 = \frac{\omega^2-\Omega^2}{(\omega+\frac{1}{2}\Gamma)^2} \geq 0. \tag{82}$$

But now, due to dissipation, $F_{\text{transmitted}} + F_{\text{reflected}} \neq 1$, and we in fact have

$$\begin{aligned} F_{\text{dissipated}} &= 1 - F_{\text{transmitted}} - F_{\text{reflected}} \\ &= 1 - \frac{\omega^2-\Omega^2}{(\omega+\frac{1}{2}\Gamma)^2} - \frac{(\Omega-\frac{1}{2}\Gamma)^2}{(\omega+\frac{1}{2}\Gamma)^2} \\ &= \frac{(\Omega+\omega)\Gamma}{(\omega+\frac{1}{2}\Gamma)^2}. \end{aligned} \tag{83}$$

— In contrast, in the superradiant case, $|\omega| < |\Omega|$, a few key signs flip. We now have

$$t = \sqrt{-\frac{(\omega-\Omega)}{(\omega+\Omega)}}\left(\frac{\omega+\Omega}{\omega+\frac{1}{2}\Gamma}\right) = \frac{\sqrt{\Omega^2-\omega^2}}{\omega+\frac{1}{2}\Gamma}. \tag{84}$$

and so in this situation

$$|t|^2 = \frac{\Omega^2-\omega^2}{(\omega+\frac{1}{2}\Gamma)^2} \geq 0. \tag{85}$$

In this superradiant situation we *must* write

$$F_{\text{transmitted}} = -|t|^2 \leq 0. \tag{86}$$

— In either situation, be it superradiant or normal, we have

$$F_{\text{transmitted}} = \frac{\omega^2-\Omega^2}{(\omega+\frac{1}{2}\Gamma)^2} = \text{sign}(k_+k_-)|t|^2. \tag{87}$$

The transmitted flux can be either positive or negative. Furthermore, in either situation, be it superradiant or normal, we now see

$$F_{\text{dissipated}} = \frac{(\Omega+\omega)\Gamma}{(\omega+\frac{1}{2}\Gamma)^2}. \tag{88}$$

Note that

$$F_{\text{dissipated}} = \frac{\Gamma F_{\text{transmitted}}}{\omega-\Omega}. \tag{89}$$

So again dissipation can actually be negative (antidissipation), if $\Gamma < 0$. (That is, if the imaginary part of the potential is negative.) This is again compatible with the Wronskian-based analysis of Richartz *et al.* [3].

Finally we have

$$F_{\text{transmitted}} + F_{\text{reflected}} + F_{\text{dissipated}} = 1. \tag{90}$$

This formula is now equally valid for both normal and superradiant regimes, and for particles incoming from either the left or the right. This is manifestly *not* conservation of *probability*; but is the perhaps more interesting statement that we have conservation of *flux*. In particular, we see that superradiance can be adequately understood using first quantization.

C. Dissipation and spontaneous emission

Spontaneous emission must again be analyzed using some of the foundational ideas from second quantization. Fortunately most of the calculation can be easily carried over (with minor modifications) from the dissipation-free case. Then absolute spontaneous emission rate of particles *per unit time per unit frequency* is

$$\frac{d^2N}{dtd\omega} = \frac{\Omega^2-\omega^2}{(\omega+\frac{1}{2}\Gamma)^2}; \qquad \omega^2 \le \Omega^2. \tag{91}$$

Note spontaneous emission occurs only within the superradiant regime.

VIII. DISCUSSION

So in all relevant situations (without dissipation), with the normalizations of this article we have

$$F_{\text{reflected}} + F_{\text{transmitted}} = 1. \tag{92}$$

which we can also cast as

$$|r|^2 + \text{sign}(k_+k_-)|t|^2 = 1. \tag{93}$$

This is a very clean and convincing result, which clearly summarizes many of the most important situations. In the presence of dissipation we must instead write

$$F_{\text{reflected}} + F_{\text{transmitted}} = 1 - F_{\text{dissipated}}. \tag{94}$$

For our particular toy model

$$\partial_x^2\psi(x) = [i\Gamma\delta(x) - (\omega - \Omega\text{sign}(x))^2]\psi(x). \tag{95}$$

we were able to explicitly evaluate

$$F_{\text{reflected}} = \frac{(\Omega-\frac{1}{2}\Gamma)^2}{(\omega+\frac{1}{2}\Gamma)^2}; \qquad F_{\text{transmitted}} = \frac{\omega^2-\Omega^2}{(\omega+\frac{1}{2}\Gamma)^2}; \tag{96}$$

and

$$F_{\text{dissipated}} = \frac{(\Omega+\omega)\Gamma}{(\omega+\frac{1}{2}\Gamma)^2}. \tag{97}$$

If the last two quantities are non-negative (the first is automatically so), then these fluxes can be reinterpreted in terms of probabilities: R, T, and P_D, for reflection, transmission, and decay, respectively. That is

$$R + T + P_D = 1. \tag{98}$$

However, if either of the last two quantities is negative (either due to superradiance or antidamping), then the formulation in terms of fluxes is more fundamental, and discussion of probabilities should be completely avoided.

ACKNOWLEDGMENTS

This research has been supported by a grant for the professional development of new academic staff from the Ratchadapisek Somphot Fund at Chulalongkorn University, by the Thailand Toray Science Foundation (TTSF), by the Thailand Research Fund (TRF), by the Office of the Higher Education Commission (OHEC), Chulalongkorn University, and by the Research Strategic plan program (A1B1), Faculty of Science, Chulalongkorn University (Grant No. MRG5680171). P. B. was additionally supported by a scholarship from the Royal Government of Thailand. T. N. was also supported by a scholarship from the Development and Promotion of Science and Technology (DPST) talent project. M. V. was supported by the Marsden Fund, and by a James Cook fellowship, both administered by the Royal Society of New Zealand.

[1] Ya. B. Zel'dovich, J. Exp. Theor. Phys. **35**, 1085 (1972).
[2] C. A. Manoge, Ann. Phys. (N.Y.) **181**, 261 (1988).
[3] M. Richartz, S. Weinfurtner, A. J. Penner, and W. G. Unruh, Phys. Rev. D **80**, 124016 (2009).
[4] M. Richartz, A. Prain, S. Weinfurtner, and S. Liberati, Classical Quantum Gravity **30**, 085009 (2013).
[5] A. Hansen and F. Ravndal, Phys. Scr. **23**, 1036 (1981).
[6] N. Dombey and A. Calogeracos, Phys. Rep. **315**, 41 (1999).
[7] A. Calogeracos and N. Dombey, Contemp. Phys. **40**, 313 (1999).
[8] W. H. Press and S. A. Teukolsky, Nature (London) **238**, 211 (1972).
[9] E. Winstanley, Phys. Rev. D **64**, 104010 (2001).
[10] V. Cardoso, O. J. C. Dias, J. P. S. Lemos, and S. Yoshida, Phys. Rev. D **70**, 044039 (2004); **70**, 049903(E) (2004).
[11] S. R. Dolan, Phys. Rev. D **76**, 084001 (2007).
[12] S. Chen and J. Jing, Classical Quantum Gravity **27**, 045003 (2010).
[13] M. Kenmoku, arXiv:0809.2634.
[14] S. R. Dolan, Phys. Rev. D **87**, 124026 (2013).

[15] C. A. R. Herdeiro, J. C. Degollado, and H. F. Rúnarsson, Phys. Rev. D **88**, 063003 (2013).
[16] S. Hod, Phys. Rev. D **88**, 064055 (2013).
[17] J. C. Degollado and C. A. R. Herdeiro, Phys. Rev. D **89**, 063005 (2014).
[18] P. Boonserm, T. Ngampitipan, and M. Visser, J. High Energy Phys. 03 (2014) 113.
[19] P. Boonserm, A. Chatrabhuti, T. Ngampitipan, and M. Visser, arXiv:1405.5678.
[20] T. Ngampitipan, P. Boonserm, A. Chatrabhuti, and M. Visser, in *Proceedings of the International Conference on Mathematical Applications in Engineering, Kuala Lumpur, Malaysia, 2014* (unpublished).
[21] R. H. Dicke, Phys. Rev. **93**, 99 (1954).
[22] A. Messiah, *Quantum Mechanics* (Dover, New York, 1999).
[23] B. Carter, Commun. Math. Phys. **10**, 280 (1968).
[24] V. P. Frolov and D. Kubiznak, Phys. Rev. Lett. **98**, 011101 (2007).
[25] R. C. Myers and M. J. Perry, Ann. Phys. (N.Y.) **172**, 304 (1986).
[26] R. Emparan and H. S. Reall, Living Rev. Relativity **11**, 6 (2008).
[27] D. Ida, Y. Uchida, and Y. Morisawa, Phys. Rev. D **67**, 084019 (2003).
[28] S. Creek, O. Efthimiou, P. Kanti, and K. Tamvakis, Phys. Lett. B **656**, 102 (2007).
[29] S. Creek, O. Efthimiou, P. Kanti, and K. Tamvakis, Phys. Rev. D **75**, 084043 (2007).
[30] P. Boonserm and M. Visser, J. Math. Phys. (N.Y.) **53**, 012104 (2012).
[31] P. Boonserm and M. Visser, Thai J. Math. **8**, 83 (2010).

PHYSICAL REVIEW D **88**, 041502(R) (2013)

Regge-Wheeler equation, linear stability, and greybody factors for dirty black holes

Petarpa Boonserm*
Department of Mathematics and Computer Science, Chulalongkorn University, Bangkok 10330, Thailand

Tritos Ngampitipan†
Department of Physics, Chulalongkorn University, Bangkok 10330, Thailand

Matt Visser‡
School of Mathematics, Statistics, and Operations Research, Victoria University of Wellington, P.O. Box 600, Wellington 6140, New Zealand

(Received 14 May 2013; published 15 August 2013)

So-called "dirty" black holes are those surrounded by nonzero stress energy, rather than vacuum. The presence of the nonzero stress energy modifies key features of the black hole, such as the surface gravity, Regge-Wheeler equation, linear stability, and greybody factors in a rather nontrivial way. Working within the inverse-Cowling approximation, (effectively the test-field limit), we shall present general forms for the Regge-Wheeler equation for linearized spin 0, spin 1, and axial spin 2 perturbations on an arbitrary static spherically symmetric background spacetime. Using very general features of the background spacetime, (in particular the classical energy conditions for the stress energy surrounding the black hole), we extract several interesting and robust bounds on the behavior of such systems, including rigorous bounds on the greybody factors for dirty black holes.

DOI: 10.1103/PhysRevD.88.041502 PACS numbers: 04.70.Dy, 04.62.+v, 04.70.Bw

I. INTRODUCTION

The "cleanest" black holes to work with are undoubtedly the Schwarzschild and Reissner-Nordström black holes. However, real physical black holes are typically surrounded by matter or fields of various types, and so are embedded in an environment of nonzero stress energy. A good model for such systems is a generic static spherically symmetric spacetime with a Killing horizon. These are the so-called "dirty" black holes [1–3]. Without any loss of generality, the metric can then be put in the form

$$\mathrm{d}s^2 = -e^{-2\phi(r)}\left[1 - \frac{2m(r)}{r}\right]\mathrm{d}t^2 + \frac{\mathrm{d}r^2}{1-2m(r)/r} + r^2\mathrm{d}\Omega^2. \tag{1}$$

The Einstein equations imply

$$m' = 4\pi\rho r^2; \qquad \phi' = -\frac{4\pi(\rho + p_r)r}{1-2m(r)/r}. \tag{2}$$

We shall assume the existence of a black hole horizon such that $2m(r_H) = r_H$. Furthermore, for simplicity we assume asymptotic flatness, so that $m(\infty)$ is finite, and we can choose $\phi(\infty) = 0$. [Asymptotically de Sitter spacetimes have an additional cosmological horizon $2m(r_C) = r_C$, where we can choose $\phi(r_C) = 0$; asymptotically anti-de Sitter spacetimes exhibit extra technical complications.]

For an asymptotically flat dirty black hole the surface gravity can easily be extracted from a straightforward calculation [1]:

$$\kappa = \frac{e^{-\phi(r_H)}}{2r_H}[1 - 2m'(r_H)]. \tag{3}$$

We shall now seek to say as much as we can about these dirty black holes, without making any particular commitment as to the specific equation of state or other but the most general features of the surrounding matter.

II. CLASSICAL ENERGY CONDITIONS

While the classical energy conditions are now known to not be fundamental physics [4], (they are typically violated by semiclassical quantum effects [5–11]), they are nevertheless a good first approximation when dealing with bulk matter and/or classical field configurations. In particular for the weak and null energy conditions we have

$$\mathrm{WEC} \Rightarrow \rho \geq 0 \Rightarrow m(r_H) \leq m(r) \leq m(\infty); \tag{4}$$

$$\mathrm{NEC} \Rightarrow \rho + p_r \geq 0 \Rightarrow \phi(r_H) \geq \phi(r) \geq 0. \tag{5}$$

Note the weak energy condition (WEC) implies the null energy condition (NEC), so the WEC implies that $\kappa \leq 1/(2r_H)$, independent of the specific nature of the matter surrounding the black hole [1]. It is this sort of model-independent result that we shall now extend first to the Regge-Wheeler equation, and subsequently to explicit bounds on the greybody factors.

*petarpa.boonserm@gmail.com
†tritos.ngampitipan@gmail.com
‡matt.visser@msor.vuw.ac.nz

III. REGGE-WHEELER EQUATION

Define a generalized *tortoise coordinate* r_* by

$$\frac{\mathrm{d}r_*}{\mathrm{d}r} = e^{+\phi(r)}\left[1 - \frac{2m(r)}{r}\right]^{-1}. \quad (6)$$

Then the spacetime metric can be written as

$$\mathrm{d}s^2 = e^{-2\phi(r)}\left[1 - \frac{2m(r)}{r}\right]\{-\mathrm{d}t^2 + \mathrm{d}r_*^2\} + r^2\mathrm{d}\Omega^2, \quad (7)$$

where r is now implicitly viewed as a function of r_*.

A. Spin zero

For a minimally coupled spin zero massless scalar field it is now a simple exercise to show that linearized perturbations are governed by a simple variant of the Regge-Wheeler equation

$$\left[\frac{\mathrm{d}^2}{\mathrm{d}r_*^2} + \omega^2 - V(r_*)\right]\psi = 0, \quad (8)$$

where now

$$V(r_*) = e^{-2\phi(r)}\left[1 - \frac{2m(r)}{r}\right]\frac{\ell(\ell+1)}{r^2} + \frac{1}{r}\frac{\mathrm{d}^2 r}{\mathrm{d}r_*^2}. \quad (9)$$

If one is considering a scalar field coupled to gravity *with no other matter present* then this result is known to be correct with the provision that $\phi(r)$ and $m(r)$ be set to values consistent with a background solution of the coupled gravity-scalar equations, which in view of the "no hair" theorems implies the background is Schwarzschild. When other nontrivial matter is present the result quoted above holds only within a variant of the inverse-Cowling approximation (wherein fluctuations of the matter fields and spacetime geometry are assumed negligible compared to fluctuations in the scalar field of interest; see Samuelsson and Andersson [12] for relevant discussion). This can alternatively be rephrased as saying that we are considering linearized scalar perturbations in the test-field limit.

Application of the Einstein equations (to the background geometry) now yields

$$\frac{1}{r}\frac{\mathrm{d}^2 r}{\mathrm{d}r_*^2} = e^{-2\phi(r)}\left[1 - \frac{2m(r)}{r}\right]\left[\frac{2m(r)}{r^3} - 4\pi(\rho - p_r)\right], \quad (10)$$

whence

$$V(r_*) = e^{-2\phi(r)}\left[1 - \frac{2m(r)}{r}\right] \times \left[\frac{\ell(\ell+1)}{r^2} + \frac{2m(r)}{r^3} - 4\pi(\rho - p_r)\right]. \quad (11)$$

This is clearly consistent with, and a significant generalization of, the standard Schwarzschild result.

B. Spin one

For the spin one Maxwell field a straightforward calculation yields

$$V(r_*) = e^{-2\phi(r)}\left[1 - \frac{2m(r)}{r}\right]\frac{\ell(\ell+1)}{r^2}. \quad (12)$$

The correctness of this result may easily be verified *a posteriori* by noting that, due to the conformal invariance of the Maxwell equations in 3 + 1 dimensions, the physics can depend only on the ratio $e^{-2\phi}(1 - 2m/r)/r^2$. Comparison with the known Schwarzschild result then fixes the proportionality constant.

If one is considering a Maxwell field coupled to gravity *with no other matter present* then this result is known to be correct with the provision that $\phi(r)$ and $m(r)$ be set to values consistent with a background solution of the coupled Einstein-Maxwell equations, which in view of the no hair theorems implies the background is Reissner-Nordström. When other nontrivial matter is present the result quoted above holds only within a variant of the inverse-Cowling approximation (wherein fluctuations of the matter fields and spacetime geometry are assumed negligible compared to fluctuations in the Maxwell field). This can be rephrased as saying that we are considering linearized Maxwell perturbations in the test-field limit.

C. Spin two axial

For the case of spin two axial perturbations the calculation is somewhat tedious. For perfect fluid stars (rather than black holes) there is general agreement that [13–15]

$$V(r_*) = e^{-2\phi(r)}\left[1 - \frac{2m(r)}{r}\right] \times \left[\frac{\ell(\ell+1)}{r^2} - \frac{6m(r)}{r^3} + 4\pi(\rho - p)\right]. \quad (13)$$

Here p is the isotropic pressure; $p = p_r = p_t$ for perfect fluids. For the specific case of boson stars, (with their intrinsically anisotropic stresses), there is a very similar result involving the radial pressure p_r [16]:

$$V(r_*) = e^{-2\phi(r)}\left[1 - \frac{2m(r)}{r}\right] \times \left[\frac{\ell(\ell+1)}{r^2} - \frac{6m(r)}{r^3} + 4\pi(\rho - p_r)\right]. \quad (14)$$

Furthermore, for generic stars supported by anisotropic stress, and subject to the inverse-Cowling approximation, (wherein fluctuations of the matter fields are assumed negligible compared to fluctuations in the spacetime geometry), Samuelsson and Andersson have argued that the above potential (14) retains its validity [12].

Note that applying the Einstein equations to the background geometry we can rewrite (14) as

$$V(r_*) = e^{-2\phi(r)}\left[1 - \frac{2m(r)}{r}\right]\left[\frac{\ell(\ell+1)}{r^2} - \frac{4m(r)}{r^3}\right] - \frac{1}{r}\frac{d^2 r}{dr_*^2}. \tag{15}$$

Formally there is no obstruction to now applying this result to other situations such as wormholes or dirty black holes. (The traversable wormhole calculations of S.-W. Kim [17–19] likewise implicitly apply a version of the inverse-Cowling approximation, and provide another consistency check on the above.)

D. Spins zero, one, and two

Now collecting all these results, we can for $S \in \{0, 1, 2\}$ write the Regge-Wheeler potential in a unified form as

$$V(r_*) = e^{-2\phi(r)}\left[1 - \frac{2m(r)}{r}\right]\left[\frac{\ell(\ell+1)}{r^2} - \frac{S(S-1)2m(r)}{r^3}\right] + \frac{1-S}{r}\frac{d^2 r}{dr_*^2}. \tag{16}$$

Equivalently:

$$V(r_*) = e^{-2\phi(r)}\left[1 - \frac{2m(r)}{r}\right]\left[\frac{\ell(\ell+1)}{r^2} + \frac{(1-S^2)2m(r)}{r^3} - (1-S)4\pi(\rho - p_r)\right]. \tag{17}$$

We now have a very general version of the Regge-Wheeler potential simultaneously applicable (within the inverse-Cowling approximation) to minimally coupled massless scalars, Maxwell fields, and axial perturbations of the spacetime geometry—for arbitrary static spherically symmetric spacetimes—and so in particular applicable to (static spherically symmetric) dirty black holes.

IV. STABILITY CONSIDERATIONS

It is well known that spacetime is linearly stable against oscillations of this type (working within the inverse-Cowling approximation) if and only if the Regge-Wheeler equation has no "negative energy" bound states, (which would correspond to pure imaginary eigenfrequencies). A *sufficient* condition for stability is $V(r_*) \geq 0$. (Thus stability is automatic for $S = 1$, and will need a little further thought for $S = 0$ and $S = 2$.) Furthermore, in view of Simon's theorem on the existence of bound states [20], a *necessary* condition for stability is $\int_{-\infty}^{+\infty} V(r_*) dr_* \geq 0$. This same integral also appears in a rather different context—it controls one of the very general and simple lower bounds one can place on the greybody factors [21]. For this reason we will merge the stability discussion with that below.

V. TRANSMISSION BOUNDS

For one-dimensional potential scattering there are a number of very general and robust bounds that can be placed on the transmission and reflection probabilities [22]. Further developments in generic contexts can be found in [23–26]. For specific applications to black hole greybody factors see [21], and further developments in [27,28]. Among the various bounds one can develop, two particularly simple ones stand out. Firstly [21,22],

$$T(\omega) \geq \mathrm{sech}^2\left\{\frac{1}{2\omega}\int_{-\infty}^{+\infty} V(r_*) dr_*\right\}. \tag{18}$$

Secondly, for any (possibly even rather crude) upper bound on the Regge-Wheeler potential of the form

$$\forall r_* \quad V(r_*) \leq V_* \leq \omega^2, \tag{19}$$

we have [21]

$$T(\omega) \geq 1 - \frac{V_*^2}{(2\omega^2 - V_*)^2} \geq 1 - \frac{V_*^2}{\omega^4}. \tag{20}$$

The second bound is the more constraining at ultrahigh frequencies, while the first bound continues to hold for arbitrarily low frequencies.

We make no particular claim that these bounds are in any sense optimal, but they are certainly robust, and make absolutely minimal assumptions regarding the form of the Regge-Wheeler potential (and so implicitly make absolutely minimal assumptions regarding the nature of the stress-energy tensor surrounding the black hole).

A. Exponential bound

Consider the integral $\int_{-\infty}^{+\infty} V(r_*) dr_*$. This can be bounded in the following manner: Observe

$$V(r_*) dr_* = e^{-\phi(r)}\left[\frac{\ell(\ell+1)}{r^2} - \frac{S(S-1)2m(r)}{r^3}\right] dr + \frac{(1-S)}{r}\frac{d}{dr}\left[e^{-\phi(r)}\left(1 - \frac{2m(r)}{r}\right)\right] dr, \tag{21}$$

which, (temporarily suppressing the argument r), equals

$$e^{-\phi}\left[\frac{\ell(\ell+1)}{r^2} - \frac{S(S-1)2m}{r^3} + \frac{(1-S)}{r^2}\left(1 - \frac{2m}{r}\right)\right] dr + (1-S)\frac{d}{dr}\left[\frac{1}{r}e^{-\phi}\left(1 - \frac{2m}{r}\right)\right] dr. \tag{22}$$

Then, in view of assumed boundary conditions at r_H and at spatial infinity, the total derivative term drops out of the integral so we have (still an exact result)

$$\int_{r_H}^{\infty} \frac{e^{-\phi}}{r^2}\left[\ell(\ell+1) + (1-S) - (S-1)^2\frac{2m}{r}\right] dr. \tag{23}$$

We shall now bound this integral from above and below.

On the one hand, merely from the definition of horizon, we must have $2m(r)/r < 1$ for $r > r_H$. Therefore perturbative sectors, and with consequent massive loss of generality. Finally, an extension to spin two polar perturbations described by a generalized Zerilli-type equation is in principle certainly possible (see for instance [19]), but is mathematically somewhat messier.

ACKNOWLEDGMENTS

P. B. was supported by a grant for the professional development of new academic staff from the Ratchadapisek Somphot Fund at Chulalongkorn University, by the Thailand Toray Science Foundation (TTSF), by the Thailand Research Fund (TRF), and by the Research Strategic plan program (A1B1), Faculty of Science, Chulalongkorn University. T. N. was supported by a scholarship from the Development and Promotion of Science and Technology talent project (DPST). M. V. was supported by the Marsden Fund, and by a James Cook fellowship, both administered by the Royal Society of New Zealand.

[1] M. Visser, Phys. Rev. D **46**, 2445 (1992).
[2] M. Visser, Phys. Rev. D **48**, 583 (1993).
[3] M. Visser, Phys. Rev. D **48**, 5697 (1993).
[4] C. Barceló and M. Visser, Int. J. Mod. Phys. D **11**, 1553 (2002).
[5] M. Visser, Phys. Lett. B **349**, 443 (1995).
[6] M. Visser, Phys. Rev. D **54**, 5103 (1996).
[7] M. Visser, Phys. Rev. D **54**, 5116 (1996).
[8] M. Visser, Phys. Rev. D **54**, 5123 (1996).
[9] M. Visser, Phys. Rev. D **56**, 936 (1997).
[10] M. Visser, arXiv:gr-qc/9710034.
[11] E. E. Flanagan and R. M. Wald, Phys. Rev. D **54**, 6233 (1996).
[12] L. Samuelsson and N. Andersson, Mon. Not. R. Astron. Soc. **374**, 256 (2007).
[13] V. Ferrari, Lect. Notes Phys. **617**, 89 (2003).
[14] V. Ferrari, Bull. Astron. Soc. India **39**, 203 (2011).
[15] K. D. Kokkotas and B. G. Schmidt, Living Rev. Relativity **2**, 2 (1999).
[16] Y. Kojima, S. Yoshida, and T. Futamase, Prog. Theor. Phys. **86**, 401 (1991).
[17] S.-W. Kim, J. Korean Phys. Soc. **45**, 193 (2004).
[18] S.-W. Kim, Prog. Theor. Phys. Suppl. **172**, 21 (2008).
[19] S.-W. Kim, J. Korean Phys. Soc. **56**, 1644 (2010).
[20] B. Simon, Ann. Phys. (N.Y.) **97**, 279 (1976).
[21] P. Boonserm and M. Visser, Phys. Rev. D **78**, 101502 (2008).
[22] M. Visser, Phys. Rev. A **59**, 427 (1999).
[23] P. Boonserm and M. Visser, J. Phys. A **42**, 045301 (2009).
[24] P. Boonserm and M. Visser, Ann. Phys. (Amsterdam) **323**, 2779 (2008).
[25] P. Boonserm and M. Visser, Ann. Phys. (Amsterdam) **325**, 1328 (2010).
[26] P. Boonserm and M. Visser, J. Math. Phys. (N.Y.) **51**, 022105 (2010).
[27] T. Ngampitipan and P. Boonserm, Int. J. Mod. Phys. D **22**, 1350058 (2013).
[28] T. Ngampitipan and P. Boonserm, J. Phys. Conf. Ser. **435**, 012027 (2013).

AIP | Journal of Mathematical Physics

Greybody factors for Myers–Perry black holes

Petarpa Boonserm, Auttakit Chatrabhuti, Tritos Ngampitipan, and Matt Visser

Citation: Journal of Mathematical Physics **55**, 112502 (2014); doi: 10.1063/1.4901127
View online: http://dx.doi.org/10.1063/1.4901127
View Table of Contents: http://scitation.aip.org/content/aip/journal/jmp/55/11?ver=pdfcov
Published by the AIP Publishing

JOURNAL OF MATHEMATICAL PHYSICS 55, 112502 (2014)

Greybody factors for Myers–Perry black holes

Petarpa Boonserm,[1,a] Auttakit Chatrabhuti,[2,b] Tritos Ngampitipan,[2,c] and Matt Visser[3,d]

[1]*Department of Mathematics and Computer Science, Faculty of Science, Chulalongkorn University, Phayathai Road, Patumwan, Bangkok 10330, Thailand*
[2]*Particle Physics Research Laboratory, Department of Physics, Faculty of Science, Chulalongkorn University, Phayathai Road, Patumwan, Bangkok 10330, Thailand*
[3]*School of Mathematics, Statistics, and Operations Research, Victoria University of Wellington, PO Box 600, Wellington 6140, New Zealand*

(Received 9 June 2014; accepted 23 October 2014; published online 10 November 2014)

The Myers–Perry black holes are higher-dimensional generalizations of the usual $(3+1)$-dimensional rotating Kerr black hole. They are of considerable interest in Kaluza–Klein models, specifically within the context of brane-world versions thereof. In the present article, we shall consider the greybody factors associated with scalar field excitations of the Myers–Perry spacetimes, and develop some rigorous bounds on these greybody factors. These bounds are of relevance for characterizing both the higher-dimensional Hawking radiation, and the super-radiance, that is expected for these spacetimes. © *2014 AIP Publishing LLC.* [http://dx.doi.org/10.1063/1.4901127]

I. INTRODUCTION

Greybody factors modulate the absorption cross-sections of classical black holes, and alter the closely related Hawking emission[1,2] probabilities of semi-classical black holes.[3–6] Physically, the incoming or outgoing wave back-scatters off the gravitational field surrounding the black hole, leading to a non-trivial transmission coefficient. In the case of Hawking radiation, this modifies the naïve Planckian spectrum by multiplying it with a frequency-dependent greybody factor. Explicitly evaluating these greybody factors is typically an impossible task, even for the simple case of the Schwarzschild black hole.[7] In view of this difficulty, techniques for placing analytic bounds on the greybody factors have now become of some interest.[7–11] (Alternatively, one might seek to extract qualitative or numerical information.[12–14])

The bounds developed in Refs. 7–11 apply to various black holes (Schwarzschild, Reissner-Nordström, Kerr, Kerr–Newman, etc.), and are all based on a very general technique for bounding one-dimensional barrier penetration probabilities; a technique that was first developed in Ref. 15, with later formal developments to be found in Refs. 16–19, and additional related discussion in Refs. 20–23. In the current article, we shall apply the same sort of formalism to the Myers–Perry rotating black holes in $(3+1+n)$ dimensions.[24,25] The Myers–Perry black holes are particularly important in that they are the simplest of the higher-dimensional rotating black holes, being of particular interest in both Kaluza–Klein scenarios and in brane-world scenarios.

We first describe the Myers-Perry spacetime,[24,25] setting up the relevant Teukolsky equation for scalar field excitations.[26] An important part of the technical analysis is the fact that we can place positivity constraints on both the separation constant and on the effective potential; without such positivity constraints progress would be severely limited. We then analyze both the greybody factors and (when relevant) super-radiant emission as a function of the angular momentum quantum number m. While zero angular momentum ($m = 0$) serves as a good template for the other cases, there are

[a]petarpa.boonserm@gmail.com
[b]dma3ac2@gmail.com
[c]tritos.ngampitipan@gmail.com
[d]matt.visser@msor.vuw.ac.nz

some significant differences to take into account. After completing the analysis and summarizing the general case, we specialize to (3+1) dimensions to verify compatibility with the usual Kerr black hole, and also consider the specific (3+1+1) five-dimensional case which is perhaps most relevant to brane-world models. We conclude with a brief discussion of the significance of our results.

II. TEUKOLSKY EQUATION FOR SCALAR FIELDS

In setting up the formalism, it is best to first focus on the geometry of the specific spacetimes under consideration, and then analyse the technical steps involved in separation of variables, leading up to the development of the Teukolsky equation for scalar field excitations. With this in hand, one can then proceed to examination of the effective potential. For some general background on black hole perturbation theory, see Refs. 27–34.

A. Myers–Perry spacetime

The Myers–Perry geometry (with only one of the angular momentum parameters being non-zero) is described by the metric[24,25]

$$\begin{aligned} ds^2 = -dt^2 + \frac{\Sigma}{\Delta}\,dr^2 + \Sigma\,d\theta^2 + (r^2+a^2)\sin^2\theta\,d\varphi^2 \\ + \frac{\mu}{r^{n-1}\Sigma}(dt - a\sin^2\theta\,d\varphi)^2 + r^2\cos^2\theta\,d\Omega_n^2. \end{aligned} \tag{1}$$

Here,

$$\Delta = r^2 + a^2 - \frac{\mu}{r^{n-1}}, \qquad \Sigma = r^2 + a^2\cos^2\theta, \tag{2}$$

and $d\Omega_n^2$ is the line-element on the unit n-sphere S^n. We choose coordinates so that

$$d\Omega_n^2 = d\theta_1^2 + \sin^2\theta_1\,d\theta_2^2 + \sin^2\theta_1\sin^2\theta_2\,d\theta_3^2 + \cdots + \left(\prod_{i=1}^{n-1}\sin^2\theta_i\right)d\theta_n^2, \tag{3}$$

whence recursively

$$d\Omega_n^2(\theta_1,\ldots,\theta_n) = d\theta_1^2 + \sin^2\theta_1\,d\Omega_{n-1}^2(\theta_2,\ldots,\theta_n). \tag{4}$$

(Several other coordinate conventions on the n-sphere are also relatively common.) This Myers–Perry spacetime has $4+n$ dimensions, 4 of them "usual" and n "extra." This is sometimes phrased as $3+1+n$ dimensions (meaning 3 of space, 1 of time, and n "extra" Kaluza–Klein dimensions). The black hole mass M_{BH}, and angular momentum J, are defined as follows:

$$M_{BH} = \frac{(n+2)\,A_{n+2}}{16\pi G}\,\mu, \qquad J = \frac{2a}{n+2}\,M_{BH}. \tag{5}$$

Here, G denotes the gravitational constant in the $(4+n)$-dimensional space-time, and the quantity $A_{n+2} = 2\pi^{(n+3)/2}/\Gamma[(n+3)/2]$ is the area of a $(n+2)$-dimensional unit sphere. The location of the black hole horizon r_H is the solution of $\Delta(r_H)=0$, such that $\mu = r_H^{n-1}(r_H^2+a^2)$ is satisfied.

- In the specific case of $n=0$, this spacetime reduces to the standard Kerr black hole, with the usual inner and outer horizons.
- In the specific case of $n=1$, we have $\mu = r_H^2 + a^2$, so then $r_H = \sqrt{\mu - a^2}$, and the horizon exists only when $a < \sqrt{\mu}$; in fact, the horizon shrinks to zero area in the extreme limit $a \to \sqrt{\mu}$. So the case $n=1$ is somewhat different from $n>1$.
- On the other hand, in the case of $n \geq 2$, for $\mu > 0$ a unique positive solution for r_H always exists for all a. Indeed, $r_H \in (0, \mu^{1/(n+1)}]$.

B. Separation of variables

In this article, we will focus on scalar field emission from the Myers–Perry black hole. The relevant excitations can be described by the Klein–Gordon equation

$$\partial_\mu \left(\sqrt{-g}\, g^{\mu\nu}\, \partial_\nu \Phi\right) = 0. \tag{6}$$

Here, the metric determinant factorizes nicely into 4-dimensional and n-dimensional pieces. Specifically, with conventions as in Eq. (3), we have

$$\sqrt{-g} = (\Sigma\, \sin\theta) \times \left(r^n \cos^n\theta\right) \times \left(\prod_{i=1}^{n-1} \sin^{n-i}\theta_i\right), \tag{7}$$

with the trailing factor arising from the unit n-sphere.

Similar to the Kerr–Newman black hole in four dimensions, the Myers–Perry solution enjoys a hidden symmetry due to the existence of a Killing–Yano tensor.[35] In view of this, we can use the separation of variables ansatz[36,37]

$$\Phi(t, r, \theta, \varphi, \theta_1, \ldots, \theta_n) = e^{-i\omega t}\, e^{im\varphi}\, \tilde{R}_{j\ell m}(r)\, S_{\ell m}(\theta)\, Y_{jn}(\theta_1, \ldots, \theta_n). \tag{8}$$

Here, the $Y_{jn}(\theta_1, \ldots, \theta_n)$ are the quite standard hyper-spherical harmonics defined on the unit n-sphere, which satisfy the differential equation[38]

$$\Delta_{S^n} Y_{jn}(\theta_1, \ldots, \theta_n) + j(j+n-1)Y_{jn} = 0. \tag{9}$$

The important observation is that for the n-sphere the Laplacian eigenvalues are $-j(j + n - 1)$. In 4 dimensions ($n \to 0$), these hyperspherical harmonics reduce to trivial constants (and $j \to 0$). In 5 dimensions ($n \to 1$), they are simply sines and cosines. If one wishes an explicit rendition of the Laplacian on the n-sphere then, with coordinates as in Eq. (3), we have

$$\sum_{k=1}^{n} \frac{1}{\prod_{i=1}^{n-1} \sin^{n-i}\theta_i} \partial_{\theta_k} \left[\left(\prod_{i=1}^{n-1} \sin^{n-i}\theta_i\right) \frac{\partial_{\theta_k} Y_{jn}}{\prod_{i=1}^{k-1} \sin^2\theta_i}\right] + j(j+n-1)Y_{jn} = 0. \tag{10}$$

We mention in passing that when you choose coordinates to write the n-sphere metric recursively, as in Eq. (4), then the Laplacian can also be expressed recursively

$$\Delta_{S^n} X = \frac{1}{\sin^{n-1}\theta_1} \frac{\partial}{\partial\theta_1}\left(\sin^{n-1}\theta_1\, \frac{\partial X}{\partial\theta_1}\right) + \frac{1}{\sin^2\theta_1}\, \Delta_{S^{n-1}} X. \tag{11}$$

In contrast to the hyper-spherical harmonics defined on the hyper-sphere S^n, the spheroidal harmonics $S_{\ell m}(\theta)\, e^{im\varphi}$ are defined on the two angular variables associated with the "usual" 4-dimensional part of the spacetime. They are the appropriate generalization of the standard spherical harmonics $Y_{\ell m}(\theta, \phi)$. The spheroidal harmonics satisfy the differential equation[12]

$$\left\{\frac{1}{\sin\theta\cos^n\theta} \frac{d}{d\theta}\left[\sin\theta\cos^n\theta \frac{d}{d\theta}\right] - \left(\omega a \sin\theta - \frac{m}{\sin\theta}\right)^2 - \frac{j(j+n-1)}{\cos^2\theta} + \lambda_{j\ell m}\right\} S_{\ell m}(\theta) = 0. \tag{12}$$

Note that going to 4 dimensions corresponds to setting $n \to 0$ *and* setting $j \to 0$, in which case this differential equation reduces to that for the Kerr (or Kerr–Newman) geometry as given in Ref. 11. These spheroidal harmonics are very closely related both to the Heun functions,[39–42] and to the hyper-spherical harmonics.[38,43]

The separation constant $\lambda_{j\ell m}$ in this spheroidal differential equation is positive. To see this let us define a new variable by $du = \sin\theta\cos^n\theta\, d\theta$, then

$$\frac{d}{d\theta} = \frac{du}{d\theta}\frac{d}{du} = \sin\theta\cos^n\theta \frac{d}{du}. \tag{13}$$

Therefore,

$$\frac{1}{\sin\theta\cos^n\theta} \frac{d}{d\theta}\left[\sin\theta\cos^n\theta \frac{dS(\theta)}{d\theta}\right] = \frac{d}{du}\left[\left(\sin\theta\cos^n\theta\right)^2 \frac{dS(\theta)}{du}\right]. \tag{14}$$

Then the angular equation (12) for the spheroidal harmonics becomes

$$\frac{\mathrm{d}}{\mathrm{d}u}\left[\left(\sin\theta\cos^n\theta\right)^2\frac{\mathrm{d}S(\theta)}{\mathrm{d}u}\right] = \left[\left(\omega a\sin\theta - \frac{m}{\sin\theta}\right)^2 + \frac{j(j+n-1)}{\cos^2\theta} - \lambda_{j\ell m}\right]S(\theta). \quad (15)$$

Multiplying the above equation by $S(\theta)$ and integrating both sides over u yields

$$\int S(\theta)\frac{\mathrm{d}}{\mathrm{d}u}\left[\left(\sin\theta\cos^n\theta\right)^2\frac{\mathrm{d}S(\theta)}{\mathrm{d}u}\right]\mathrm{d}u$$
$$= \int\left[\left(\omega a\sin\theta - \frac{m}{\sin\theta}\right)^2 + \frac{j(j+n-1)}{\cos^2\theta} - \lambda_{j\ell m}\right]S^2(\theta)\,\mathrm{d}u. \quad (16)$$

Integrate the left hand side by parts, using periodicity to discard boundary terms, and then rearrange to obtain

$$\lambda_{j\ell m}\int S^2(\theta)\,\mathrm{d}u = \int\left[\left(\omega a\sin\theta - \frac{m}{\sin\theta}\right)^2 + \frac{j(j+n-1)}{\cos^2\theta}\right]S^2(\theta)\,\mathrm{d}u$$
$$+\int\left[\left(\sin\theta\cos^n\theta\right)^2\left(\frac{\mathrm{d}S(\theta)}{\mathrm{d}u}\right)^2\right]\mathrm{d}u. \quad (17)$$

Now the right hand side of this equation is manifestly positive, as is the factor $\int S^2\,\mathrm{d}u$ on the left hand side. Therefore, the separation constant $\lambda_{j\ell m}$ is guaranteed to be positive.

C. Effective potential

We now construct the effective potential, starting from the radial part of the variable-separated Klein–Gordon equation.[12–14] We have

$$\left\{\frac{1}{r^n}\frac{\mathrm{d}}{\mathrm{d}r}\left[r^n\Delta\frac{\mathrm{d}}{\mathrm{d}r}\right] + \frac{[(r^2+a^2)\omega - ma]^2}{\Delta} - \frac{j(j+n-1)a^2}{r^2} - \lambda_{j\ell m}\right\}\tilde{R}_{j\ell m}(r) = 0. \quad (18)$$

Let us now define a new radial mode function

$$\tilde{R}_{j\ell m}(r) = \frac{r^{-\frac{n}{2}}R_{j\ell m}(r)}{\sqrt{r^2+a^2}}. \quad (19)$$

It is now a quite standard calculation to show that the radial Teukolsky equation (the Regge–Wheeler-like equation governing the radial modes), is given by Refs. 12–14

$$\left\{\frac{\mathrm{d}^2}{\mathrm{d}r_*^2} - U_{j\ell m}(r)\right\}R_{j\ell m}(r) = 0, \quad (20)$$

where r_* is the standard "tortoise coordinate"

$$\mathrm{d}r_* = \frac{r^2+a^2}{\Delta(r)}\,\mathrm{d}r. \quad (21)$$

Note that the tortoise coordinates can be expressed as

$$r_* = \int_{r_H}^{r}\frac{r^2+a^2}{\Delta(r)}dr \sim A_n\ln(r-r_H) + B_n(r), \quad (22)$$

where the exact expressions for the coefficients A_n and functions $B_n(r)$ depend on the number of extra dimensions n. However, we can quite generally observe that as $r \to r_H$ we have $r_* \to -\infty$, and as $r \to \infty$ we have $r_* \to \infty$. So the region $r > r_H$ outside the black hole, (the domain of outer communication), maps into the entire real line $-\infty \le r_* \le +\infty$ in terms of the tortoise coordinate.

The Teukolsky potential (sometimes called the Regge–Wheeler–Teukolsky potential), is now seen to be

$$U_{j\ell m}(r) = \frac{\Delta(r)}{\left(r^2+a^2\right)^2}\left[\lambda_{j\ell m} + \frac{j(j+n-1)a^2}{r^2} + \frac{n(n-2)\Delta(r)}{4r^2} + \frac{n\Delta'(r)}{2r} - \frac{3r^2\Delta(r)}{(r^2+a^2)^2} + \frac{[r\Delta(r)]'}{r^2+a^2}\right] - \left(\omega - \frac{ma}{r^2+a^2}\right)^2. \tag{23}$$

Note that for $j = n = 0$ this reduces to the Teukolsky potential for the ordinary Kerr black hole in 4 dimensional space-time. (See Ref. 11.) For purposes of calculation, we now define quantities

$$\varpi(r) = \frac{a}{a^2+r^2}, \tag{24}$$

and more specifically

$$\Omega_H = \frac{a}{a^2+r_H^2}. \tag{25}$$

Here, $\varpi(r)$ is related to frame dragging, while Ω_H is the "angular velocity" of the event horizon.[11] We can now re-express the Teukolsky potential as

$$U_{j\ell m}(r) = V_{j\ell m}(r) - (\omega - m\varpi)^2, \tag{26}$$

with

$$V_{j\ell m}(r) = \frac{\Delta(r)}{\left(r^2+a^2\right)^2}\left[\lambda_{j\ell m} + \frac{j(j+n-1)a^2}{r^2} + \frac{n(n-2)\Delta(r)}{4r^2} + \frac{n\Delta'(r)}{2r} - \frac{3r^2\Delta(r)}{(r^2+a^2)^2} + \frac{[r\Delta(r)]'}{r^2+a^2}\right]. \tag{27}$$

D. Positivity properties

To show positivity of $V_{j\ell m}(r)$, we start by noting that $\Delta(r) > 0$ outside the horizon (that is for $r > r_H$). This is standard for $n = 0$, and trivial for $n = 1$. For $n \geq 1$, we generically re-express $\Delta(r)$ as

$$\begin{aligned}\Delta(r) &= r^2 + a^2 - r^{1-n}\mu \\ &= r^2 + a^2 - (r/r_H)^{1-n}(r_H^2 + a^2) \\ &\geq (r_H^2 + a^2)\left(1 - (r_H/r)^{n-1}\right).\end{aligned} \tag{28}$$

Since $r \geq r_H$, we can see that $\Delta(r) \geq 0$ for $n \geq 1$. Using this result, we make the following observations. First, for $n \geq 1$ we have

$$\begin{aligned}\frac{[r\Delta(r)]'}{r^2+a^2} - \frac{3r^2\Delta(r)}{(r^2+a^2)^2} &\propto [r\Delta(r)]'(r^2+a^2) - 3r^2\Delta(r) \\ &= a^2(r^2+a^2) + \frac{\mu}{r^{n-1}}\left[(n+1)r^2 + (n-2)a^2\right] \\ &= a^2\Delta(r) + \frac{\mu}{r^{n-1}}\left[(n+1)r^2 + (n-1)a^2\right] \\ &\geq 0.\end{aligned} \tag{29}$$

Note that the equivalent result for $n = 0$ was already derived in Ref. 11 for the Kerr–Newman spacetime. Second, for $n \geq 0$, we also have

$$\begin{aligned}\frac{n(n-2)\Delta(r)}{4r^2} + \frac{n\Delta'(r)}{2r} &\propto n\{(n-2)\Delta(r) + 2r\Delta'(r)\} \\ &= n\{(n+2)r^2 + (n-2)a^2 + n\mu r^{1-n}\}.\end{aligned} \tag{30}$$

Now for $n \geq 2$ this quantity is certainly positive. For $n = 0$, this quantity is identically zero. For $n = 1$, this quantity reduces to $3r^2 - a^2 + \mu = 3r^2 - r_H^2 \geq 0$ (provided the horizon exists). In all situations, the relevant quantity is non-negative. Thus, by now combining these results with the fact that $\lambda_{j\ell m} > 0$, and the fact that both $n \geq 0$ and $j \geq 0$, we can conclude that $V_{j\ell m}(r)$ is always positive for all values of j, ℓ, m, and r.

E. Super-radiance

Now note that the effective potential is

$$U_{j\ell m}(r) = V_{j\ell m}(r) - (\omega - m\varpi)^2; \qquad V_{j\ell m}(r) \geq 0. \tag{31}$$

However, the quantity $\omega - m\varpi$ can under suitable circumstances change sign. This is the harbinger of super-radiance. Some rather-general analyses can be found in Refs. 44 and 45, while a specific analysis closely related to the current situation can be found in Ref. 11. The key point is that super-radiance is a phenomenon in which the reflected wave is larger in its amplitude than the incident wave. From mathematical point of view, super-radiance is a phenomenon in which $|r| > 1$, where r is the reflection coefficient. Super-radiance will occur once $\omega - m\varpi$ changes sign in the domain of outer communication which, given the asymptotic behaviour of ϖ, occurs whenever $0 < \omega < m\Omega_H$, that is, $m > m_* \equiv \omega/\Omega_H$. Once super-radiance occurs, the bound on the greybody factor becomes a bound on the spontaneous emission amplitude. A detailed discussion of this particular issue can be found in Ref. 11.

III. ANALYTIC BOUND FOR SCALAR TRANSMISSION

From Ref. 15 (see also Refs. 16–19 for further developments and applications), we have the extremely general result that

$$T_{j\ell m} \geq \operatorname{sech}^2\left(\int_{-\infty}^{\infty} \vartheta \, \mathrm{d}r_*\right), \tag{32}$$

where

$$\vartheta = \frac{\sqrt{[h'(r_*)]^2 + \left[U_{j\ell m}(r_*) + h^2(r_*)\right]^2}}{2h(r_*)}, \tag{33}$$

for any positive function $h(r_*)$. Equivalently,

$$\vartheta = \frac{\sqrt{[h'(r_*)]^2 + \left[V_{j\ell m}(r_*) - (\omega - m\varpi)^2 + h^2(r_*)\right]^2}}{2h(r_*)}. \tag{34}$$

We shall now use the positivity properties of $\lambda_{j\ell m}$ and $V_{j\ell m}$, together with the super-radiant/non-super-radiant distinction, to systematically analyse this bound in various cases. In particular

- The modes $m < m_* \equiv \omega/\Omega_H$ are not super-radiant.
- The modes $m \geq m_* \equiv \omega/\Omega_H$ are super-radiant.

In situations where super-radiance occurs, in addition to the greybody factor $T_{j\ell m}$, there is a closely related spontaneous emission rate which satisfies the bound[11]

$$\Gamma_{j\ell m} \leq \omega \sinh^2\left(\int_{-\infty}^{\infty} \vartheta \, \mathrm{d}r_*\right). \tag{35}$$

IV. NON-SUPER-RADIANT MODES ($m < m_*$)

It is convenient to split the discussion of non-super-radiant modes into three sub-cases:

- $m = 0$ zero-angular-momentum modes: This is the most fundamental case, and most straightforward case to analyze. This case provides a useful template for the more complicated situations.
- $m \neq 0$ nonzero-angular-momentum modes: These are most conveniently further split into two sub-cases
  - $m < 0$ negative-angular-momentum modes.
  - $m \in (0, m_*)$ low-lying positive-angular-momentum modes.

A. Zero angular momentum modes ($m = 0$)

We choose $\bar{h}(r_*) = \omega > 0$ and $m = 0$, then

$$U_{j\ell,m=0}(r) = \frac{\Delta(r)}{\left(r^2+a^2\right)^2}\left[\lambda_{j\ell,m=0} + \frac{j(j+n-1)a^2}{r^2} + \frac{n(n-2)\Delta(r)}{4r^2} + \frac{n\Delta'(r)}{2r} - \frac{3r^2\Delta(r)}{(r^2+a^2)^2} + \frac{[r\Delta(r)]'}{r^2+a^2}\right] - \omega^2. \tag{36}$$

Then

$$\begin{aligned} T &\geq \operatorname{sech}^2\left(\frac{1}{2\omega}\int_{-\infty}^{\infty}|V|\,\mathrm{d}r_*\right) \\ &= \operatorname{sech}^2\left(\frac{1}{2\omega}\int_{r_h}^{\infty}|V(r)|\,\frac{r^2+a^2}{\Delta(r)}\mathrm{d}r\right) \\ &= \operatorname{sech}^2\left[\frac{1}{2\omega}\int_{r_h}^{\infty}\left|\frac{1}{r^2+a^2}\left\{\lambda_{j\ell,m=0} + \frac{j(j+n-1)a^2}{r^2} + \frac{n(n-2)\Delta(r)}{4r^2} - \frac{3r^2\Delta(r)}{(r^2+a^2)^2} + \frac{n\Delta'(r)}{2r} + \frac{[r\Delta(r)]'}{r^2+a^2}\right\}\right|\mathrm{d}r\right]. \end{aligned} \tag{37}$$

For $n \geq 1$ and $r \geq r_H$, in view of the positivity properties of the separation constant and effective potential, we can replace $\int|\cdots|\,\mathrm{d}r \to |\int\cdots\mathrm{d}r|$. Therefore,

$$T \geq \operatorname{sech}^2\left|\frac{1}{2\omega}\int_{r_h}^{\infty}\frac{1}{r^2+a^2}\left\{\lambda_{j\ell,m=0} + \frac{j(j+n-1)a^2}{r^2} + \frac{n(n-2)\Delta(r)}{4r^2} - \frac{3r^2\Delta(r)}{(r^2+a^2)^2} + \frac{n\Delta'(r)}{2r} + \frac{[r\Delta(r)]'}{r^2+a^2}\right\}\mathrm{d}r\right|. \tag{38}$$

We would like to integrate this equation term by term. Start by considering the first term

$$\int_{r_H}^{\infty}\frac{\lambda_{j\ell,m=0}}{r^2+a^2}\,\mathrm{d}r = \frac{\lambda_{j\ell,m=0}}{a}\arctan\frac{r}{a}\Big|_{r_H}^{\infty} = \frac{\lambda_{j\ell,m=0}}{a}\arctan\frac{a}{r_H}. \tag{39}$$

For the last two integrals, we can show that they can be simplified as follows:

$$\int_{r_H}^{\infty}\frac{1}{r^2+a^2}\left[-\frac{3r^2\Delta(r)}{(r^2+a^2)^2} + \frac{[r\Delta(r)]'}{r^2+a^2}\right]\mathrm{d}r = \int_{r_H}^{\infty}\frac{r^2\Delta(r)}{(r^2+a^2)^3}\,\mathrm{d}r. \tag{40}$$

This can be explicitly integrated (for instance, by using Mathematica) and we arrive at

$$\int_{r_H}^{\infty}\frac{r^2\Delta(r)}{(r^2+a^2)^3}\mathrm{d}r = \frac{n}{8r_H} - \frac{n(n-2)(r_H^2+a^2)}{8(n+2)r_H^3}\,{}_2F_1\left(1, \frac{n+2}{2}, \frac{n+4}{2}, -\frac{a^2}{r_H^2}\right) - \frac{a^2}{4r_H(r_H^2+a^2)} + \frac{1}{2a}\arctan\frac{a}{r_H}. \tag{41}$$

Here, ${}_2F_1(z_1, z_2, z_3, z_4)$ is the hypergeometric function. Let us now consider the j-dependent integral

$$\int_{r_H}^{\infty}\frac{j(j+n-1)a^2}{r^2(r^2+a^2)}dr = \frac{j(j+n-1)}{r_H} - \frac{j(j+n-1)}{a}\arctan\frac{a}{r_H}. \tag{42}$$

We can also integrate the n-dependent terms as

$$\int_{r_H}^{\infty} \frac{1}{r^2+a^2}\left[\frac{n(n-2)\Delta(r)}{4r^2}+\frac{n\Delta'(r)}{2r}\right]dr = \frac{n^2(r_H^2+a^2)}{4(n+2)r_H^3}\,{}_2F_1\left(1,\frac{n+2}{2},\frac{n+4}{2},-\frac{a^2}{r_H^2}\right) + \frac{n(n-2)}{4r_H}+\frac{n}{a}\arctan\frac{a}{r_H}. \tag{43}$$

Finally, combining the results from Eqs. (39), (41)–(43), we obtain

$$T_{j\ell,m=0} \geq \operatorname{sech}^2\left|\frac{1}{2\omega r_H} I_{j\ell,m=0}\right|, \tag{44}$$

where we define

$$\begin{aligned} I_{j\ell,m=0} &= \frac{n(2n-3)}{8}+j(j+n-1)+\frac{a^2}{4(r_H^2+a^2)} \\ &+\left(\frac{2n+1}{2}-j(j+n-1)+\lambda_{j\ell,m=0}\right)\frac{r_H}{a}\arctan\frac{a}{r_H} \\ &+\frac{n(r_H^2+a^2)}{8r_H^2}\,{}_2F_1\left(1,\frac{n+2}{2},\frac{n+4}{2},-\frac{a^2}{r_H^2}\right). \end{aligned} \tag{45}$$

For a consistency check, consider the limit $a \to 0$ (with both $n = 0$ and $j = 0$),

$$\begin{aligned} \lim_{a\to 0} I_{j=0,\ell,m=0} &= \lim_{a\to 0}\left[-\frac{a^2}{4(r_H^2+a^2)}+\left(\frac{1}{2}+\lambda_{j=0,\ell,m=0}\right)\frac{r_H}{a}\arctan\frac{a}{r_H}\right] \\ &= \frac{1}{2}+\lambda_{j=0,\ell,m=0}. \end{aligned} \tag{46}$$

This is the same result as for the Kerr black hole (the Kerr–Newman black hole for $Q = 0$), as is to be expected.

B. Non-zero angular momentum mode ($m \neq 0$)

From the basic inequality, we have

$$T_{jlm} \geq \operatorname{sech}^2\left[\int_{\infty}^{\infty}\frac{\sqrt{[\bar{h}'(r_*)]^2+\left[\bar{U}_{j\ell m}(r_*)+\bar{h}^2(r_*)\right]^2}}{2\bar{h}(r_*)}\mathrm{d}r_*\right], \tag{47}$$

for all $\bar{h}(r_*) > 0$. By now using the triangle inequality

$$|a|+|b| \geq \sqrt{a^2+b^2}, \tag{48}$$

we have

$$\begin{aligned} T_{jlm} &\geq \operatorname{sech}^2\left[\int_{\infty}^{\infty}\frac{\left|\bar{h}'(r_*)\right|+\left|\bar{U}_{j\ell m}(r_*)+\bar{h}^2(r_*)\right|}{2\bar{h}(r_*)}\mathrm{d}r_*\right] \\ &\geq \operatorname{sech}^2\left[\int_{-\infty}^{\infty}\frac{\left|\bar{h}'(r_*)\right|}{2\bar{h}(r_*)}\mathrm{d}r_*+\int_{-\infty}^{\infty}\frac{\left|\bar{U}_{j\ell m}(r_*)+\bar{h}^2(r_*)\right|}{2\bar{h}(r_*)}\mathrm{d}r_*\right]. \end{aligned} \tag{49}$$

Provided that $\bar{h}'(r_*)$ is monotone, we have

$$\int_{-\infty}^{\infty}\frac{|\bar{h}'(r_*)|}{2\bar{h}(r_*)}\mathrm{d}r_* = \begin{cases} \frac{1}{2}\ln\frac{\bar{h}(\infty)}{\bar{h}(-\infty)} & \text{for } \bar{h}'(r_*) > 0; \\ -\frac{1}{2}\ln\frac{\bar{h}(\infty)}{\bar{h}(-\infty)} & \text{for } \bar{h}'(r_*) < 0. \end{cases} \tag{50}$$

Let us now rewrite the potential as

$$U_{j\ell m} = V_{j\ell,m} - (\omega - m\,\varpi(r))^2. \tag{51}$$

This form of potential is exactly the same as for the 4-dimensional Kerr–Newman black hole, and thus we simply choose

$$\tilde{h}(r_*) = h(r) = \omega - m\varpi(r). \tag{52}$$

Note that this choice for $h(r)$ is always monotonic as a function of r. However, we can see that $h(r)$ is positive if and only if $\omega > m\Omega_H$. This condition is satisfied for $m < \omega/\Omega_H$, (that is, $m < m_*$), where the mode does not suffer from super-radiant instability.

1. Negative-angular-momentum modes ($m < 0$)

Note that in this case, for $h(r)$ defined in Eq. (52),

$$\frac{\tilde{h}(\infty)}{\tilde{h}(-\infty)} = \frac{h(\infty)}{h(r_H)} = \frac{\omega}{\omega - m\Omega_H} = \frac{1}{1 - m\Omega_H/\omega} < 1. \tag{53}$$

Then

$$\frac{1}{2}\left|\ln\left[\frac{\tilde{h}(\infty)}{\tilde{h}(-\infty)}\right]\right| = \frac{1}{2}\ln(1 - m\Omega_H/\omega). \tag{54}$$

Note also that in this case we have $\omega - m\Omega_H > h(r) > \omega$, so

$$\int_{-\infty}^{\infty} \frac{|U_{j\ell m} + h^2(r)|}{2h(r)}\mathrm{d}r_* = \int_{-\infty}^{\infty} \frac{|V_{j\ell m}|}{2h(r)}\mathrm{d}r_* < \int_{-\infty}^{\infty} \frac{V_{j\ell m}}{2\omega}\mathrm{d}r_*. \tag{55}$$

Then

$$T_{j\ell,m<0} \geq \operatorname{sech}^2\left\{\frac{1}{2}\ln(1 - m\Omega_H/\omega) + \int_{-\infty}^{\infty}\frac{V_{j\ell,m<0}}{2\omega}\mathrm{d}r_*\right\}, \tag{56}$$

$$\geq \operatorname{sech}^2\left\{\frac{1}{2}\ln(1 - m/m_*) + \frac{1}{2\omega r_H} I_{j\ell,m<0}\right\}. \tag{57}$$

It is easy to see that this result is very similar to the result we have for $m = 0$, with the replacement $\lambda_{j\ell,m=0} \to \lambda_{j\ell,m<0}$. We can write down $I_{j\ell m}$ explicitly as

$$\begin{aligned} I_{j\ell m} = {} & \frac{n(2n-3)}{8} + j(j+n-1) + \frac{a^2}{4(r_H^2 + a^2)} \\ & + \left(\frac{2n+1}{2} - j(j+n-1) + \lambda_{j\ell m}(a\omega)\right)\frac{r_H}{a}\arctan\frac{a}{r_H} \\ & + \frac{n(r_H^2 + a^2)}{8r_H^2}\,{}_2F_1\left(1, \frac{n+2}{2}, \frac{n+4}{2}, -\frac{a^2}{r_H^2}\right). \end{aligned} \tag{58}$$

2. Low-lying positive-angular-momentum modes ($m \in (0, m_*)$)

Recall that for $m_* > m > 0$, $h(r)$ is positive and monotonic as a function of r, for this situation we first consider

$$\frac{\tilde{h}(\infty)}{\tilde{h}(-\infty)} = \frac{h(\infty)}{h(r_H)} = \frac{\omega}{\omega - m\Omega_H} = \frac{1}{1 - m\Omega_H/\omega} > 1. \tag{59}$$

Then, we have

$$\frac{1}{2}\left|\ln\left[\frac{\tilde{h}(\infty)}{\tilde{h}(-\infty)}\right]\right| = -\frac{1}{2}\ln(1 - m\Omega_H/\omega). \tag{60}$$

Note also that in this case we have $\omega - m\Omega_H < h(r) < \omega$, so

$$\int_{-\infty}^{\infty} \frac{|U_{j\ell m} + h^2(r)|}{2h(r)} dr_* = \int_{-\infty}^{\infty} \frac{|V_{j\ell,m>0}|}{2h(r)} dr_* < \int_{-\infty}^{\infty} \frac{V_{j\ell,m>0}}{2(\omega - m\Omega_H)} dr_*. \tag{61}$$

Then, we arrive at the result

$$T_{j\ell\, m>0} \geq \operatorname{sech}^2 \left\{ -\frac{1}{2} \ln(1 - m\Omega_H/\omega) + \int_{-\infty}^{\infty} \frac{V_{j\ell,m>0}}{2(\omega - m\Omega_H)} dr_* \right\}, \tag{62}$$

$$\geq \operatorname{sech}^2 \left\{ -\frac{1}{2} \ln(1 - m/m_*) + \frac{1}{2r_H\omega(1 - m/m_*)} I_{j\ell,m>0} \right\}, \tag{63}$$

where $I_{j\ell,m>0}$ is defined by Eq. (58).

V. SUPER-RADIANT MODES ($m \geq m_*$)

It is a good strategy to split the super-radiant modes into two sub-classes depending on the relative sizes of ω^2 and $(\omega - m\Omega_H)^2$. Note that $\omega^2 = (\omega - m\Omega_H)^2$ when $m = 2\omega/\Omega_H = 2m_*$. This suggests that it might be useful to split the super-radiant modes as follows:

- $m \in [m_*, 2m_*)$.
- $m \in [2m_*, \infty)$.

A. Low-lying super-radiant modes ($m \in [m_*, 2m_*)$)

In this region, we have $\omega^2 > (\omega - m\Omega_H)^2$ and we choose

$$h(r) = \max\{\omega - m\varpi(r), m\Omega_H - \omega\}. \tag{64}$$

We can see that $h(r) > 0$ and monotone decreasing as we move from spatial infinity to the horizon, and become a flat horizontal line near the horizon. Note that $h(r) \geq m\Omega_H - \omega$ everywhere. By using $h(r)$ as defined in Eq. (64), we have

$$\int_{-\infty}^{\infty} \frac{|h'(r)|}{h(r)} dr_* = |\ln h(r)|_{r_H}^{\infty} = \ln\left(\frac{\omega}{m\Omega_H - \omega}\right) = -\ln(m/m_* - 1). \tag{65}$$

It is now straightforward to show that

$$\int_{-\infty}^{\infty} \frac{V_{j\ell m}}{2h(r)} dr_* \leq \int_{-\infty}^{\infty} \frac{V_{j\ell m}}{2(m\Omega_H - \omega)} dr_*' = \frac{I_{j\ell m}}{2(m\Omega_H - \omega)r_H} = \frac{I_{j\ell m}}{2\omega(m/m_* - 1)r_H}, \tag{66}$$

where $I_{j\ell m}$ is defined in Eq. (58). The last integral we need to perform is

$$J_m^{\text{low}} = \int_{-\infty}^{\infty} \frac{h(r)^2 - (\omega - m\varpi(r))^2}{2h(r)} dr_*. \tag{67}$$

Note that with our choice of $h(r)$, the integrand in above integral is zero over much of the relevant range. To be more precise, we are interested only in

$$J_m^{\text{low}} = \int_{r_H}^{r_0} \frac{(\omega - m\Omega_H)^2 - (\omega - m\varpi(r))^2}{2(m\Omega_H - \omega)} \frac{r^2 + a^2}{\Delta} dr. \tag{68}$$

The upper limit of integration r_0 is defined by the condition

$$m[\Omega_H + \varpi(r_0)] = 2\omega, \tag{69}$$

or we can write down r_0 explicitly as

$$r_0 = \sqrt{r_H^2 + \frac{2(m - m_*)}{2m_* - m}(r_H^2 + a^2)}. \tag{70}$$

Notice that the upper limit $r_0 > r_H$ for $m \in [m_*, 2m_*)$. Then

$$J_m^{\text{low}} = \frac{m}{2(m\Omega_H - \omega)} \int_{r_H}^{r_0} (\Omega_H - \varpi(r))(m\varpi(r) + m\Omega_H - 2\omega)\frac{r^2+a^2}{\Delta}\,\mathrm{d}r. \tag{71}$$

However, for the relevant domain of integration we have

$$0 \le (m\varpi(r) + m\Omega_H - 2\omega) \le 2(m\Omega_H - \omega). \tag{72}$$

Then we can conclude that

$$J_m^{\text{low}} \le m\int_{r_H}^{r_0} (\Omega_H - \varpi(r))\frac{r^2+a^2}{\Delta}\,\mathrm{d}r = m\Omega_H\int_{r_H}^{r_0} \frac{r^{n-1}(r-r_H)(r+r_H)}{r^{n-1}(r^2+a^2) - r_H^{n-1}(r_H^2+a^2)}\,\mathrm{d}r. \tag{73}$$

This integral is finite, and one can evaluate it exactly for each value of n. (The *integrand* is in fact finite as $r \to r_H$ by the l'Hôpital rule.) By now combining all these results, we have

$$T_{j\ell,m\in[m_*,2m_*)} \ge \operatorname{sech}^2\left\{-\frac{1}{2}\ln(m/m_* - 1) + \frac{I_{j\ell,m\in[m_*,2m_*)}}{2r_H\omega(m/m_* - 1)} + J_m^{\text{low}}\right\}. \tag{74}$$

B. Highly super-radiant modes ($m \ge 2m_*$)

In this region, we have $(\omega - m\Omega_H)^2 > \omega^2$, so we can choose

$$h(r) = \max\{m\varpi(r) - \omega, \omega\}. \tag{75}$$

It is not difficult to see that $h(r)$ is both positive and monotone decreasing as we move from the horizon to spatial infinity. Note also that $h(r) \ge \omega$ for the relevant domain. By using Eq. (75), we have

$$\int_{-\infty}^{\infty} \frac{|h'(r)|}{h(r)}\,\mathrm{d}r_* = |\ln h(r)|_{r_H}^{\infty} = \ln\left(\frac{m\Omega_H - \omega}{\omega}\right) = \ln(m/m_* - 1). \tag{76}$$

We also obtain

$$\int_{-\infty}^{\infty} \frac{V_{j\ell m}}{2h(r)}\,\mathrm{d}r_* \le \int_{-\infty}^{\infty} \frac{V_{j\ell m}}{2\omega}\mathrm{d}r_* = \frac{I_{j\ell m}}{2\omega r_H}, \tag{77}$$

where $I_{j\ell m}$ is defined in Eq. (58) as for the previous cases. Finally, we are left with the integral

$$J_m^{\text{high}} = \int_{-\infty}^{\infty} \frac{h(r)^2 - (\omega - m\varpi(r))^2}{2h(r)}\,\mathrm{d}r_*. \tag{78}$$

Again the integrand is zero over much of the domain of integration. That is, we are only interested in

$$J_m^{\text{high}} = \int_{r_0}^{\infty} \frac{\omega^2 - (\omega - m\varpi(r))^2}{2\omega}\frac{r^2+a^2}{\Delta}\,\mathrm{d}r. \tag{79}$$

Here, the lower bound of integration, r_0, is now defined by

$$m\varpi(r_0) = 2\omega, \tag{80}$$

implying

$$r_0 = a\sqrt{\frac{m}{2\omega a} - 1}. \tag{81}$$

Recall that $m \ge 2m_*$ in this region, we have

$$r_0 \ge a\sqrt{\frac{m_*}{\omega a} - 1} = a\sqrt{\frac{r_H^2 + a^2}{a^2} - 1} = r_H. \tag{82}$$

The integral J_m^{high} is finite. (In fact, the *integrand* is finite as $r \to r_0$, and falls of as $1/r^2$ as $r \to \infty$.) After assembling all results we have, we finally obtain

$$T_{j\ell,m\geq 2m_*} \geq \text{sech}^2\left\{\frac{1}{2}\ln(m/m_* - 1) + \frac{I_{j\ell,m\geq 2m_*}}{2r_H\omega} + J_m^{\text{high}}\right\}. \tag{83}$$

VI. SUMMARY OF THE GENERAL CASE

Collecting the results for the low-lying and highly super-radiant modes, together with the non-super-radiant modes, we have the following bounds for the transmission probabilities:

$$T_{j\ell m} \geq \begin{cases} \text{sech}^2\left\{\frac{1}{2}\ln(1-m/m_*) + \frac{1}{2r_H\omega} I_{j\ell m}\right\} & \text{for } m < 0; \\ \text{sech}^2\left\{\frac{1}{2r_H\omega} I_{j\ell m}\right\} & \text{for } m = 0; \\ \text{sech}^2\left\{-\frac{1}{2}\ln(1-m/m_*) + \frac{1}{2r_H\omega(1-m/m_*)} I_{j\ell m}\right\} & \text{for } 0 < m < m_*; \\ \text{sech}^2\left\{-\frac{1}{2}\ln(m/m_* - 1) + \frac{1}{2r_H\omega(m/m_*-1)} I_{j\ell m} + J_m^{\text{low}}\right\} & \text{for } m_* \leq m < 2m_*; \\ \text{sech}^2\left\{\frac{1}{2}\ln(m/m_* - 1) + \frac{1}{2r_H\omega} I_{j\ell m} + J_m^{\text{high}}\right\} & \text{for } m \geq 2m_*. \end{cases} \tag{84}$$

Here, m_* is the "critical" azimuthal angular momentum defined by $m_* = \omega/\Omega_H$, while the quantity $I_{j\ell m}$ is defined in Eq. (58).

VII. FOUR-DIMENSIONAL CASE $n = 0$

When $n = 0$ the Myers–Perry spacetime reduces to the usual Kerr spacetime. Furthermore, the separation constant and effective potential reduce to those discussed in Ref. 11. Ultimately, the bounds on the greybody factors reduce (as they should) to those of Ref. 11.

VIII. FIVE-DIMENSIONAL CASE $n = 1$

Let us now take a look at a special case with only *one* extra dimension $n = 1$. These are the (3+1+1)-dimensional [five-dimensional] Myers–Perry black holes. In this case, we have the simplification

$$\Delta \to r^2 + a^2 - \mu. \tag{85}$$

A brief computation, starting from Eq. (58), now yields

$$I_{j\ell m}^{n=1} = \left(\frac{3}{8a\Omega_H} - \frac{1}{8} + j^2 - \frac{a\Omega_H}{4}\right) + \left(\frac{3}{2} - j^2 - \frac{3}{8a\Omega_H} + \lambda_{j\ell m}\right)\frac{r_H}{a}\arctan\left(\frac{a}{r_H}\right). \tag{86}$$

Interestingly, J_m^{low} has a very simple bound in five-dimensional space-time. For $n = 1$, we have

$$J_m^{\text{low}}\Big|_{n=1} \leq m\Omega_H(r_0 - r_H) = \omega\frac{m}{m_*}(r_0 - r_H). \tag{87}$$

Let us now consider J_m^{high}; this also takes a simpler form in five-dimensional space-time

$$J_m^{\text{high}}\big|_{n=1} = \int_{r_0}^{\infty} \frac{ma}{2\omega}\left[\frac{2\omega - m\varpi(r)}{(r-r_H)(r+r_H)}\right] \mathrm{d}r. \tag{88}$$

For the relevant domain of integration, $2\omega > m\varpi(r)$, then we can conclude that

$$J_m^{\text{high}}\big|_{n=1} \leq ma\int_{r_0}^{\infty} \frac{1}{(r-r_H)(r+r_H)}\,\mathrm{d}r = \frac{ma}{r_H}\ln\sqrt{\frac{r_0+r_H}{r_0-r_H}}. \tag{89}$$

Collecting results, we finally deduce a quite explicit bound for scalar emission from five-dimensional simply rotating Myers–Perry black holes. The bound is given by

$$T_{j\ell m}^{(n=1)} \geq \begin{cases} \operatorname{sech}^2 \left\{ \frac{1}{2} \ln(1 - m/m_*) + \frac{1}{2r_H\omega} I_{j\ell m}^{n=1} \right\} & \text{for } m < 0; \\ \operatorname{sech}^2 \left\{ \frac{1}{2r_H\omega} I_{j\ell m}^{n=1} \right\} & \text{for } m = 0; \\ \operatorname{sech}^2 \left\{ -\frac{1}{2} \ln(1 - m/m_*) + \frac{1}{2r_H\omega(1-m/m_*)} I_{j\ell m}^{n=1} \right\} & \text{for } 0 < m < m_*; \\ \operatorname{sech}^2 \left\{ -\frac{1}{2} \ln(m/m_* - 1) + \frac{1}{2r_H\omega(m/m_*-1)} I_{j\ell m}^{n=1} + \omega \frac{m}{m_*}(r_0 - r_H) \right\} & \text{for } m_* \leq m < 2m_*; \\ \operatorname{sech}^2 \left\{ \frac{1}{2} \ln(m/m_* - 1) + \frac{1}{2r_H\omega} I_{j\ell m}^{n=1} + \frac{ma}{r_H} \ln \sqrt{\frac{r_0+r_H}{r_0-r_H}} \right\} & \text{for } m \geq 2m_*. \end{cases} \tag{90}$$

Here, $I_{j\ell m}^{n=1}$ is as given in Eq. (86).

IX. DISCUSSION

In this article, we have established certain rigorous bounds on the greybody factors (mode dependent transmission probabilities) for the Myers–Perry black holes. We have also obtained (mutatis mutandis) certain rigorous bounds on the emission rates for the super-radiant modes. In the absence of exact results (the relevant differential equations seem highly resistant to explicit analytic solution), quantitative bounds along these lines seem to be the best one can do.

ACKNOWLEDGMENTS

This project was funded by Ratchadapisek Sompoch Endowment Fund, Chulalongkorn University (Sci-Super 2014-032), by a grant for the professional development of new academic staff from the Ratchadapisek Somphot Fund at Chulalongkorn University, by the Thailand Toray Science Foundation (TTSF), by the Thailand Research Fund (TRF), by the Office of the Higher Education Commission (OHEC), Faculty of Science, Chulalongkorn University (MRG5680171), and by the Research Strategic plan program (A1B1). A.C. was supported by the Thailand Toray Science Foundation (TTSF) and Thailand Excellence in Physics project (THEP). P.B. was additionally supported by a scholarship from the Royal Government of Thailand. T.N. was also additionally supported by a scholarship from the Development and Promotion of Science and Technology talent project (DPST). M.V. was supported by the Marsden Fund, and by a James Cook fellowship, both administered by the Royal Society of New Zealand.

[1] S. W. Hawking, "Black hole explosions," Nature (London) **248**, 30 (1974).

[2] S. W. Hawking, "Particle creation by black holes," Commun. Math. Phys. **43**, 199 (1975) [Erratum **46**, 206 (1976)].

[3] D. N. Page, "Particle emission rates from a black hole: Massless particles from an uncharged, nonrotating hole," Phys. Rev. D **13**, 198 (1976).

[4] D. N. Page, "Particle emission rates from a black hole. 2. Massless particles from a rotating hole," Phys. Rev. D **14**, 3260 (1976).

[5] J. D. Bekenstein and A. Meisels, "Einstein A and B coefficients for a black hole," Phys. Rev. D **15**, 2775 (1977).

[6] J. Escobedo, "Greybody factors: Hawking radiation in disguise," M.Sc. thesis, University of Amsterdam, 2008.

[7] P. Boonserm and M. Visser, "Bounding the greybody factors for Schwarzschild black holes," Phys. Rev. D **78**, 101502 (2008); e-print arXiv:0806.2209 [gr-qc].

[8] T. Ngampitipan and P. Boonserm, "Bounding the greybody factors for non-rotating black holes," Int. J. Mod. Phys. **D22**, 1350058 (2013); e-print arXiv:1211.4070 [math-ph].

[9] T. Ngampitipan and P. Boonserm, "Bounding the greybody factors for the Reissner–Nordström black holes," J. Phys. Conf. Ser. **435**, 012027 (2013); e-print arXiv:1301.7527 [math-ph].

[10] P. Boonserm, T. Ngampitipan, and M. Visser, "Regge-Wheeler equation, linear stability, and greybody factors for dirty black holes," Phys. Rev. D **88**, 041502 (2013); e-print arXiv:1305.1416 [gr-qc].

[11] P. Boonserm, T. Ngampitipan, and M. Visser, "Bounding the greybody factors for scalar field excitations of the Kerr-Newman spacetime," J. High Energy Phys. (**2014**) 113; e-print arXiv:1401.0568 [gr-qc].

[12] D. Ida, Y. Uchida, and Y. Morisawa, "The scalar perturbation of higher-dimensional rotating black holes," Phys. Rev. D **67**, 084019 (2003); e-print arXiv:gr-qc/0212035.

[13] S. Creek, O. Efthimiou, P. Kanti, and K. Tamvakis, "Scalar emission in the bulk in a rotating black hole background," Phys. Lett. B **656**, 102–111 (2007); e-print arXiv:0709.0241 [hep-th].

[14] S. Creek, O. Efthimiou, P. Kanti, and K. Tamvakis, "Greybody factors for brane scalar fields in a rotating black-hole background," Phys. Rev. D **75**, 084043 (2007); e-print arXiv:hep-th/0701288.

[15] M. Visser, "Some general bounds for 1-D scattering," Phys. Rev. A **59**, 427–38 (1999); e-print arXiv:quant-ph/9901030.

[16] P. Boonserm and M. Visser, "Transmission probabilities and the Miller–Good transformation," J. Phys. A **42**, 045301 (2009); e-print arXiv:0808.2516 [math-ph].

[17] P. Boonserm and M. Visser, "Bounding the Bogoliubov coefficients," Ann. Phys. **323**, 2779 (2008); e-print arXiv:0801.0610 [quant-ph].

[18] P. Boonserm and M. Visser, "Analytic bounds on transmission probabilities," Ann. Phys. **325**, 1328 (2010); e-print arXiv:0901.0944 [math-ph].

[19] P. Boonserm and M. Visser, "Reformulating the Schrödinger equation as a Shabat–Zakharov system," J. Math. Phys. **51**, 022105 (2010); e-print arXiv:0910.2600 [math-ph].

[20] P. Boonserm and M. Visser, "Quasi-normal frequencies: Key analytic results," J. High Energy Phys. (**2011**) 073; e-print arXiv:1005.4483 [math-ph].

[21] P. Boonserm and M. Visser, "One dimensional scattering problems: A pedagogical presentation of the relationship between reflection and transmission amplitudes," Thai J. Math. **8**, 83–97 (2010).

[22] P. Boonserm and M. Visser, "Compound transfer matrices: Constructive and destructive interference," J. Math. Phys. **53**, 012104 (2012); e-print arXiv:1101.4014 [math-ph].

[23] P. Boonserm and M. Visser, "Bounds on variable-length compound jumps," J. Math. Phys. **54**, 092105 (2013); e-print arXiv:1301.7524 [math-ph].

[24] R. C. Myers and M. J. Perry, "Black holes in higher dimensional space-times," Ann. Phys. **172**, 304 (1986).

[25] R. Emparan and H. S. Reall, "Black holes in higher dimensions," Liv. Rev. Relat. **11**, 6 (2008); e-print arXiv:0801.3471 [hep-th].

[26] W. H. Press and S. A. Teukolsky, "Perturbations of a rotating black hole. II. Dynamical stability of the Kerr metric," Astrophys. J. **185**, 649–673 (1973).

[27] M. Shibata, M. Sasaki, H. Tagoshi, and T. Tanaka, "Gravitational waves from a particle orbiting around a rotating black hole: Post-Newtonian expansion," Phys. Rev. D **51**, 1646–1663 (1995).

[28] H. Tagoshi, M. Shibata, T. Tanaka, and M. Sasaki, "Post-Newtonian expansion of gravitational waves from a particle in circular orbits around a rotating black hole: Up to $O(v^8)$ beyond the quadrupole formula," Phys. Rev. D **54**, 1439–1459 (1996).

[29] K. D. Kokkotas and B. G. Schmidt, "Quasinormal modes of stars and black holes," Liv. Rev. Relat. **2**, 2 (1999); e-print arXiv:gr-qc/9909058.

[30] M. Sasaki and H. Tagoshi, "Analytic black hole perturbation approach to gravitational radiation," Liv. Rev. Relat. **6**, 6 (2003); e-print arXiv:gr-qc/0306120.

[31] V. Ferrari, "Stellar perturbations," Lect. Notes Phys. **617**, 89–112 (2003).

[32] L. Samuelsson and N. Andersson, "Neutron star asteroseismology: Axial crust oscillations in the cowling approximation," Mon. Not. R. Astron. Soc. **374**, 256 (2007); e-print arXiv:astro-ph/0609265.

[33] R. A. Konoplya and A. Zhidenko, "Quasinormal modes of black holes: From astrophysics to string theory," Rev. Mod. Phys. **83**, 793 (2011); e-print arXiv:1102.4014 [gr-qc].

[34] V. Ferrari, "Gravitational waves from perturbed stars," Bull. Astron. Soc. India **39**, 203–224 (2011); e-print arXiv:1105.1678 [gr-qc].

[35] V. P. Frolov and D. Kubiznak, "Hidden symmetries of higher dimensional rotating black holes," Phys. Rev. Lett. **98**, 011101 (2007); e-print arXiv:gr-qc/0605058 [gr-qc].

[36] B. Carter, "Hamilton-Jacobi and Schrodinger separable solutions of Einstein's equations," Commun. Math. Phys. **10**, 280 (1968).

[37] M. Vasudevan, K. A. Stevens, and D. N. Page, "Particle motion and scalar field propagation in Myers–Perry black hole spacetimes in all dimensions," Class. Quant. Grav. **22**, 1469 (2005); e-print arXiv:gr-qc/0407030.

[38] C. Muller, *Lecture Notes in Mathematics: Spherical Harmonics* (Springer-Verlag, Berlin, 1966).

[39] R. S. Maier, "The 192 solutions of the Heun equation," Math. Comput. **76**, 811–843 (2007); e-print arXiv:math/0408317.

[40] *Heun's Differential Equations*, edited by A. Ronveaux (Clarendon Press, England, 1995).

[41] B. D. Sleeman and V. B. Kuznetzov, "Heun functions," in *NIST Handbook of Mathematical Functions*, edited by F. W. J. Olver, D. M. Lozier, R. F. Boisvert, and C. W. Clark (Cambridge University Press, England, 2010).

[42] G. Valent, "Heun functions versus elliptic functions," *Difference Equations, Special Functions and Orthogonal Polynomials* (World Scientific, Singapore, 2007), pp. 664–686; e-print arXiv:math-ph/0512006.

[43] E. D. Fackerell and R. G. Crossman, "Spin-weighted angular spheroidal functions," J. Math. Phys. **18**, 1849–1854 (1977).

[44] M. Richartz, S. Weinfurtner, A. J. Penner, and W. G. Unruh, "General universal superradiant scattering," Phys. Rev. D **80**, 124016 (2009); e-print arXiv:0909.2317 [gr-qc].

[45] Ya. B. Zel'dovich, "Amplification of cylindrical electromagnetic waves reflected from a rotating body," JETP **35**, 1085 (1972).

Conference Proceedings

Proceedings of the 12th Asia Pacific Physics Conference
JPS Conf Proc 1, 013100 (2014)

Transmission Probability for Charged Dilatonic Black Holes in Various Dimensions

Tritos Ngampitipan[1] and Petarpa Boonserm[2]

[1]*Department of Physics, Faculty of Science, Chulalongkorn University, Bangkok 10330, Thailand*
[2]*Department of Mathematics and Computer Science, Faculty of Science, Chulalongkorn University, Bangkok 10330, Thailand*

E-mail: tritos.ngampitipan@gmail.com

(Received June 18, 2013)

A dilaton is a theoretical particle, which results from the Plank mass raised to a dynamical field. In this paper, the rigorous bounds on the transmission probabilities for charged black holes, coupled to a dilaton field in various dimensions, are calculated. The results show that in the absence of the cosmological constant, the black holes in (2 + 1) dimensions have only one event horizon. Moreover, the charges of the black holes can increase the transmission probabilities. However, for the black holes in (3 + 1) dimensions, the charges of the black holes can filter Hawking radiation.

KEYWORDS: dilaton, transmission probability, (2 + 1) dimensions, (3 + 1) dimensions

1. Introduction

According to Stephen Hawking, black holes can emit radiation, which became known as Hawking radiation [1]. This phenomenon was predicted by the quantum field theory in curved spacetime. The gravitational potential surrounding the black hole can modify Hawking radiation. Therefore, Hawking radiation is not considered as blackbody radiation because some of the radiation is reflected back into the black hole and the rest is transmitted to the spatial infinity. The transmission probability is of interest because it is a characteristic property of black hole, which depends only on mass, angular momentum, and charge of the black hole. In this paper, the rigorous bounds on the transmission probabilities for the charged dilatonic black holes in (2 + 1) and (3 + 1) dimensions are derived.

2. The Charged Dilatonic Black Holes in (2 + 1) Dimensions

The charged dilatonic metric in (2 + 1) dimensions is given by [2, 3]

$$ds^2 = -f(r)dt^2 + \frac{4r^2}{f(r)}dr^2 + r^2 d\theta^2, \tag{1}$$

where

$$f(r) = -2Mr + 8\Lambda r^2 + 8Q^2. \tag{2}$$

For $M > 8Q\sqrt{\Lambda}$, this spacetime describes a black hole with two event horizons

$$r_\pm = \frac{M \pm \sqrt{M^2 - 64Q^2\Lambda}}{8\Lambda}. \tag{3}$$

We are only interested in $\Lambda = 0$. In this case, the black hole has only one event horizon located at

$$r_h = \frac{4Q^2}{M}. \tag{4}$$

The Schrödinger-like equation is given by

$$\left[\frac{d^2}{dr_*^2}+\omega^2-V(r)\right]u(r)=0, \tag{5}$$

where

$$dr_*=\frac{2r}{f(r)}dr \tag{6}$$

and

$$V(r)=\left(\frac{5M^2}{8}+2m^2M\right)\frac{1}{r}-\left(4MQ^2+8m^2Q^2\right)\frac{1}{r^2}+\frac{6Q^4}{r^3}. \tag{7}$$

The $(2+1)$ charged dilatonic potential is plotted with $m=1$ and $M=2$ for $Q=1,2$ as shown in Fig. 1. It can be seen that the potential for $Q=2$ is higher than that of $Q=1$. The coordinate r_* can explicitly be written as

$$r_*=-\frac{r_h}{M}\ln|r-r_h|-\frac{r}{M}. \tag{8}$$

When $r\to r_h$, $r_*\to\infty$ and when $r\to\infty$, $r_*\to-\infty$. The general and robust bounds on the transmission probability can be found in [4]. They are applied to generic systems [5–7] and black hole greybody factors [3, 8]. The lower bounds on the transmission probabilities are given by [4, 8–10]

$$T\geq\operatorname{sech}^2\left(\int_{-\infty}^{\infty}\vartheta dr_*\right), \tag{9}$$

where

$$\vartheta=\frac{\sqrt{(h')^2+(\omega^2-V-h^2)^2}}{2h}, \tag{10}$$

for some positive function h. We set $h=\omega$, then

$$\begin{aligned}
T &\geq \operatorname{sech}^2\left[\frac{1}{2\omega}\int_{-\infty}^{\infty}V dr_*\right]\\
&= \operatorname{sech}^2\left[\frac{1}{2\omega}\int_{\infty}^{r_h}\left\{\left(\frac{5M^2}{8}+2m^2M\right)\frac{1}{r}-\left(4MQ^2+8m^2Q^2\right)\frac{1}{r^2}+\frac{6Q^4}{r^3}\right\}\frac{2r}{f(r)}dr\right]\\
&= \operatorname{sech}^2\left[\left(\frac{5M+16m^2}{16\omega}\right)\ln\left|\frac{r_{\max}-r_h}{r_{\min}}\right|-\frac{3M}{16\omega}\right].
\end{aligned} \tag{11}$$

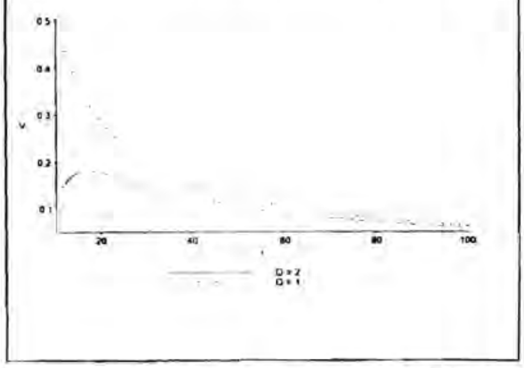

Fig. 1. The $(2+1)$ charged dilatonic potential with $m=1$ and $M=2$ for $Q=1,2$.

where $r_{\min} - r_h \to 0$ and $r_{\max} >> r_h$. The dependence of the transmission probability on the energy of an emitted particle is plotted with $m = 1$, $M = 2$ and $Q = 1, 2$ as shown in Fig. 2. The dependence of the transmission probability on the charges of the black hole is plotted with $m = 1$, $M = 2$ and $\omega = 30$. as shown in Fig. 3. Both the graphs show that the transmission probability increases with Q.

3. The Charged Dilatonic Black Holes in (3 + 1) Dimensions

The charged dilatonic metric in (3 + 1) dimensions is given by [3, 11]

$$ds^2 = -f(r)dt^2 + \frac{1}{f(r)}dr^2 + R^2(r)d\Omega^2, \tag{12}$$

where

$$f(r) = 1 - \frac{r_+}{r} \text{ and } R^2(r) = r^2\left(1 - \frac{r_-}{r}\right), \tag{13}$$

with

$$r_+ = 2M \text{ and } r_- = \frac{Q^2}{M}. \tag{14}$$

By the coordinate transformation

$$r = \frac{r_- + \sqrt{4R^2 + r_-^2}}{2}, \tag{15}$$

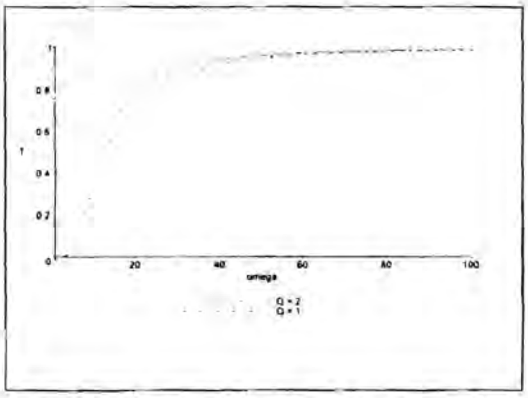

Fig. 2. The transmission probability versus the energy of an emitted particle with $m = 1$, $M = 2$ and $Q = 1, 2$.

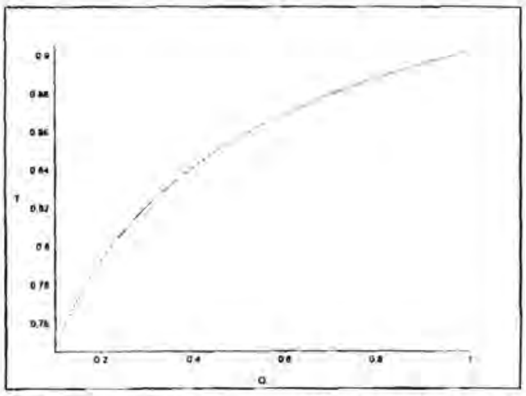

Fig. 3. The transmission probability versus the charges of the black hole with $m = 1$, $M = 2$ and $\omega = 30$.

the metric (12) can be rewritten as

$$ds^2 = -F(R)dt^2 + \frac{1}{F(R)H^2(R)}dR^2 + R^2 d\Omega^2, \tag{16}$$

where

$$F(R) = 1 - \frac{2r_+}{r_- + \sqrt{4R^2 + r_-^2}} \tag{17}$$

and

$$H(R) = \frac{4R^2}{4R^2 + r_-^2}. \tag{18}$$

Introducing the tortoise coordinate

$$dR_* = \frac{dR}{F(R)H(R)}, \tag{19}$$

the equation of motion is given by

$$\frac{\partial^2 U}{\partial t^2} - \frac{\partial^2 U}{\partial R_*^2} + V(R) = 0, \tag{20}$$

where

$$V(R) = F(R)\left[\frac{H(R)}{R}\frac{d}{dR}(F(R)H(R)) + \frac{l(l+1)}{R^2}\right]. \tag{21}$$

The (3 + 1) charged dilatonic potential is plotted with $l = 0$, $r_+ = 4$, and $r_- = 0.5$ as shown in Fig. 4. If $r_- = 0$, we obtain $R = r$, and the (3 + 1) charged dilatonic potential $V(R)$ is reduced to the Schwarzschild potential [12]

$$V_{\text{sch}}(r) = \left(1 - \frac{r_+}{r}\right)\left[\frac{l(l+1)}{r^2} + \frac{r_+}{r^3}\right]. \tag{22}$$

The comparison between the (3 + 1) charged dilatonic potential and the Schwarzschild potential is shown in Fig. 5. The lower bound on the transmission probability for $l = 0$ is

$$T \geq \operatorname{sech}^2\left[\frac{1}{2\omega}\int_{-\infty}^{\infty} V(R)dR_*\right]$$

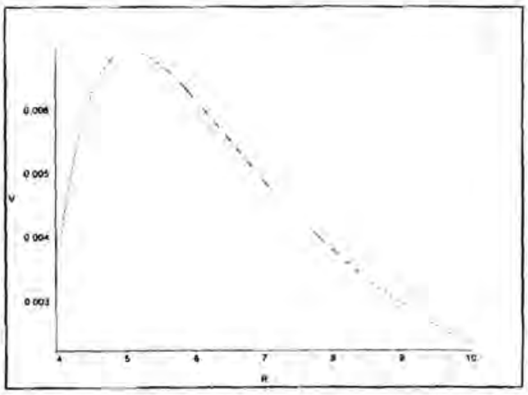

Fig. 4. The (3 + 1) charged dilatonic potential with $l = 0$, $r_+ = 4$, and $r_- = 0.5$.

$$
\begin{aligned}
&= \operatorname{sech}^2\left[\frac{1}{2\omega}\int_{\sqrt{r_+(r_+-r_-)}}^{\infty}\frac{1}{R}\frac{d}{dR}(F(R)H(R))dR\right] \\
&= \operatorname{sech}^2\left[\frac{r_- - r_+}{2\omega r_-^2}\ln\left|\frac{r_+}{r_+ - r_-}\right| + \frac{1}{2\omega r_-}\right],
\end{aligned} \tag{23}
$$

for $r_- \neq 0$. If $r_- = 0$, the transmission probability for $l = 0$ becomes

$$
T \geq \operatorname{sech}^2\left(\frac{1}{4\omega r_+}\right), \tag{24}
$$

which is the transmission probability for the Schwarzschild black hole [12]. The transmission probability is plotted with $r_+ = 4$ and $r_- = 2, 0.5, 0$ as shown in Fig. 6. The graph shows that the transmission probability decreases as r_- increases. This indicates that the charges behave as good barriers to resist the tunneling of the uncharged scalar particles. This is in agreement with [3] as it should be because in this paper, we have just rewritten the metric in terms of the new variable R instead of r.

4. Conclusion

In this paper, we have calculated the rigorous bounds on the transmission probabilities for the charged dilatonic black holes in (2 + 1) and (3 + 1) dimensions. For the charged dilatonic black holes in (2 + 1) dimensions, we are only interested in the absence of the cosmological constant. The results

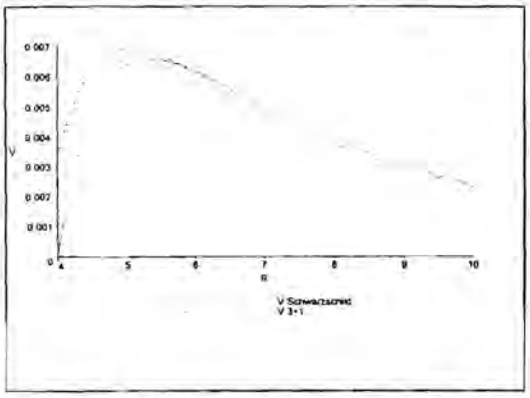

Fig. 5. The comparison between the (3 + 1) charged dilatonic potential and the Schwarzschild potential with $l = 0$, $r_+ = 4$, and $r_- = 0.5$.

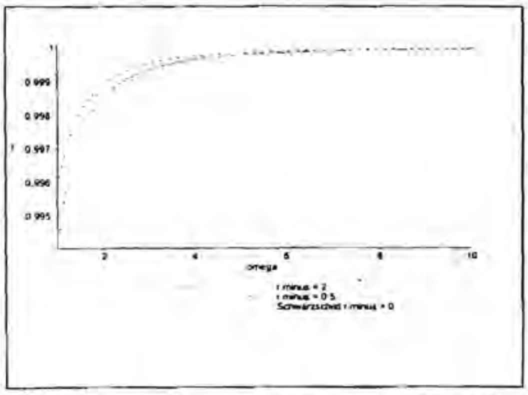

Fig. 6. The transmission probability versus the energy of an emitted particle with $r_+ = 4$ and $r_- = 2, 0.5, 0$.

show that the black hole has only one event horizon instead of two event horizons as in the case of the presence of the cosmological constant. The results also show that the transmission probability increases with the charge of the black holes. This result contrasts with the case of the presence of the cosmological constant.

For the charged dilatonic black holes in (3 + 1) dimensions, we have transformed the coordinates to rewrite the metric in terms of the new variables. The results show that the charges act as a good barrier.

Acknowledgment

This research has been supported by a grant for the professional development of new academic staff from the Ratchadapisek Somphot Fund at Chulalongkorn University, by the Thailand Toray Science Foundation (TTSF), by the Thailand Research Fund (TRF), the Office of the Higher Education Commission (OHEC), Chulalongkorn University, and by the Research Strategic plan program (A1B1), Faculty of Science, Chulalongkorn University (MRG5680171). PB was additionally supported by a scholarship from the Royal Government of Thailand. TN was also additionally supported by a scholarship from the Development and Promotion of Science and Technology talent project (DPST). TN gives special thanks to Dr. Auttakit Chatrabuti for his invaluable advice. We also thank Prof. Matt Visser for his extremely useful suggestions and comments.

References

[1] S. W. Hawking: *Commun. Math. Phys.* **43** (1975) 199.
[2] S. Fernando: *Gen. Relativ. Gravit.* **37** (2005) 461.
[3] T. Ngampitipan and P. Boonserm: *Int. J. Mod. Phys.* D **22** (2013) 1350058, arXiv:1211.4070 [math-ph].
[4] M. Visser: *Phys. Rev.* A **59** (1999) 427, quant-ph/9901030.
[5] P. Boonserm and M. Visser: *J. Phys.* A **42** (2009) 045301, arXiv:0808.2516 [math-ph].
[6] P. Boonserm and M. Visser: *Ann. Phys.* **325** (2010) 1328, arXiv:0901.0944 [math-ph].
[7] P. Boonserm and M. Visser: *J. Math. Phys.* **51** (2010) 022105, arXiv:0910.2600 [math-ph].
[8] T. Ngampitipan and P. Boonserm: *J. Phys.: Conf. Ser* **435** (2013) 012027, arXiv:1301.7527 [math-ph].
[9] P. Boonserm and M. Visser: *Ann. Phys.* **323** (2008) 2779, arXiv:0801.0610 [quant-ph].
[10] P. Boonserm: *Rigorous bounds on Transmission, Reflection, and Bogoliubov coefficients*, Ph.D. thesis, Victoria University of Wellington, 2009, arXiv:0907.0045 [math-ph].
[11] W. Kim and J. J. Oh: *Journal of Korean Physical Society* **52** (2008) 986.
[12] P. Boonserm and M. Visser: *Phys. Rev.* D **78** (2008) 101502(R), arXiv:0806.2209 [gr-qc].

Spin zero Hawking radiation for non-zero-angular momentum mode

Tritos Ngampitipan, Petarpa Bonserm, and Matt Visser

Citation: AIP Conference Proceedings **1660**, 050066 (2015); doi: 10.1063/1.4915699
View online: http://dx.doi.org/10.1063/1.4915699
View Table of Contents: http://scitation.aip.org/content/aip/proceeding/aipcp/1660?ver=pdfcov
Published by the AIP Publishing

Spin Zero Hawking Radiation for Non-Zero-Angular Momentum Mode

Tritos Ngampitipan[a], Petarpa Bonserm[b] and Matt Visser[c]

[a] *Department of Physics, Chulalongkorn University, Bangkok 10330, Thailand*
[b] *Department of Mathematics and Computer Science, Chulalongkorn University, Bangkok 10330, Thailand*
[c] *School of Mathematics, Statistics, and Operations Research, Victoria University of Wellington, PO Box 600, Wellington 6140, New Zealand*

Abstract. Black hole greybody factors carry some quantum black hole information. Studying greybody factors may lead to understanding the quantum nature of black holes. However, solving for exact greybody factors in many black hole systems is impossible. One way to deal with this problem is to place some rigorous analytic bounds on the greybody factors. In this paper, we calculate rigorous bounds on the greybody factors for spin zero hawking radiation for non-zero-angular momentum mode from the Kerr-Newman black holes.

Keywords: greybody factors, Kerr-Newman black holes, rigorous bounds.
PACS: 04.70.Dy, 04.62.+v, 04.70.Bw

INTRODUCTION

Classically, a black hole can absorb everything entering it even light. However, this picture was changed when we took into account quantum effects. In 1974, Stephen Hawking discovered that a black hole could indeed emit radiation. This radiation became known as "Hawking radiation" [1]. Some black hole information is contained in the greybody factor. Therefore, understanding the greybody factors may lead to understanding the universe. However, in most systems, solving the equation for the greybody factors is very complicated. Instead of finding exact solutions, we place some rigorous analytic bound on the greybody factors. In this paper, we calculate rigorous bounds on the greybody factors for spin zero hawking radiation for non-zero-angular momentum mode from the Kerr-Newman black holes.

KERR-NEWMAN BLACK HOLE

The Kerr-Newman metric is given by [2, 3]

$$ds^2 = -\frac{\Delta}{\Sigma}\left(dt - a\sin^2\theta\, d\phi\right)^2 + \frac{\sin^2\theta}{\Sigma}\left[a\,dt - (r^2+a^2)\,d\phi\right]^2 + \frac{\Sigma}{\Delta}dr^2 + \Sigma\, d\theta^2, \tag{1}$$

where

$$\Delta = r^2 - 2Mr + a^2 + Q^2 = (r-r_+)(r-r_-), \qquad \Sigma = r^2 + a^2\sin^2\theta. \tag{2}$$

Here a is the angular momentum per unit mass of the black holes, M is the black hole mass, Q is the black hole electric charge, r_- is the inner event horizon, and r_+ is the outer event horizon. The horizon radii are given by

$$r_\pm = M \pm \sqrt{M^2 - a^2 - Q^2}. \tag{3}$$

In this work, we are interested in scalar excitation to the Kerr-Newman black holes. The equation of motion takes the form

$$\left\{\frac{d^2}{dr_*^2} - U_{lm}(r)\right\}R_{lm}(r) = 0 \tag{4}$$

where the tortoise coordinate r_* is defined by

International Conference on Mathematics, Engineering and Industrial Applications 2014 (ICoMEIA 2014)
AIP Conf. Proc. 1660, 050066-1–050066-6; doi: 10.1063/1.4915699

$$dr_* = \frac{r^2+a^2}{\Delta}dr = \frac{r^2+a^2}{(r-r_+)(r-r_-)}dr \tag{5}$$

and the effective potential $U_{\ell m}(r)$ is given by

$$U_{\ell m}(r) = \frac{\Delta}{(r^2+a^2)^2}\left[\lambda_{\ell m}(a\omega) + \frac{(r\Delta)'}{r^2+a^2} - \frac{3r^2\Delta}{(r^2+a^2)^2}\right] - \left(\omega - \frac{ma}{r^2+a^2}\right)^2 \tag{6}$$

Here

$$\lambda_{\ell m}(a\omega) = \ell(\ell+1) - 2ma\omega + (H_{\ell+1,m} - H_{\ell m})(a\omega)^2, \tag{7}$$

where ℓ is the angular momentum quantum number, m is the azimuthal quantum number, ω is the energy of an emitted particle, and $H_{\ell m}$ is given by [4]

$$H_{\ell m} = \frac{2\ell(\ell^2-m^2)}{4\ell^2-1} \tag{8}$$

We can write

$$U_{\ell m}(r) = V_{\ell m}(r) - (\omega - m\varpi)^2, \tag{9}$$

where

$$\varpi = \frac{a}{a^2+r^2} \tag{10}$$

and

$$V_{\ell m}(r) = \frac{\Delta}{(r^2+a^2)^2}\left[\lambda_{\ell m}(a\omega) + \frac{(r\Delta)'}{r^2+a^2} - \frac{3r^2\Delta}{(r^2+a^2)^2}\right] \tag{11}$$

RIGOROUS BOUNDS ON GREYBODY FACTORS

Because of impossibility of finding exact solutions, we calculate the rigorous bounds on the greybody factors instead. These bounds can be found in [5]. They are applied to generic systems in [6-8] and to black hole greybody factors [9, 10]. These bounds are given by [11, 12]

$$T \geq \mathrm{sech}^2\left(\int_{-\infty}^{\infty} \vartheta dr_*\right), \tag{12}$$

where

$$\vartheta = \frac{\sqrt{[h'(r)]^2 + [U_{\ell m}(r) + h(r)^2]^2}}{2h(r)} \tag{13}$$

Using the triangle inequality, we obtain

$$T_{\ell m} \geq \mathrm{sech}^2\left[\frac{1}{2}\left|\ln\frac{h(\infty)}{h(-\infty)}\right| + \frac{1}{2}\int_{-\infty}^{\infty}\frac{|U_{\ell m}(r) + h(r)^2|}{2h(r)}dr_*\right] \tag{14}$$

Here, $h(r)$ is any positive function. In this work, we choose $h(r) = \omega - m\varpi$. Therefore,

$$T_{\ell m} \geq \mathrm{sech}^2\left[\frac{1}{2}\left|\ln\frac{h(\infty)}{h(-\infty)}\right| + \int_{-\infty}^{\infty}\frac{V_{\ell m}}{2\omega}dr_*\right] \tag{15}$$

We are interested in the non-zero-angular-momentum modes ($m \neq 0$). We shall divide the non-zero-angular-momentum modes into two cases: negative-angular-momentum modes $m < 0$ and low-lying positive-angular-momentum modes $m \in (0, \omega/\Omega_+)$.

Negative-Angular-Momentum Modes

In this case, we obtain

$$T_{\ell m\omega} \geq \mathrm{sech}^2 \left\{ \frac{1}{2} \ln(1 + \ell \Omega_+ / \omega) + \frac{\lambda_{\ell m}(a\omega) - \frac{\arctan(a / r_+)}{a / r_+} + K_{MQJ}}{2 r_+ \omega} \right\}, \tag{16}$$

where

$$\Omega_+ = \frac{a}{a^2 + r_+^2} \tag{17}$$

and

$$K_{MQJ} = \frac{r_+}{8} \frac{(r_+^2 + a^2)(3a^2 + r_+ r_-)\arctan(a / r_+) + a(a^2[r_+ - 2r_-] - r_+^2 r_-)}{a^3 (r_+^2 + a^2)} \tag{18}$$

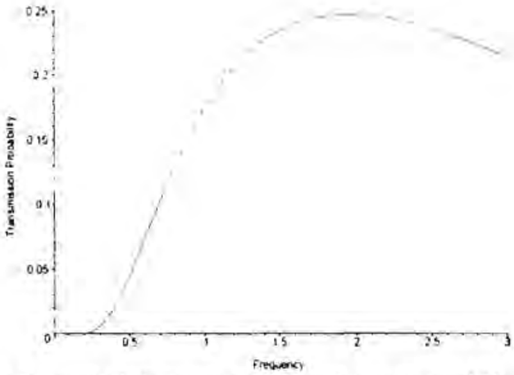

FIGURE 1. The bounds on the greybody factors as a function of ω with $a = 2, Q = 2, \ell = 2, m = -1$ and $M = 3$

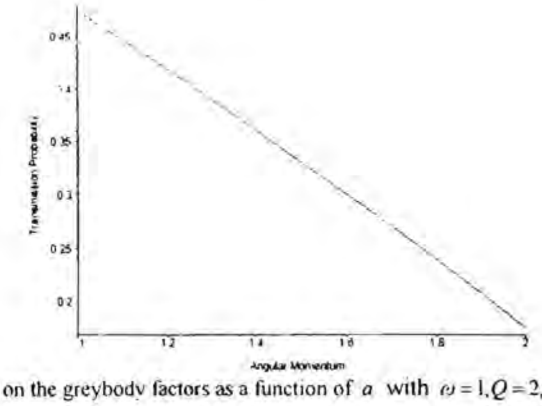

FIGURE 2. The bounds on the greybody factors as a function of a with $\omega = 1, Q = 2, \ell = 2, m = -1$ and $M = 3$

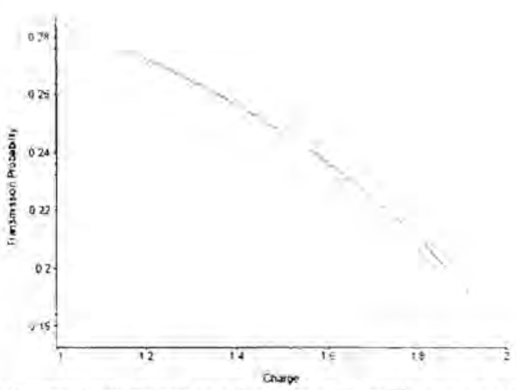

FIGURE 3. The bounds on the greybody factors as a function of Q with $\omega = 1, a = 2, \ell = 2, m = -1$ and $M = 3$

Fig. 1 shows the rigorous bound on the greybody factors as a function of frequency. We can see that the bound increases with increasing frequency until it reaches the maximum and after that it decreases with increasing frequency. Fig. 2 shows the rigorous bound on the greybody factors as a function of angular momentum. The graph indicates that the bound decreases when the angular momentum increases. Fig. 3 shows the rigorous bound on the greybody factors as a function of electric charge. The graph states that the bound decreases with increasing the electric charge.

Low-Lying Positive-Angular-Momentum Modes

In this case, we obtain

$$T_{\ell,m>0} \geq \operatorname{sech}^2\left\{ -\frac{1}{2}\ln(1-(\Omega_+/\omega)) + \frac{\lambda_{\ell m}(a\omega)\dfrac{\arctan(a/r_+)}{a/r_+} + K_{MQJ}}{2r_+(\omega - m\Omega_+)} \right\} \tag{19}$$

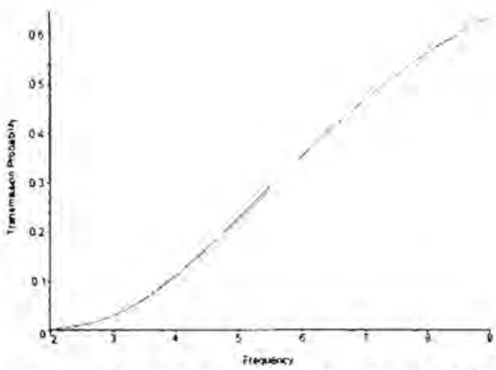

FIGURE 4. The bounds on the greybody factors as a function of ω with $a = 0.2, Q = 0.21, \ell = 2, m = 1$ and $M = 0.3$

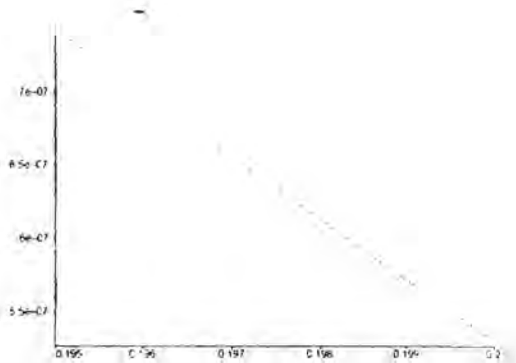

FIGURE 5. The bounds on the greybody factors as a function of a with $\omega = 1, Q = 0.21, \ell = 2, m = 1$ and $M = 0.3$

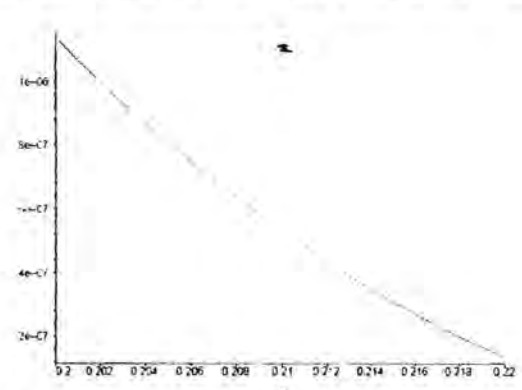

FIGURE 6. The bounds on the greybody factors as a function of Q with $\omega = 1, a = 0.2, \ell = 2, m = 1$ and $M = 0.3$

Fig. 4 shows the rigorous bound on the greybody factors as a function of frequency. Unlike the negative-angular-momentum modes, we can see that the bound increases with increasing frequency. Fig. 5 shows the rigorous bound on the greybody factors as a function of angular momentum. The graph indicates that the bound decreases when the angular momentum increases. Fig. 6 shows the rigorous bound on the greybody factors as a function of electric charge. The graph states that the bound decreases with increasing the electric charge.

CONCLUSIONS

In this paper, we have obtained the rigorous bounds on the greybody factors for spin zero Hawking radiation from the Kerr-Newman black holes. The results show that the bounds increase with increasing frequency but with decreasing angular momentum and electric charge.

ACKNOWLEDGMENTS

This research has been supported by a grant for the professional development of new academic staff from the Ratchadapisek Somphot Fund at Chulalongkorn University, by Thailand Toray Science Foundation (TTSF), by the Thailand Research Fund (TRF), the Office of the Higher Education Commission (OHEC), Chulalongkorn University, and by the Research Strategic plan program (A1B1), Faculty of Science, Chulalongkorn University (MRG5680171). PB was additionally supported by a scholarship from the Royal Government of Thailand. TN was also additionally supported by a scholarship from the Development and Promotion of Science and Technology talent project (DPST). TN gives special thanks to Dr. Auttakit Chatrabuti for his invaluable advice. MV was additionally supported by the Marsden Fund, and by a James Cook fellowship, both administered by the Royal Society of New Zealand.

REFERENCES

1. S. Hawking, *Commun. Math. Phys.* **43**, 199-220 (1975)
2. E. T. Newman and A. I. Janis, *J. Math. Phys.* **6**, 915-917 (1965)
3. E. T. Newman, R. Couch, K. Chinnapared, A. Exton, A. Prakash, and R. Torrence, *J. Math. Phys.* **6**, 918-919 (1965)
4. M. Sasaki and H. Tagoshi, *Living Rev. Relativity* **6**, (2003) [arXiv: gr-qc/0306120]
5. M. Visser, *Phys. Rev.* A **59**, 427-438 (1999), [arXiv: quant-ph/9901030]
6. P. Boonserm and M. Visser, *J. Phys.* A **42**, 045301 (2009) [arXiv: 0808.2516 [math-ph]]
7. P. Boonserm and M. Visser, *Ann. Phys.* **325**, 1328-1339 (2010, [arXiv: 0901.0944 [math-ph]]
8. P. Boonserm and M. Visser, *J. Math. Phys.* **51**, 022105 (2010), [arXiv: 0910.2600 [math-ph]]
9. T. Ngampitipan and P. Boonserm, *Int. J. Mod. Phys.* D **22**, 1350058 (2013), [arXiv: 1211.4070 [math-ph]]
10. T. Ngampitipan and P. Boonserm, *Phys.: Conf. Ser.* **435**, 012027 (2013) [arXiv: 1301.7527 [math-ph]]
11. P. Boonserm and M. Visser, *Ann. Phys.* **323**, 2779-2798 (2008) [arXiv: 0801.0610 [quant-ph]]
12. P. Boonserm, "Rigorous bounds on transmission, reflection, and Bogoliubov coefficients", Ph.D. Thesis, Victoria University of Wellington, Wellington, New Zealand, 2009 [arXiv: 0907.0045 [math-ph]]

International Journal of Engineering and Technology, Vol. 8, No. 4, April 2016

Rigorous Bounds on Greybody Factors: Scalar Emission of Negative Angular Momentum Modes from Myers-Perry Black Holes

Tritos Ngampitipan, Petarpa Boonserm, Auttakit Chatrabhuti, and Matt Visser

Abstract—**When taking into account the quantum effects, a black hole can emit the so-called Hawking radiation. This Hawking radiation propagates in a curved spacetime due to the presence of a black hole. In this paper, the Myers-Perry black hole is considered, which is an uncharged, rotating black hole occurring in higher dimensions. Scalar Hawking radiation emitted from the Myers-Perry black hole is studied. The rigorous bounds on the greybody factors for massless scalar field of negative-angular-momentum modes are also derived.**

Index Terms—**Greybody factor, hawking radiation, myers-perry black hole, rigorous bound.**

I. Introduction

The existence of black holes has been predicted by Einstein's general theory of relativity. The first solutions of the Einstein's field equation were discovered by Karl Schwarzschild. His solutions predicted the presence of Schwarzschild black holes, which are the uncharged, non-rotating black holes. The second type of black hole was obtained by solving the Einstein's field equation in conjunction with Maxwell's equation. This was done by Hans Reissner and Gunnar Nordström. Their solutions represented the Reissner- Nordström black holes, which are the charged, non-rotating black holes. The third set of solutions of the Einstein's field equation was discovered by Roy Kerr [1]. His solutions described the Kerr black holes, which are the uncharged, rotating black holes. The Kerr solutions were generalized to higher dimensions by Myers and Perry [2], [3]. Their results led to the prediction of Myers-Perry black holes, which are the uncharged, rotating black holes in higher dimensions.

When studying the quantum effects of black holes, Stephen Hawking showed that black holes can emit thermal radiation which became known as Hawking radiation [4]. The curvature of spacetime due to the presence of a black hole acts as the gravitational potential barrier. The scattering of Hawking radiation from this potential can be viewed as one-dimensional scattering problem in quantum mechanics. The term 'greybody factor' can be defined as the transmission probability.

In this paper, the rigorous bounds on the greybody factors for massless scalar field of negative-angular-momentum modes emitted from a Myers-Perry black hole will be derived.

II. Myers-Perry Spacetime

The Myers-Perry spacetime can be described by the metric [2], [3], [5]

$$ds^2 = -dt^2 + \frac{\Sigma}{\Delta}dr^2 + \Sigma d\theta^2 + (r^2+a^2)\sin^2\theta d\varphi^2 + \frac{\mu}{r^{n-1}\Sigma}(dt - a\sin^2\theta d\varphi)^2 + r^2\cos^2\theta d\Omega_n^2, \quad (1)$$

where

$$\Delta = r^2 + a^2 - \frac{\mu}{r^{n-1}} \text{ and } \Sigma = r^2 + a^2\cos^2\theta \qquad (2)$$

Here $d\Omega_n^2$ is the metric on the unit n-sphere S^n which is given by

$$d\Omega_n^2 = \left(\prod_{i=1}^{n-1}\sin^2\theta_i\right)d\theta_n^2 \qquad (3)$$

The solutions of $\Delta(r)=0$ provide the location of the black hole event horizons. In this paper, we focus on massless scalar field emitted from the Myers-Perry black hole. The equation of motion of this scalar field can be described by the Klein-Gordon equation

$$\partial_\mu\left(\sqrt{-g}\,g^{\mu\nu}\partial_\nu\Phi\right) = 0, \qquad (4)$$

where

$$\sqrt{-g} = (\Sigma\sin\theta)\times(r^n\cos^n\theta)\times\left(\prod_{i=1}^{n-1}\sin^{n-i}\theta_i\right) \qquad (5)$$

This Klein-Gordon equation governs how the scalar field Φ propagates in the Myers-Perry background. We use the separation of variables in this form

Manuscript received October 3, 2014; revised January 12, 2015.

T. Ngampitipan and A. Chatrabhuti is with the Particle Physics Research Laboratory, Department of Physics, Faculty of Science, Chulalongkorn University, Bangkok 10330, Thailand (e-mail: tritos.ngampitipan@gmail.com, dma3ac2@gmail.com)).

P. Boonserm is with the Department of Mathematics and Computer Science, Faculty of Science, Chulalongkorn University, Bangkok 10330, Thailand (e-mail: petarpa.boonserm@gmail.com).

M. Visser is with the School of Mathematics, Statistics, and Operations Research, Victoria University of Wellington, PO Box 600, Wellington, New Zealand (e-mail: matt.visser@msor.vuw.ac.nz)

DOI: 10.7763/IJET.2016.V8.904

$$\Phi(t,r,\theta,\varphi,\theta_1,\ldots,\theta_n) = e^{-i\omega t+im\varphi}\tilde{R}_{j\ell m}(r)S_{\ell m}(\theta)Y_{jn}(\theta_1,\ldots,\theta_n), \quad (6)$$

where $S_{\ell m}(\theta)e^{im\varphi}$ are the spheroidal harmonics and $Y_{jn}(\theta_1,\ldots,\theta_n)$ are the hyper-spherical harmonics. The spheroidal harmonics satisfy

$$\left\{\frac{1}{\sin\theta\cos^n\theta}\frac{d}{d\theta}\left[\sin\theta\cos^n\theta\frac{d}{d\theta}\right]-\left(\omega a\sin\theta-\frac{m}{\sin\theta}\right)^2 -\frac{j(j+n-1)}{\cos^2\theta}+\lambda_{j\ell m}\right\}S_{\ell m}(\theta)=0 \quad (7)$$

while the hyper-spherical harmonics satisfy

$$\Delta_{S^n}Y_{jn}(\theta_1,\ldots,\theta_n)+j(j+n-1)Y_{jn}(\theta_1,\ldots,\theta_n)=0, \quad (8)$$

where Δ_{S^n} is the Laplacian. Then, the radial Teukolsky equation is obtained [6]-[8]

$$\left[\frac{d^2}{dr_*^2}-U_{j\ell m}(r)\right]R_{j\ell m}(r)=0, \quad (9)$$

where the tortoise coordinate r_* is defined by

$$dr_* = \frac{r^2+a^2}{\Delta(r)}dr. \quad (10)$$

The relationship between the tortoise coordinate and the ordinary coordinate is plotted as shown in Fig. 1.

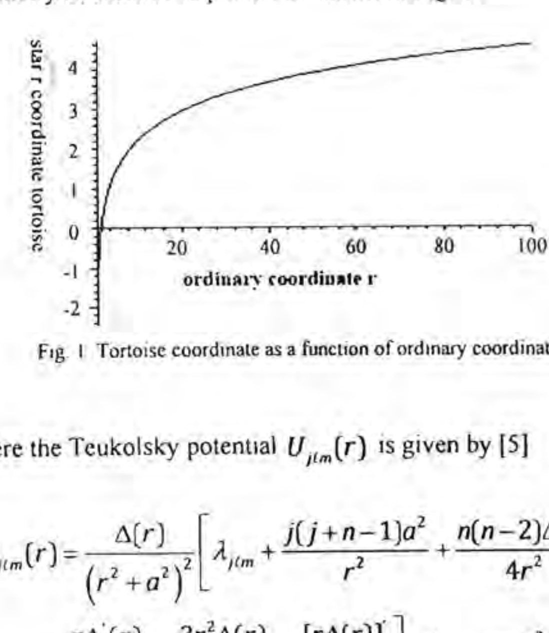

Fig. 1. Tortoise coordinate as a function of ordinary coordinate

Here the Teukolsky potential $U_{j\ell m}(r)$ is given by [5]

$$U_{j\ell m}(r)=\frac{\Delta(r)}{\left(r^2+a^2\right)^2}\left[\lambda_{j\ell m}+\frac{j(j+n-1)a^2}{r^2}+\frac{n(n-2)\Delta(r)}{4r^2} +\frac{n\Delta'(r)}{2r}-\frac{3r^2\Delta(r)}{(r^2+a^2)^2}+\frac{[r\Delta(r)]'}{r^2+a^2}\right]-\left(\omega-m\varpi\right)^2, \quad (11)$$

where

$$\varpi=\frac{a}{r^2+a^2}. \quad (12)$$

This Teukolsky potential can be expressed in another form as

$$U_{j\ell m}(r)=V_{j\ell m}(r)-(\omega-m\varpi)^2, \quad (13)$$

where

$$V_{j\ell m}(r)=\frac{\Delta(r)}{\left(r^2+a^2\right)^2}\left[\lambda_{j\ell m}+\frac{j(j+n-1)a^2}{r^2}+\frac{n(n-2)\Delta(r)}{4r^2} +\frac{n\Delta'(r)}{2r}-\frac{3r^2\Delta(r)}{(r^2+a^2)^2}+\frac{[r\Delta(r)]'}{r^2+a^2}\right] \quad (14)$$

The potential $V_{j\ell m}(r)$ is plotted as shown in Fig. 2 for five and six dimensions which correspond to $n = 1$ and $n = 2$, respectively.

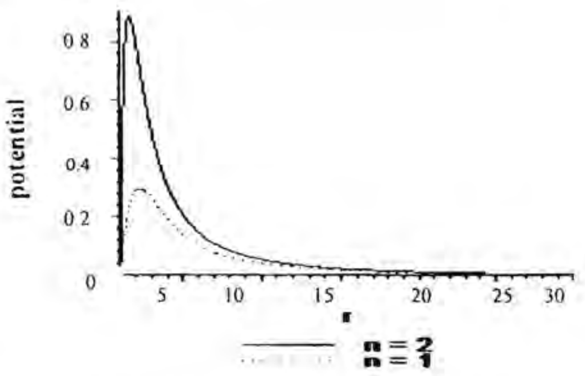

Fig. 2. The potential $V_{j\ell m}(r)$ for $n = 1$ and $n = 2$

III. Rigorous Bounds on Greybody Factors

We can model the scattering of the massless scalar field from the Teukolsky potential as one-dimensional scattering problem in quantum mechanics. The term 'greybody factor' in black hole systems can be defined as the 'transmission probability'. In general situations, finding exact greybody factors is difficult due to complicated potentials. Therefore, in this paper, some rigorous bounds will be placed on greybody factors. These bounds were first developed in [9]. Their further developments can be found in [10]-[13] and their applications can be found in [14]-[19]. For the radial Teukolsky equation in (9), the rigorous bounds on the greybody factors are given by

$$T_{j\ell m} \geq \operatorname{sech}^2\left[\int_{-\infty}^{\infty}\frac{|\tilde{h}'(r_*)|}{2\tilde{h}(r_*)}dr_* + \int_{-\infty}^{\infty}\frac{|\tilde{U}_{j\ell m}(r_*)+\tilde{h}^2(r_*)|}{2\tilde{h}(r_*)}dr_*\right], \quad (15)$$

for any positive functions $h(r_*)$. In this paper, we choose

$$\tilde{h}(r_*)=h(r)=\omega-m\varpi(r), \quad (16)$$

where $m < 0$. In this case, we obtain

$$\tilde{h}'(r_*) = \frac{2mar\Delta(r)}{\left(r^2+a^2\right)^3} > 0 \quad (17)$$

Then, we obtain the first integral

$$\int_{-\infty}^{\infty} \frac{|\tilde{h}'(r_*)|}{2\tilde{h}(r_*)} dr_* = \frac{1}{2}\ln\frac{\tilde{h}(\infty)}{\tilde{h}(-\infty)} = \frac{1}{2}\ln(1-m/m_*), \quad (18)$$

where

$$m_* = \frac{\omega}{\Omega_H}, \quad \Omega_H = \frac{a}{a^2+r_H^2}, \quad (19)$$

and r_H is the event horizon radius. Since $\omega - m\Omega_H > h(r) > \omega$, we have an inequality

$$\int_{-\infty}^{\infty} \frac{|U_{j\ell m} + h^2(r)|}{2h(r)} dr_* = \int_{-\infty}^{\infty} \frac{|V_{j\ell m}|}{2h(r)} dr_* < \int_{-\infty}^{\infty} \frac{V_{j\ell m}}{2\omega} dr_*. \quad (20)$$

Using (14), we can write

$$\int_{-\infty}^{\infty} \frac{V_{j\ell m<0}}{2\omega} dr_* = \frac{1}{2\omega}\int_{-\infty}^{\infty} \frac{\Delta(r)}{\left(r^2+a^2\right)^2}\left[\lambda_{j\ell m<0} + \frac{j(j+n-1)a^2}{r^2} + \frac{n(n-2)\Delta(r)}{4r^2} + \frac{n\Delta'(r)}{2r} - \frac{3r^2\Delta(r)}{(r^2+a^2)^2} + \frac{[r\Delta(r)]'}{r^2+a^2}\right] dr_*. \quad (21)$$

Using (10), we can change the variable r_* to r

$$\int_{-\infty}^{\infty} \frac{V_{j\ell m<0}}{2\omega} dr_* = \frac{1}{2\omega}\int_{r_H}^{\infty} \frac{\Delta(r)}{\left(r^2+a^2\right)^2}\left[\lambda_{j\ell m<0} + \frac{j(j+n-1)a^2}{r^2} + \frac{n(n-2)\Delta(r)}{4r^2} + \frac{n\Delta'(r)}{2r} - \frac{3r^2\Delta(r)}{(r^2+a^2)^2} + \frac{[r\Delta(r)]'}{r^2+a^2}\right]\frac{r^2+a^2}{\Delta(r)} dr \quad (22)$$

The above equation can be simplified to

$$\int_{-\infty}^{\infty} \frac{V_{j\ell m<0}}{2\omega} dr_* = \frac{1}{2\omega}\int_{r_H}^{\infty} \frac{1}{r^2+a^2}\left[\lambda_{j\ell m<0} + \frac{j(j+n-1)a^2}{r^2} + \frac{n(n-2)\Delta(r)}{4r^2} + \frac{n\Delta'(r)}{2r} - \frac{3r^2\Delta(r)}{(r^2+a^2)^2} + \frac{[r\Delta(r)]'}{r^2+a^2}\right] dr \quad (23)$$

Therefore,

$$T_{j\ell,m<0} \geq \operatorname{sech}^2\left[\frac{1}{2}\ln(1-m/m_*) + \frac{1}{2\omega r_H} I_{j\ell,m<0}\right], \quad (24)$$

where

$$I_{j\ell m<0} = \frac{n(2n-3)}{8} + j(j+n-1) + \frac{a^2}{4(r_H^2+a^2)} + \left(\frac{2n+1}{2} - j(j+n-1) + \lambda_{j\ell m}(a\omega)\right)\frac{r_H}{a}\arctan\frac{a}{r_H} + \frac{n(r_H^2+a^2)}{8r_H^2}\,{}_2F_1\left(1, \frac{n+2}{2}, \frac{n+4}{2}, -\frac{a^2}{r_H^2}\right) \quad (25)$$

Here the hypergeometric function ${}_2F_1(a, b, c, z)$ is defined by

$${}_2F_1(a,b,c,z) = \sum_{n=0}^{\infty} \frac{(a)_n (b)_n}{(c)_n} \frac{z^n}{n!} \quad (26)$$

The bounds on the greybody factors are plotted as shown in Fig. 3.

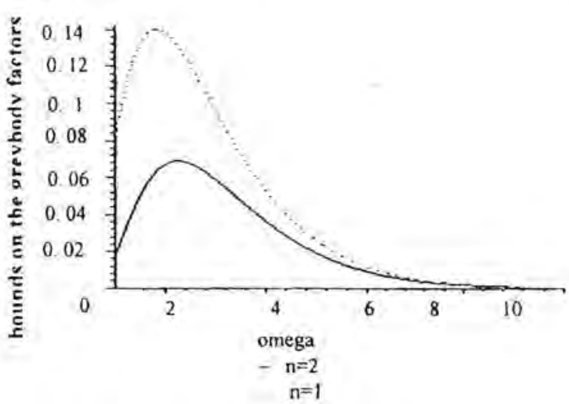

Fig. 3. The bounds on the greybody factors for $n = 1$ and $n = 2$.

In the limit $a \to 0$ and $n = j = 0$, the quantity $I_{j\ell m<0}$ reduces to

$$I_{j=0,\ell,m<0} = \frac{1}{2} + \lambda_{j=0,\ell,m<0}, \quad (27)$$

which is the result for the Schwarzschild black hole [14].

IV. Conclusion

In this paper, the rigorous bounds on the greybody factors for massless scalar field of negative-angular-momentum modes emitted from the Myers-Perry black hole have been established. To obtain these bounds, the appropriate function $h(r_*)$ has been chosen. The number of dimensions of spacetime, the angular momentum of the black holes, and the mass of the black hole have been determined to have effects on these bounds. Note that for $n = 0$, these bounds reduce to bounds for Kerr black holes. For outlook, we can choose other forms of $h(r_*)$ in order to derive better bounds.

ACKNOWLEDGMENT

This project was funded by Ratchadapisek Sompoch Endowment Fund, Chulalongkorn University (Sci-Super 2014-032), by a grant for the professional development of new academic staff from the Ratchadapisek Somphot Fund at Chulalongkorn University, by the Thailand Toray Science Foundation (TTSF), by the Thailand Research Fund (TRF), by the Office of the Higher Education Commission (OHEC), Faculty of Science, Chulalongkorn University (MRG5680171), and by the Research Strategic plan program (A1B1). AC was supported by the Thailand Toray Science Foundation (TTSF) and Thailand Excellence in Physics project (THEP). PB was additionally supported by a scholarship from the Royal Government of Thailand. TN was also additionally supported by a scholarship from the Development and Promotion of Science and Technology talent project (DPST). MV was supported by the Marsden Fund, and by a James Cook fellowship, both administered by the Royal Society of New Zealand.

REFERENCES

[1] R. P. Kerr, "Gravitational field of a spinning mass as an example of algebraically special metrics," *Physical Review Letter*, vol. 11, pp. 237-238, September 1963.

[2] R. C. Myers and M. J. Perry, "Black holes in higher dimensional space-times," *Annals of Physics*, vol. 172, pp. 304-347, December 1986.

[3] R. Emparan and H. S. Reall, "Black holes in higher dimensions," *Living Reviews in Relativity*, vol. 11, September 2008.

[4] S. W. Hawking, "Particle creation by black holes," *Communications in Mathematical Physics*, vol. 43, pp. 199-220, April 1975.

[5] T. Ngampitipan, P. Boonserm, A. Chatrabhuti, and M. Visser, "Spin-zero hawking radiation: Bounds on the zero-angular-momentum mode emission from Myers-Perry black holes," in *Proc. the International Conference on Multi-Hazard Approaches to Civil Infrastructure Engineering*, 2014.

[6] D. Ida, Y. Uchida, and Y. Morisawa, "The scalar perturbation of higher-dimensional rotating black holes," *Physical Review D*, vol. 67, April 2003.

[7] S. Creek, O. Efthimiou, P. Kanti, and K. Tamvakis, "Scalar emission in the bulk in a rotating black hole background," *Physics Letter B*, vol. 656, pp. 102-111, November 2007.

[8] S. Creek, O. Efthimiou, P. Kanti, and K. Tamvakis, "Greybody factors for brane scalar fields in a rotating black-hole background," *Physical Review D*, vol. 75, April 2007.

[9] M. Visser, "Some general bounds for 1-D scattering," *Physical Review A*, vol. 59, pp. 427-438, January 1999.

[10] P. Boonserm and M. Visser, "Transmission probabilities and the Miller-Good transformation," *Journal of Physics A: Mathematical and Theoretical*, vol. 42, January 2009.

[11] P. Boonserm and M. Visser, "Bounding the Bogoliubov coefficients," *Annals of Physics*, vol. 323, pp. 2779-2798, November 2008.

[12] P. Boonserm and M. Visser, "Analytic bounds on transmission probabilities," *Annals of Physics*, vol. 325, pp. 1328-1339, April 2010.

[13] P. Boonserm and M. Visser, "Reformulating the equation as a Shabat-Zakharov system," *Journal of Mathematical Physics*, vol. 51, February 2010.

[14] P. Boonserm and M. Visser, "Bounding the greybody factors for Schwarzschild black holes," *Physical Review D*, vol. 78, November 2008.

[15] T. Ngampitipan and P. Boonserm, "Bounding the greybody factors for non-rotating black holes," *International Journal of Modern Physics D*, vol. 22, June 2013.

[16] T. Ngampitipan and P. Boonserm, "Bounding the greybody factors for the Reissner-Nordström black holes," *Journal of Physics: Conference Series*, vol. 435, May 2013.

[17] P. Boonserm, T. Ngampitipan, and M. Visser, "Regge-Wheeler equation, stability, and greybody factors for dirty black holes," *Physical Review D*, vol. 88, August 2013.

[18] P. Boonserm, T. Ngampitipan, and M. Visser, "Bounding the greybody factors for scalar field excitations of the Kerr-Newman spacetime," *Journal of High Energy Physics*, vol. 1403, p. 113, March 2014.

[19] P. Boonserm, A. Chatrabhuti, T. Ngampitipan, and M. Visser, "Greybody factors for Myers-Perry black holes," *Journal of Mathematical Physics*, vol. 55, November 2014.

Tritos Ngampitipan received the B.Sc., M.Sc., and Ph.D. degrees in physics from Chulalongkorn University, Bangkok, Thailand, in 2008, 2011, and 2015, respectively.

He is a researcher at the Department of Physics, Faculty of Science, Chulalongkorn University, Bangkok, Thailand. His current research interests include quantum theory and general relativity.

Petarpa Boonserm received the BSc., MSc., and Ph.D. degrees in mathematics from Victoria University of Wellington, Wellington, New Zealand, in 2004, 2006, and 2009, respectively.

She is an assistant professor at the Department of Mathematics and Computer Science, Faculty of Science, Chulalongkorn University, Bangkok, Thailand. Her current research interests include differential equations, applied mathematics, quantum theory, and general relativity.

Auttakit Chatrabhuti received the Ph.D. degree from Durham University, Durham, United Kingdom, in 2002.

He is an assistant professor at the Department of Physics, Faculty of Science, Chulalongkorn University, Bangkok, Thailand. His current research interests include quantum field theory, string theory, and supersymmetry.

Matt Visser received the Ph.D. degree from University of California at Berkeley, California, USA. He is a professor at the School of Mathematics, Statistics, and Operations Research, Victoria University of Wellington, Wellington, New Zealand. He is best known for his contributions to the theory of traversable wormholes, chronology protection, and analogue spacetimes. His research interests include general relativity, quantum field theory, and cosmology.

Conservation of Flux in Superradiance Phenomenon

Petarpa Boonserm, Tritos Ngampitipan, and Matt Visser

Abstract—**For a usual occurrence of wave scattering, the amplitude of the reflected wave is less than that of the incident wave because the incident wave loses energy to the reflective obstacle. However, for the so-called superradiance phenomenon, the amplitude of the reflected wave is more than that of the incident wave since the incident wave extracts energy from the reflective obstacle. In this paper, a simple toy model of superradiance is presented. The results show that for the case of superradiance, we derive a conservation of flux instead of the conservation of probability.**

Index Terms—**Conservation, flux, probability, superradiance.**

I. INTRODUCTION

The phenomena of scattering can be described by the interaction of wave with a reflective physical obstacle. In a general situation, the incident wave loses some of its energy to the obstacle, resulting in the amplitude of the reflected wave being less than that of the incident wave. However, in some systems, the incident wave gains energy from the obstacle instead of losing energy. Therefore, the amplitude of the reflected wave becomes greater than that of the incident wave. This unusual phenomenon is called superradiance. Matters of superradiance in literature can be found in [1]-[20].

Despite a long scientific history, superradiance still generates some degree of confusion. Part of the confusion comes from a lack of understanding of the differences between fluxes and probabilities. In this paper, a simple toy model of superradiance is presented to clarify the concept.

II. SUPERRADIANCE

In non-relativistic quantum mechanics, superradiance does not take place [21]. To see this, consider the Schrödinger equation

$$i\hbar\partial_t\psi(x,t)=-\frac{\hbar^2}{2m}\partial_x^2\psi(x,t)+V(x)\psi(x,t) \qquad (1)$$

Assuming the solution

$$\psi(x,t)=e^{-i\omega t/\hbar}\psi(x). \qquad (2)$$

The Schrödinger equation becomes

$$\frac{\hbar^2}{2m}\partial_x^2\psi(x)=[V(x)-\omega]\psi(x) \qquad (3)$$

On the other hand, in the relativistic regime we have the Klein-Gordon equation

$$\left[-(\partial_t-i\varpi(x))^2+\partial_x^2-V(x)\right]\psi(t,x)=0 \qquad (4)$$

For a neutral scalar field, we assume the solution

$$\psi(x,t)=e^{-i\omega t}\psi(x) \qquad (5)$$

The Klein-Gordon equation becomes

$$\partial_x^2\psi(x)=[V(x)-\{\omega-\varpi(x)\}^2]\psi(x) \qquad (6)$$

In this case, superradiance can occur. We see that the term $[\omega-\varpi(x)]^2$ is responsible for superradiance. For a charged scalar field, we obtain

$$\partial_x^2\psi(x)=[V(x)-\{\omega-\varpi(x)-q\Phi(x)\}^2]\psi(x), \qquad (7)$$

where q is the charge of the scalar field. The term $[\omega-\varpi(x)-q\Phi(x)]^2$ is also responsible for superradiance.

III. FLUXES IN SUPERRADIANCE PHENOMENON

In ordinary phenomena of wave scattering, we are familiar with the term 'probability' through both 'reflection probability' and 'transmission probability'. For a more general situation, including the case of superradiance, it is preferable to calculate the quantities in terms of fluxes rather than probabilities. The general conservation law can be described by

$$F_{\text{reflected}}+F_{\text{transmitted}}=1-F_{\text{dissipated}} \qquad (8)$$

In this paper, we are interested in cases of non-dissipation, where $F_{\text{dissipated}}=0$. The general cases, including dissipation, can be found in [21]. In ordinary cases, if the transmitted flux is non-negative $F_{\text{transmitted}}\geq 0$, it can be reduced to transmission probability $F_{\text{transmitted}}=T$. Moreover, the reflected flux also reduces to reflection probability $F_{\text{reflected}}=R$. Therefore (8) becomes

Manuscript received October 3, 2014; revised January 13, 2015.

P. Boonserm is with the Department of Mathematics and Computer Science, Faculty of Science, Chulalongkorn University, Bangkok 10330, Thailand (e-mail: petarpa.boonserm@gmail.com).

T. Ngampitipan is with the Particle Physics Research Laboratory, Department of Physics, Faculty of Science, Chulalongkorn University, Bangkok 10330, Thailand (e-mail: tritos.ngampitipan@gmail.com).

M. Visser is with the School of Mathematics, Statistics, and Operations Research, Victoria University of Wellington, PO Box 600, Wellington, New Zealand (e-mail: matt.visser@msor.vuw.ac.nz).

DOI: 10.7763/IJET.2016.V8.903

$$R+T=1 \tag{9}$$

This is the familiar conservation law of probabilities. On the other hand, in the case of superradiance, we have $F_{transmitted} < 0$. It cannot be interpreted as the transmission probability. Thus, in any situation, we should work with quantities in terms of fluxes rather than probabilities.

IV. Toy Model for Superradiance

Consider the Klein-Gordon equation in 1+1 dimensions

$$\left[-(\partial_t - i\varpi(x))^2 + c^2\partial_x^2 - V(x)\right]\psi(t,x) = 0 \tag{10}$$

Assuming the solution $\psi(t,x) = e^{-i\omega t}\psi(x)$, we obtain

$$c^2\,\partial_x^2\psi(x) = [V(x) - \{\omega - \varpi(x)\}^2]\psi(x) \tag{11}$$

Now, we simplify the problem by letting $V(x) \to 0$ and taking

$$\varpi(x) = \Omega \mathrm{sign}(x), \tag{12}$$

where Ω is a constant. Moreover, we set $c=1$. Therefore, (11) becomes

$$\partial_x^2\psi(x) = -[\omega - \Omega\mathrm{sign}(x)]^2\psi(x) \tag{13}$$

The solutions to (13) are given by

$$\psi(x) = \begin{cases} e^{ik_- x} + re^{-ik_- x} & \text{for} \quad x<0 \\ te^{ik_+ x} & \text{for} \quad x>0 \end{cases} \tag{14}$$

where r is the reflection amplitude, t is the transmission amplitude, and

$$k_\pm^2 = (\omega \mp \Omega)^2. \tag{15}$$

Note that

$$k_+ k_- = \omega^2 - \Omega^2 \tag{16}$$

Thus, we obtain

$$\mathrm{sign}(k_+ k_-) = \mathrm{sign}(\omega^2 - \Omega^2) \tag{17}$$

Assuming that wave moves from left to right and crosses the border at the origin, we have

$$e^{ik_- x} + re^{-ik_- x} \S \quad te^{ik_+ x}. \tag{18}$$

The continuity of the wave function leads to

$$1+r=t. \tag{19}$$

The continuity of the derivative of the wave function leads to

$$k_-(1-r) = k_+ t \tag{20}$$

Solving the equations, we obtain

$$1+r = \frac{k_-}{k_+}(1-r) \tag{21}$$

Rearranging it gives

$$r = -\frac{k_+ - k_-}{k_+ + k_-} = -\frac{(\omega-\Omega)-(\omega+\Omega)}{(\omega-\Omega)+(\omega+\Omega)} = +\frac{\Omega}{\omega} \tag{22}$$

Since the reflection amplitude is normalization independent, the result is valid. The reflected flux is given by

$$F_{reflected} = |r|^2 = \frac{\Omega^2}{\omega^2} \tag{23}$$

However, the transmission amplitude depends on the normalization. For the relativistic Klein-Gordon equation, the normalization factor is

$$\frac{e^{ik_- x}}{\sqrt{2|k_-|}} \tag{24}$$

Therefore, the normalized solutions to (13) are given by

$$\psi(x) = \begin{cases} \dfrac{e^{ik_- x}}{\sqrt{2|k_-|}} + \dfrac{re^{-ik_- x}}{\sqrt{2|k_-|}} & \text{for} \quad x<0 \\ \dfrac{te^{ik_+ x}}{\sqrt{2|k_+|}} & \text{for} \quad x>0 \end{cases} \tag{25}$$

The continuity of the wave function leads to

$$\frac{1+r}{\sqrt{2|k_-|}} = \frac{t}{\sqrt{2|k_+|}} \tag{26}$$

The continuity of the derivative of the wave function leads to

$$\frac{k_-}{\sqrt{2|k_-|}}(1-r) = \frac{k_+}{\sqrt{2|k_+|}}t \tag{27}$$

Solving the equations, we obtain

$$\frac{1+r}{\sqrt{2|k_-|}} = \frac{k_-}{k_+}\frac{1-r}{\sqrt{2|k_-|}} \tag{28}$$

Rearranging it gives

$$r = -\frac{k_+ - k_-}{k_+ + k_-} = -\frac{(\omega-\Omega)-(\omega+\Omega)}{(\omega-\Omega)+(\omega+\Omega)} = +\frac{\Omega}{\omega} \tag{29}$$

Substituting in (26), we obtain

$$t=\sqrt{\frac{|k_+|}{|k_-|}}\left(1+\frac{\Omega}{\omega}\right)=\sqrt{\frac{|\omega-\Omega|}{|\omega+\Omega|}}\left(\frac{\omega+\Omega}{\omega}\right). \quad (27)$$

The reflected flux is given by

$$F_{\text{reflected}}=|r|^2=\frac{\Omega^2}{\omega^2}. \quad (28)$$

If $|\omega|>|\Omega|$, we have

$$t=\sqrt{\frac{\omega-\Omega}{\omega+\Omega}}\left[\frac{\omega+\Omega}{\omega}\right]=\frac{\sqrt{\omega^2-\Omega^2}}{\omega}$$
$$=\text{sign}(\omega)\sqrt{1-\frac{\Omega^2}{\omega^2}}. \quad (29)$$

Therefore, the transmitted flux is given by

$$|t|^2=1-\frac{\Omega^2}{\omega^2}\geq 0. \quad (30)$$

We see that

$$F_{\text{reflected}}+|t|^2=1. \quad (31)$$

In this case, we can write

$$F_{\text{transmitted}}=|t|^2\geq 0. \quad (32)$$

On the other hand, if $|\omega|<|\Omega|$, we have

$$t=\sqrt{-\frac{(\omega-\Omega)}{(\omega+\Omega)}}\left(\frac{\omega+\Omega}{\omega}\right)=\frac{\sqrt{\Omega^2-\omega^2}}{\omega}$$
$$=\text{sign}(\omega)\sqrt{\frac{\Omega^2}{\omega^2}-1} \quad (33)$$

The transmitted flux is given by

$$|t|^2=\frac{\Omega^2}{\omega^2}-1. \quad (34)$$

We see that

$$F_{\text{reflected}}-|t|^2=1. \quad (35)$$

In this case, we can write

$$F_{\text{transmitted}}=-|t|^2\leq 0. \quad (36)$$

We summarize both the cases by

$$F_{\text{transmitted}}=\text{sign}(k_+k_-)|t|^2=1-\frac{\Omega^2}{\omega^2}. \quad (37)$$

Thus, we can write

$$F_{\text{reflected}}+F_{\text{transmitted}}=1. \quad (38)$$

Using (17), this can be rewritten as

$$|r|^2+\text{sign}(k_+k_-)|t|^2=1. \quad (39)$$

Explicitly, this is not a conservation of probability, but rather, a conservation of flux.

V. Conclusion

Superradiance is a phenomenon of scattering in which the amplitude of the reflected wave is more than that of the incident wave because the incident wave extracts energy from the reflective obstacle. In this paper, a simple toy model of superradiance has been presented. In the case of superradiance, we have achieved the conservation of flux instead of the conservation of probability. The concept of conservation of probability is only valid in the absence of superradiance. So, in any situation (both with and without superradiance) we can write the conservation of flux

$$F_{\text{reflected}}+F_{\text{transmitted}}=1 \quad (40)$$

if there is no dissipation. This can be rewritten as

$$|r|^2+\text{sign}(k_+k_-)|t|^2=1 \quad (41)$$

Acknowledgment

This project was funded by Ratchadapisek Sompoch Endowment Fund, Chulalongkorn University (Sci-Super 2014-032), by a grant for the professional development of new academic staff from the Ratchadapisek Somphot Fund at Chulalongkorn University, by the Thailand Toray Science Foundation (TTSF), by the Thailand Research Fund (TRF), by the Office of the Higher Education Commission (OHEC), Faculty of Science, Chulalongkorn University (MRG5680171), and by the Research Strategic plan program (A1B1). PB was additionally supported by a scholarship from the Royal Government of Thailand. TN was also supported by a scholarship from the Development and Promotion of Science and Technology talent project (DPST). MV was supported by the Marsden Fund, and by a James Cook fellowship, both administered by the Royal Society of New Zealand.

References

[1] Y. B. Zel'dovich, "Amplification of cylindrical electromagnetic waves reflected from a rotating body," *Journal of Experimental and Theoretical Physics*, vol. 35, pp. 1085-1087, December 1972.

[2] C. A. Manoge, "The Klein paradox and super-radiance," *Annals of Physics*, vol. 181, pp. 261-283, February 1988.

[3] M. Richartz, S. Weinfurtner, A. J. Penner, and W. G. Unruh, "General universal super-radiant scattering," *Physical Review D*, vol. 80, December 2009.

[4] M. Richartz, A. Prain, S. Weinfurtner, and S. Liberati, "Super-radiant scattering of dispersive fields," *Classical and Quantum Gravity*, vol. 30, March 2013.

[5] A. Hansen and F. Ravndal, "Klein's paradox and its resolution," *Physica Scripta*, vol. 23, January 1981.

[6] N. Dombey and A. Calogeracos, "Seventy years of the Klein paradox," *Physics Reports*, vol. 315, pp. 41-58, July 1999.

[7] A. Calogeracos and N. Dombey, "History and physics of the Klein paradox," *Contemporary Physics*, vol. 40, pp. 313-321, 1999.

[8] W. H. Press and S. A. Teokolsky, "Floating orbits, super-radiant scattering and the black-hole bomb," *Nature*, vol. 238, pp. 211-212, July 1972.

[9] E. Winstanley, "On classical super-radiance in Kerr-Newman - anti-de Sitter black holes," *Physical Review D*, vol. 64, October 2001.

[10] V. Cardoso, O. J. C. Dias, J. P. S. Lemos, and S. Yoshida, "The black hole bomb and super-radiant instabilities," *Physical Review D*, vol. 70, August 2004.

[11] S. R. Dolan, "Instability of the massive Klein-Gordon-field on the Kerr spacetime," *Physical Review D*, vol. 76, October 2007.

[12] S. Chen and J. Jing, "Phantom scalar emission in the Kerr black hole spacetime," *Classical and Quantum Gravity*, vol. 27, January 2010.

[13] M. Kenmoku. (May 2009). Normal modes, quasi-normal modes and super-radiant modes for scalar fields in Kerr anti-de Sitter spacetime. Available. [Online]. http://www.arxiv.org/pdf/0809.2634v3.pdf

[14] S. R. Dolan, "Super-radiant instabilities of rotating black holes in the time domain," *Physical Review D*, vol. 87, June 2013.

[15] C. A. R. Herdeiro, J. C. Degollado, and H. F. Runarsson, "Rapid growth of super-radiant instabilities for charged black holes in a cavity," *Physical Review D*, vol. 88, September 2013.

[16] S. Hod, "Analytic treatment of the charged black-hole-mirror bomb in the highly explosive regime," *Physical Review D*, vol. 88, September 2013.

[17] J. C. Degollado and C. A. R. Herdeiro, "Time evolution of superradiant instabilities for charged black holes in a cavity," *Physical Review D*, vol. 89, March 2014.

[18] P. Boonserm, T. Ngampitipan, and M. Visser, "Bounding the greybody factors for scalar field excitations of the Kerr-Newman spacetime," *Journal of High Energy Physics*, pp. 113, March 2014.

[19] P. Boonserm, A. Chatrabhuti, T. Ngampitipan, and M. Visser, "Greybody factors for Myers-Perry black holes," *Journal of Mathematical Physics*, vol. 55, November 2014.

[20] T. Ngampitipan, P. Boonserm, A. Chatrabhuti, and M. Visser, "Spin-zero Hawking radiation: Bounds on the zero-angular-momentum mode emission from Myers-Perry black holes," in *Proc. the International Conference on Mechanical and Aerospace Engineering*, 2014.

[21] P. Boonserm, T. Ngampitipan, and M. Visser, "Superradiance and flux conservation," *Physical Review D*, vol. 90, September 2014.

Petarpa Boonserm received the BSc., MSc., and Ph.D. degrees in mathematics from Victoria University of Wellington, Wellington, New Zealand, in 2004, 2006, and 2009, respectively.

She is an assistant professor at the Department of Mathematics and Computer Science, Faculty of Science, Chulalongkorn University, Bangkok, Thailand. Her current research interests include differential equations, applied mathematics, quantum theory, and general relativity.

Tritos Ngampitipan received the B.Sc., M.Sc., and Ph.D. degrees in physics from Chulalongkorn University, Bangkok, Thailand, in 2008, 2011, and 2015, respectively.

He is a researcher at the Department of Physics, Faculty of Science, Chulalongkorn University, Bangkok, Thailand. His current research interests include quantum theory and general relativity.

Matt Visser received the Ph.D. degree from University of California at Berkeley, California, USA.

He is a professor at the School of Mathematics, Statistics, and Operations Research, Victoria University of Wellington, Wellington, New Zealand. He is best known for his contributions to the theory of traversable wormholes, chronology protection, and analogue spacetimes. His research interests include general relativity, quantum field theory, and cosmology.

ICMAE 2014

ENGINEERING MATHEMATICS WITHOUT BOUNDS

HOME

CONFERENCE VENUE

TOPICS & SUBMISSION GUIDELINES

REGISTRATION & ABSTRACT SUBMISSION

PUBLICATION

FULL PAPER SUBMISSION

MATHEMATICAL PHYSICS AND PARTIAL DIFFERENTIAL EQUATIONS

1. Author(s): Farrukh Mukhamedov and Hasan Akin

Affiliation: Department of Computational & Theoretical Sciences, Faculty of Sciences, International Islamic University Malaysia, 25200 Kuantan

Paper Title:A class of p-adic rational dynamical systems

2. Author(s): Abdumalik Rakhimov

Affiliation: Department of Science in Engineering, Faculty of Engineering, International Islamic University Malaysia, 50728 Kuala Lumpur

Paper Title: The uniformly convergence of the eigenfunction expansions in a closed domain

3. Author(s): Azeddine Messikh, Gharib M. Subhi, Bakhram Umarov and Mohamed Ridza Wahiddin

Affiliation: Department of Computer Science, Kulliyyah of Information and Communication Technology, International Islamic University Malaysia, 50728 Kuala

Last updated : 8, September 2014

VISITORS

Lumpur

Paper Title : Atomic Coupler with Two-Mode Squeezed Vacuum States

4. Author(s): Gharib Mahmoud, Azeddine Messikh, Torla Hassan and Raihan Othman

Affiliation: Department of Science in Engineering, Faculty of Engineering, International Islamic University Malaysia, 50728 Kuala Lumpur

Paper Title : Spectrum-Reconstruction Method and High Performance Liquid Chromatography to Calculate Concentrations of Total Carotenoids and Chlorophylls a and b of Chlorella vulgaris B

5. Author(s): Gharib Mahmoud, Azeddine Messikh, and Torla Hassan

Affiliation: Department of Science in Engineering, Faculty of Engineering, International Islamic University Malaysia, 50728 Kuala Lumpur

Paper Title : Evolution of the Two-Mode Entangled States with the Liner Quantum Coupler

6. Author(s): Nasir Ganikhodjaev and Mohd Hirzie Mohd Rodzhan

Affiliation: Department of Computational & Theoretical Sciences, Faculty of Sciences, International Islamic University Malaysia, 25200 Kuantan, Malaysia

Paper Title : On Phase Diagram of Ising Model on the Cayley Tree with Competing Interactions up to the Third-Nearest-Neighbor Generation

7. Author(s): Bakhram Umarov and Nor Amirah Busul Aklan

Affiliation: Department of Physics, Faculty of Sciences, International Islamic University Malaysia, 25200 Kuantan, Malaysia

Paper Title : Soliton Scattering on the External Potential in Weakly Nonlocal Nonlinear Media

8. Author(s): Somayyeh Azizi and Atsushi Yagi

Affiliation: Department of Applied Physics, University Suita, Osaka 565-0871, Japan

Paper Title : One-Dimensional Simulations of Growing Crystal under Molecular Beam Epitaxy

9. Author(s): Reza Soheilifard

Affiliation: Department of Mechanical Engineering, Hakim Sabzevari University, Sabzevar, Iran

Paper Title : Using Collective Coordinates in the Coarse-Graining of the Dynamics of Linear Systems

10. Author(s): F.Kh. Abdullaev, M. Salerno, B. Umarov, M.S.A. Hadi

Affiliation: Department of Computational & Theoretical Sciences, Faculty of Sciences, International Islamic University Malaysia, 25200 Kuantan, Malaysia

Paper Title : Compaction Matter Waves of Binary Mixtures under Strong Nonlinear Management

11. Author(s): Kartini Ahmad

Affiliation: Department of Science in Engineering, Faculty of Engineering, International Islamic University Malaysia, 50728 Kuala Lumpur

Paper Title : MHD Flow and Heat Transfer of a Jeffrey Fluid over a Stretching Sheet with Viscous Dissipation

12. Author(s): Annie Gorgey

Affiliation: Department of Mathematics, Faculty of Science and Mathematics, Universiti Pendidikan Sultan Idris, 35900 Tanjong Malim 35900 Tanjong Malim, Perak

Paper Title : Extrapolation of Linear Two-Point Boundary Value Problems and Parabolic Equations

13. Author(s): Tritos Ngampitipan, Petarpa Boonserm, Auttakit Chatrabhuti, and Matt Visser

Affiliation: Department of Physics, Faculty of Science, Chulalongkorn University, Bangkok 10330, Thailand

Paper Title : Spin-Zero Hawking Radiation: Bounds on the Zero-Angular-Momentum Mode Emission from Myers-Perry Black Holes

14. Author(s): Zahriddin Muminov and Fudziah Ismail

Affiliation: Department of Mathematics, Faculty of Science, Universiti Putra Malaysia, 43400 UPM Serdang

Paper Title : Threshold Resonances and Eigenvalues of Some Schrödinger Operators on Lattices

15.Author(s): A.A. Okhunov, G.Sh. Mamathonova, M.X. Ismoilov, Torla Hassan

Affiliation: Department of Science in Engineering, Faculty of Engineering, International Islamic University Malaysia, 50728 Kuala Lumpur

Paper Title : Normalization of Wave Function of the

Band States

16.Author(s): Pah Chin Hee

Affiliation: Department of Computational & Theoretical Sciences, Faculty of Sciences, International Islamic University Malaysia, 25200 Kuantan, Malaysia

Paper Title :Dirichlet's Theorem related Prime Gap Statistics

Malaysian Journal of Mathematical Sciences *(S): **-** (201*)
Special Issue: Name of conference (Conf201*)

MALAYSIAN JOURNAL OF MATHEMATICAL SCIENCES
PERTANIKA
Journal homepage: http://einspem.upm.edu.my/journal

Spin-Zero Hawking Radiation: Bounds on the Zero-Angular-Momentum Mode Emission from Myers-Perry Black Holes

Ngampitipan T*[1], Boonserm P[2], Chatrabhuti A[1], and Visser M[3]

[1]*Department of Physics, Chulalongkorn University, Bangkok 10330, Thailand*
[2]*Department of Mathematics and Computer Science, Chulalongkorn University, Bangkok 10330, Thailand*
[3]*School of Mathematics, Statistics, and Operations Research, Victoria University of Wellington, PO Box 600, Wellington 6140, New Zealand*

E-mail: tritos.ngampitipan@gmail.com
**Corresponding author*

ABSTRACT

From the quantum point of view, black holes are unstable and emit so-called Hawking radiation. Specifically, the Myers-Perry black holes are generalized rotating Kerr black holes in higher-dimensions, popular in both Kaluza-Klein and braneworld scenarios, which might in principle be detected through their Hawking radiation. One specific black hole characteristic is the greybody factor, defined in terms of the transmission probability of Hawking radiation back-scattered from the black hole gravitational potential barrier. In this paper, some rigorous bounds on the greybody factor for spin-zero Hawking radiation emitted in the zero-angular-momentum mode from the Myers-Perry black holes are calculated. This calculation serves as a template for other angular momentum modes.

Keywords: Hawking radiation, greybody factors, Myers-Perry black holes, rigorous bounds

1. Introduction

Classically anything and everything, even light, which enters a black hole cannot escape. As a consequence, no one can (directly) see the black hole. However from the quantum point of view, black holes are unstable and emit so-called Hawking radiation, see ref. (Hawking (1975)). When Hawking radiation propagates in the black hole spacetime, it is modified by the curvature of spacetime resulting from that black hole. In particular, when Hawking radiation is back scattered from the black hole gravitational potential barrier, only the transmitted radiation can be observed from spatial infinity. This modified Hawking radiation, therefore, can be thought of as greybody radiation. The quantity known as the greybody factor is defined in terms of the transmission probability.

In this paper some rigorous bounds are calculated for the greybody factors for spin-zero Hawking radiation, emitted in the zero-angular-momentum mode from Myers-Perry black holes.

2. Myers-Perry Black Holes

The Myers-Perry black holes are the generalization of four-dimensional Kerr black holes to $(4+n)$ dimensions. The $(4+n)$-dimensional Myers-Perry black holes can be described by the $(4+n)$-dimensional Myers-Perry metric (Myers et al. (1986)), (Emparan et al. (2008))

$$ds^2 = -dt^2+\frac{\Sigma}{\Delta}dr^2+\Sigma d\theta^2+(r^2+a^2)\sin^2\theta d\phi^2+\frac{\mu}{r^{n-1}\Sigma}(dt-a\sin^2\theta d\phi)^2+r^2\cos^2\theta d\Omega_n^2, \tag{1}$$

where

$$\Delta = r^2+a^2-\frac{\mu}{r^{n-1}}, \Sigma = r^2+a^2\cos^2\theta, \tag{2}$$

and $d\Omega_n^2$ is the metric on n-sphere which is given by

$$d\Omega_n^2 = d\theta_1^2+\sin^2\theta_1 d\theta_2^2+\sin^2\theta_1\sin^2\theta_2 d\theta_3^2+\ldots+\left(\prod_{i=1}^{n-1}\sin^2\theta_i\right)d\theta_n^2. \tag{3}$$

Here μ is a free parameter that determines the mass and angular momentum of the black hole. In particular, the mass and angular momentum of the black hole are defined by

$$M_{\rm BH} = \frac{(n+2)A_{n+2}}{16\pi G}\mu \text{ and } J = \frac{2a}{n+2}M_{\rm BH}, \tag{4}$$

where A_{n+2} is the area of an $(n+2)$-dimensional unit sphere which is given by

$$A_{n+2} = \frac{2\pi^{(n+3)/2}}{\Gamma[(n+3)/2]}. \tag{5}$$

The event horizon is located at r_{H} which can be found from $\Delta(r_{\mathrm{H}}) = 0$. We are interested in spin zero (scalar field) Hawking radiation emitted from Myers-Perry black holes. The equation of motion for scalar fields on the Myers-Perry black hole background takes the form

$$\partial_\mu \left(\sqrt{-g} g^{\mu\nu} \partial_\nu \Phi\right) = 0. \tag{6}$$

By separation of variables,

$$\Phi(t, r, \theta, \phi, \theta_1, \ldots, \theta_n) = e^{-i\omega t} e^{im\phi} \tilde{R}_{j\ell m}(r) S_{\ell m}(\theta) Y_{jn}(\theta_1, \ldots, \theta_n), \tag{7}$$

the radial equation is given by (Boonserm et al. (2014b))

$$\left[\frac{d^2}{dr_*^2} - U_{j\ell m}(r)\right] R_{j\ell m}(r) = 0. \tag{8}$$

Here r_* is the tortoise coordinate given by

$$dr_* = \frac{r^2 + a^2}{\Delta(r)} dr. \tag{9}$$

This can explicitly be expressed as

$$r_* = \int_{r_{\mathrm{H}}}^{r} \frac{r^2 + a^2}{\Delta(r)} dr \sim A_n \ln(r - r_{\mathrm{H}}) + B_n(r). \tag{10}$$

The quantity $U_{j\ell m}(r)$ is the Teukolsky potential given by

$$\begin{aligned} U_{j\ell m}(r) &= \frac{\Delta(r)}{(r^2+a^2)^2} \left[\lambda_{j\ell m} + \frac{j(j+n-1)a^2}{r^2} + \frac{n(n-2)\Delta(r)}{4r^2} + \frac{n\Delta'(r)}{2r} \right. \\ &\quad \left. - \frac{3r^2\Delta(r)}{(r^2+a^2)^2} + \frac{(r\Delta(r))'}{r^2+a^2}\right] - \left(\omega - \frac{ma}{r^2+a^2}\right)^2. \end{aligned} \tag{11}$$

Here $\lambda_{j\ell m}$ is the separation constant. In this work, we are interested in the zero-angular-momentum mode ($m = 0$). Therefore, the Teukolsky potential becomes

$$\begin{aligned} U_{j\ell, m=0}(r) &= \frac{\Delta(r)}{(r^2+a^2)^2} \left[\lambda_{j\ell, m=0} + \frac{j(j+n-1)a^2}{r^2} + \frac{n(n-2)\Delta(r)}{4r^2} \right. \\ &\quad \left. + \frac{n\Delta'(r)}{2r} - \frac{3r^2\Delta(r)}{(r^2+a^2)^2} + \frac{(r\Delta(r))'}{r^2+a^2}\right] - \omega^2. \end{aligned} \tag{12}$$

We can rewrite the Teukolsky potential as

$$U_{j\ell,m=0}(r) = V_{j\ell,m=0}(r) - \omega^2, \tag{13}$$

where

$$\begin{aligned} V_{j\ell,m=0}(r) &= \frac{\Delta(r)}{(r^2+a^2)^2}\left[\lambda_{j\ell,m=0} + \frac{j(j+n-1)a^2}{r^2} + \frac{n(n-2)\Delta(r)}{4r^2}\right. \\ &\quad \left. + \frac{n\Delta'(r)}{2r} - \frac{3r^2\Delta(r)}{(r^2+a^2)^2} + \frac{(r\Delta(r))'}{r^2+a^2}\right]. \end{aligned} \tag{14}$$

Figures 1 and 2 shows the potential $V_{j\ell,m=0}(r)$ in five ($n = 1$) and six ($n = 2$) dimensions.

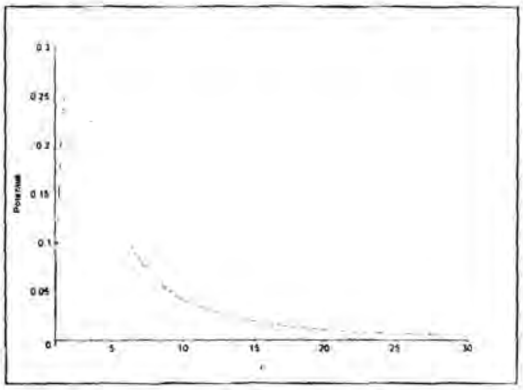

Figure 1: The Myers-Perry potential for $n = 1$.

3. Rigorous Bounds on Greybody Factors

In general, the exact greybody factors are impossible to obtain even for the Schwarzschild black hole, which is by far the simplest case. Thus, it is of interest to develop new methods in calculating the greybody factors. One of them is to place some rigorous bounds on the greybody factors. The relevant bounds were first developed in Visser (1999). They were further developed in Boonserm et al. (2008a), Boonserm et al. (2009), Boonserm (2009), Boonserm et al. (2010a) and Boonserm et al. (2010b). These bounds have been specifically applied to black hole systems (Boonserm et al. (2008b), Ngampitipan et al. (2013a), Ngampitipan et al. (2013b), Boonserm et al. (2013) and Boonserm et al. (2014a)). General and robust bounds on the greybody factors are given by

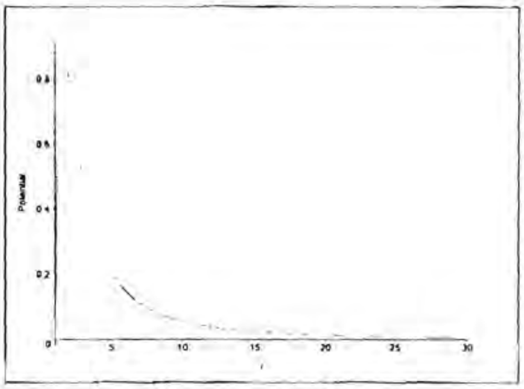

Figure 2: The Myers-Perry potential for $n = 2$.

(Visser (1999), Boonserm et al. (2008a) and Boonserm et al. (2009))

$$T_{j\ell m} \geq \text{sech}^2 \left(\int_{-\infty}^{\infty} \vartheta dr_* \right), \tag{15}$$

where

$$\vartheta = \frac{\sqrt{[h'(r_*)]^2 + [U_{j\ell m}(r_*) + h^2(r_*)]^2}}{2h(r_*)}. \tag{16}$$

and $h(r_*)$ is any positive function. We choose $h(r_*) = \omega$ and consider the $m = 0$ case. Then,

$$\begin{aligned} T \;\; \geq \;\; & \text{sech}^2 \left[\frac{1}{2\omega} \int_{r_H}^{\infty} \left| \frac{1}{r^2 + a^2} \left\{ \lambda_{j\ell, m=0} + \frac{j(j+n-1)a^2}{r^2} + \frac{n(n-2)\Delta(r)}{4r^2} \right. \right. \right. \\ & \left. \left. \left. + \frac{n\Delta'(r)}{2r} - \frac{3r^2\Delta(r)}{(r^2+a^2)^2} + \frac{(r\Delta(r))'}{r^2+a^2} \right\} \right| dr \right]. \end{aligned} \tag{17}$$

We can show that the argument of the absolute value is positive for $r > r_H$. Thus, we can write

$$\begin{aligned} T \;\; \geq \;\; & \text{sech}^2 \left[\frac{1}{2\omega} \int_{r_H}^{\infty} \frac{1}{r^2 + a^2} \left\{ \lambda_{j\ell, m=0} + \frac{j(j+n-1)a^2}{r^2} + \frac{n(n-2)\Delta(r)}{4r^2} \right. \right. \\ & \left. \left. + \frac{n\Delta'(r)}{2r} - \frac{3r^2\Delta(r)}{(r^2+a^2)^2} + \frac{(r\Delta(r))'}{r^2+a^2} \right\} dr \right]. \end{aligned} \tag{18}$$

Performing the first integral, we obtain

$$\int_{r_H}^{\infty} \frac{\lambda_{j\ell, m=0}}{r^2 + a^2} dr = \frac{\lambda_{j\ell, m=0}}{a} \arctan \frac{r}{a} \Big|_{r_H}^{\infty} = \frac{\lambda_{j\ell, m=0}}{a} \arctan \frac{a}{r_H}. \tag{19}$$

By integrating by parts, we can show that

$$\int_{r_H}^{\infty} \frac{1}{r^2+a^2}\left[-\frac{3r^2\Delta(r)}{(r^2+a^2)^2}+\frac{(r\Delta(r))'}{r^2+a^2}\right]dr = \int_{r_H}^{\infty} \frac{r^2\Delta(r)}{(r^2+a^2)^3}dr. \tag{20}$$

This integral can be explicitly performed and gives

$$\begin{aligned}\int_{r_H}^{\infty} \frac{r^2\Delta(r)}{(r^2+a^2)^3}dr &= \frac{n}{8r_H} - \frac{n(n-2)\left(r_H^2+a^2\right)}{8(n+2)r_H^3}\,{}_2F_1\left(1,\frac{n+2}{2},\frac{n+4}{2},-\frac{a^2}{r_H^2}\right)\\ &\quad -\frac{a^2}{4r_H\left(r_H^2+a^2\right)}+\frac{1}{2a}\arctan\frac{a}{r_H}.\end{aligned} \tag{21}$$

Here ${}_2F_1\left(z_1,z_2,z_3,z_4\right)$ is the hypergeometric function. The j-dependent integral yields

$$\int_{r_H}^{\infty} \frac{j(j+n-1)a^2}{r^2\left(r^2+a^2\right)}dr = \frac{j(j+n-1)}{r_H} - \frac{j(j+n-1)}{a}\arctan\frac{a}{r_H}. \tag{22}$$

Calculating the n-dependent integral, we obtain

$$\begin{aligned}\int_{r_H}^{\infty} \frac{1}{r^2+a^2}\left[\frac{n(n-2)\Delta(r)}{4r^2}+\frac{n\Delta'(r)}{2r}\right]dr &= \frac{n^2\left(r_H^2+a^2\right)}{4(n+2)r_H^3}\,{}_2F_1\left(1,\frac{n+2}{2},\frac{n+4}{2},-\frac{a^2}{r_H^2}\right)\\ &\quad +\frac{n(n-2)}{4r_H}+\frac{n}{a}\arctan\frac{a}{r_H}.\end{aligned} \tag{23}$$

Collecting all the results, we obtain

$$T_{j\ell,m=0} \geq \operatorname{sech}^2\left|\frac{1}{2\omega r_H}I_{j\ell,m=0}\right|. \tag{24}$$

Here

$$\begin{aligned}I_{j\ell,m=0} &= \frac{n(2n-3)}{8}+j(j+n-1)+\frac{n\left(r_H^2+a^2\right)}{8r_H^2}\,{}_2F_1\left(1,\frac{n+2}{2},\frac{n+4}{2},-\frac{a^2}{r_H^2}\right)\\ &\quad +\frac{a^2}{4\left(r_H^2+a^2\right)}+\left[\frac{2n+1}{2}-j(j+n-1)+\lambda_{j\ell,m=0}\right]\frac{r_H}{a}\arctan\frac{a}{r_H}\end{aligned} \tag{25}$$

In the limit $a\to 0$, $n=0$ and $j=0$, we obtain

$$\lim_{a\to 0} I_{j=0,\ell,m=0} = \lim_{a\to 0}\left[-\frac{a^2}{4\left(r_H^2+a^2\right)}+\left(\frac{1}{2}+\lambda_{j=0,\ell,m=0}\right)\frac{r_H}{a}\arctan\frac{a}{r_H}\right] = \frac{1}{2}+\lambda_{j=0,\ell,m=0}. \tag{26}$$

Figures 3 and 4 show the bounds on the greybody factors as a function of ω in five ($n=1$) and six ($n=2$) dimensions, respectively. Figures 5 and 6 show the bounds on the greybody factors as a function of the black hole angular momentum in five ($n=1$) and six ($n=2$) dimensions, respectively.

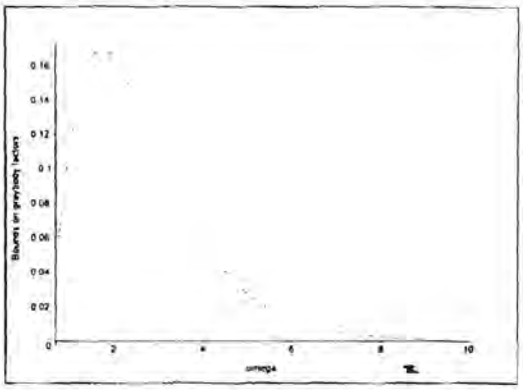

Figure 3: The bounds on the greybody factors as a function of ω for $n = 1$.

4. Conclusion

In this paper, we have obtained rigorous bounds on the greybody factors for spin-zero Hawking radiation emitted in the zero-angular-momentum mode from the Myers-Perry black holes. Qualitatively, the bounds seem to decrease in higher dimensions. In five dimensions corresponding to n = 1, the bounds decrease when increasing the black hole angular momentum. In six dimensions corresponding to n = 2, the bounds increase to reach the maximum and start to decrease when increasing the black hole angular momentum.

Acknowledgments

This research has been supported by Ratchadapisek Sompoch Endowment Fund, Chulalongkorn University (Sci-Super 2014-032), by a grant for the professional development of new academic staff from the Ratchadapisek Somphot Fund at Chulalongkorn University, by the Thailand Toray Science Foundation (TTSF), by the Thailand Research Fund (TRF), by the Office of the Higher Education Commission (OHEC), Chulalongkorn University (MRG5680171), and by the Research Strategic plan program (A1B1). AC was supported by the Thailand Toray Science Foundation (TTSF) and Thailand Excellence in Physics project (THEP). PB was additionally supported by a scholarship from the Royal Government of Thailand. TN was also additionally supported by a scholarship from the Development and Promotion of Science and Technology talent project (DPST). MV was supported by the Marsden Fund, and by a James Cook fellowship, both administered by the Royal Society of New

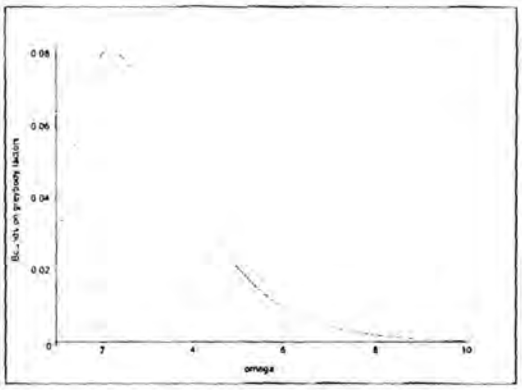

Figure 4: The bounds on the greybody factors as a function of ω for $n = 2$.

Zealand.

References

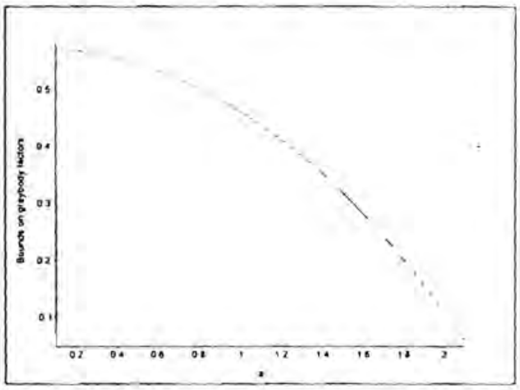

Figure 5: The bounds on the greybody factors as a function of the black hole angular momentum for $n = 1$.

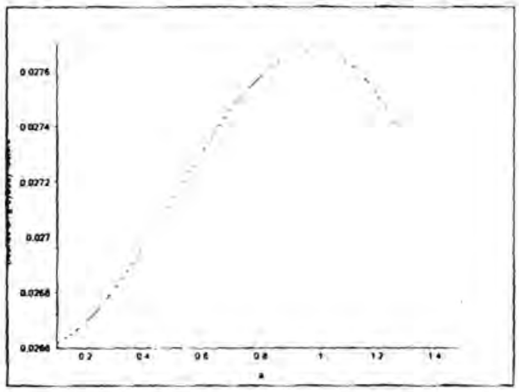

Figure 6: The bounds on the greybody factors as a function of the black hole angular momentum for $n = 2$.

บทความสำหรับการเผยแพร่

การหาขอบเขตล่างของความน่าจะเป็นของการส่งผ่านในปัญหาการกระเจิงทางควอนตัมใน 1 มิติ

Lower bounds on transmission probabilities in one-dimensional quantum scattering problems

ไตรทศ งามปิติพันธ์[1*] *และ เพชรอาภา บุญเสริม*[2]

บทคัดย่อ

กลศาสตร์ควอนตัมเป็นทฤษฎีที่ใช้อธิบายพลศาสตร์ของอนุภาคขนาดเล็ก ๆ เช่น อะตอมหรือโมเลกุล เป็นต้น ในบทความนี้สนใจศึกษากลศาสตร์ควอนตัมในส่วนที่เป็นกลศาสตร์คลื่นของชเรอดิงเงอร์ สมการศูนย์กลางของกลศาสตร์คลื่นนี้คือสมการชเรอดิงเงอร์ โดยการแก้สมการนี้ ทำให้สามารถอธิบายพลศาสตร์ของระบบทางควอนตัมได้ นอกจากนี้ยังได้ศึกษาปัญหาการกระเจิงทางควอนตัมใน 1 มิติ คำนวณหาฟังก์ชันคลื่นโดยการหาผลเฉลยแม่นตรงของสมการชเรอดิงเงอร์ในกรณีของพลังงานศักย์แบบฟังก์ชันเดลต้าและพลังงานศักย์แบบสี่เหลี่ยมมุมฉาก และนำฟังก์ชันคลื่นที่ได้มาคำนวณหาความน่าจะเป็นของการส่งผ่านและการสะท้อน รวมทั้งนำเสนอการหาขอบเขตล่างของความน่าจะเป็นของการส่งผ่าน และนำมาประยุกต์ใช้ในปัญหาพลังงานศักย์แบบฟังก์ชันเดลต้าและพลังงานศักย์แบบสี่เหลี่ยมมุมฉาก ผลลัพธ์ที่ได้บ่งชี้ว่าความน่าจะเป็นของการส่งผ่านที่หาจากผลเฉลยแม่นตรงของฟังก์ชันคลื่นมีความสอดคล้องกับขอบเขตล่างของความน่าจะเป็นของการส่งผ่าน

Abstract

Quantum mechanics is the theory that describes dynamics of small objects such as atom and molecule. In this paper, Schrodinger's wave mechanics, a part of quantum mechanics, is studied. The central equation of this wave mechanics is the Schrodinger's equation. Solving this equation, quantum system dynamics can be described. In this work, the quantum scattering problem in one dimension is studied. Wave functions are obtained by exactly solving the Schrodinger's equation in case of the delta function potential and the rectangular potential. The transmission and reflection probabilities are calculated from the obtained wave functions. Lower bounds on the transmission probabilities are presented. Finally, the lower bounds on the transmission probabilities are applied to the delta function potential and the rectangular potential problems. The results show that the exact transmission probabilities satisfy the lower bounds on the transmission probabilities.

---

[1] ภาควิชาฟิสิกส์ คณะวิทยาศาสตร์ จุฬาลงกรณ์มหาวิทยาลัย กรุงเทพมหานคร 10330

[*] tritos.ngampitipan@gmail.com

[2] ภาควิชาคณิตศาสตร์และวิทยาการคอมพิวเตอร์ คณะวิทยาศาสตร์ จุฬาลงกรณ์มหาวิทยาลัย กรุงเทพมหานคร 10330

คำสำคัญ: กลศาสตร์ควอนตัม สมการชเรอดิงเงอร์ ขอบเขตล่างของความน่าจะเป็นของการส่งผ่าน พลังงานศักย์แบบฟังก์ชันเดลต้า พลังงานศักย์แบบสี่เหลี่ยมมุมฉาก

Keywords: Quantum mechanics, Schrodinger equation, lower bound on the transmission probability, the delta function potential, the rectangular potential.

1. บทนำ

ในช่วงปลายศตวรรษที่ 19 ความรู้ทางฟิสิกส์ประกอบไปด้วยวิชาหลัก ๆ คือ กลศาสตร์แบบดั้งเดิม แม่เหล็กไฟฟ้า และอุณหพลศาสตร์ กลศาสตร์แบบดั้งเดิมใช้ทำนายการเคลื่อนที่ของวัตถุตั้งแต่วัตถุบนโลกจนกระทั่งวัตถุในเอกภพ แม่เหล็กไฟฟ้าใช้อธิบายสนามและคลื่นแม่เหล็กไฟฟ้า และอุณหพลศาสตร์ใช้อธิบายความร้อน งาน พลังงาน อุณหภูมิ และเครื่องยนต์ ทั้งหมดนี้รวมเรียกว่าฟิสิกส์แบบดั้งเดิม ความสำเร็จของฟิสิกส์แบบดั้งเดิมทำให้นักฟิสิกส์หลาย ๆ คนเชื่อกันว่าฟิสิกส์สามารถอธิบายปรากฏการณ์ธรรมชาติได้ทั้งหมด อย่างไรก็ตามในช่วงต้นศตวรรษที่ 20 ได้ค้นพบปรากฏการณ์บางอย่างที่ฟิสิกส์แบบดั้งเดิมไม่สามารถอธิบายได้ เช่น พฤติกรรมของค่าความจุความร้อนต่อโมลแบบปริมาตรคงที่ของก๊าซไฮโดรเจน เมื่ออุณหภูมิมีค่าตั้งแต่ต่ำมากจนกระทั่งสูงมาก เป็นต้น ในปีค.ศ. 1905 อัลเบิร์ต ไอน์สไตน์ได้เสนอทฤษฎีสัมพัทธภาพพิเศษและได้แสดงให้เห็นว่ากลศาสตร์แบบดั้งเดิมของนิวตันใช้ไม่ได้เมื่อความเร็วของอนุภาคสูงมาก (นั่นคือเมื่อความเร็วของอนุภาคใกล้เคียงกับความเร็วแสง) นอกจากนี้ฟิสิกส์แบบดั้งเดิมยังไม่สามารถอธิบายปรากฏการณ์ของอนุภาคขนาดเล็ก เช่น ปัญหาการแผ่รังสีของวัตถุดำ ปรากฏการณ์โฟโตอิเล็กทริก เป็นต้น ในปีค.ศ. 1900 แม็ก พลังค์ได้นำเสนอแนวคิด**ควอนตัม**ของพลังงานซึ่งมีใจความว่า การแลกเปลี่ยนพลังงานระหว่างคลื่นแม่เหล็กไฟฟ้ากับสสารจะเกิดขึ้นได้เมื่อพลังงานที่แลกเปลี่ยนนั้นมีค่าเป็นจำนวนเต็มคูณกับ hf เท่านั้น โดยที่ h เรียกว่าค่าคงที่ของพลังค์ และ f คือความถี่ของคลื่น และเรียกพลังงานที่ไม่ต่อเนื่องนี้ว่า**ควอนตัม** จากแนวคิดนี้ทำให้สามารถอธิบายปัญหาการแผ่รังสีของวัตถุดำได้สำเร็จ ในปีค.ศ. 1905 ไอน์สไตน์ได้นำแนวคิดของพลังค์มาอธิบายปรากฏการณ์โฟโตอิเล็กทริก ไอน์สไตน์ได้เสนอว่าแสงประกอบด้วยอนุภาคเล็ก ๆ ที่เรียกว่าโฟตอน โดยที่โฟตอนแต่ละตัวมีพลังงานเท่ากับ hf ทำให้สามารถอธิบายปรากฏการณ์โฟโตอิเล็กทริกได้สำเร็จ ในปีค.ศ. 1913 นีลส์ บอร์ ได้นำเสนอแบบจำลองอะตอมของไฮโดรเจน และอธิบายว่าการแลกเปลี่ยนพลังงานระหว่างอะตอมกับคลื่นแม่เหล็กไฟฟ้าจะเกิดขึ้นได้เมื่อพลังงานที่แลกเปลี่ยนนั้นมีค่าเป็นจำนวนเต็มคูณกับ hf เท่านั้น ทำให้เขาสามารถอธิบายการทดลองได้ อย่างไรก็ตามแนวคิดของบอร์ยังไม่มีทฤษฎีที่นำมารองรับ ในปีค.ศ. 1923 หลุยส์ เดอบรอยล์ได้นำเสนอว่าไม่เพียงแต่คลื่นที่สามารถประพฤติตัวเป็นอนุภาคได้ แต่อนุภาคก็สามารถประพฤติตัวเป็นคลื่นได้เช่นกัน ในปีค.ศ. 1925 ทฤษฎีที่เชื่อมโยงผลการทดลองเข้ากับแนวคิดของบอร์ก็ได้ถือกำเนิดขึ้น ทฤษฎีนี้เรียกว่า**กลศาสตร์ควอนตัม** ตามประวัติศาสตร์ มีผู้วางรากฐานของกลศาสตร์ควอนตัมไว้สองแนวทาง แนวทางแรกเรียกว่า**กลศาสตร์เมทริกซ์** โดยเวอร์เนอร์ ไฮเซนเบิร์กเป็นผู้ให้กำเนิดกลศาสตร์เมทริกซ์นี้ในปีค.ศ. 1925 ซึ่งได้แทนปริมาณทางพลศาสตร์เช่น ตำแหน่งของอนุภาค พลังงาน โมเมนตัม เป็นต้น ในรูปของเมทริกซ์ ทำให้ได้ปัญหาค่าไอเกนซึ่งสามารถอธิบายพลศาสตร์ของระบบขนาดเล็ก ๆ ได้ แนวทางที่สองเรียกว่า**กลศาสตร์คลื่น** โดยเออร์วิน ชเรอดิงเงอร์เป็นผู้ให้กำเนิดกลศาสตร์คลื่นนี้ในปีค.ศ. 1926 ซึ่งพัฒนาทฤษฎีนี้มาจากแนวคิดของเดอบรอยล์ ทฤษฎีนี้อธิบายพลศาสตร์ของอนุภาคที่มีขนาดเล็ก ๆ ด้วยคลื่นในรูปของสมการคลื่น สมการนี้เรียกว่าสมการ**ชเรอดิงเงอร์**ซึ่งเป็นสมการเชิงอนุพันธ์ คำตอบของสมการนี้จะให้ค่าพลังงานของอนุภาคและฟังก์ชันคลื่นของระบบ ในปีค.ศ. 1927 แม็ก บอร์น ได้นำเสนอว่า กำลังสองของขนาดของฟังก์ชันคลื่นซึ่งเป็นคำตอบของสมการชเรอดิงเงอร์จะแสดงถึงความน่าจะเป็นที่จะพบอนุภาค ภายหลังชเรอดิงเงอร์สามารถพิสูจน์ได้ว่ากลศาสตร์เมทริกซ์ของไฮเซนเบิร์กและกลศาสตร์คลื่นของชเรอดิงเงอร์มีความสมมูลกัน (Zettili, 2009)

โดยสรุป กลศาสตร์ควอนตัมเป็นทฤษฎีที่ใช้อธิบายปรากฏการณ์ของอนุภาคขนาดเล็กที่มองไม่เห็นด้วยตาเปล่า เช่น อนุภาคในระดับโมเลกุลหรืออะตอม เป็นต้น กลศาสตร์ควอนตัมเป็นรากฐานของฟิสิกส์ของของแข็ง เลเซอร์ สารกึ่งตัวนำ ตัวนำยิ่งยวด พลาสมา นอกจากนี้ กลศาสตร์ควอนตัมยังเป็นรากฐานของเคมีและชีววิทยาด้วย

ปัญหาการกระเจิงทางควอนตัมใน 1 มิติเป็นการนำสมการชเรอดิงเงอร์มาอธิบายปัญหาการกระเจิงใน 1 มิติ การประยุกต์ใช้สมการชเรอดิงเงอร์เช่นนี้ช่วยให้สามารถเปรียบเทียบความแตกต่างระหว่างปรากฏการณ์แบบดั้งเดิมและแบบควอนตัมได้ ปัญหาการกระเจิงเกิดขึ้นเมื่อฟลักซ์ของอนุภาค (กลุ่มของอนุภาคที่มีมวลและความเร็วเท่ากัน) วิ่งจากบริเวณหนึ่งไปยังอีกบริเวณหนึ่งที่มีพลังงานศักย์ต่างกันโดยที่ค่าพลังงานศักย์นั้นน้อยกว่าค่าพลังงานรวมของแต่ละอนุภาค ในปรากฏการณ์แบบดั้งเดิมอนุภาคจะทะลุผ่านทั้งหมด ไม่มีอนุภาคตัวใดสะท้อนกลับมาเลย อย่างไรก็ตาม ในปรากฏการณ์แบบควอนตัม จะมีอนุภาคบางส่วนสะท้อนกลับมาได้ ถึงแม้ว่าพลังงานรวมของอนุภาคเหล่านั้นจะมากกว่าพลังงานศักย์ก็ตาม ในทางตรงกันข้าม ถ้า ฟลักซ์ของอนุภาควิ่งจากบริเวณหนึ่งที่ค่าพลังงานศักย์น้อยกว่าค่าพลังงานรวมไปยังอีกบริเวณหนึ่งที่ค่าพลังงานศักย์มากกว่าค่าพลังงานรวม อนุภาคจะสะท้อนกลับทั้งหมดในกรณีของปรากฏการณ์แบบดั้งเดิม อย่างไรก็ตาม ในปรากฏการณ์แบบควอนตัม อนุภาคบางส่วนจะทะลุผ่านได้ ปรากฏการณ์เช่นนี้เรียกว่าปรากฏการณ์ขุดอุโมงค์ (เพชรอาภา, 2556) การศึกษาหรือการทำความเข้าใจปรากฏการณ์ทางควอนตัมในลักษณะเช่นนี้ล้วนแล้วแต่เกี่ยวข้องกับการคำนวณค่าความน่าจะเป็นของการส่งผ่านและค่าความน่าจะเป็นของการสะท้อนทั้งสิ้น

ในปัญหาการกระเจิงทางควอนตัมใน 1 มิติ พลังงานศักย์จะมีค่าแตกต่างกันไปในแต่ละระบบ โดยในบางระบบ พลังงานศักย์มีรูปแบบไม่ซับซ้อน สามารถคำนวณหาผลเฉลยแม่นตรงของความน่าจะเป็นของการส่งผ่านได้ อย่างไรก็ตาม ในบางระบบพลังศักย์มีรูปแบบซับซ้อนมากจนกระทั่งไม่สามารถหาผลเฉลยแม่นตรงของความน่าจะเป็นของการส่งผ่านได้ ในกรณีเช่นนี้ อาจต้องหาคำตอบเชิงตัวเลขหรือคำตอบแบบประมาณ ในกรณีที่ไม่ต้องการความแม่นยำเชิงตัวเลข Visser (1999) ได้นำเสนอการหาขอบเขตล่างของความน่าจะเป็นของการส่งผ่านในปัญหาการกระเจิงทางควอนตัมใน 1 มิติ วิธีการนี้จะช่วยในการทำความเข้าใจระบบในเชิงคุณภาพได้ ในบทความนี้ จะนำวิธีการดังกล่าวมาประยุกต์ใช้กับปัญหาพลังงานศักย์แบบฟังก์ชันเดลต้าและพลังงานศักย์แบบสี่เหลี่ยมมุมฉากซึ่งมีผลเฉลยแม่นตรง

2. การหาฟังก์ชันคลื่นในปัญหา 1 มิติ

ในบทความนี้ เราสนใจศึกษากลศาสตร์คลื่นของชเรอดิงเงอร์ พลศาสตร์ของอนุภาคที่มีขนาดเล็ก ๆ สามารถอธิบายได้ด้วยสมการชเรอดิงเงอร์

$$-\frac{\hbar^2}{2m}\frac{d^2\psi(x)}{dx^2}+V(x)\psi(x)=E\psi(x) \tag{2.1}$$

โดยที่ $\psi(x)$ คือฟังก์ชันคลื่น $V(x)$ คือพลังงานศักย์ E คือพลังงานรวมของอนุภาค และ m คือมวลของอนุภาค พจน์แรกอธิบายพลังงานจลน์ของอนุภาค พจน์ที่สองอธิบายพลังงานศักย์ และพจน์ที่สามอธิบายพลังงานรวมของอนุภาค เราสามารถเขียนสมการชเรอดิงเงอร์ใหม่ได้ดังนี้ (เพชรอาภา, 2556)

$$\frac{d^2\psi(x)}{dx^2}+\frac{2m}{\hbar^2}\left[E-V(x)\right]\psi(x)=0 \tag{2.2}$$

ในการแก้สมการเพื่อหาฟังก์ชันคลื่น เราจำเป็นต้องทราบค่าพลังงานศักย์ ในบทความนี้ได้เลือกศึกษาพลังงานศักย์แบบฟังก์ชันเดลต้าและพลังงานศักย์แบบสี่เหลี่ยมมุมฉาก

2.1 พลังงานศักย์แบบฟังก์ชันเดลต้า

พลังงานศักย์แบบฟังก์ชันเดลต้ามีรูปแบบดังนี้

$$V(x) = \alpha\delta(x) \tag{2.3}$$

โดยที่ α คือค่าคงที่บวกและ $\delta(x)$ คือฟังก์ชันเดลต้าซึ่งนิยามโดย

$$\delta(x) = \begin{cases} \infty & \text{เมื่อ } x \neq 0 \\ 0 & \text{เมื่อ } x = 0 \end{cases} \tag{2.4}$$

กราฟของฟังก์ชันเดลต้าแสดงในรูปที่ 1

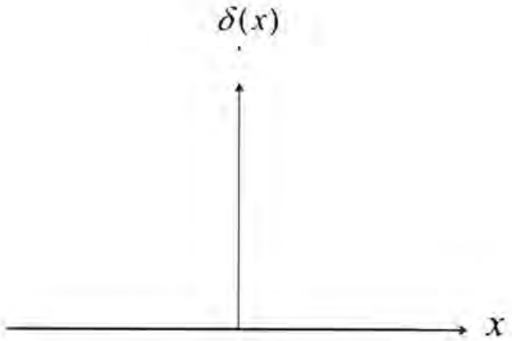

รูปที่ 1 ฟังก์ชันเดลต้า

พิจารณากรณี $E > 0$ เรานิยามปริมาณต่าง ๆ ดังนี้

$$k^2 = \frac{2mE}{\hbar^2} \text{ และ } k_0 = \frac{m\alpha}{\hbar^2} \tag{2.5}$$

สมการชเรอดิงเงอร์คือ

$$\frac{\mathrm{d}^2\psi(x)}{\mathrm{d}x^2} + \frac{2m}{\hbar^2}[E - \alpha\delta(x)]\psi(x) = 0 \tag{2.6}$$

เมื่อ $x \neq 0$ จะได้

$$\frac{\mathrm{d}^2\psi(x)}{\mathrm{d}x^2} + k^2\psi(x) = 0 \tag{2.7}$$

คำตอบของสมการนี้คือ

$$\psi(x) = \begin{cases} \psi_1(x) = Ae^{ikx} + Be^{-ikx} & \text{เมื่อ } x < 0 \\ \psi_2(x) = Ce^{ikx} & \text{เมื่อ } x > 0 \end{cases} \tag{2.8}$$

ฟังก์ชันคลื่นมีความต่อเนื่องที่ $x = 0$ ดังนั้น $\psi_1(0) = \psi_2(0)$ นั่นคือ

$$A + B = C \tag{2.9}$$

เนื่องจากพลังงานศักย์มีค่าเป็นอนันต์ที่ $x = 0$ ดังนั้นอนุพันธ์ของฟังก์ชันคลื่นจึงไม่ต่อเนื่องที่จุดนี้ นั่นคือ

$$\left.\frac{\mathrm{d}\psi(x)}{\mathrm{d}x}\right|_{x=0^+} - \left.\frac{\mathrm{d}\psi(x)}{\mathrm{d}x}\right|_{x=0^-} = c \tag{2.10}$$

โดยที่ $c \neq 0$ เราสามารถหาค่า c ได้โดยการเขียนสมการ (2.6) ใหม่ดังนี้

$$\frac{d^2\psi(x)}{dx^2}+k^2\psi(x)=2k_0\delta(x)\psi(x) \tag{2.11}$$

อินทิเกรตสมการข้างต้นทั้งสองข้างจาก $-\epsilon$ ถึง ϵ

$$\int_{-\epsilon}^{\epsilon}\frac{d^2\psi(x)}{dx^2}dx+\int_{-\epsilon}^{\epsilon}k^2\psi(x)dx=\int_{-\epsilon}^{\epsilon}2k_0\delta(x)\psi(x)dx \tag{2.12}$$

ดังนั้น

$$\left.\frac{d\psi(x)}{dx}\right|_{-\epsilon}^{\epsilon}+\int_{-\epsilon}^{\epsilon}k^2\psi(x)dx=2k_0\psi(0) \tag{2.13}$$

ให้ $\epsilon\to 0$ จะได้

$$\left.\frac{d\psi(x)}{dx}\right|_{x=0^+}-\left.\frac{d\psi(x)}{dx}\right|_{x=0^-}=2k_0\psi(0) \tag{2.14}$$

แทนสมการ (2.8) ลงในสมการ (2.14) จะได้

$$ikC-ikA+ikB=2k_0(A+B) \tag{2.15}$$

เราสามารถแก้สมการ (2.9) และสมการ (2.15) เพื่อได้ค่า B และ C ในรูปของ A

$$B=\frac{k_0A}{ik-k_0} \text{ และ } C=\frac{ikA}{ik-k_0} \tag{2.16}$$

ความน่าจะเป็นของการส่งผ่านและการสะท้อนมีค่าดังนี้

$$T=\left|\frac{C}{A}\right|^2 \text{ และ } R=\left|\frac{B}{A}\right|^2 \tag{2.17}$$

ดังนั้น

$$T=\frac{k^2}{k^2+k_0^2} \text{ และ } R=\frac{k_0^2}{k^2+k_0^2} \tag{2.18}$$

ผลลัพธ์นี้เป็นไปตามกฎอนุรักษ์ความน่าจะเป็นที่กล่าวไว้ว่า $T+R=1$

2.2 พลังงานศักย์แบบสี่เหลี่ยมมุมฉาก

พลังงานศักย์แบบสี่เหลี่ยมมุมฉากมีรูปแบบดังนี้

$$V(x)=\begin{cases}V_0 & \text{เมื่อ } |x|\le a\\ 0 & \text{เมื่อ } |x|>a\end{cases} \tag{2.19}$$

กราฟของพลังงานศักย์แบบสี่เหลี่ยมมุมฉากแสดงในรูปที่ 2

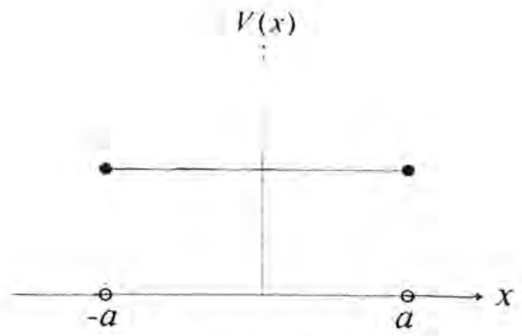

รูปที่ 2 พลังงานศักย์แบบสี่เหลี่ยมมุมฉาก

พิจารณากรณี $E > V_0 > 0$ เรานิยามปริมาณต่าง ๆ ดังนี้

$$k^2 = \frac{2mE}{\hbar^2} \quad q^2 = \frac{2m(E-V_0)}{\hbar^2} \text{ และ } k_0^2 = \frac{2mV_0}{\hbar^2} = k^2 - q^2 \tag{2.20}$$

สมการชเรอดิงเงอร์คือ

$$\frac{\mathrm{d}^2\psi(x)}{\mathrm{d}x^2} + \frac{2m}{\hbar^2}[E - V(x)]\psi(x) = 0 \tag{2.21}$$

เมื่อ $|x| \le a$ จะได้

$$\frac{\mathrm{d}^2\psi(x)}{\mathrm{d}x^2} + q^2\psi(x) = 0 \tag{2.22}$$

เมื่อ $|x| > a$ จะได้

$$\frac{\mathrm{d}^2\psi(x)}{\mathrm{d}x^2} + k^2\psi(x) = 0 \tag{2.23}$$

คำตอบของสมการเหล่านี้คือ

$$\psi(x) = \begin{cases} \psi_1(x) = Ae^{ikx} + Be^{-ikx} & \text{เมื่อ } x < -a \\ \psi_2(x) = Ce^{iqx} + De^{-iqx} & \text{เมื่อ } -a \le x \le a \\ \psi_3(x) = Ee^{ikx} & \text{เมื่อ } x > a \end{cases} \tag{2.24}$$

ฟังก์ชันคลื่นมีความต่อเนื่องที่ $x = -a$ ดังนั้น $\psi_1(-a) = \psi_2(-a)$ นั่นคือ

$$Ae^{-ika} + Be^{ika} = Ce^{-iqa} + De^{iqa} \tag{2.25}$$

ฟังก์ชันคลื่นยังมีความต่อเนื่องที่ $x = a$ ดังนั้น $\psi_2(a) = \psi_3(a)$ นั่นคือ

$$Ee^{ika} = Ce^{iqa} + De^{-iqa} \tag{2.26}$$

เนื่องจากพลังงานศักย์มีค่าอันตะ ดังนั้นอนุพันธ์ของฟังก์ชันคลื่นมีความต่อเนื่องที่จุดเหล่านี้เช่นกัน ที่ $x = -a$ จะได้

$$Ae^{-ika} - Be^{ika} = \frac{q}{k}Ce^{-iqa} - \frac{q}{k}De^{iqa} \tag{2.27}$$

ที่ $x = a$ จะได้

$$Ee^{ika} = \frac{q}{k}Ce^{iqa} - \frac{q}{k}De^{-iqa} \tag{2.28}$$

เราสามารถแก้สมการ (2.25)-(2.28) เพื่อได้ค่า B และ E ในรูปของ A

$$\frac{B}{A}=\frac{\left(k^2-q^2\right)\left(e^{2iqa}-e^{-2iqa}\right)}{(k-q)^2e^{2iqa}-(k+q)^2e^{-2iqa}}e^{-2ika} \text{ และ } \frac{E}{A}=-\frac{4kqe^{-2ika}}{(k-q)^2e^{2iqa}-(k+q)^2e^{-2iqa}} \tag{2.29}$$

ความน่าจะเป็นของการส่งผ่านและการสะท้อนมีค่าดังนี้

$$T=\left|\frac{E}{A}\right|^2=\frac{4k^2q^2}{4k^2q^2+k_0^4\sin^2(2qa)} \text{ และ } R=\left|\frac{B}{A}\right|^2=\frac{k_0^4\sin^2(2qa)}{4k^2q^2+k_0^4\sin^2(2qa)} \tag{2.30}$$

ผลลัพธ์นี้เป็นไปตามกฎอนุรักษ์ความน่าจะเป็นที่กล่าวไว้ว่า $T+R=1$

สำหรับพลังงานศักย์ที่มีรูปแบบที่ซับซ้อนมากขึ้น การแก้สมการหาผลเฉลยแม่นตรงอาจไม่สามารถทำได้ จึงต้องอาศัยเทคนิคการประมาณมาช่วยในการหาค่าความน่าจะเป็นของการส่งผ่านและการสะท้อน เพชรอาภา (2556) ได้นำเสนอเทคนิคการประมาณค่าแบบดับเบิลยูเคบีมาช่วยในการหาค่าเหล่านั้นในกรณีที่พลังงานศักย์มีค่ามากกว่าพลังงานรวม $\left(V(x)>E\right)$ ในบทความนี้จะนำเสนออีกเทคนิคหนึ่งซึ่งช่วยในการคำนวณความน่าจะเป็นของการส่งผ่านและการสะท้อนในกรณีที่พลังงานรวมมีค่ามากกว่าพลังงานศักย์ $\left(E>V(x)\right)$ นั่นคือการหาขอบเขตล่างของความน่าจะเป็นของการส่งผ่าน

3. การหาขอบเขตล่างของความน่าจะเป็นของการส่งผ่าน

ในหัวข้อนี้ เป็นการนำเสนอเนื้อหาส่วนหนึ่งของบทความ (Visser, 1999; Boonserm and Visser, 2008; Boonserm, 2009) ซึ่งเกี่ยวกับการหาขอบเขตล่างของความน่าจะเป็นของการส่งผ่าน พิจารณาสมการชเรอดิงเงอร์ใน 1 มิติ

$$\frac{\mathrm{d}^2\psi(x)}{\mathrm{d}x^2}+k^2(x)\psi(x)=0 \tag{3.1}$$

โดยที่

$$k^2(x)=\frac{2m}{\hbar^2}[E-V(x)] \tag{3.2}$$

และ $V(x)$ คือพลังงานศักย์ที่ลู่เข้าสู่ค่าคงที่เมื่อ x มีค่าเป็นบวกอนันต์หรือลบอนันต์

$$V(x\to\pm\infty)\to V_{\pm\infty} \tag{3.3}$$

คำตอบของสมการ (3.1) ที่ตำแหน่งระยะอนันต์คือ

$$\psi(x\to\pm\infty)\approx\begin{cases}\alpha\dfrac{e^{ik_{-\infty}x}}{\sqrt{k_{-\infty}}}+\beta\dfrac{e^{-ik_{-\infty}x}}{\sqrt{k_{-\infty}}} & \text{เมื่อ } x\to-\infty\\[2ex] \dfrac{e^{ik_{\infty}x}}{\sqrt{k_{\infty}}} & \text{เมื่อ } x\to\infty\end{cases} \tag{3.4}$$

โดยที่

$$k_{\pm\infty}=\frac{\sqrt{2m(E-V_{\pm\infty})}}{\hbar} \tag{3.5}$$

ความน่าจะเป็นของการสะท้อนและการส่งผ่านมีค่าดังนี้คือ

$$R=\left|\frac{\beta}{\alpha}\right|^2 \text{ และ } T=\left|\frac{1}{\alpha}\right|^2 \tag{3.6}$$

โดยใช้กฎการอนุรักษ์ความน่าจะเป็น ($T+R=1$) จะได้

$$|\alpha|^2-|\beta|^2=1 \tag{3.7}$$

ที่ตำแหน่งใด ๆ ที่ไม่ใช่ระยะอนันต์ เราสมมติคำตอบในรูป

$$\psi(x)=a(x)\frac{e^{i\varphi(x)}}{\sqrt{\varphi'(x)}}+b(x)\frac{e^{-i\varphi(x)}}{\sqrt{\varphi'(x)}} \tag{3.8}$$

โดยที่ $\varphi'(x)\neq 0$ และ $\varphi(x)$ เป็นจำนวนจริง $a(x)$ และ $b(x)$ เป็นจำนวนเชิงซ้อน คำตอบนี้ต้องลู่เข้าสู่คำตอบในสมการ (3.4) เมื่อ x มีค่าเป็นบวกอนันต์หรือลบอนันต์ นั่นคือ

$$\varphi'(x\to\pm\infty)\to k_{\pm\infty}\quad a(x\to-\infty)\to\alpha\quad a(x\to\infty)\to 1\quad b(x\to-\infty)\to\beta\quad b(x\to\infty)\to 0 \tag{3.9}$$

ในทำนองเดียวกัน อนุพันธ์ของฟังก์ชันคลื่นในสมการ (3.8) ต้องลู่เข้าสู่อนุพันธ์ของฟังก์ชันคลื่นในสมการ (3.4) เมื่อ x มีค่าเป็นบวกอนันต์หรือลบอนันต์ ดังนั้นจึงมีเงื่อนไขเกจ

$$\frac{\mathrm{d}}{\mathrm{d}x}\left[\frac{a(x)}{\sqrt{\varphi'(x)}}\right]e^{i\varphi(x)}+\frac{\mathrm{d}}{\mathrm{d}x}\left[\frac{b(x)}{\sqrt{\varphi'(x)}}\right]e^{-i\varphi(x)}=0 \tag{3.10}$$

ดังนั้นอนุพันธ์ของฟังก์ชันคลื่นในสมการ (3.8) มีค่าดังนี้

$$\frac{\mathrm{d}\psi(x)}{\mathrm{d}x}=i\sqrt{\varphi'(x)}\left[a(x)e^{i\varphi(x)}-b(x)e^{-i\varphi(x)}\right] \tag{3.11}$$

นำสมการ (3.11) มาคำนวณอนุพันธ์อันดับสองได้เป็น

$$\begin{aligned}\frac{\mathrm{d}^2\psi(x)}{\mathrm{d}x^2} &= -\frac{[\varphi'(x)]^2}{\sqrt{\varphi'(x)}}\left[a(x)e^{i\varphi(x)}+b(x)e^{-i\varphi(x)}\right]+\frac{2i\varphi'(x)}{\sqrt{\varphi'(x)}}\frac{\mathrm{d}a(x)}{\mathrm{d}x}e^{i\varphi(x)}-i\frac{\varphi''(x)}{\sqrt{\varphi'(x)}}b(x)e^{-i\varphi(x)}\\ &= -\frac{[\varphi'(x)]^2}{\sqrt{\varphi'(x)}}\left[a(x)e^{i\varphi(x)}+b(x)e^{-i\varphi(x)}\right]-\frac{2i\varphi'(x)}{\sqrt{\varphi'(x)}}\frac{\mathrm{d}b(x)}{\mathrm{d}x}e^{-i\varphi(x)}+i\frac{\varphi''(x)}{\sqrt{\varphi'(x)}}a(x)e^{i\varphi(x)}\end{aligned} \tag{3.12}$$

เปรียบเทียบสมการข้างต้นกับสมการ (3.1) จะได้

$$\begin{aligned}\frac{\mathrm{d}a(x)}{\mathrm{d}x} &= \frac{1}{2\varphi'(x)}\left[\varphi''(x)b(x)e^{-2i\varphi(x)}+i\left\{k^2(x)-\varphi'(x)^2\right\}\left\{a(x)+b(x)e^{-2i\varphi(x)}\right\}\right]\\ \frac{\mathrm{d}b(x)}{\mathrm{d}x} &= \frac{1}{2\varphi'(x)}\left[\varphi''(x)a(x)e^{2i\varphi(x)}-i\left\{k^2(x)-\varphi'(x)^2\right\}\left\{b(x)+a(x)e^{2i\varphi(x)}\right\}\right]\end{aligned} \tag{3.13}$$

สำหรับจำนวนเชิงซ้อนใด ๆ

$$\frac{\mathrm{d}|a(x)|}{\mathrm{d}x}=\frac{1}{2|a(x)|}\left[a^*(x)\frac{\mathrm{d}a(x)}{\mathrm{d}x}+a(x)\frac{\mathrm{d}a^*(x)}{\mathrm{d}x}\right] \tag{3.14}$$

จากสมการ (3.13) จะได้

$$\begin{aligned}\frac{\mathrm{d}|a(x)|}{\mathrm{d}x} &= \frac{1}{2|a(x)|}\frac{1}{2\varphi'(x)}\Big[\varphi''(x)\left\{a^*(x)b(x)e^{-2i\varphi(x)}+a(x)b^*(x)e^{2i\varphi(x)}\right\}\\ &\quad +i\left\{k^2(x)-\varphi'(x)^2\right\}\left\{a^*(x)b(x)e^{-2i\varphi(x)}+a(x)b^*(x)e^{2i\varphi(x)}\right\}\Big]\end{aligned} \tag{3.15}$$

จัดรูปใหม่จะได้

$$\frac{\mathrm{d}|a(x)|}{\mathrm{d}x}=\frac{1}{2|a(x)|}\frac{1}{2\varphi'(x)}\mathrm{Re}\left(\left[\varphi''(x)+i\left\{k^2(x)-\varphi'(x)^2\right\}\right]a^*(x)b(x)e^{-2i\varphi(x)}\right) \tag{3.16}$$

จากอสมการรูปสามเหลี่ยมสำหรับจำนวนเชิงซ้อนใด ๆ

$$\mathrm{Re}(AB)\le|A||B| \tag{3.17}$$

จะได้

$$\frac{\mathrm{d}|a(x)|}{\mathrm{d}x}\le\vartheta(x)|b(x)| \tag{3.18}$$

โดยที่

$$\vartheta(x)=\frac{\sqrt{[\varphi''(x)]^2+\left[k^2(x)-\{\varphi'(x)\}^2\right]^2}}{2|\varphi'(x)|} \tag{3.19}$$

เรานิยามฟังก์ชันใหม่ซึ่งมีค่าบวกเสมอดังนี้ $h(x)\equiv|\varphi'(x)|$ ดังนั้น

$$\vartheta(x)=\frac{\sqrt{[h'(x)]^2+\left[k^2(x)-h^2(x)\right]^2}}{2h(x)} \tag{3.20}$$

จากสมการ (3.7) จะได้

$$|a(x)|^2-|b(x)|^2=1 \tag{3.21}$$

ดังนั้น

$$\frac{\mathrm{d}|a(x)|}{\mathrm{d}x}\le\vartheta(x)\sqrt{a^2(x)-1} \tag{3.22}$$

อินทิเกรตอสมการข้างต้นจะได้

$$\left[\cosh^{-1}|a(x)|\right]_{x_i}^{x_f}\le\int_{x_i}^{x_f}\vartheta(x)\mathrm{d}x \tag{3.23}$$

ใช้เงื่อนไขในสมการ (3.9) เมื่อ $x_i\to-\infty$ และ $x_f\to\infty$ จะได้

$$\cosh^{-1}|\alpha|\le\int_{-\infty}^{\infty}\vartheta(x)\mathrm{d}x \tag{3.24}$$

ดังนั้น

$$|\alpha|\le\cosh\left[\int_{-\infty}^{\infty}\vartheta(x)\mathrm{d}x\right] \tag{3.25}$$

จากสมการ (3.6) เราจะได้

$$T\ge\mathrm{sech}^2\left[\int_{-\infty}^{\infty}\vartheta(x)\mathrm{d}x\right] \tag{3.26}$$

อินทิกรัลด้านขวามือของอสมการ (3.26) คือค่าต่ำสุดที่เป็นไปได้ของค่าความน่าจะเป็นของการส่งผ่าน ดังนั้นอสมการนี้จึงให้ค่าขอบเขตล่างของความน่าจะเป็นของการส่งผ่าน

4. การประยุกต์ใช้เทคนิคในการหาฟังก์ชันคลื่นในพลังงานศักย์แบบต่าง ๆ

4.1 พลังงานศักย์แบบฟังก์ชันเดลต้า

จากอสมการ (3.26) ขอบเขตล่างของความน่าจะเป็นของการส่งผ่านสำหรับพลังงานศักย์แบบฟังก์ชันเดลต้ามีค่า

$$T \geq \operatorname{sech}^2\left[\int_{-\infty}^{\infty} \frac{\sqrt{[h'(x)]^2+\left[k^2-2k_0\delta(x)-h^2(x)\right]^2}}{2h(x)}\,\mathrm{d}x\right] \tag{4.1}$$

เลือก $h(x)=k$ ดังนั้น

$$T \geq \operatorname{sech}^2\left[\int_{-\infty}^{\infty} \frac{\sqrt{\left[-2k_0\delta(x)\right]^2}}{2k}\,\mathrm{d}x\right]=\operatorname{sech}^2\left[\int_{-\infty}^{\infty} \frac{\left|-2k_0\delta(x)\right|}{2k}\,\mathrm{d}x\right]=\operatorname{sech}^2\left[\int_{-\infty}^{\infty} \frac{k_0\delta(x)}{k}\,\mathrm{d}x\right]=\operatorname{sech}^2\left[\frac{k_0}{k}\right] \tag{4.2}$$

เมื่อนำผลเฉลยแม่นตรงที่ได้จากสมการ (2.17) มาเปรียบเทียบกับขอบเขตล่างในอสมการ (4.2) นี้ ได้ผลลัพธ์ดังแสดงในรูปที่ 3

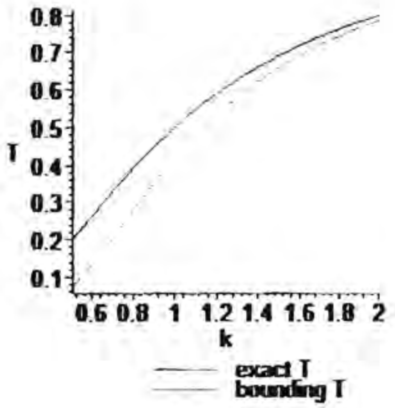

รูปที่ 3 กราฟแสดงการเปรียบเทียบความน่าจะเป็นของการส่งผ่านที่เป็นผลเฉลยแม่นตรงกับขอบเขตล่างในกรณีพลังงานศักย์แบบฟังก์ชันเดลต้า

กราฟนี้ได้แสดงว่าผลเฉลยแม่นตรง (2.17) มีค่ามากกว่าค่าขอบเขตล่างที่ปรากฏในอสมการ (4.2) นั่นคืออสมการ (3.26) เป็นจริง นอกจากนี้ รูปที่ 3 ได้แสดงว่า ในกรณีของผลเฉลยแม่นตรง ความสัมพันธ์ระหว่างความน่าจะเป็นของการส่งผ่านและค่าพลังงานของอนุภาคเหมือนกันกับในกรณีของค่าขอบเขตล่าง นั่นคือ ความน่าจะเป็นของการส่งผ่านมีค่ามากขึ้นเมื่อพลังงานของอนุภาคมีค่ามากขึ้น ดังนั้น อสมการ (4.2) สามารถใช้อธิบายคุณสมบัติเชิงคุณภาพของการกระเจิงของอนุภาคในพลังงานศักย์แบบฟังก์ชันเดลต้าได้

4.2 พลังงานศักย์แบบสี่เหลี่ยมมุมฉาก

จากอสมการ (3.26) ขอบเขตล่างของความน่าจะเป็นของการส่งผ่านสำหรับพลังงานศักย์แบบสี่เหลี่ยมมุมฉากมีค่า

$$T \geq \operatorname{sech}^2\left[\int_{-\infty}^{-a}\frac{\sqrt{[h'(x)]^2+\left[k^2-h^2(x)\right]^2}}{2h(x)}\mathrm{d}x+\int_{-a}^{a}\frac{\sqrt{[h'(x)]^2+\left[q^2-h^2(x)\right]^2}}{2h(x)}\mathrm{d}x\right.$$

$$\left.+\int_{a}^{\infty}\frac{\sqrt{[h'(x)]^2+\left[k^2-h^2(x)\right]^2}}{2h(x)}\mathrm{d}x\right] \tag{4.3}$$

เลือก $h(x)=k$ ดังนั้น

$$T \geq \operatorname{sech}^2\left[\int_{-a}^{a}\frac{\sqrt{\left(q^2-k^2\right)^2}}{2k}\mathrm{d}x\right]=\operatorname{sech}^2\left[\int_{-a}^{a}\frac{\left|q^2-k^2\right|}{2k}\mathrm{d}x\right]=\operatorname{sech}^2\left[\frac{k^2-q^2}{2k}2a\right]=\operatorname{sech}^2\left[\frac{k_0^2 a}{k}\right] \tag{4.4}$$

เมื่อนำผลเฉลยแม่นตรงที่ได้จากสมการ (2.29) มาเปรียบเทียบกับขอบเขตล่างในอสมการ (4.4) นี้ ได้ผลลัพธ์ดังแสดงในรูปที่ 4

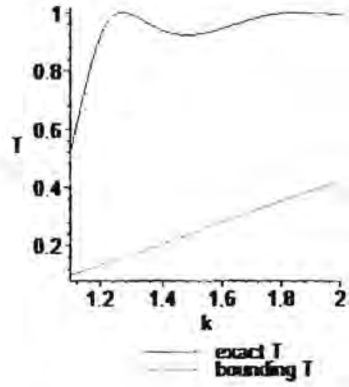

รูปที่ 4 กราฟแสดงการเปรียบเทียบความน่าจะเป็นของการส่งผ่านที่เป็นผลเฉลยแม่นตรงกับขอบเขตล่างในกรณีพลังงานศักย์แบบสี่เหลี่ยมมุมฉาก

กราฟนี้ได้แสดงว่าผลเฉลยแม่นตรง (2.29) มีค่ามากกว่าค่าขอบเขตล่างที่ปรากฏในอสมการ (4.4) นั่นคืออสมการ (3.26) เป็นจริง นอกจากนี้ รูปที่ 4 ได้แสดงว่า ในกรณีของผลเฉลยแม่นตรง ความสัมพันธ์ระหว่างความน่าจะเป็นของการส่งผ่านและค่าพลังงานของอนุภาคเหมือนกันกับในกรณีของค่าขอบเขตล่าง นั่นคือ ความน่าจะเป็นของการส่งผ่านมีค่ามากขึ้นเมื่อพลังงานของอนุภาคมีค่ามากขึ้น ดังนั้น อสมการ (4.4) สามารถใช้อธิบายคุณสมบัติเชิงคุณภาพของการกระเจิงของอนุภาคในพลังงานศักย์แบบสี่เหลี่ยมมุมฉากได้

5. บทสรุป

กลศาสตร์ควอนตัมสามารถใช้อธิบายปรากฏการณ์ของอนุภาคขนาดเล็ก ๆ ได้ เช่น อะตอม โมเลกุล เป็นต้น ในขณะที่ฟิสิกส์แบบดั้งเดิมไม่สามารถอธิบายได้ รากฐานของกลศาสตร์ควอนตัมมีสองแบบคือ กลศาสตร์เมทริกซ์และกลศาสตร์คลื่น ใน

บทความนี้ได้ศึกษากลศาสตร์คลื่นซึ่งพิจารณาว่าอนุภาคประพฤติตัวเป็นคลื่นตามสมมติฐานของเดอบรอยล์ สมการที่ใช้อธิบายคลื่นดังกล่าวคือสมการชเรอดิงเงอร์

นอกจากนี้ยังได้แสดงการหาฟังก์ชันคลื่นในปัญหา 1 มิติโดยการหาผลเฉลยแม่นตรงของสมการชเรอดิงเงอร์ในกรณีพลังงานศักย์แบบฟังก์ชันเดลต้าและพลังงานศักย์แบบสี่เหลี่ยมมุมฉาก และนำมาคำนวณหาความน่าจะเป็นของการส่งผ่านและการสะท้อน นอกจากนั้นยังได้นำเสนอการหาขอบเขตล่างของความน่าจะเป็นของการส่งผ่านและนำมาประยุกต์ใช้ในปัญหาพลังงานศักย์แบบฟังก์ชันเดลต้าและพลังงานศักย์แบบสี่เหลี่ยมมุมฉาก พบว่าความน่าจะเป็นของการส่งผ่านที่หาจากผลเฉลยแม่นตรงของฟังก์ชันคลื่นมีความสอดคล้องกับขอบเขตล่างของความน่าจะเป็นของการส่งผ่าน

ขอบเขตล่างของความน่าจะเป็นของการส่งผ่าน สามารถนำมาใช้อธิบายคุณสมบัติเชิงคุณภาพของปรากฏการณ์การกระเจิงต่าง ๆ ในกลศาสตร์ควอนตัม โดยเฉพาะอย่างยิ่ง ในปัญหาที่ไม่สามารถหาผลเฉลยแม่นตรงได้

กิตติกรรมประกาศ

การวิจัยครั้งนี้ผู้วิจัยขอขอบคุณโครงการพัฒนาและส่งเสริมผู้มีความสามารถพิเศษทางวิทยาศาสตร์และเทคโนโลยี (พสวท.) กองทุนรัชดาภิเษกสมโภช จุฬาลงกรณ์มหาวิทยาลัย (Sci-Super 2014-032) และสำนักงานกองทุนสนับสนุนการวิจัย (สกว.) สำนักงานคณะกรรมการการอุดมศึกษา (สกอ.) และจุฬาลงกรณ์มหาวิทยาลัย (MRG5680171) ที่ให้ทุนสนับสนุนการทำวิจัยจนทำให้งานวิจัยนี้สำเร็จลุล่วงด้วยดี

เอกสารอ้างอิง

ไตรทศ งามปิติพันธ์. (2557). ขอบเขตล่างของตัวประกอบวัตถุเทาสำหรับหลุมดำชนิดต่าง ๆ. วิทยานิพนธ์วิทยาศาสตร์ดุษฎีบัณฑิต , จุฬาลงกรณ์มหาวิทยาลัย. กรุงเทพมหานคร. 82 หน้า.

นรา จิรภัทรมล. (2553). กลศาสตร์ควอนตัม. พิมพ์ครั้งที่ 1. กรุงเทพฯ: สำนักพิมพ์แห่งจุฬาลงกรณ์มหาวิทยาลัย. หน้า 19-31

เพชรอาภา บุญเสริม. (2556). วิธีการทางคณิตศาสตร์สำหรับสมการชเรอดิงเงอร์และวิธีประมาณค่าแบบดับเบิลยูเคบี. วารสารวิทยาศาสตร์ มข. เล่มที่ 41 (ฉบับที่ 1): 109-110

สิทธิชัย โภไคยอุดม. (2552). กลศาสตร์ควอนตัมพื้นฐาน. พิมพ์ครั้งที่ 1. กรุงเทพฯ. มหาวิทยาลัยเทคโนโลยีมหานคร. หน้า 5.71-5.76

Boonserm, P. and Visser, M. (2008). Bounding the Bogoliubov coefficients. Annals of Physics 323 (11): 2779-2798.

Boonserm, P. (2009). Rigorous bounds on transmission reflection and Bogoliubov coefficients. Ph. D. Thesis, Victoria University of Wellington [arXiv:0907.0045 [math-ph]]. 347 pages.

Visser, M. (1999). Some general bounds for 1-D scattering. Physical Review A 59: 427–438.

Zettili, N. (2009). Quantum mechanics: concepts and applications. Second edition. West Sussex: John Wiley & Sons Ltd. pp. 1-4.